l'université nantes angers le mans
PÔLE DE RECHERCHE ET D'ENSEIGNEMENT SUPÉRIEUR

ECOLE DES MINES DE NANTES

Thèse de Doctorat

Cristian Barca

Mémoire présenté en vue de l'obtention du grade de ***Docteur de l'Ecole des Mines de Nantes***

Sous le label de l'Université Nantes Angers Le Mans

Discipline : *Génie des Procédés*

Laboratoire : Laboratoire de Génie des Procédés Environnement Agro-alimentaire (GEPEA)

Soutenue le 17 octobre 2012

École doctorale : Science Pour l'Ingénieur, Géosciences, Architecture (SPIGA)

Thèse N°2012EMNA0045

Steel slag filters to upgrade phosphorus removal in small wastewater treatment plants

Mise au point de filtres garnis de matériaux réactifs destinés au traitement des eaux usées au sein de petites installations

JURY

Rapporteurs :	**Mme Alessandra CARUCCI**, Professeur, Université de Cagliari (Italie)
	M. Christophe DAGOT, Professeur, Université de Limoges (France)
Examinateurs :	**M. Yves COMEAU,** Professeur, Ecole Polytechnique de Montréal (Canada)
	M. Stéphane TROESCH, Docteur, Epur Nature SAS, Caumont sur Durance (France)
Invité :	**M. Dirk ESSER**, Ingénieur, Société d'Ingénierie Nature et Technique, La Chapelle du Mont du Chat (France)
Directeur de Thèse :	**M. Yves ANDRES**, Professeur, Ecole des Mines de Nantes (France)
Co-encadrant de Thèse :	**M. Florent CHAZARENC**, Maître assistant, Ecole des Mines de Nantes (France)

Scientific production

Papers published in peer reviewed journals

Barca C., Gérente C., Meyer D., Chazarenc F., Andrès Y., 2012. Phosphate removal from synthetic and real wastewater using steel slags produced in Europe. Water Research 46 (7), 2376-2384. http://dx.doi.org/10.1016/j.watres.2012.02.012

Barca C., Troesch S., Meyer D., Drissen P., Andrès Y., Chazarenc F., 2013. Steel slag filters to upgrade phosphorus removal in constructed wetlands: two years of field experiments. Environmental Science & Technology 47 (1), 549-556.
http://pubs.acs.org/doi/abs/10.1021/es303778t

Paper under preparation

Barca C. et al. Steel slag filters to upgrade phosphorus removal in small wastewater treatment plants: two years of column experiments. Manuscript.

Oral presentation at international conferences

Barca C., Troesch S., Meyer D., Drissen P., Andres Y., Chazarenc F.. Steel slag filters to upgrade phosphorus removal in small wastewater treatment plants: two years of field experiments. 13th International Conference on Wetland Systems for Water Pollution Control. 25-29 Nov. 2012, Perth, Australia, International Water Association (IWA). Full paper in proceedings.

Barca C., Troesch S., Meyer D., Robinet A., Esser D., Andrès Y., Chazarenc F.. The use of steel slag filters for upgrading phosphorus removal from constructed wetlands: full scale experiments in France. Joint Meeting of Society of Wetland Scientists, Wetpol and Wetland Biogeochemistry Symposium. 3-8 July 2011, Prague, Czech Republic.

Meyer D., Liira M., Barca C., Andrès Y., Chazarenc F.. The use of slag filters for upgrading phosphorus removal from constructed wetlands: lab scale column experiments. Joint Meeting of Society of Wetland Scientists, Wetpol and Wetland Biogeochemistry Symposium. 3-8 July 2011, Prague, Czech Republic.

Barca C., Chazarenc F., Gérente C., Andrès Y., Drissen P.. The use of slag as a sorbent to treat wastewater in Europe. 6th European Slag Conference EUROSLAG 2010. 20-22 Oct. 2010, Madrid, Spain. Full paper in proceedings.

Chazarenc F., Barca C., Gerente, C., Andres, Y.. The use of a industrial by-product (Steel slag) as a substrate to treat wastewater. 12th International Waste Management and Landfill Symposium. 5-9 October 2009, Cagliari, Sardinia, Italy. Full paper in proceedings.

Poster presentation at international conferences

Meyer D., Barca C., Drissen P., Rex M., Andres Y., Chazarenc F.. Slag filters for upgrading phosphorus removal from constructed wetlands: two years of lab scale column experiments. 13th International Conference on Wetland Systems for Water Pollution Control. 25-29 Nov. 2012, Perth, Australia, International Water Association (IWA). Full paper in proceedings.

Barca C., Meyer D., Gérente C., Andrès Y., Troesch S., Chazarenc F.. The use of steel slag as a substrate to treat wastewater: an integrated approach. 13th International Waste Management and Landfill Symposium. 3-7 Oct. 2011, Cagliari, Sardinia, Italy. Full paper in proceedings.

Barca C., Gérente C., Meyer D., Andrès Y., Chazarenc F.. Steel slag produced in Europe as potential filter media for phosphorus removal from wastewater. 12th International Conference on Wetland Systems for Water Pollution Control. 4-8 Oct. 2010, Venice, Italy, International Water Association (IWA).

Acknowledgments

This thesis comes from the collaboration between the Département Systèmes Energétiques et Environnement (DSEE) of the Ecole des Mines de Nantes and the company Epur Nature within the framework of the European project SLASORB (Research Fund for Coal and Steel (RFCS) research program under grant agreement n° RFSP-CT-2009-00028).

First and foremost I would like to thank my supervisor, Assoc. Professor Florent Chazarenc, since he is the person who made all this possible from the beginning. I really appreciated his help and his enthusiasm in doing research. I would express my sincerest gratitude to my director, Professor Yves Andrès, for his excellent guidance, caring, patience, and providing me with an excellent atmosphere for doing research. I would also like to thank Assoc. Professor Claire Gérente, who helped me to develop my background in aquatic chemistry. I really appreciated her help and support. Special thanks go to Professor Alessandra Carucci, University of Cagliari, Italy, and Professor Christophe Dagot, University of Limoges, France, who accepted to review this manuscript.

Part of the experimental work was performed at the company Epur Nature, Avignon, France. I would like to express my gratitude to Christian Pietri, Stéphane Troesch, Vincent Leboeuf, and all the workers in Epur Nature for their help and support during my fellowship and later collaboration. I very appreciated the scientific advice and the interesting discussion with Professor Yves Comeau and his research team of the Laboratoire de Génie de l'Environnement of the Ecole Polytechnique of Montréal, Canada, where I spent a two month period internship. I am really grateful to all them.

I am particularly grateful to Daniel Meyer, for his great support in column experiments, he also helped me to develop my background about hydraulics, Gwendoline Belbeze, for sampling and chemical analyses, Martin Liira, University of Tartu, Estonia, for his very appreciated support in mineralogical investigations, I have really learned a lot from him about the mineralogy of Ca phosphates, Peter Drissen, FEhS Institute of Duisburg, Germany, for chemical and mineralogical analyses, Mark Fixaris, Arcelor Mittal, for providing the steel slag samples. I would also to thank all the other colleagues and partners of the project SLASORB, Dirk Esser, Heribert Rustige, and Martin Rex. I really appreciate the interesting discussions we had during the project meetings.

I want to thank the master students Arthur Robinet and Hernan Ruiz for their great help in sampling and monitoring of slag filters. I really appreciated their great involvement in the

experimental work. Special thanks go to the administrative staff of the department DSEE, Dominique Briand and Marie-Laure Lefebvre. They have always been very supportive and of great help. Also, many thanks go to Thomas Bergantz, Eric Chevrel, Yvan Gouriou, François-Xavier Blanchet, Patrick Brion, Jerome Martin, Nicolas Le Quéré, and other workers in the laboratory of the DSEE for technical support. My research would not have been possible without their helps.

I want to thank all the friends, co-workers and colleagues, master students, PhD students, Postdoctoral researchers, and teachers that I met at the Ecole des Mines de Nantes during my studies. I thank all them for their company, understanding, interesting discussions and help. I really enjoyed the time spent with them, and I will miss all them. Special thanks go to Audrey Forthomme, Vanessa Maroga Mboula and Rafat Khalafallah: we shared the same office during our doctoral studies, thank you for supporting me, for helping me and for understanding me. I will keep always a pleasant memory of the three years we spent together.

Finally, yet importantly, I would like to thank my parents, Mario and Elena, and my sisters, Paola and Daniela. They were always supporting me and encouraging me with their best wishes. This thesis is dedicated to them.

Abstract

This thesis aimed at developing the use of electric arc furnace steel slag (EAF-slag) and basic oxygen furnace steel slag (BOF-slag) in filters designed to upgrade phosphorus (P) removal in small wastewater treatment plants. An integrated approach was followed, with investigation at different scales: (i) Batch experiments were performed to establish an overview of the P removal capacities of steel slag produced in Europe, and then to select the most suitable samples for P removal; (ii) Continuous flow column experiments were performed to investigate the effect of various parameters including slag size and composition, and column design on treatment and hydraulic performances of lab-scale slag filters; (iii) Finally, field experiments were performed to investigate hydraulic and treatment performances of demonstration-scale slag filters designed to remove P from the effluent of a constructed wetland. The experimental results indicated that the major mechanism of P removal was related to CaO-slag dissolution followed by precipitation of Ca phosphate and crystallization into hydroxyapatite (HAP). After 100 weeks of continuous feeding of a synthetic P solution (mean inlet total P 10.2 mg P/L), columns filled with small-size slag (6-12 mm BOF-slag; 5-16 mm EAF-slag) removed >98% of inlet total P, whereas columns filled with big-size slag (20-50 mm BOF-slag and 20-40 mm EAF-slag) removed 56 and 86% of inlet total P, respectively. Most probably, the smaller was the size of slag, the greater was the specific surface for CaO-slag dissolution and adsorption of Ca phosphate precipitates. Field experiments confirmed that steel slag is an efficient substrate for P removal from the effluent of a constructed wetland (mean inlet total P 8.3 mg P/L). Over a period of 85 weeks of operation, EAF-slag removed 36% of inlet total P, whereas BOF-slag removed 59% of inlet total P. P removal efficiencies increased with increasing temperature and void hydraulic retention time (HRTv), most probably because the increase in temperature and HRTv affected the rate of CaO dissolution and Ca phosphate precipitation. However, it was found that long HRTv (>3 days) may produce high pH of the effluents (>9), as the result of excessive CaO-slag dissolution. However, the results of field experiments demonstrated that at shorter HRTv (1-2 days), slag filters produced pH that were elevated only during the first 5 weeks of operation, and then stabilized below a pH of 9. Finally, a dimensioning equation based on the experimental results was proposed.

Keywords: phosphorus removal; steel slag filter; constructed wetlands; hydroxyapatite.

Table of Contents

List of Tables

Chapter 1 Phosphorus removal from wastewater

Chapter 2 Phosphate removal from synthetic and real wastewater using steel slag produced in Europe

Chapter 3 Steel slag filters to upgrade phosphorus removal in small wastewater treatment plants: two years of column experiments

Chapter 4 Steel slag filters to upgrade phosphorus removal in constructed wetlands: two years of field experiments

List of Figures

Chapter 1 Phosphorus removal from wastewater

Chapter 2 Phosphate removal from synthetic and real wastewater using steel slag produced in Europe

Chapter 3 Steel slag filters to upgrade phosphorus removal in small wastewater treatment plants: two years of column experiments

GENERAL INTRODUCTION

Municipal wastewater drainages are significant sources of phosphorus (P) loads into water bodies such as rivers, lakes or lagoons. These P loads usually result in the enrichment in P of the receiving water body, and this promotes an abnormal growth of algae and aquatic plants. As algae and aquatic plants die, they decay by microbial decomposition reducing the concentration of dissolved oxygen. When this happens, this can cause the death of fish and aquatic species that need oxygen to survive. This phenomenon of water quality degradation due to excessive intake of P is commonly referred to as "eutrophication".

Nowadays, it is well known that reduction of P loads is needed to prevent eutrophication. Therefore, legislation on P rejects into the surrounding environment is becoming stricter worldwide, including for municipal wastewater treatment plants (European Union Directives 91/271/EEC and 2000/60/EC). Conventional techniques for P removal based on processes of chemical precipitation and biological uptake present several technical and cost limitations, especially when employed to remove P in small and extensive wastewater treatment plants such as constructed wetland systems. Therefore, research on alternative low cost techniques to upgrade P removal in small wastewater treatment plants has become a priority for scientists in the last two decades. Several international studies have demonstrated that filtration through filters filled with replaceable reactive materials with high affinities for P binding is a viable technique to upgrade P removal in small and extensive wastewater treatment plants.

Since the 1980s, the affinity of steel slag for P binding has been studied with the aim of using a by-product of the steel industry as filter substrate to treat wastewater. Steel and iron industry produces mostly four types of slag: blast furnace slag (BF-slag), which originates from the iron production in a blast furnace; basic oxygen furnace slag (BOF-slag), which originates from the further refining of iron in a basic oxygen furnace; electric arc furnace slag (EAF-slag), which is derived from melting recycled scrap in an electric arc furnace; melter slag, which is produced when iron sand is converted to melter iron. Steel slag is primarily made of iron (Fe) and calcium oxide (CaO), as a result of the use of fluxing agents (mainly lime) during the steelmaking process. A large number of laboratory scale investigations including batch and continuous flow column experiments have demonstrated that steel slag is an efficient substrate for P removal from wastewater. Nowadays, only a few demonstration scale experiments have been conducted (USA, Canada and New Zeeland) to determine P removal performances of steel slag under real operating conditions, and further field-scale experiments are needed to define P removal mechanisms, treatment performances and hydraulic behaviour

of steel slag filters depending on the real operating parameters such as temperature, climate and wastewater composition.

This thesis comes from the collaboration between the Ecole des Mines de Nantes (France) and the company Epur Nature (Caumont sur Durance, France) within the framework of the European project SLASORB. The main objective was to develop a full scale system using steel slag produced in Europe to upgrade phosphorus removal in small wastewater treatment plants. An integrated approach was followed, with investigations at different scales:

i. Batch experiments were performed to establish an overview of the PO_4-P removal capacities of steel slag produced in Europe, and then to select the most suitable samples for P removal;

ii. Continuous flow column experiments were performed to investigate the effect of various parameters including slag size and composition, and column design on treatment and hydraulic performances of slag filters;

iii. Field experiments were performed to investigate the hydraulic and treatment performances of two demonstration-scale slag filters (one filled with EAF-slag, one filled with BOF-slag) designed to remove P from the effluent of a constructed wetland, and to propose design equations based on the experimental results.

Batch tests and continuous flow column experiments were performed at the Département Systèmes Energétiques et Environnement (DSEE) of the Ecole des Mines de Nantes, whereas field experiments were conducted at the wastewater treatment plant of La Motte D'Aigues (Vaucluse, France), under the technical supervision of the company Epur Nature.

This manuscript consists of 4 Chapters. Chapter 1 was written in the form of literature review, whereas Chapters 2, 3 and 4 were written in the form of research papers, as follows:

- Chapter 1: "Phosphorus removal from wastewater". This Chapter shows an overview of the main mechanisms of P removal from aqueous solutions and presents a short review of selected relevant studies that tested reactive filter materials to upgrade P removal in small wastewater treatment plants;

- Chapter 2: "Phosphate removal from synthetic and real wastewater using steel slags produced in Europe", a research paper published in Water Research 46 (2012), 2376-

2384. This paper describes objectives, experimental methods, results and conclusions of batch experiments;

- Chapter 3: “Steel slag filters to upgrade phosphorus removal in small wastewater treatment plants: two years of column experiments”, manuscript describing objectives, experimental methods, results and conclusions of column experiments;

- Chapter 4: “Steel slag filters to upgrade phosphorus removal in constructed wetlands: two years of field experiments”, a research paper published in Environmental Science and Technology 47 (2013), 549-556. This paper describes objectives, experimental methods, results and conclusions of column experiments.

The results of this study demonstrated that EAF-slag and BOF-slag produced in Europe are efficient filter substrates for P removal from wastewater.

LITERATURE REVIEW

CHAPTER 1 Phosphorus removal from wastewater

1.1 Phosphorus pollution

Phosphorus (P) is an essential nutrient for biomass growth. However, an excessive intake of P into water bodies such as rivers, lakes or lagoons causes an abnormal growth of algae and aquatic plants resulting in the degradation of the water quality. These aquatic species covering the surfaces of water limit the transfer of oxygen from air to water by diffusion (Shukla et al., 2008). When algae and aquatic plants die, they sink to the bottom of the water body and decay by microbial decomposition, thus reducing the concentration of dissolved oxygen and forming P-rich sediments. Over time, these sediments release P that is available for biomass growth, thus resulting in a trophic cycle and algal blooms (Recknagel et al., 1995). This phenomenon of water quality degradation due to excessive trophic cycle is commonly referred to as "eutrophication" (Crouzet et al., 1999).

Municipal and industrial drainages and agricultural runoffs are the major sources of P loads into water bodies, and their P contents derived primarily from human and animal dejections, food waste, P-based detergents and P-based fertilisers. Nowadays, it is well known that reduction of P loads is needed to reduce eutrophication. Therefore, legislation on P rejects into the surrounding environment is becoming stricter worldwide, especially in areas that present a high risk of eutrophication. The European Union Directive on urban wastewater treatment (91/271/EEC) established the following requirements for discharges from urban waste water treatment plants (WWTPs) to sensitive areas that are subject to eutrophication:

i. Medium WWTPs (10000 -100000 p.e[1]): annual average effluent total P concentration (TP) of 2 mg P/L and reduction of 80% of the influent TP;

ii. Big WWTPs (> 100000 p.e): annual average effluent TP of 1 mg P/L, and reduction of 80% of the influent TP.

[1] The people equivalent (p.e.) is a unit of measurement of biodegradable organic pollution representing the average load of such pollution produced per capita per day. It is specified in the directive as 60 g of BOD_5 (biochemical oxygen demand in five days) per day.

However, in several European countries (France, Sweden) these limits are (or are expected to become) more stringent and TP concentrations must be reduced below 0.5 mg P/L. Typical P concentrations of municipal wastewater range from 4 to 16 mg P/L (Metcalf and Eddy, 2003), and the use of techniques specifically targeted at P removal is usually required to meet the minimum standards of treatment established by the law. The conventional techniques for P removal in wastewater treatment plants are the chemical precipitation with calcium, aluminium and iron salts, adsorption on P-adsorbent materials, and the biological removal process.

1.2 Forms of phosphorus in wastewater

P in wastewater exists in three main forms, phosphates, polyphosphates and organic phosphorus (Roques, 1990). Each of these P forms presents a different reactivity and affinity for processes of chemical precipitation, adsorption and biological removal. Therefore, the efficiency of the conventional P removal technique depends considerably on the form of P that predominantly occurs in the wastewater.

The phosphates are referred to as the salts of the phosphoric acid (H_3PO_4). Phosphoric acid dissociates in solution producing the phosphate forms $H_2PO_4^-$, HPO_4^{2-} and PO_4^{3-} (PO_4-P). The chemical equilibria between the different PO_4-P forms depend on the pH of the solution as shown in Figure 1.1. $H_2PO_4^-$ is the primary form when pH ranges from 2 to 7, HPO_4^{2-} is the primary form when the pH ranges from 7 to 12, and PO_4^{3-} is the primary form when the pH is higher than 12.

Phosphate is a form of P that is readily available for chemical precipitation, adsorption, and biological removal. Therefore, the ratio of phosphate to total phosphorus of the wastewater is a parameter of great importance when evaluating the efficiency of conventional techniques for P removal.

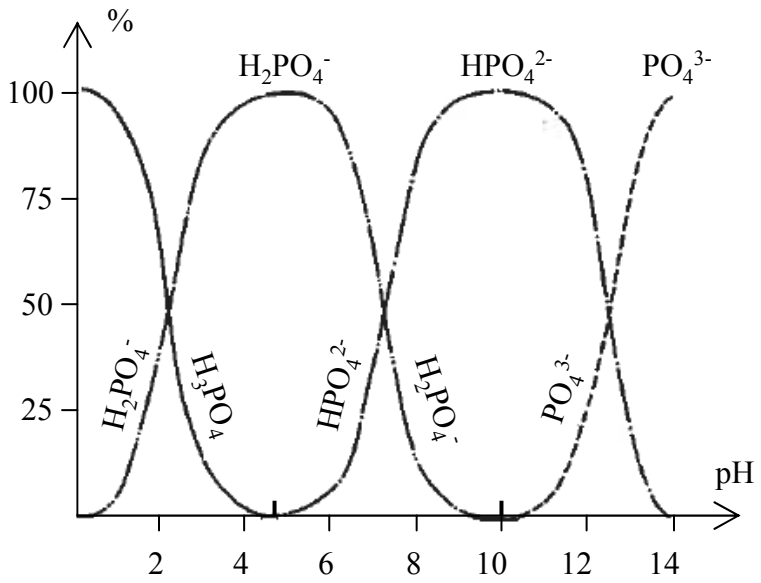

Figure 1.1. Chemical equilibria of phosphates depending on the pH (adapted from Roques, 1990).

The polyphosphates are the salts or ester of polyphosphoric acid. They consist of chains of phosphates bound to each other through one atom of oxygen (Roques, 1990). Polyphosphates in wastewater derive primarily from household detergents. Over the last 20 years, the phosphorus content in detergents has been considerably lowered in many countries in Europe (Crouzet et al., 1999). Therefore, the polyphosphate content in wastewater has been markedly reduced.

The organic phosphorus content in municipal wastewater derives primarily from human dejections. Among the organic phosphorus compounds, some of these are insoluble in water (such as phospholipids, phosphoproteins, nucleic acids and polysaccharides-phosphates), whereas others are soluble (such as glucose-1-phosphate, adenosine diphosphate, inositol mono- and hexa-phosphate, glycerophosphates, phosphocreatine) (Roques, 1990). In France, the average output of organic phosphorus per capita per day is around 1.5 g/(p.e.)d (Roque, 1990). This means that, considering a consumption of water per capita per day of about 150 L/(p.e.)*d, the expected concentration of organic phosphorus in fresh wastewater is around a value of 10 mg P/L.

The polyphosphates and the organic phosphorus decay by hydrolysis and/or by microbial decomposition to produce phosphate. Because phosphorus changes form over time, in the analytic practice it is usual to determine the total phosphorus content (TP), which is measured

by spectrophotometry after the conversion of all forms of phosphorus to phosphate via a pre-treatment of acid digestion and the formation of a colored compound (EN ISO 6878, 2004).

1.3 Mechanisms of phosphorus removal from wastewater

The most common techniques for P removal in wastewater treatment plants refer to processes of chemical precipitation, adsorption and biological removal. The fully understanding of the P removal mechanisms that occur when treating P is essential for the enhancement of the techniques in order to improve the efficiencies of P treatment. Mechanisms of P removal from wastewater may be summarized into three main categories: chemical precipitation, adsorption and biological uptake.

1.3.1 Chemical precipitation

Dissolution of a solute in a solvent is usually a limited phenomenon. A solution is saturated when, at constant temperature, no more solute can be dissolved in the solvent, and a maximum concentration of solute in the solvent is reached. This maximum concentration is referred to as “solubility”. The solubility depends on several parameters, including the nature of the solute and of the solvent, the temperature and the pressure. Precipitation occurs when the concentration of the solute in the solvent is higher than the solubility.

The solubility product constant (Ksp) is the parameter that controls the equilibrium between dissolution and precipitation, and it is usually determined under standard conditions (25°C). The value of Ksp for a general reaction of dissolution-precipitation (1.1) is given by the equation (1.2) (Stumm and Morgan, 1996).

$$A_a B_b(s) \leftrightarrow aA(aq) + bB(aq) \tag{1.1}$$

$$K_{SP} = \frac{[A]_{eq}^{a}[B]_{eq}^{b}}{[A_a B_b]_{eq}} \tag{1.2}$$

The ionic product (IP) of a solution is the product of the concentrations of the ions in a solution at any moment in time, including at non-equilibrium condition. The value of IP for a general reaction of dissolution-precipitation (1.1) is given by the equation (1.3).

$$IP = \frac{[A]^{a}[B]^{b}}{[A_a B_b]} \tag{1.3}$$

The state of saturation of a solution is defined by comparing the ionic product IP to the solubility product constant Ksp:

i. IP < Ksp: the reaction 1.1 will tend to the right until equilibrium is reached. The solution is under saturated and no precipitation will occur;

ii. IP > Ksp: the reaction 1.1 will tend to the left until equilibrium is reached. The solution is supersaturated and precipitation will occur;

iii. IP = Ksp: the reaction 1.1 is at equilibrium. The solution is saturated and no reaction will occur.

The solubility product constant Ksp is also used to compare the stability of different precipitates each other: the lower the Ksp, the greater the stability of the precipitate.

Conventional treatments for phosphorus removal from wastewater most often refer to chemical precipitation. Several salts including aluminium sulphate ($Al_2(SO_4)_3$), ferric chloride ($FeCl_3$) and lime (CaO) are commonly added to wastewater to remove phosphate by precipitation as Al phosphate, Fe phosphate and Ca phosphate, respectively. The solubility of these complexes depends on several parameters, including the pH, as shown in Figure 1.2 (Stumm and Morgan, 1996). Al and Fe phosphates are the most stable forms when the pH of the solution is < 6, whereas Ca phosphates are the most stable forms when pH is > 8.

Figure 1.2. Solubility diagrams of Al, Fe and Ca phosphates depending on pH. The solubility of Ca phosphate has been calculated under the assumption that Ca^{2+} concentration was 10^{-3} M (Stumm and Morgan, 1996).

1.3.1.1 Al phosphate precipitation

Aluminium sulphate ($Al_2(SO_4)_3$) is a salt of Al that is commonly used for phosphorus removal from wastewater. Aluminium sulphate dissolves in solution producing Al^{3+} ions. Then, the Al^{3+} ions react with the phosphates to form Al phosphate (variscite), as shown in equation (1.4) (Stumm and Morgan, 1996).

$$Al^{3+} + PO_4^{3-} + 2H_2O \leftrightarrow AlPO_4 \bullet 2H_2O \qquad \text{Ksp at 25 °C} = 10^{-21} \qquad (1.4)$$

As shown in Figure 1.2, the best pH condition for P removal via Al phosphate precipitation is around a value of 6. However, precipitation of Al hydroxide ($AlOH_3$) may lead to a competing consumption of Al^{3+} ions, as shown in equation (1.5) (Stumm and Morgan, 1996), thus limiting the precipitation of Al phosphate.

$$Al^{3+} + 3H_2O \leftrightarrow AlOH_3 + 3H^+ \qquad \text{Ksp at 25 °C} = 10^{-16.9} \qquad (1.5)$$

1.3.1.2 Fe phosphate precipitation

Ferric chloride $FeCl_3$ is a salt of Fe that is commonly used for phosphorus removal from wastewater. Ferric chloride dissolves in solution producing Fe^{3+} ions. Then, the Fe^{3+} ions react with the phosphates to form Fe phosphate (strengite), as shown in equation (1.6) (Stumm and Morgan, 1996).

$$Fe^{3+} + PO_4^{3-} + 2H_2O \leftrightarrow FePO_4 \bullet 2H_2O \qquad \text{Ksp at 25 °C} = 10^{-26} \qquad (1.6)$$

As shown in Figure 1.2, the best pH condition for P removal via Fe phosphate precipitation is around a value of 5. However, precipitation of Fe hydroxide ($Fe(OH)_3$) may lead to a competing consumption of Fe^{3+} ions, as shown in equation (1.7) (Stumm and Morgan, 1996), thus limiting the Fe phosphate precipitation.

$$Fe^{3+} + 3H_2O \leftrightarrow FeOH_3 + 3H^+ \qquad \text{Ksp at 25 °C} = 10^{-12.6} \qquad (1.7)$$

1.3.1.3 Ca phosphate precipitation

Free lime (CaO) and hydrated lime ($Ca(OH)_2$) are commonly used to remove phosphorus from wastewater via Ca phosphate precipitation. They dissociate in solution producing Ca^{2+} and OH^- ions (equations 1.8 and 1.9, respectively) (Roques, 1990).

$$CaO + H_2O \leftrightarrow Ca^{2+} + 2OH^- \qquad (1.8)$$

$$Ca(OH)_2 \leftrightarrow Ca^{2+} + 2OH^- \quad (1.9)$$

Then, Ca^{2+} ions react with the phosphates to form Ca phosphates. Several Ca phosphates may be formed depending on the pH values, Ca^{2+} and PO_4-P concentrations of the solutions: amorphous Ca phosphate (ACP), dicalcium phosphate (DCP), dicalcium phosphate dihydrate (DCPD), octacalcium phosphate (OCP), tricalcium phosphate (TCP), hydroxyapatite (HAP) and fluorapatite (FAP) (Table 1.1).

The molar ratios of Ca to P of these Ca-P compounds range from 1 (DCP and DCPD) to 1.67 (HAP and FAP). As shown by comparing the values of Ksp at 25 °C (Table 1.1), the most stable Ca phosphates are HAP and FAP. These Ca phosphates are formed from precipitation of PO_4^{3-} ion, which is the primary phosphate form for high pH solutions (>12) (Figure 1.1). Moreover, precipitation of HAP directly involves OH^- ions (basic solution), thus suggesting that basic aqueous conditions may be required to achieve an efficient P removal via HAP precipitation.

Precipitation of Ca phosphate is also affected by the temperature. Mc Dowell et al. (1977) have shown that solubility of HAP decreased with increasing temperature up 15 °C. This suggested that the efficiency of P removal via HAP precipitation increases with increasing temperature.

Table 1.1. Ca phosphates: molar ratios Ca to P and solubility product constants Ksp at 25 °C (Roques, 1990; Stumm and Morgan, 1996).

Ca phosphate: name, abbreviation	Formula	Molar ratio Ca/P	Ksp (at 25 °C)
Amorphous Ca phosphate (ACP)	variable	~ 1.5	variable
Dicalcium phosphate (DCP)	$CaHPO_4$	1	$10^{-6.6}$
Dicalcium phosphate dihydrate (DCPD)	$CaHPO_4 \cdot 2H_2O$	1	$10^{-6.6}$
Octacalcium phosphate (OCP)	$Ca_4H(PO_4)_3$	1.33	$10^{-46.9}$
Tricalcium phosphate (TCP)	$Ca_3(PO_4)_2$	1.5	10^{-26}
Hydroxyapatite (HAP)	$Ca_{10}(PO_4)_6OH_2$	1.67	10^{-114}
Fluorapatite (FAP)	$Ca_{10}(PO_4)_6F_2$	1.67	10^{-118}

Spontaneous Ca phosphate precipitation at neutral pH may occur, but only when the wastewater is naturally rich in Ca (>100 mg Ca/L) and the initial P concentration is higher than 50 mg P/L (de-Bashan and Bashan, 2004). However, these chemical conditions are very unusual in municipal wastewater and the addition of CaO and/or $Ca(OH)_2$ is needed to enable Ca phosphate precipitation.

Several studies have demonstrated that calcium carbonate ($CaCO_3$) precipitation leads to a competing consumption of Ca^{2+}, thus limiting Ca phosphate precipitation (Johansson and Gustafsson, 2000; Jang and Kang, 2002). The carbonate alkalinity of the wastewater and the dissolution of atmospheric CO_2 may represent the sources of carbonate that enable $CaCO_3$ precipitation. As shown in equation (1.10), the precipitation of one mole of $CaCO_3$ consumes one mole of Ca (Stumm and Morgan, 1996).

$$CaCO_3 \leftrightarrow Ca^{2+} + CO_3^{2-} \qquad \text{Ksp at 25 °C} = 10^{-8.3} \qquad (1.10)$$

The chemical equilibria between the carbonate forms in aqueous solution at 25 °C are shown in equation (1.11) (adapted from Stumm and Morgan, 1996).

$$H_2CO_3 \neg \xrightarrow{pK=6.4} H^+ + HCO_3^- \neg \xrightarrow{pK=10.3} 2H^+ + CO_3^{2-} \qquad (1.11)$$

As shown in equation (1.11), $CaCO_3$ precipitation involves CO_3^{2-} ions, which is the primary carbonate form at high pH (>10.3). Therefore, on the hand high pH values of the solutions favour HAP precipitation, on the other hand they favour also $CaCO_3$ precipitation, which may limit HAP precipitation by competing consumption of Ca^{2+} ions.

To conclude, it appears that the amount of CaO and/or $Ca(OH)_2$ to be added to the wastewater is a parameter of great importance for an efficient P removal via Ca phosphate precipitation. The production of Ca^{2+} and OH^- ions due to CaO and/or $Ca(OH)_2$ dissolution have to be great enough to:

i. Increase the pH of the solutions to the range of values that supports Ca phosphates precipitation;

ii. Neutralise the carbonate alkalinity of the wastewater via $CaCO_3$ precipitation;

iii. Enable Ca phosphate precipitation.

1.3.1.4 Ca phosphate crystallisation

After the deposition of amorphous precipitates, the Ca phosphates can reorganize their internal structure to produce crystals with regularly repeating internal structures and external plane faces. This process is referred to as "crystallisation process". The crystallisation of Ca phosphates is important because it insure a permanent P retention. In fact, it is well known that crystalline forms are more stable than amorphous forms (Valsami-Jones, 2001).

Several international studies have confirmed that the precipitation of Ca phosphates follows the so-called "Ostwald's rule" (rule of stages): first, precipitation of less stable Ca phosphates (ACP, DCP, DCPD); then, these precipitates recrystallize into the most stable HAP (Valsami-Jones, 2001; Lundager-Madsen, 2008).

Almost all the authors in the literature agree that HAP is the final product of the crystallization process. However, their opinions often diverge about the precursor phase to HAP crystallisation. In general, the authors' opinions can be summarized into two main sequences of precipitation-crystallization, as follows:

a. Crystallisation of DCPD, then transformation to OCP, and finally recrystallisation to HAP (Zoltec, 1974; Lundager-Madsen, 2008);

b. Precipitation of ACP, then transformation to OCP, and finally recrystallisation to HAP (Arends and Ten Cate, 1981; Meyer J.L., 1983).

Therefore, two different kinetics should be considered when studying Ca-P removal from wastewater (Valsami-Jones, 2001): first, the Ca-P precipitation kinetic, which can be easily studied in the laboratory by batch experiments; then, the crystal growth kinetic, which is more complex to determine, because it may be affected by a large number of parameters.

Among the organic and inorganic compounds in wastewater, several of them may inhibit / promote HAP crystallisation. They are referred as inhibitors / promoters of HAP crystallisation. The main inhibitors / promoters of HAP crystallisation are listed in Table 1.2.

Table 1.2. Main inhibitors and promoters of HAP crystallisation.

Inhibitors
Mg^{2+} (Kibalczyc et al., 1990)
CO_2 and carbonates (Valsami-Jones, 2001; House, 1999)
Humic, fulvic and tannic acids (Inskeep and Silvertooth, 1988)
Citrate (Var der Houwen and Valsami-Jones, 2001)
Promoters
F^- (Moreno and Varughese, 1981)
Pb^{2+} (Lundager-Madsen, 2008)
HAP seed-crystals (Zoltek 1974; Moreno and Varughese, 1981; Kim et al., 2006)

The adsorption of the inhibitor on the surface of the crystal is often the major cause of the crystal growth inhibition (Lundager-Madsen, 2008). The inhibition effect of Mg^{2+} on HAP crystallisation was studied by Kibalczyc et al. (1990). They found that some atoms of Mg^{2+} can be incorporated in the crystals of HAP, but this causes structural changes inhibiting further HAP crystallisation. However the Mg^{2+} appeared to not affect Ca-P precipitation and crystallisation of less stable Ca phosphate such as DCPD (House, 1999). CO_2 and carbonates are also strong inhibitors of HAP crystallisation (Valsami-Jones, 2001; House, 1999), because they block phosphate nucleation and induce $CaCO_3$ precipitation.

Several organic compounds have an inhibiting effect on precipitation of Ca phosphate and on its crystallisation. Inskeep and Silvertooth (1988) observed that humic, fulvic and tannic acids inhibit the HAP precipitation, because they "obstruct the active crystal growth site by the adsorbed ligands" (Valsami-Jones, 2001). On the other hand, microorganisms and biotic compounds commonly present in surface water as well as the metabolites released during the biological wastewater treatment (activated sludge) did not appear to disturb the process of HAP crystallisation (Lucas and Prevot, 1984).

Among the promoters, it was found that elements such as F^- and Pb^{2+} are efficient precursors for HAP crystallisation, most probably because they react with phosphates to form fluorapatite (FAP) and hydroxypyromorphite ($Pb_5(PO_4)_3OH$), which is isomorphous with HAP (Lundager Madsen, 2008).

Several authors found that the presence of seed crystals of HAP is a precursor of HAP crystallisation, and the faces of existing HAP crystals are efficient supports for the growth of new HAP crystals (Zoltek, 1974; Moreno and Varughese, 1981; Jang and Kang, 2002; Molle et al., 2005a; Kim et al., 2006). A certain super saturation level of the solution is needed to spontaneous HAP precipitation in the absence of seed crystals (Lundager-Madsen et al, 1995). Kim et al. (2006) performed a series of batch experiments to determine the solubility and super solubility curves of HAP depending on the pH values and the initial phosphate concentrations (Figure 1.3). The super solubility curve defines the limiting conditions for pH and phosphate concentrations enabling spontaneous HAP precipitation, whereas the solubility curve defines the residual phosphate concentrations remaining in the solutions after HAP crystallisation in the presence of seed crystals of HAP. Then, they defined a meta-stable zone ranging between the solubility and supersolubility curves, where HAP crystallisation is possible in the presence of pre-existent HAP crystals (seeds). The findings of previous studies appeared also to confirm the existence of a meta-stable zone for HAP crystallization depending on pH, calcium and phosphate concentrations (Ferguson et al., 1973; Zoltek, 1974; Moreno and Varughese, 1981; Jang and Kang, 2002). As shown in Figure 1.3, the meta-stable zone of Kim et al. (2006) tends to lower pH as the initial phosphate concentration increases, and vice versa.

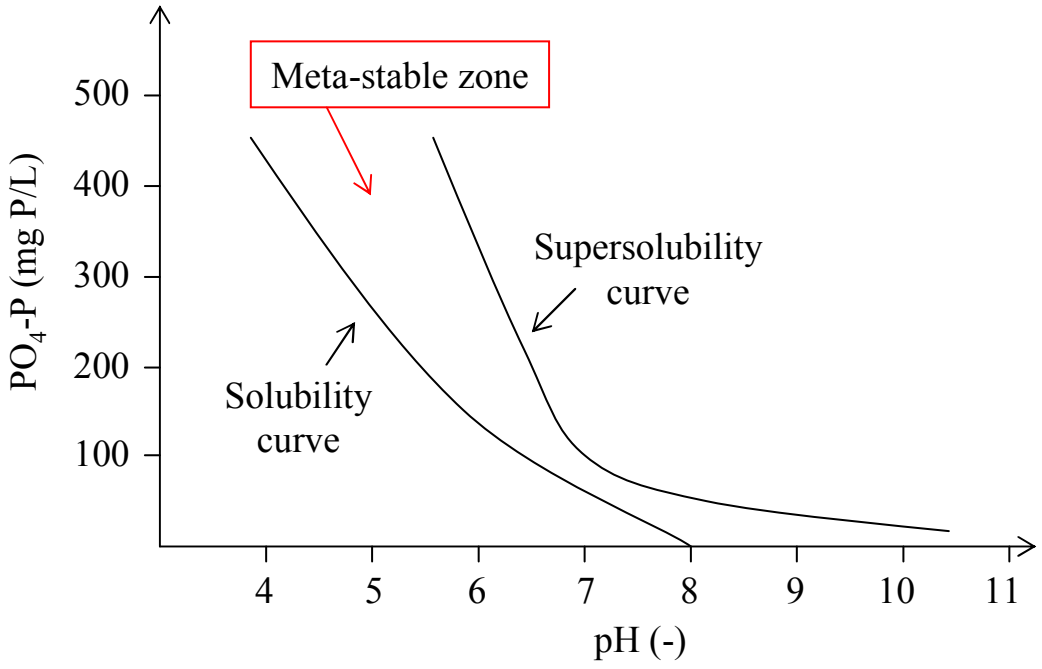

Figure 1.3. Metastable zone for HAP crystallisation according to pH and phosphate concentration (adapted from Kim et al., 2006).

1.3.2 Adsorption

Adsorption is a phenomenon in which atoms, ions or molecules (adsorbate) are removed from a gas or a liquid stream by adhering to the surface of a solid (adsorbent). The adsorption of different types of pollutants on the surface of an adsorbent may depend on a variety of mechanisms, which may be considered independently from each other (Valsaraj, 2000).

Adsorption usually depends on electrical, physical and/or chemical properties of the adsorbent and/or the adsorbate:

i. Electrical adsorption: electrical adsorption involves electrical forces between the adsorbate and the adsorbent. This happens, for example, in clay materials, when the partial substitution of cations can lead to a surface charge of the particles. Then, this surface charge may be balanced by compensating ions and/or molecules from water (Das et al., 2006);

ii. Physical adsorption: physical adsorption involves intermolecular attraction between one molecule and the neighbouring molecules (van der Waals forces). In physical adsorption, the individually of the adsorbate and of the adsorbent is preserved.

iii. Chemical adsorption: in contrast to electrical and physical adsorption, chemical adsorption involves the formation of chemical bonds between the adsorbent and the adsorbate. The chemical adsorption reversibility depends on the natures of the chemical bonds. Chemical adsorption happens, for example, when anion exchange materials are used to remove phosphate from water (Blaney et al., 2007). Equation (1.12) summarizes a typical reaction of phosphate adsorption by anion exchange (Bellier, 2005).

$$Me-(OH)_2 + HPO_4^{2-} \rightarrow Me-(HPO)_4 + 2OH^- \quad (1.12)$$

1.3.2.1 Capacity of adsorption

The equilibrium capacity of adsorption Qe (mg/g) defines the amount of adsorbate (mg) that may be removed by adsorption on the surface of the adsorbent (g) until equilibrium in residual pollution concentration is reached. The value of Qe depends on the nature of the adsorbent and of the adsorbate, on the initial concentration, and on the temperature. Qe represents a parameter of great importance to evaluate the ability of an adsorbent to remove a pollutant (Desjardins, 1997). The value of Qe for the adsorption of a pollutant on an adsorbent

is determined empirically, via batch experiments and using equation (1.13), where Cin is the initial pollutant concentration (mg/L), Ce is the pollutant concentration at equilibrium (mg/L), V is the volume of the batch solution (L) and M is the mass of adsorbent (g).

$$Q_e = \frac{(C_{in} - C_e)V}{M} \qquad (1.13)$$

1.3.2.2 Isotherms of adsorption

The affinity of an adsorbent for the adsorption of a pollutant is commonly studied by batch experiments of adsorption from solutions at different initial pollutant concentration. Several adsorption models are employed to describe the Q_e as a function of the residual pollutant concentrations at the equilibrium C_e (mg/L). These models are usually referred to as "isotherms of adsorption", since they refer to standard temperature conditions (Stumm and Morgan, 1996).

The isotherms of Langmuir (equation 1.14) and those of Freundlich (equation 1.15) are the most used to describe the phenomena of phosphate adsorption on various adsorbents.

$$Q_e = Q_{max} \frac{K_L C_e}{1 + K_L C_e} \qquad (1.14)$$

$$Q_e = K_F C_e^{1/n} \qquad (1.15)$$

The isotherm of Langmuir (1.14) is defined by the constants K_L (L/mg) and Q_{max} (mg/g). K_L describes the affinity of the material for phosphate adsorption, and is graphically represented by the initial slope of the curve. The constant Q_{max} represent the maximum phosphate adsorption capacity at equilibrium (mg P/L), and is graphically represented by an asymptote according to the increase in C_e. The model of Langmuir is based on the assumption of the monolayer adsorption: there are several adsorption sites on the adsorbent surface, and each site can adsorb only one molecule: therefore, a single layer of molecules can be adsorbed. The isotherm of Freundlich (1.15) is graphically defined by the constants K_F (L/g) and n. The Freundlich model is largely used to model phosphate adsorption because of its simplicity. However, it can not be used to determine the maximum phosphate adsorption capacity at equilibrium.

1.3.2.3 Kinetics of adsorption

The knowledge of the pollutant adsorption kinetic of a material is of a great importance when dimensioning filters for pollutant removal. The adsorption kinetic is usually determined by batch experiments, monitoring the pollutant concentrations over time until equilibrium in pollutant adsorption is reached.

In most of the study in the literature, the experimental capacities of pollutant adsorption were plotted according to the pseudo-first order kinetic equation of Lagergren (1898) (equation 1.16), and the pseudo-second order kinetic equation as modified by Ho and McKay (1998) (equation 1.17). The parameters Q_e and Q_t represent the capacities of pollutant adsorption at equilibrium and at time t (mg/g), t is the time (d), k_1 is the rate constant of pseudo-first order adsorption (1/d), and k_2 is the rate constant of pseudo-second order adsorption (g/mg*d).

$$\ln(Q_e - Q_t) = \ln Q_e - k_1 t \quad (1.16)$$

$$\frac{1}{(Q_e - Q_t)} = \frac{1}{Q_e} - k_2 t \quad (1.17)$$

The pseudo-first order kinetic is employed to describe pseudo-first order reactions, whereas the pseudo-second order kinetic is employed to describe pseudo-second order reactions (Ho and McKay, 1998). If pseudo-first order kinetic is applicable, this suggests a reaction whose rate of reaction is determined by the concentration of one chemical species. Whereas, if pseudo-second order kinetic is applicable, this suggests a reaction whose rate of reaction is determined by the concentration of two chemical species.

1.3.2.4 Adsorption of phosphate

In most of the studies presented in the literature, the major mechanisms of phosphate adsorption were the adsorption on the surface of metal hydroxides (Das et al., 2006) and the phosphate-anion exchange (Blaney et al., 2007).

Das et al. (2006) found that phosphate adsorption on metal hydroxides is a spontaneous and exothermic process in nature, and it follows a first order kinetic. They studied also the effect of competing anions on phosphate adsorption, and they found that divalent anions (SO_4^{2-}, SeO_3^{2-}) have higher interfering effect compared to monovalent anions (NO_3^-, Cl^-), most probably because divalent anions competed with divalent phosphates (HPO_4^{2-}) for the adsorption sites on metal hydroxides. Several international studies have demonstrated that the

Al and Fe hydroxides formed during the chemical precipitation with Al and Fe salts are efficient supports for phosphate adsorption (Boisvert et al., 1997; Fytianos et al., 1998).

Phosphate anion exchange occurs when adsorbent materials presenting anion exchange groups are put in contact with phosphate in aqueous solutions (Blaney et al., 2007). However, anions such as chloride, nitrate and sulphate, which commonly occur in wastewater may compete with phosphate in the process of anion exchange, thus limiting the efficiency of P removal.

1.3.3 Biological P uptake

Phosphorus is an essential element for the growth of many microorganisms. It is stored within the cells in the nucleic acids and polyphosphates (DNA, RNA, ATP). The polyphosphates are the primary actors in the energy metabolism: in fact, they store chemical energy within the cells (Roques, 1990). However, the needs in phosphorus of the heterotrophic biomass commonly used for biological treatment are markedly lower than the amount of phosphorus that is available in wastewater. Consequently, the conventional biological treatment plants usually show poor performances of phosphorus removal. Equation (1.18) and (1.19) describe the chemical formula of heterotrophic biomass (Roques, 1990).

$$C_{118}H_{170}O_{51}N_{17}P \quad (1.18)$$

$$C_{106}H_{180}O_{45}N_{16}P \quad (1.19)$$

As shown by equations (1.18) and (1.19), the molar ratio of C to P is around 100, thus indicating that the metabolic need of P is significantly lower than the need of C. Over the last four decades, technologies based on the ability of bacteria to accumulate polyphosphates over the metabolic needs have been developed (Levin and Sharipo, 1965; Harold, 1966).

Fuhs and Chen (1975) studied the ability of acinetobacter to accumulate polyphosphate over the metabolic needs, thus alternating anaerobic and aerobic phases:

i. Anaerobic condition: the microorganisms use the energy deriving from the hydrolysis of polyphosphate to accumulate C in the form of poly-β-hydroxybutyric acid (PHB);

ii. Aerobic condition: the microorganisms metabolize the PHB and adsorb phosphates from the water, thus accumulating polyphosphates over the metabolic needs.

However, the biological removal of phosphorus is a complex and unstable technique. In fact, it requires the continuous control of the alternation of anaerobic and aerobic phases, and this results in high operating costs. Moreover, polyphosphates accumulated within microorganism cells are not stable, and an unexpected change from aerobic to anaerobic conditions may lead to a sudden release of phosphate that may be difficult to control. For this reason, in the practice the biological treatments are often combined with chemical treatments.

1.4 P removal from wastewaters via filtration through reactive materials

Conventional techniques based on processes of chemical precipitation and biological removal of P present several limitations, especially when employed to remove P in small (< 10000 p.e.) and extensive wastewater treatment plants such as constructed wetland systems. In fact, the technique of chemical precipitation with the addition of Al, Fe, and Ca usually requires the strict control of the chemical parameters, such as pH and alkalinity, which enable P precipitation. Moreover, an additional cost is given by removal, disposal and treatment of the precipitate-sludge. The biological removal process requires the employment of qualified workers and high energy costs due to the strict control of the anaerobic-aerobic phases.

A promising technique to upgrade P removal in small and extensive wastewater treatment plants is filtration through materials with high affinities for P binding.

1.4.1 Potential substrates for P removal

Several international studies have demonstrated that filtration through materials with high affinities for P binding is an appropriate technology to improve P removal in small and extensive wastewater treatment plants. Since common filter substrates (such as sand and gravel) have limited P removal capacities (Arias et al., 2001), research on alternative materials has become a priority. In the last two decades, a large number of potential substrates has been tested. These substrates can be classified according to their source of origin into three main categories (Johansson-Westholm, 2006): natural materials, industrial by-products and man-made products.

1.4.1.1 Natural materials

A large number of natural materials have been tested in the literature, including mineral and rocks (bauxite, apatite, limestone, dolomite, zeolite), soils (opoka, peat) and sediments

(shallsand, maerl). Most of these materials have a high content of Ca, Al, and/or Fe, which are elements with a strong affinity for P binding (Johansson-Westholm, 2006).

1.4.1.2 Industrial by-products

Various industrial by-products, including iron and steel slags, ashes of thermal incineration plants (oil shale ashes, fly ashes), and waste of the alumina industry (red mud) have been tested for P removal with the aim of valorising by-products of the industry in wastewater treatments.

Iron and steel slags derive from the steel-making industry. Three main types of iron and steel slag are produced in Europe: blast furnace slag (BF-slag), which originates from the iron production in a blast furnace; basic oxygen furnace slag (BOF-slag), which originates from the further refining of iron in a basic oxygen furnace; electric arc furnace slag (EAF-slag), which is derived from melting recycled scrap in an electric arc furnace (Proctor et al., 2000). According to EUROSLAG statistics, more than 45 million tons of iron and steel slag was produced in Europe in 2006: about 80% was used in several fields of application (cement production, road construction) and 10% was recycled internally. However, about 10% was still disposed of in specialised landfill sites. This suggests an interesting potential market for wastewater treatment. Steel slag is primarily made of iron (Fe) and calcium oxide (CaO), as a result of the use of fluxing agents (mainly lime) during the steelmaking process (Motz and Geiseler, 2001).

Oil shale ashes derived from the thermal incineration of oil shale in Estonia. Estonian oil shale is primarily composed of calcareous minerals, which are decomposed during thermal incineration to produce aches and sediments rich in free lime (CaO) and anhydrite ($CaSO_4$) (Vohla et al., 2011). Fly ashes derived from coal combustion in thermal plants. Fly ashes consist mainly of silica (SiO_2), alumina (Al_2O_3) and iron oxides.

Red mud is the by-product of the process of alumina production from bauxite. It is produced in large amount from the alumina industry: “for every tonne of alumina produced, approximately 1 or 2 tonnes of red mud (dry weight) are generated” (Huang et al., 2008). The main components of red mud are Fe and Al oxides.

1.4.1.3 Man-made products

Several adsorbent materials including lightweight expanded clay aggregates (such as LECA, filtralite P®, polonite®), and anion exchange fibres have been specifically produced for P

removal from wastewater. Most of these man-made products are based on the synthesis of natural materials such as clay minerals with high content in Ca, Mg, and metal hydroxides (Chitrakar et al., 2006; Adam et al., 2007; Li et al., 2009).

Anion exchange fibres are usually produced by the synthesis of polystyrene matrices with amino groups to produce polymers with hydrophilic characteristics and which prefer phosphates in the presence of competing ions such as chloride and nitrate (Blaney et al., 2007; Awual et al., 2011). These fibres have a strong affinity to bind with the monovalent and divalent forms of phosphate ($H_2PO_4^-$, HPO_4^{2-}), which are the primary forms of phosphate in the range of pH of the wastewater (Kadlec and Wallace, 2009).

After P saturation, most of these man-made adsorbents may be regenerated by P desorption with the use of aqueous basic solutions of NaOH. In fact, the use of basic solutions promote desorption of P from the surface of metal hydroxides and provide a source of high quality P available for the fertilizer industry. After regeneration, these materials may be reused for a new cycle of P treatment (Awual et al., 2011).

1.4.2 Batch experiments

Batch experiments are usually performed to evaluate the phosphate removal capacities (PRCs) of candidate materials. In fact, PRC is an important parameter when comparing and selecting candidate materials to be used as filter media (Drizo et al., 2002).

1.4.2.1 P removal capacities

Main results from selected batch studies that tested PRCs of candidate substrates are reported in Table 1.3 (natural materials), Table 1.4 (industrial by-products) and Table 1.5 (man-made products). The maximum PRCs varied by several orders of magnitude, from less than 0.5 to up than 100 mg P/g (Tables 1.3, 1.4 and 1.5). Among the materials tested, anion exchange fibres, BF and BOF slag presented the highest PRCs (> 44 g P/g).

Table 1.3. Natural materials: maximum experimental PRCs observed in selected batch experiments (adapted from Vohla et al., 2011).

Authors	Material tested	Ca content (%)	Particle size (mm)	Ratio slag to solution (g/mL)	Initial PO_4-P (mg P/L)	Agitation mode	Contact time (h)	PO_4-P removed (%)	Maximum PRC (mg P/g)
Sakadevan and Bavor, 1998	Zeolite	N.A.	N.A.	0.1	0-10000	100 rpm	48	N.A.	2.15 [a]
Drizo et al., 1999	Zeolite	N.A.	N.A.	0.04	40	60 rpm	24	25	0.25
Drizo et al., 1999	Bauxite	N.A.	N.A.	0.04	40	60 rpm	24	60	0.60
Drizo et al., 1999	Limestone	N.A.	N.A.	0.04	40	60 rpm	24	55	0.55
Gray et al., 2000	Maerl	80 ($CaCO_3$)	N.A.	0.04	5000	200 rpm	48	32	39.5
Johansson and Gustafsson, 2000	Opoka	50 ($CaCO_3$)	0-2	0.02	10	70 rpm	20	20	0.1
Pant et al., 2001	Dolomite	N.A.	N.A.	0.02	1-100	N.A.	24	N.A.	0.3[a]
Molle et al., 2005a	Apatite	37.3	d_{60}[b] < 1 mm	0.04	0-500	25 rpm	24	N.A.	4.76 [a]
Bellier et al., 2006	Apatite	7	2.5-10	0.05	5-150	N.A.	24	N.A.	0.41[a]
Adam et al., 2007	Shell sand	32.7	3-7	0.033	480	N.A.	24	67	9.6

[a] Calculated using the Langmuir equation.

[b] Diameter of the sieve which passes 60% (weight) of the particles.

Table 1.4. Industrial by-product: maximum experimental PRCs observed in selected batch experiments (adapted from Vohla et al., 2011).

Authors	Material tested	Ca content (%)	Particle size (mm)	Ratio slag to solution (g/mL)	Initial PO_4-P (mg P/L)	Agitation mode	Contact time (h)	PO_4-P removed (%)	Maximum PRC (mg P/g)
Drizo al., 1999	Fly ash	N.A.	N.A.	0.04	40	60 rpm	24	70	0.70
Xu et al., 2006	Fly ash	8.6 (CaO)	N.A.	0.05	1000	200 rpm	24	42	8.5
Drizo et al., 1999	Oil shale ash	N.A.	N.A.	0.04	40	60 rpm	24	42	0.42
Kaasik et al., 2008	Oil shale ash	29.2 (CaO)	< 0.01	0.01	98	75 rpm	48	67	6.5
Huang et al., 2008	Red mud	N.A.	N.A.	0.008	1	70 rpm	6	20	0.29
Sakadevan and Bavor, 1998	BF slag	38-43 (CaO)	N.A.	0.1	0-10000	100 rpm	48	N.A.	44.2 [a]
Johansson and Gustafsson, 2000	BF slag	33.7 (CaO)	0.25-4	0.02	20	70 rpm	20	65	0.65
Drizo et al., 2002	EAF slag	21.7	2.5-10	0.05	320	175 rpm	24	60	3.9
Xiong et al., 2008	EAF slag	45.6 (CaO)	< 2	0.04	45	200 rpm	2	71	0.8
Jha et al., 2008	BOF slag	38.5 (CaO)	< 0.02	0.002	320	N.A.	24	49	78.9
Xue et al., 2008	BOF slag	45.4 (CaO)	< 0.6	0.01	500	N.A.	3	86	43.1
Bowden et al., 2009	BOF slag	42-44 (CaO)	< 6	N.A.	500	150 rpm	24	18	89.9

[a] Calculated using the Langmuir equation.

Table 1.5. Man-made product: maximum experimental PRCs observed in selected batch experiments (adapted from Vohla et al., 2011).

Authors	Material tested	Ca content (%)	Particle size (mm)	Ratio slag to solution (g/mL)	Initial PO_4-P (mg P/L)	Agitation mode	Contact time (h)	PO_4-P removed (%)	Maximum PRC (mg P/g)
Drizo et al., 1999	LECA	N.A.	N.A.	0.04	40	60 rpm	24	55	0.55
Vohla et al., 2005	LECA	N.A.	4-40	0.04	5-1000	N.A.	48	N.A.	0.1-0.2
Adam et al., 2007	Filtralite P®	3	0.5-4	0.033	480	N.A.	24	17	2.5
Awual et al., 2011	Anion exchange fibres	N.A.	N.A.	0.001	300	85 rpm	24	54 (pH 5)	161(pH 5)
								46 (pH 7)	139 (pH 7)
								29 (pH 8.5)	87 (pH 8.5)

1.4.2.2 Limitations of batch experiments

As already observed by Cucarella and Renman (2009), there is not a standard procedure for batch experiments, and this leads to difficulties in comparing the results of the different studies. As shown in Tables 1.3, 1.4 and 1.5, the main experimental parameters affecting the results of batch experiments are the size of the material, the ratio of material to solution, contact time, agitation mode, and initial phosphate (PO_4-P) concentrations. Overall, PRCs increased with increasing the initial PO_4-P concentration, and decreasing the particle size and/or the ratio of slag to solution, most probably because the contact surface of material to solution was enlarged.

In addition, batch experiments are usually performed by using synthetic P solutions in laboratory conditions and steady state. For these reasons, batch experiments are not able to provide complete information to evaluate P removal efficiency of the filter media under real wastewater and continuous process conditions.

1.4.3 Column experiments

The term "column experiments" usually refers to laboratory experiments of filtration that are performed by using small scale filters (columns) fed with synthetic P solutions. These experiments are usually performed to evaluate the hydraulic efficiency, P removal kinetic, and P removal efficiency of candidate substrates to be used as filter media.

1.4.3.1 Hydraulic efficiency

The hydraulic efficiency of a filter depends on the filter design, on the flow rate, and on the physical properties of the filter material (Alcocer et al., 2012). The hydraulic efficiency is studied empirically, by tracer test. A tracer is an ion or molecule that is introduced into a system and can be followed through the course of a process, providing information about the dynamics of the system. The tracer must be inert during the passage through the filter, because, for a good outcome of the test, the recovery of the tracer at the outlet of the filter is needed. Fluorescein, rhodamine and salts of lithium and bromine are commonly used as tracers in hydraulic studies.

Tracer tests are performed by the injection of a well-known amount of the tracer to the inlet of the filter. Then, the outlet tracer concentrations are monitored over time until the total amount of the tracer injected is recovered at the outlet of the filter, and several statistical parameters are determined as follows:

i. The time needed to recover 10%, 50% and 90% of the mass of the tracer injected (T_{10}, T_{50} and T_{90}, respectively);

ii. The peak time T_P, the time corresponding to the peak in outlet concentration;

iii. The average time T_{AVE}, the average time that is needed for a generic mass of tracer to exit from the filter: it is calculated by equation (1.20), where Ci (mg/L) is the tracer concentration at the time ti (h) and Δti (h) is the interval between two consecutive measures (adapted from Metcalf and Eddy, 2003).

$$T_{AVE} = \frac{\sum ti \times Ci \times \Delta ti}{\sum Ci \times \Delta ti} \quad (1.20)$$

These statistical times (T_{10}, T_{50}, T_{90}, T_P, and T_{AVE}) are compared with the theoretical void hydraulic retention time (HRTv), which is determined by equation (1.21), dividing the void volume of the filter Vv (m^3) to the average flow Q (m^3/h).

$$HRTv = \frac{V_V}{Q} \quad (1.21)$$

In ideal plug flow conditions, the time required for the tracer to exit the filter corresponds exactly to the HRTv, because it is well known that in plug flow reactors the velocity of the fluid is assumed to be constant across any cross-section of the filters. Therefore, in ideal plug flow conditions equation (1.22) is true.

$$T_{10} = T_{50} = T_{90} = T_P = T_{AVE} = HRTv \quad (1.22)$$

Instead, in real conditions, a fraction of the tracer will exit the filter before the HRTv, while another fraction will exit with a delay, and equation 1.22 is not true. This is due to the phenomena of short-circuiting paths, dead volume, and diffusion / dispersion of the tracer in the filter (Alcocer et al., 2012; Chazarenc et al., 2003).

The short-circuiting effect depends on preferential paths in which the fluid flows at a velocity that is greater than the theoretical velocity, reaching the outlet in advance with respect to the theoretical HRTv. Instead, the dead volume indicates a fraction of fluid that stagnates in the reactor and will exit the filter with a delay with respect to the theoretical HRTv (Chazarenc, 2003).

High diffusion and dispersion usually indicate a higher level of mixing of the tracer inside the filter. This usually results in larger differences between T_{10}, T_{50}, T_{90}, T_P, T_{AVE} and HRTv. As well known from the theory of the mass transfer, diffusion depends primarily on chemical properties, and the diffusive flux increases with increasing the difference of concentration. Instead, dispersion depends primarily on the flow regime, and dispersion flow increases with increasing the difference of velocities (Metcalf and Eddy, 2003).

The difference between the values of T_{10}, T_{50}, T_{90}, T_P, T_{AVE} and HRTv, gives important information about the hydraulic behaviour of the filter: the smaller the difference, the more the behaviour of the filter is close to an ideal plug flow reactor.

Several empirical flow models have been proposed in the literature to study the internal hydrodynamics of filters (Ogata and Banks, 1961; Wolf and Resnick, 1963; Rebhun and Argaman, 1965). Most of these models were developed to reproduce the experimental retention time distribution of the flow in filter systems, and they are based on the theories of the continuous stirred tank reactor (CSTR) and of the plug flow reactor (PFR) (Werner and Kadlec, 2000).

Wolf and Resnick (1963) and Rebhun and Argaman (1965) proposed equation (1.23) to estimate the fractions of plug flow (PF) and dead volume (DV) in real hydraulic systems. In equation (1.23), F(t) is the cumulative fraction of the tracer that exited the filter at the time t (-), t is the time from the tracer injection (h) and T is the theoretical HRTv (h). The equation (1.24) of Wolf and Resnick (1963) is valid for instantaneous puff injection of the tracer.

$$F(t) = 1 - \exp\left[\left(\frac{t/T}{(1-PF)(1-DV)} - \frac{PF}{1-PF}\right)\right] \qquad (1.23)$$

A recent study (Alcocer et al., 2012) employed equation (1.23) to investigate the effect of different filter design, influent loading rate and size of porous media on internal hydrodynamics of sub-surface horizontal flow filters.

They observed that, in general, plug flow increased with increasing the ratio length to width of the filters (from 1:1 to 1.5:1), most probably because the longer length allowed the dissipation of the initial turbulence of the system. Instead, plug flow decreased with increasing the loading rates, most probably because the higher the flow, the higher the linear velocity of the fluid, thus favouring dispersion. It was also observed that, in general, larger

porous media yielded higher plug flow. This most probably because the larger was the pore space, the lower was the linear velocity of the fluid, thus reducing dispersion.

Alcocer et al. (2012) have also shown that dead volume decreases with increasing the loading rate and decreasing the size of the filter media, thus indicating that the volume of the filters was more effectively exploited. Most probably, the use of smaller pore size and higher loading rate have favoured a more uniform distribution of the fluid flow across any cross-section of the filters, as confirmed by smaller short-circuiting effects and retention times closer to theoretical retention times.

To conclude, the results of tracer tests in small scale filters (columns) give important information for the correct design of field scale filters, this considering that the type of behaviour that is desirable to optimize treatment in sub-surface flow filters is characterized by high plug flow, low dispersion, low dead volume and low short-circuiting effects (Kadlec and Knight, 2009),

1.4.3.2 P removal kinetic

The kinetics of P removal in column experiments are usually studied empirically, by the analyses of the P concentrations of water samples taken from piezometers placed at different distances from the inlet of the filters. Then, the experimental data are modelled by using kinetic equations to determine the rate constants of P removal.

In 1988, USEPA recommended the use of the first order kinetic equation (1.24) to model pollutant removal in sub-surface horizontal flow filters. In equation (1.24), C_0 is the inlet P concentration (mg P/L), C is the P concentration at the distance x from the inlet (mg P/L), k_V is the volumetric rate constant of the first order (1/h), HRTv is the theoretical retention time (h), x is the distance from the inlet (m) and L is the length of the filter (m).

$$\frac{C}{C_0} = \exp\left(-k_V \times HRTv \times \frac{x}{L}\right) \qquad (1.24)$$

Kadlec and Knight (1996) modified the first kinetic plug flow model with the addition of the parameter C* (equation 1.25), which represents the background P concentration of the water (mg P/L) and defines the minimum P level that can be achieved in the effluent. This made the first kinetic plug flow model more realistic, because it sets a limit in P removal that corresponds to the background concentration of the water.

$$\frac{C - C^*}{C_0 - C^*} = \exp\left(-k_V \times HRTv \times \frac{x}{L}\right) \quad (1.25)$$

The volumetric rate constant (k_V) depends on the temperature, as shown in the equation (1.26), where k_V20 is the volumetric constant rate at 20 °C (1/h), θ is the empiric constant (-) and T is the temperature (°C). The value of θ is usually determined empirically, performing experiments at different temperature conditions.

$$k_V T = k_V 20 \times \theta^{(T-20)} \quad (1.26)$$

The k-C* model (equation 1.25) is based on the assumptions of plug flow and that k_V and C* are constants, except for possible effects due to temperature (Kadlec, 2000). However, the kinetic of P removal of a material may change over time depending on changes in the removal mechanisms during the life of the filters. For example, Molle et al. (2011) observed a first phase of rapid decrease of k_V when using apatite materials to remove P via adsorption mechanisms; then, when the adsorption sites were saturated, a new phase of P precipitation started, thus changing the rate of k_V decrease. For this reason, presenting the k_V as a function of the P saturation level of the material appeared to be more appropriate.

The value of the volumetric rate constant (k_V) may be used in equation (1.27) and/or (1.28) to determine the volume of the filter to achieve an expected outlet P concentration at different HRTv. The equations (1.27) and (1.28) derived from the first kinetic equations (1.24) and (1.25), respectively: V is the void volume of the filter (m^3), Q is the wastewater flow (m^3/d), k_V is the volumetric rate constant of the first order (1/h), C_0 is the inlet P concentration (mg P/L), C_E is the expected outlet P concentration (mg P/L) and C* is the background P concentration (mg P/L).

$$V = \frac{Q}{k_V} \ln\left(\frac{C_0}{C_E}\right) \quad (1.27)$$

$$V = \frac{Q}{k_V} \ln\left(\frac{C_0 - C^*}{C_E - C^*}\right) \quad (1.28)$$

1.4.3.3 P removal efficiencies

Main results from selected column studies that tested P removal performances of candidate substrates are presented in Table 1.6 (natural materials), Table 1.7 (industrial by-products) and Table 1.8 (man-made products).

Table 1.6. Natural materials: main operating parameters and P removal performances of selected column studies (adapted from Vohla et al., 2011).

Authors	Material	Ca content (%)	Size (mm)	Inlet TP (mg/L)	HRTv (h)	Duration (week)	TP removal (%)	TP removed (mg P/g)
Molle et al., 2005a	Apatite	37.3	d_{60} < 1 mm	20	5.6	78	N.A.	13.9
Bellier et al., 2006	Apatite	7	2.5-10	30	1.5	6	50	0.4
Adam et al., 2007	Shell sand	32.7	3-7	10	1.5	43	92	0.5

Table 1.7. Industrial by-products: main operating parameters and P removal performances of selected column studies (adapted from Vohla et al., 2011).

Authors	Material	Ca content (%)	Size (mm)	Inlet TP (mg/L)	HRTv (h)	Duration (week)	TP removal (%)	TP removed (mg P/g)
Gustafsson et al., 2008	BF-slag	21.6	0-4	4.5 (mean)	7	68	86	1.0-3.1
Drizo et al., 2002	EAF-slag	21.7	2.5-10	350-400	8.3	40	N.A.	1.35
Drizo et al., 2006	EAF-slag	30.4 (CaO)	2.5-10	20-400	24	26	>99	2.2
Chazarenc et al., 2007	EAF-slag	27.7 (CaO)	2-5	6-12	2-4	52	80	0.3
Bowden et al., 2009	BOF-slag	42-44 (CaO)	<20	100-300	8	44	24	8.4
Shilton et al., 2005	Melter slag	N.A.	N.A.	10	12	30	27	N.A.
Liira et al., 2009	Oil shale ash	29.2 (CaO)	2-5	8-15	6-8-12	22	>40	N.A.

Table 1.8. Man-made products: main operating parameters and P removal performances of selected column studies (adapted from Vohla et al., 2011).

Authors	Material	Ca content (%)	Size (mm)	Inlet TP (mg/L)	HRTv (h)	Duration (week)	TP removal (%)	TP removed (mg P/g)
Gustafsson et al., 2008	Polonite	24.5	2-5.6	4.5	8	68	96.7	1.9-7.4
Gustafsson et al., 2008	Filtra P	31.2	2-13	4.5	6	35	98.2	2.5-19.4
Adam et al., 2007	Filtralite P	3	0.5-4	10	3.5	43	54	0.5

As shown in Tables 1.6-8, apatite (Molle et al., 2005a) and EAF-slag (Drizo et al., 2006) presented the highest TP retention level (13.9 mg P/g) and TP removal efficiency (>99%), respectively. However, the TP removal performances appeared to vary as a function of the experimental parameters that were often arbitrarily established, thus leading to difficulties in comparing the results of the different studies. The main parameters influencing TP removal efficiencies were the granular size of the materials, the void hydraulic retention time (HRTv) and the inlet TP concentrations.

Overall, the TP removal efficiencies increased when the particle size decreased and/or the HRTv increased, most probably because the contact time for P adsorption, precipitation and crystallisation was enhanced. However, Shilton et al. (2005) found that this relationship between the increase in HRTv and the increase in TP removal performances is not linear, and increasing the HRTv up to values of 12 h did not lead to significant improvement in TP removal efficiencies. In addition, in CaO-rich materials, long HRTv may promote CaO dissolution, hydration (equation 1.29) and carbonation (equation 1.30), thus causing high pH, volume expansion of grains and filter clogging (Wang et al., 2010; Gunning et al., 2010).

$$CaO + H_2O \leftrightarrow Ca(OH)_2 \quad (1.29)$$

$$Ca(OH)_2 + H_2CO_3 \leftrightarrow CaCO_3 + 2H_2O \quad (1.30)$$

In most of the studies presented in Tables 1.6-8, TP saturation levels were not reached, and TP retention values increased with increasing initial PO_4-P concentration and duration of the experiments, thus suggesting that most of the material tested had a very high potential for P removal.

1.4.3.4 Limitations of column experiments

Column experiments of P removal are usually performed with synthetic P solutions, which do not contain all components occurring in real wastewater that may affect P removal (e.g., humic acids, organic colloids, competing anions) (Valsami-Jones, 2001; Pratt et al., 2007). Indeed, remarkable differences in filter performance were observed when treating real wastewater (Shilton et al., 2005; Chazarenc et al., 2007). In addition, column experiments are usually performed in the laboratory under controlled temperature conditions. For these reasons, column experiments are not able to provide complete information to evaluate the performances of filters under real operating conditions.

1.4.4 P removal mechanisms of potential substrates

As shown in Tables 1.3-8, P removal efficiencies seemed to increase with increasing CaO content of the materials, as already observed by Vohla et al (2011). This suggests that the main mechanism of P removal was related to CaO dissolution followed by Ca phosphate precipitation.

Various chemical techniques, including X-ray based investigations and wet chemical extractions, are commonly used to investigate the chemical and mineralogical surface of the materials before and after the experiments of P removal. These investigations give fundamental information to elucidate the key mechanisms of P removal achieved by the use of potential filter substrates.

1.4.4.1 X-ray based investigations

Scanning electron microscopy (SEM), energy dispersive X-ray fluorescence (XRF), and X-ray diffraction analyses (XRD) are usually carried out to examine the chemical and mineralogical surface of a solid sample. SEM, XRF and XRD use a focused beam of high-energy electrons to generate a variety of signals deriving from electron-sample interactions, including secondary electrons, characteristic X-rays and diffracted backscattered electrons. Secondary electrons provide high magnification, high resolution images (SEM observation), characteristic X-rays provide elemental composition, and diffracted backscattered electrons provide information about the crystalline structure and orientation of minerals on the surface of the sample. Table 1.9 summarizes the results of SEM, XRF and XRD analyses from selected studies that investigated P removal mechanisms of potential filter substrates. In most of these studies, the surface of the filter substrates after P removal was covered by a secondary layer of precipitates including amorphous and crystalline Ca phosphates (indicating Ca phosphate precipitation and crystallisation) and crystals of calcite (indicating Ca carbonate precipitation followed by crystallisation). The formation of crystals of calcite on the surface of the filter media may favour further P retention, as calcite has been recognized to provide sorption sites for P (Freeman and Rowell, 1981). Moreover, several studies showed that co-precipitation of calcite with P is possible, with calcite incorporating P into the calcite crystals (House, 1999; Plant and House, 2002). These mechanisms of P sorption on calcite and P co-precipitation with calcite may be significant for the long-time successful operation of the filters, in terms of system longevity (Bowden et al., 2009).

Table 1.9. Results of SEM, XRF and XRD analyses from selected studies that investigated the surface of filter media after P saturation.

Study	Material	Scale and duration of experiment	SEM observation and XRF analyses	XRD analyses
Molle et al., 2005a	Apatite	Column (10 months)	Precipitates mainly composed of Ca and P	N.A.
Liira et al., 2009	Oil shale ash	Column (5 months)	Acicular (>10µm) and spherical aggregates of secondary precipitates	$CaCO_3$ crystals and amorphous Ca phosphates
Kim et al., 2006	BOF-slag	Mixed reactor (1 month)	Finely distributed crystalline layer	$CaCO_3$ and HAP crystals
Bowden et al., 2009	BOF-slag	Column (12 months)	Spherical crystals (<5µm)	OCP and HAP crystals
Drizo et al., 2006	EAF-slag	Column (11 months)	N.A.	HAP crystals
Claveau-Mallet et al., 2012	EAF-slag	Column (16 months)	Fibrous and acicular crystals (5-40 nm)	HAP crystals (>95%)

1.4.4.2 P chemical extractions

Several studies in the literature used a five step sequential extraction procedure (adapted from Tiessen and Moir, 1993) to quantify 5 main inorganic fractions of P bound to the surface of saturated filter substrates:

i. The exchangeable P fraction, which is extracted with a highly concentrated anion solution. This fraction is defined as the total amount of P that can be mobilized via anion exchange;

ii. The bicarbonate extractable P fraction, which is extracted with a highly concentrated bicarbonate solution (0.5 M $NaHCO_3$). This fraction represents a further P fraction that is likely exchangeable in carbonate solutions;

iii. The hydroxide extractable P fraction, which is extracted with a basic solution (0.1 NaOH). This fraction is defined as Fe and Al associated P;

iv. The diluted HCl extractable P fraction, which is extracted with an acid solution (1 M HCl). This fraction is defined as Ca associated P, since Fe and Al associated P were previously extracted by basic solution, and remaining Fe and Al associated P are usually insoluble in acid;

v. The residual P fraction is extracted with a highly concentrated acid solution (~12 M HCl). This fraction is defined as P bound in very stable residual pools, and may include the most stable form of Ca-P as HAP crystals.

Drizo et al. (2002) adopted this sequential extraction procedure to investigate samples of EAF-slag after 278 days of P solution (350-400 mg P/L) application in column experiments. The high fractions of Fe bound P (46.5%), Ca bound P (12.1%) and Ca bound P in very stable residual pools (26.5%) suggested that the main mechanisms of P removal in EAF-slag were P adsorption on Fe hydroxides and Ca phosphate precipitation followed by crystallisation.

Korkusuz et al. (2007) employed the same technique to determine the fraction of P bound to the surface of BF-slag after 12 months of field experiments of P filtration in a constructed wetland system (average inlet TP 6.6 mg P/L). The high fractions of loosely bound P (49%) and Ca bound P (43%) suggested that the main mechanisms of P removal in BF-slag was Ca phosphate precipitation.

1.5 Reactive filters to upgrade phosphorus removal in constructed wetlands

1.5.1 Constructed wetlands to treat wastewater

The constructed treatment wetlands (CWs) are artificial wetland areas specifically designed for wastewater treatment. In these plants, pollutant treatment can be obtained by the biological activity of plants, animals, and microorganisms, which constitute the ecosystem of the wetland, and the natural energy of the sun. They represent also a clear example of ecological WWTPs and one of the least expensive WWTPs to operate and maintain (Kadlec and Wallace, 2009).

The CWs can be classified into three main categories, according to the design and the hydrologic flow (Kadlec and Wallace, 2009):

i. Free water surface constructed wetlands (FWSCWs) are characterized by free water surface areas, and they are similar in appearance to natural wetlands. They can be planted with floating, submerged and/or emergent species;

ii. Horizontal subsurface flow constructed wetlands (HSFCWs): they consist usually of a gravel or sand bed planted with wetland vegetation. The wastewater flows below the surface of the bed, and its flow is horizontal from the inlet to the outlet of the bed (Figure 1.4);

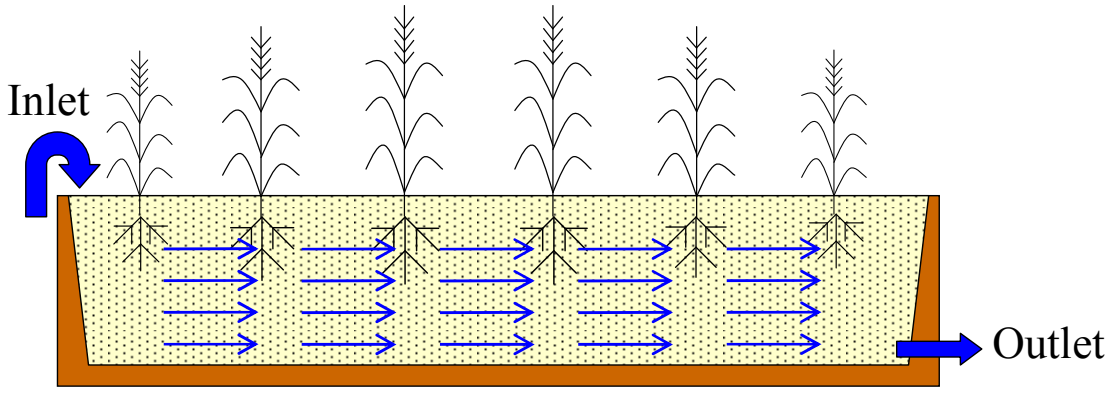

Figure 1.4. Cross section of typical HSFCWs.

iii. Vertical flow constructed wetlands (VFCWs): they consist usually of a gravel or sand bed planted with wetland vegetation. The water is distributed across the surface of the bed and it percolates through the bed according to a vertical flow (Figure 1.5).

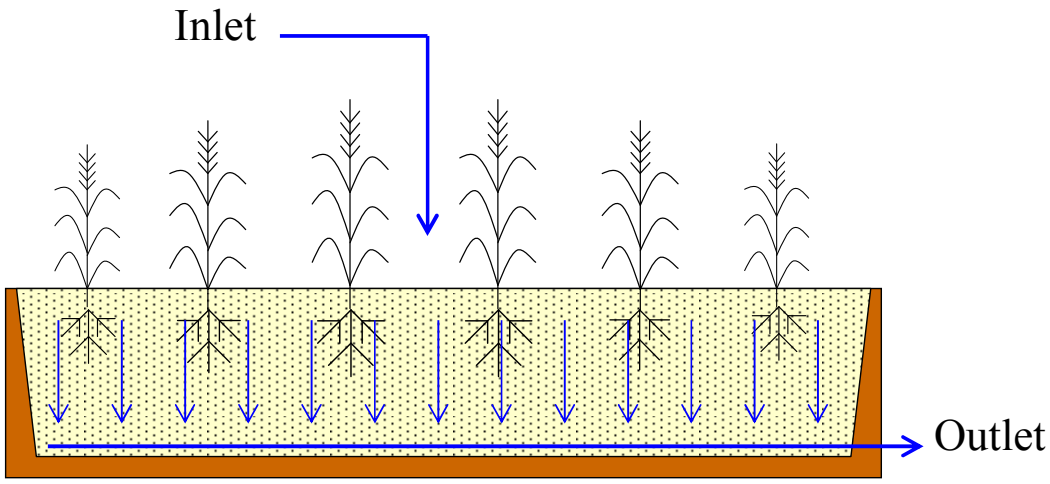

Figure 1.5. Cross section of typical VFCWs.

1.5.2 The French constructed wetland system

The most common design for CWs in France is the two stage VFCW. The French VFCW system is characterized by the fact that the raw wastewater is directly sent to the VFCW without any pre-treatment. The use of VFCWs has been developed in France since the 1980s (Liénard et al., 1987), and has gained a growing consensus over time, to become nowadays one of the most adopted treatment systems in small communities (Molle et al., 2004).

The French VFCW system, if well designed, is highly efficient for COD and total suspended solid (TSS) removal and nitrification. Molle et al. (2005b) analysed the treatment performances of more than 80 two stage VFCWs in France, and they observed average performances of about 90%, 95% and 85% for COD, TSS and total Kjeldahl nitrogen (TKN) removal, respectively (Table 1.10).

As shown in Table 1.10, treatment performances of VFCWs in France meet the requirements of the European Union Directive 91/271/EEC, with the exception of phosphorus.

Table 1.10. Average treatment performances of two stage VFCWs in France (Molle et al., 2005b; Molle, 2008), compared to the requirements for discharges established by the European Union Directive 91/271/EEC.

Pollutant	VFCW treatment performances		Requirements of 91/271/EEC	
	Outlet Concentration	Percentage of removal	Outlet Concentration	Percentage of removal
COD (mg O_2/L)	65	90	125	75
TSS (mg/L)	15	95	60[a]	70[a]
TKN (mg N/L)	8	85	15[b,c,d]	70-80[b,c,d]
TP (mg P/L)	N.A.	<20	2[c,d]	80[c,d]

[a] discharges from agglomerations of 2000-10000 p.e.;

[b] total nitrogen (TN);

[c] discharges to sensitive areas that are subject to eutrophication;

[d] discharges from agglomerations of 10000-100000 p.e..

1.5.3 P removal in constructed wetlands

P removal in constructed wetlands depends on the biotic and abiotic phenomena that occur when wastewater percolates through the materials that constitute the bed of the constructed wetland (Kadlec and Wallace, 2009). Among these, P sorption by plants and P sorption on the bed material are suggested to be the major P removal mechanisms in VFCWs (Molle, 2008):

i. P sorption by plants: the aquatic plants adsorb P for their metabolism and growth. Tanner (1996) studied the uptake of P of 8 emergent plants commonly used in wetland and reported maximum accumulation of P ranging from 1 to 8 mg P/g. In constructed wetlands, the maximum P retention that can be achieved with plants range from about 30 to 150 kg P/ha per year, and the surfaces needed to reach the minimum standards of P treatment are too high and unsustainable (Molle, 2008). In addition, P sorption depends on the plant growth cycle, and acceptable levels of P removal can be achieved only during the growing season;

ii. P sorption on the bed material: the amount of P that can be removed by sorption on the bed material is a function of the initial P concentration and of the properties of the bed material (Kadlec and Wallace, 2009). Rustige et al. (2003) observed that P sorption is markedly influenced by the content of iron, aluminium and calcium of the materials

used to construct the bed, thus suggesting that adsorption on Al and Fe oxides and/or Ca-P precipitation on the bed material were the major mechanisms of P removal. However, the bed materials that are commonly used in constructed wetland (such as sand and gravel) usually present low P removal capacities, and are P saturated with few years of operation (Arias et al., 2001). For these reasons, the use of separate filters filled with replaceable material having high affinity for P binding appears to be a suitable solution to upgrade P removal in constructed wetlands (Vohla et al., 2011).

1.5.4 Reactive filters to upgrade P removal - Field experiments

Latest researches in the field of P removal in constructed wetlands aim to upgrade P removal efficiency by the application of separate filters filled with replaceable reactive materials. Instead of sand and gravel, reactive materials are able to induce chemical changes in water, in terms of pH and chemical composition, this primarily by means of reactions of ions release and/or metal oxide dissolution.

Among the reactive materials, CaO-rich materials are the most promising for P treatment, because they release large amounts of Ca^{2+} and OH^- ions, thus favouring Ca-P precipitation. Despite CaO-rich materials are rare in nature because unstable and highly reactive, several industrial by-products coming from high temperature processes, including ashes from thermal combustion and steel slags, have high CaO-content. This derives primarily from thermal decomposition of the original $CaCO_3$ content of the raw materials and/or the fluxing agents added during the melting process (mainly limestone). Equation (1.31) shows a sample reaction of thermal decomposition of the $CaCO_3$ producing CaO and CO_2 (Gunning et al., 2010).

$$CaCO_3 \xrightarrow{\text{Heat}} CaO + CO_2 \qquad (1.31)$$

1.5.4.1 P removal efficiencies

Main results from selected field experiments that used CaO-rich materials in filters designed to upgrade P removal performances of CWs are summarized in Table 1.11. These experiments showed that CaO-rich materials are very efficient in P removal from the effluent of constructed wetlands, and P removal efficiencies over the full periods of experimentation were always higher than 50% (Table 1.11).

The results of Weber et al. (2007) and Lee et al. (2010) confirmed that P removal performances of EAF-filters increased with increasing HRTv. However, they also observed

that HRTv affected the pH of the effluents: at short HRTv (12-24 hours), the effluent pH was elevated (up to 10) only during the first 30 days of operation, and then it stabilized below a pH of 9. Instead, Lee et al. (2010) found that at longer HRTv (up to 60 hours) pH was elevated (up to 11) for a long period of operation, and this most probably depended on excessive CaO-slag dissolution.

As already observed in column experiments (Shilton et al., 2005), P removal performances of reactive filters appeared to increase with increasing temperature. Shilton et al. (2006) showed a clear seasonal cycle of TP concentrations of the effluents from melter slag filters, indicating high removal efficiencies during the warm seasons and low removal efficiencies during the cold season. This suggested that reactive filters are more efficient in warmer climates (Shilton et al., 2005).

The effect of wastewater composition on P removal performances of Ca-rich ash filters has been studied by Koiv et al. (2010). They found that the presence of known inhibitor ions (chlorine, sulphate etc.) did not influence P removal. However, they observed that the P removal efficiency depended on the inlet P concentration, and P removal efficiencies decreased drastically when initial P concentration fell below 0.2 mg P/L. This suggests that there is a limit for P treatment, and that this limit likely is the background P concentration of the water.

1.5.4.2 Mechanism of P removal

The results of the studies reported in Table 1.11 seemed to indicate that removal mechanisms depended on the chemical composition of the reactive materials. CaO dissolution followed by Ca phosphate precipitation seemed to be the major mechanism of P removal when using BF-slag, BOF-slag and oil shale ash, most probably because they are particularly rich in CaO (Table 1.11). Instead, P adsorption on Al and Fe hydroxides and Fe-phosphate precipitation seemed to be the major removal mechanisms on melter slag (Shilton et al., 2006; Pratt et al., 2007), which is the poorest in CaO among the other CaO-rich materials listed in Table 1.11.

1.5.4.3 Estimating lifespan of reactive filters

Nowadays, it is difficult to assess the lifespan of reactive filters because the number of field experiments is too limited and, to our knowledge, only a study in the literature has presented the long time performances of reactive filters (Shilton et al., 2006). Shilton et al. (2006) reported high P removal efficiencies by using melter slag until a P saturation level of 1.23 g P/kg was reached after 5 years of field scale operation. Since estimating the lifespan of other

types of reactive filters by using data from meter slag is very approximate, further long term studies are urged to determine the P saturation levels of the other CaO-rich materials under field conditions.

Table 1.11. Selected field experiments that used CaO-rich industrial by-products to upgrade P removal in CWs (adapted from Vohla et al., 2011).

Authors	Filter material	Experimental design, Flow type[a] (filter vol.)	Size (mm)	CaO (% w.)	Inlet TP (mg/L)	HRTv (day)	Duration (month)	TP removal (%)	TP removed (mg P/g)
Koiv et al., 2010	Sediments of oil shale ash	1 UVF (0.86 m^3) 1 HF (1.24 m^3) in series	5-20	29.2	4.9	5-15	6	>99	0.69 (VF) 0.61 (HF)
Korkusuz et al., 2007	BF-slag (50% of volume bed)	1 UVF (18 m^3)	<3	33.5	6.6	3	12	52	0.08[b]
Cassini et al., 2010	BOF-slag	1 HF (7.2 m^3)	d_{10}[c] < 32	40	7.8	1.7	5	>99	N.A.
Shilton et al., 2006	Melter slag	10 HF (1440 m^3 each) in parallel	10-20	15.9	8.4	3	10 years	72 (first 5 years) 37 (last 5 years)	1.23 (5 years) 1.5 (10 years)
Weber et al., 2007	EAF-filters	4 SVF (0.02 m^3 each)[d] in parallel	5-14	N.A.	N.A.	0.5-1	9	79-81	1.67-1.7
Lee et al., 2010	EAF-filters	3 HF (0.94 m^3) in parallel	N.A.	N.A.	46[e]	2.5-5	7	>99	N.A.

[a] Horizontal Flow (HF), Saturated Vertical Flow (SVF), Unsaturated Vertical Flow (UVF).

[b] Determined by P extraction experiment.

[c] Diameter of the sieve which passes 10% (weight) of the particles.

[d] Pore volume only, total volume of the filters not available

[e] Dissolved reactive phosphorus (mg P/L).

1.6 Recovery of saturated filter substrates

1.6.1 Regeneration of P removal capacity

Several studies in the literature have demonstrated that P retention capacities of P saturated substrates may be regenerated by physical techniques, including drying, agitation and crushing of P saturated slag (Drizo et al., 2002, Drizo et al., 2008; Pratt et al., 2009). These techniques may favour HAP crystallisation (drying) and also unclog adsorption sites to create fresh surface for CaO dissolution and P adsorption (agitation and crushing). Drizo et al. (2002; 2008) demonstrated that rejuvenation techniques may improve P retention capacities of EAF-slag of more than 50%. However, Pratt et al. (2009) demonstrated that physical treatments were not effective for long-term rejuvenation, and, after just two months from regeneration, P removal efficiencies of regenerated slag fell back to a similar level to that exhibited by exhausted slag. Latest studies focus on chemical treatments to regenerate P retention capacities of exhausted filter substrates. Pratt and Shilton (2010) showed that acid washes (1M HCl) were an effective technique to strip P from exhausted melter slag and hence to regenerate its P removal capacities. Moreover, they suggested that P recovered from exhausted slag may represent a high quality P resource for the industry of fertilizer.

1.6.2 Reuse as fertilizer

Nowadays, mined P-rich rock (apatite) represents the only primary source of P for fertilizer production (Valsami-Jones, 2001). P-rich rocks are natural, abundant and relatively low cost sources of P (de-Bashan and Bashan, 2004). However, at the current rate of exploitation, the high quality portion of these natural resources is expected to be largely depleted in less than 100 years (Driver et al., 1999; Isherwood, 2000). Therefore, the research on alternative high-quality sources of P for fertilizer production has become a priority.

P recovered from WWTPs might represent one viable source of P for the agricultural use. Filter materials that retained P in WWTPs might be used as fertilizer and the availability of P for plant sorption will depend on the solubility of the P-complexes and/or mobility of P bound to the surface of the materials. In most of the studies presented in Tables from 1.3 to 1.10 the major mechanism of P removal was Ca-P precipitation followed by HAP crystallisation. Since HAP is very stable and poorly soluble (Valsami-Jones, 2001), P retained on Ca-rich materials might be not likely available for plant sorption (Johansson and Gustafsson, 2000).

However, the role of phosphate solubilizing bacteria and/or fungi (PSB, PSF) may represent a cheap and effective means of HAP solubilization (Richardson, 2001; Ramaekers et al., 2010).

In fact, these microorganisms, which are common in almost all agricultural and forest soils, produce organic acids strong enough to dissolve HAP (de-Bashan and Bashan, 2004). The plant availability of P retained on Ca-rich filter substrates was confirmed by pot experiments (Hylander and Siman, 2001; Cucarella et al., 2007).

1.6.3 Reuse in civil engineering

Exhausted filter substrates may be reused as aggregates in civil engineering, with the condition that they show technical proprieties and environmental compatibility. Technical properties are usually determined by laboratory tests, and they include: bulk density, resistance to fragmentation, water adsorption, resistant to freezing, volume stability and resistance to abrasion (Motz and Geiseler, 2001).

The environmental compatibility of exhausted filter materials is usually established by the potential production of hazardous leachates, which is determined by leaching tests (EN 12457-1:2002; EN 12457-2:2002). The Decision 2003/33/EC of the European Council established the limit leachate concentrations for waste acceptable at landfills for inert waste. If these values are respected, the exhausted filter materials are defined as not-hazardous waste, and they can be used as aggregates in civil engineering or sent to landfills for inert waste.

References of Chapter 1

EN 12457-1: 2002. Characterisation of waste. Leaching. Compliance test for leaching of granular waste materials and sludges. One stage batch test at a liquid to solid ratio of 2 l/kg for materials with high solid content and with particle size below 4 mm (without or with size reduction).

EN 12457-2: 2002. Characterisation of waste. Leaching. Compliance test for leaching of granular waste materials and sludges. One stage batch test at a liquid to solid ratio of 10 l/kg for materials with high solid content and with particle size below 4 mm (without or with size reduction).

EN ISO 6878, 2004. Water quality - Determination of phosphorus - Ammonium molybdate spectrometric method.

Adam K., Krogstad T., Vrale L., Søvik A.K., Jenssen P.D., 2007. Phosphorus retention in the filter materials shellsand and Filtralite-P®—Batch and column experiment with synthetic P solution and secondary wastewater. Ecological Engineering 29, 200-208.

Alcocer R.D.J., Giacoman V.G., Champagne P., 2012. Assessment of the plug flow and dead volume ratios in a sub-surface horizontal-flow packed-bed reactor as a representative model of a sub-surface horizontal constructed wetland. Ecological Engineering 40, 18-26.

Arends J., Ten Cate J.M., 1981. Tooth enamel remineralization. Journal of Crystal Growth 53(1), 135-147.

Arias C.A., Del Bubba M., Brix H., 2001. Phosphorus removal by sands for use as media in subsurface flow constructed reed beds. Water Research 35(5), 1159-1168.

Awual Md.R., Jyo A., El-Safty S.A., Tamada M., Seko N., 2011. A weak-base fibrous anion exchanger effective for rapid phosphate removal from water. Journal of Hazardous Materials 188(1-3), 164-171.

Bellier N., 2005. Potentiel et efficacité d'enlèvement du phosphore par des apatites d'Amérique du nord. PhD thesis, Université de Montréal (Canada).

Bellier N., Chazarenc F., Comeau Y., 2006. Phosphorus removal from wastewater using north american apatites. Water Research 40(15), 2965-2971.

Blaney L.M., Cinar S., SenGupta A.K, 2007. Hybrid anion exchanger for trace phosphate removal from water and wastewater. Water Research 41(7), 1603-1613.

Boisvert J.P., To T.C., Berrak A., Jolicoeur C., 1997. Phosphate adsorption in flocculation processes of aluminium sulphate and polyaluminium-silicate-sulphate. Water Research 31(8), 1939-1946.

Bowden L.I., Jarvis A.P., Younger P.L., Johnson K.L., 2009. Phosphorus removal from wastewaters using basic oxygen steel slag. Environmental Science and Technology 43(7), 2476-2481.

Cassini S.T., Avelar J.C., Gonçalves R.F., Pinotti L.M., Keller R., 2010. Evaluation of steel slag as filter bed of constructed wetland in post treatment of anaerobic baffled reactor treating wastewater. Proceedings of the 12th International Conference on Wetland Systems for Water Pollution Control. Venice, Italy, 4-7 Oct. 2010.

Chazarenc F., 2003. Optimisation des systèmes de traitement des eaux usées domestiques par filtres plantés de macrophytes. PhD thesis, Université de Savoie (France).

Chazarenc F., Merlin G., Gonthier Y., 2003. Hydrodynamics of horizontal subsurface flow constructed wetlands. Ecological Engineering 21 (2-3), 165-173.

Chazarenc F., Brisson J., Comeau Y., 2007. Slag columns for upgrading phosphorus removal from constructed wetland effluents. Water Science and Technology 56(3), 109-115.

Chitrakar R., Tezuka S., Sonoda A., Sakane K., Ooi K., Hirotsu T., 2006. Phosphate adsorption on synthetic goethite and akaganeite. Journal of Colloid Interface Science 298(2), 602–608

Claveau-Mallet D., Wallace S., Comeau Y., 2012. Model of phosphorus precipitation and crystal formation in electric arc furnace steel slag filters. Environmental Science and Technology 46 (3), 1465-1470.

Crouzet P., Leonard J., Nixon S., Rees Y., Parr W., Laffon L., Bogestrand J., Kristensen P., Lallana C., Izzo G., Bokn T., Bak J., 1999. Nutrients in European Ecosystems. European Environment Agency, www.eea.eu.int, Environmental Assessment Report n° 4.

Cucarella V., Zaleski T., Mazurek R., Renman G., 2007. Fertilizer potential of calcium-rich substrates used for phosphorus removal from wastewater. Polish Journal of Environmental Studies 16(6), 817-822.

Cucarella V., Renman G., 2009. Phosphorus sorption capacity of filter materials used for on-site wastewater treatment determined in batch experiments. A comparative study. Journal of Environmental Quality 38(2), 381-392.

Das J., Patra B.S., Baliarsingh N., Parida K.M., 2006. Adsorption of phosphate by layered double hydroxides in aqueous solutions. Applied Clay Science 32(3-4), 252-260.

de-Bashan L.E., Bashan Y., 2004. Recent advances in removing phosphorus from wastewater and its future use as fertilizer (1997–2003). Water Research 38(19), 4222-4246.

Desjardins R., 1997. Le Traitement des Eaux. Editions de l'Ecole Polytechnique de Montréal, Canada.

Driver J., Lijmbach D., Steen I. (1999) Why recover phosphorus for recycling and how? Environmental Technoogy 20(7), 651-662.

Drizo A., Frost C.A., Grace J., Smith K.A., 1999. Physico-chemical screening of phosphate-removing substrates for use in constructed wetland systems. Water Resource 33(17), 3595-3602.

Drizo A., Comeau Y., Forget C., Chapuis R. P., 2002. Phosphorus saturation potential: a parameter for estimating the longevity of constructed wetland systems. Environmental Science and Technology 36(21), 4642-4648.

Drizo A., Forget C., Chapuis R.P., Comeau Y., 2006. Phosphorus removal by electric arc furnace steel slag and serpentinite. Water Research 40(8), 1547-1554.

Drizo A., Cummings J., Weber D., Twohig E., Druschel G., Bourke B., 2008. New evidence for rejuvenation of phosphorus retention capacity in EAF steel slag. Environmental Science and Technology 42(16), 6191-6197.

Ferguson J.F., Jenkins D., Eastman J., 1973. Calcium phosphate precipitation at slightly alkaline pH values. Journal Water Pollution Control Federation 45(4), 620-631.

Freeman J.S, Rowel D.L., 1981. The adsorption and precipitation of phosphate onto calcite. International Journal of Soil Science 32(1), 75-84.

Fytianos K., Voudrias E., Raikos N., 1998. Modelling phosphorus removal from aqueous and wastewater samples using ferric iron. Environmental Pollution 101(1), 123-130.

Fush G.W., Chen M., 1975. Microbiological basis of phosphate removal in the activated sludge process for the treatment of wastewater. Microbial Ecology 2(2), 119-138.

Gray S., Kinros J., Read P., Marland A., 2000. The nutrient assimilative capacity of maerl as a substrate in constructed wetland systems for waste treatment. Water Research 34(8), 2183-2190.

Gunning P.J., Hills C.D., Carey P.J., 2010. Accelerated carbonation treatment of industrial wastes. Waste Management 30(6), 1081-1090.

Gustafsson J.P., Renman A., Renman G., Poll K., 2008. Phosphate removal by mineral-based sorbents used in filters for small-scale wastewater treatment. Water Research 42 (1-2), 189-197.

Harold F.M., 1966. Inorganic polyphosphates in biology: structure, metabolism and function. Bacteriological Reviews 30(4), 772-794.

Ho Y.S., McKay G., 1998. A comparison of chemisorption kinetic models applied to pollutant removal on various sorbents. Process Safety and Environmental Protection 76(4), 332-340.

House W.A., 1999. The physico-chemical conditions for the precipitation of phosphate with calcium. Environmental Technology 20(7), 727-733.

Huang W., Wang S., Zhu Z., Li L., Yao X., Rudolph V., Haghseresht F., 2008. Phosphate removal from wastewater using red mud. Journal of Hazardous Materials 158(1), 35-42.

Hylander L., Siman G., 2001. Plant availability of phosphorus sorbed to potential wastewater treatment materials. Biology and Fertility of Soils 34(1), 42-48.

Inskeep W.P., Silvertooth J.C., 1988. Inhibition of hydroxyapatite precipitation in the presence of fulvic, humic and tannic acids. Soil Science Society of American Journal 52(4), 941-946.

Isherwood K.F., 2000. Mineral fertilizer distribution and the environment. International Fertilizer Industry Association. United Nations Environment Programme, Paris, pp. 106.

Jang H., Kang S.H., 2002. Phosphorus removal using cow bone in hydroxyapatite crystallization. Water Research 36(5), 1324-1330.

Jha V.K., Kameshima Y., Nakajima A., Okada K., 2008. Utilization of steel-making slag for the uptake of ammonium and phosphate ions from aqueous solution. Journal of Hazardous Materials 156(1-3), 156-162.

Johansson L., Gustafsson J.P., 2000. Phosphate removal using blast furnace slags and opoka - mechanisms. Water Research 34(1), 259-265.

Johansson-Westholm L., 2006. Substrates for phosphorus removal-potential benefits for on-site wastewater treatment? Water Research 40(1), 23-36.

Kaasik A., Vohla C., Motlep R., Mander U., Kirsimae K., 2008. Hydrated calcareous oil-scale ash as potential filter media for phosphorus removal in constructed wetlands. Water Research 42(4-5), 1315-1323.

Kadlec R. H., Knight R. L., 1996. Treatment Wetlands. Lewis Publishers, USA (Florida), pp. 893.

Kadlec R.H., 2000. The inadequacy of first-order treatment wetland models. Ecological Engineering 15 (1-2), 105-119.

Kadlec R.T., Wallace S.D., 2009. Treatment wetlands. Second edition. Taylor and Francis Group, USA (Florida), pp. 1016.

Kibalczyc W., Christoffersen J., Christoffersen M.R., Zielenkiewicz A., Zielenkiewicz W., 1990. The effect of magnesium ions on the precipitation of calcium phosphates. Journal of Crystal Growth 106(2-3), 355-366.

Kim E.H., Yim S., Jung H., Lee E., 2006. Hydroxyapatite crystallization from a highly concentrated phosphate solution using powdered converter slag as a seed material. Journal of Hazardous Materials 136(3), 690-697.

Koiv M., Liira M., Mander U., Motlep R., Vohla C., Kirsimae K., 2010. Phosphorus removal using Ca-rich hydrated oil shale ash as filter material – The effect of different phosphorus loadings and wastewater compositions. Water Research 44(18), 5232-5239.

Korkusuz E.A., Beklioglu M., Demirer G.,N., 2007. Use of blast furnace granulated slag as a substrate in vertical flow reed beds: field application. Bioresource Technology 98(11), 2089-2101.

Lagergren S., 1898. About the theory of so-called adsorption of soluble substances, Kungliga Svenska Vetenskapsakademiens. Handlingar 24(4), 1-39.

Lee M.S., Drizo A., Rizzo D.M., Druschel G., Hayden N., Twohig E., 2010. Evaluating the efficiency and temporal variation of pilot-scale constructed wetlands and steel slag phosphorus removing filters for treating dairy wastewater. Water Research 44(14), 4077-4086.

Levin G.V., Sharipo J., 1965. Metabolic uptake of phosphorus by wastewater organisms. Journal of the Water Pollution Control Federation 37, 800-821.

Li Z., Tang X., Chen Y., Wang Y., 2009. Behaviour and mechanism of enhanced phosphate sorption on loess modified with metals: equilibrium study. Journal of Chemical Technology and Biotechnology 84(4), 595–603.

Liénard A., 1987. Domestic wastewater treatment in tanks with Emergent Hydrophytes: latest results of a recent plant in France. Water Science and Technology 19(12), 373-375.

Liira M., Kõiv M., Mander Ü., Mõtlep R., Vohla C., Kirsimäe K., 2009. Active filtration of phosphorus on Ca-rich hydrated oil-shale ash: does longer retention time improve the process? Environmental Science and Technology 43(10), 3809-3814.

Lucas J., Prevot L., 1984. Synthèse de l'apatite par voie bactérienne à partir de matière organique phosphatée et de divers carbonates de calcium dans des eaux douce et marine naturelles. Chemical Geology 42(1-4), 101-118.

Lundager-Madsen H.E., Christensson F., Polyak L.E., Suvorova E.I., Kliya M.O., Chernov A.A., 1995. Calcium phosphate crystallization under terrestrial and microgravity conditions. Journal of Crystal Growth 152(3), 191-202.

Lundager-Madsen H.E., 2008. Influence of foreign metal ions on crystal growth and morphology of brushite ($CaHPO_4,2H_2O$) and its transformation to octacalcium phosphate and apatite. Journal of Crystal Growth 310(10), 2602-2612.

Meyer J.L., 1983. Phase-transformations in the spontaneous precipitation of calcium phosphate. Croatica Chemica Acta 56, 753-767.

Metcalf and Eddy, Inc. 2003. Wastewater Engineering - Treatment and reuse. 4th edition, McGraw-Hill, USA (New York).

Mc Dowell H., Gregory T.M., Brown W.E., 1977. Solubility of Ca5(PO4)3(OH) in the system Ca(OH)2-H3PO4-H2O at 5, 15, 25 and 37°C, Journal of Research, National Bureau of Standards, 81A(2-3), 273-281.

Molle P., Liénard A., Boutin C., Merlin G., Iwema A., 2004. Traitement des eaux usées domestiques par marais artificiels: état de l'art et performances des filtres plantés de roseaux en France. Ingénieries n° spécial, p. 23-32.

Molle P., Lienard A., Grasmick A., Iwema A., Kabbabi A., 2005a. Apatite as an interesting seed to remove phosphorus from wastewater in constructed wetlands. Water Science and technology 51(9), 193-203.

Molle P., Liénard A., Boutin C., Merlin G., Iwema A., 2005b. How to treat raw sewage with constructed wetlands: an overview of the French system. Water Science and Technology 51(9), 11-21.

Molle P., 2008. Élimination du phosphore par filtres plantés de roseaux. Technique de l'Ingénieur RE101, pp. 8.

Molle P., Martin S., Esser D., Besnault S., Morlay C., Harouiya N., 2011. Phosphorous removal by the use of apatite in constructed wetlands: design recommendations. Water Practice and Technology 6 (3), doi:10.2166/wpt.2011.046.

Moreno E.C., Varughese K., 1981. Crystal growth of calcium apatites from dilute solutions. Journal of Crystal Growth 53(1), 20-30.

Motz H., Geiseler J., 2001. Products of steel slags: an opportunity to save natural resources. Waste Management 21(3), 285-293.

Ogata A., Banks R.B., 1961. A solution of the differential equation of longitudinal dispersion in porous media. United States Geological Survey Professional Paper 411-A:7.

Pant H.K., Reddy K.R., Lemon E., 2001. Phosphorus retention capacity of root bed media of sub-surface flow constructed wetland. Ecological Engineering 17(4), 345-355.

Plant L.J., House W.A., 2002. Precipitation of calcite in the presence of inorganic phosphate. Colloid and Surfaces A – Physicochemical and Engineering Aspects 203(1-3), 143-153.

Pratt C., Shilton A., Pratt S., Haverkamp R.G., Bolan N.S., 2007. Phosphorus removal mechanisms in active slag filters treating waste stabilization pond effluent. Environmental Science and Technology 41(9), 3296-3301.

Pratt C., Shilton A., Haverkamp R.G., Pratt S., 2009. Assessment of physical techniques to regenerate active slag filters removing phosphorus from wastewater. Water Research 43(2), 277-282.

Pratt C., Shilton A., 2010. Active slag filters – simple and sustainable phosphorus removal from wastewater using steel industry by-product. Water Science and Technology 62(8), 1713-1718.

Proctor D.M., Fehling K.A., Shay E.C., Wittenborn J.L., Green J.J., Avent C., Bigham R.D., Connolly M., Lee B., Shepker T.O., Zak M.A., 2000. Physical and chemical characteristics of blast furnace, basic oxygen furnace, and electric arc furnace steel industry slags. Environmental Science and Technology 34(8), 1576-1582.

Ramaekers L., Remans R., Rao I.M., Blair M.W., Vanderleyden J., 2010. Strategies for improving phosphorusacquisition efficiency of crop plants. Field Crops research 117(2-3), 169-176.

Rebhun M., Argaman Y., 1965. Evaluation of hydraulic efficiency of sedimentation basin. Journal of Sanitary Engineering Division, ASCE, 91 (SA5), 37-45.

Recknagel F., Hosomi M., Fukushima T., Kong D.S., 1995. Short and long term control of external and internal phosphorus loads in lakes. A scenario analysis. Water Research 29(7), 1767-1779.

Richardson A.E., 2001. Prospects for using soil microorganisms to improve the acquisition of phosphorus by plants. Journal of Plant Physiology 28, 897-906.

Roques H., 1990. Fondements théoriques du traitement chimique des eaux. Volume II, Technique et Documentation – Lavoisier, Paris (France), pp. 382.

Rustige H., Tomac I., Honer G., 2003. Investigations on phosphorus retention in subsurface flow constructed wetlands. Water Science and Technology 48(5), 67-74.

Sakadevan K., Bavor H.J., 1998. Phosphate adsorption characteristics of soils, slags and zeolite to be used as substrates in constructed wetland systems. Water Research 32(2), 393-399.

Shilton A. N., Pratt S., Drizo A., Mahmood B., Banker S., Billings L., Glenny S., Luo D., 2005. Active filters for upgrading phosphorus removal from pond systems. Water Science and Technology 51(12), 111-116.

Shilton A. N., Elmetri I., Drizo A., Pratt S., Haverkamp R. G., Bilby S. C., 2006. Phosphorus removal by an “active” slag filter - a decade of full scale experience. Water Research 40(1), 113-118.

Shukla J.B., Misra A.K., Chandra P., 2008. Modelling and analysis of the algal bloom in a lake caused by discharge of nutrients. Applied Mathematics and Computation 196, 782-790.

Stumm W., Morgan J.J., 1996. Aquatic chemistry – Chemical equilibria and rates in natural waters. 3rd edition, Wiley-Interscience Publication, USA (Iowa), pp. 1022.

Tanner C.C., 1996. Plants for constructed wetland treatment systems – A comparison of the growth and nutrient uptake of eight emergent species. Ecological Engineering 7(1), 59-83.

Tiessen H., Moir J.O., 1993. Characterization of available P by sequential extraction. In: Soil sampling and methods of analysis. M.R. Carter Editor, Canadian Society of Soil Science. Lewis Publisher, London, Ch. 10, 75-86.

USEPA, 1988. Constructed wetlands and aquatic plant systems for municipal wastewater treatment – Design manual. United States Environmental Protection Agency, pp. 92.

Valsami-Jones E., 2001. Mineralogical controls on phosphorus recovery from wastewaters. Mineralogical Magazine 65(5), 611-620.

Valsaraj K.T., 2000. Elements of Environmental Engineering: Thermodynamics and Kinetics. 2nd edition, Lewis Publishers, USA (Florida), pp 679.

Van der Houwen J.A.M., Valsami-Jones E., 2001. The application of calcium phosphate precipitation chemistry to phosphorus recovery: the influence of organic ligands. Environmental Technology 22(11), 1325-1335.

Vohla C., Poldvere E., Noorvee A., Kuusemets V., Mander U., 2005. Alternative filter media for phosphorus removal in a horizontal subsurface flow constructed wetland. Journal of Environmental Science and Health 40(6-7), 1251-1264.

Vohla C., Kõiv M., Bavor H.J., Chazarenc F., Mander U., 2011. Filter materials for phosphorus removal from wastewater in treatment wetlands – A review. Ecological Engineering 37(1), 70-89.

Wang G., Wang Y., Gao Z., 2010. Use of steel slag as a granular material: Volume expansion prediction and usability criteria. Journal of Hazardous Materials 184(1-3), 555-560.

Weber D., Drizo A., Twohig E., Bird S., Ross D., 2007. Upgrading constructed wetlands phosphorus reduction from a dairy effluent using electric arc furnace steel slag filters. Water Science and Technology 56(3), 135-143.

Werner T.M., Kadlec R.H., 2000. Wetland residence time distribution modelling. Ecological Engineering 15(1-2), 77-90.

Wolf, D., Resnick, W. 1963. Residence time distribution in real system. Journal of Industrial and Engineering Chemical Fundamentals, 2(4):28-293.

Xiong J., He Z., Mahmood Q., Liu D., Yang X., Islam E., 2008. Phosphate removal from solution using steel slag through magnetic separation. Journal of Hazardous Materials 152(1), 211-215.

Xu D., Xu J., Wu J., Muhammad A., 2006. Studies on the phosphorus sorption capacity of substrates used in constructed wetland systems. Chemosphere 63(2), 344-352.

Xue Y., Hou H., Zhu S., 2009. Characteristics and mechanisms of phosphate adsorption onto basic oxygen furnace slag. Journal of Hazardous Materials 162(2-3), 973-980.

Zoltek J., 1974. Phosphorus removal by orthophosphate nucleation. Journal Water Pollution Control Federation 46, 2498-2520.

EXPERIMENTAL PART

CHAPTER 2 Phosphate removal from synthetic and real wastewater using steel slags produced in Europe

Abstract

Electric arc furnace steel slags (EAF-slags) and basic oxygen furnace steel slags (BOF-slags) were used to remove phosphate from synthetic solutions and real wastewater. The main objective of this study was to establish an overview of the phosphate removal capacities of steel slags produced in Europe. The influences of parameters, including pH, and initial phosphate and calcium concentrations, on phosphate removal were studied in a series of batch experiments. Phosphate removal mechanisms were also investigated via an in-depth study. The maximum capacities of phosphate removal from synthetic solutions ranged from 0.13 to 0.28 mg P/g using EAF-slags and from 1.14 to 2.49 mg P/g using BOF-slags. Phosphate removal occurred predominantly via the precipitation of Ca-phosphate complexes (most probably hydroxyapatite) according to two consecutive reactive phases: first, dissolution of CaO-slag produced an increase in Ca^{2+} and OH^- ion concentrations; then the Ca^{2+} and OH^- ions reacted with the phosphates to form hydroxyapatite. It was found that the release of Ca^{2+} from slag was not always enough to enable hydroxyapatite precipitation. However, our results indicated that the Ca^{2+} content of wastewater represented a further source of Ca^{2+} ions that were available for hydroxyapatite precipitation, thus leading to an increase in phosphate removal efficiencies.

2.1 Introduction

Phosphorus (P) is an essential nutrient for biomass growth. However, an excessive intake of P in water bodies such as rivers, lakes or lagoons causes an abnormal growth of algae and aquatic plants resulting in the degradation of the water quality. Therefore, legislation on P disposal into the surrounding environment is becoming stricter worldwide, including for small wastewater treatment plants (WWTPs). One appropriate technology for improving P removal in small WWTPs is filtration through materials with high affinities for P binding. Since common filter substrates (such as sand and gravel) have limited P removal capacities, research on alternative materials has become a priority. In the last two decades, a large number of potential substrates, including natural materials (rocks, soils and sediments), industrial by-products (steel slag, burnt oil shale and fly ash) and man-made products (light-weight aggregates specifically produced for P removal), have been tested (Vohla et al., 2011). Most of these materials have a high content of Ca, Al, and/or Fe, which are elements with a strong affinity for P binding (Johansson-Westholm, 2006). Batch experiments are commonly performed to evaluate the phosphate removal capacity (PRC) of a potential filter material. In fact, PRC is an important parameter when comparing and selecting candidate materials (Drizo et al., 2002). Cucarella and Renman (2009) reviewed a large number of relevant studies that used batch experiments to determine the PRCs of potential filter materials. They observed that there is not a standard procedure for batch experiments and PRCs varied by several orders of magnitude depending on the experimental batch parameters that were arbitrarily established, thus leading to difficulties in comparing the results. The main parameters affecting the results of batch experiments are the size and form of the material, the ratio of material to solution, contact time, agitation mode, temperature, pH and initial phosphate (PO_4-P) concentrations (Cucarella and Renman, 2009).

Since the 1980s, the affinity of steel slag for P binding has been studied with the aim of using a by-product of the steel industry to treat wastewater (first study by Yamada et al., 1986). According to EUROSLAG statistics, more than 16 million tons of steel slag was produced in Europe in 2006: about 80% was used in several fields of application (cement production, road construction) and 10% was recycled internally. However, about 10% was still disposed of in specialised landfill sites. This suggests an interesting potential market for wastewater treatment. The steel industry produces mostly two types of slag derived from two different steelmaking processes: BOF-slag, which originates from the further refining of iron in a basic oxygen furnace, and EAF-slag, which is derived from melting recycled scrap in an electric arc

furnace (Proctor et al., 2000). Steel slag is primarily made of iron (Fe) and calcium oxide (CaO), as a result of the use of fluxing agents (mainly lime) during the steelmaking process (Motz and Geiseler, 2001). Several international studies have demonstrated that steel slag is a suitable substrate for PO_4-P removal from wastewater via Ca-P precipitation mechanisms (Drizo et al., 2006; Kim et al., 2006a; Kim et al., 2006b; Bowden et al., 2009). PRCs reported from batch experiments range from less than 1 to up to 80 mg P/g (Drizo et al., 2002; Jha et al., 2008; Xiong et al., 2008; Xue et al., 2009; Bowden et al., 2009). However, the large discrepancy in experimental batch parameters leads to difficulties in comparing the results of different studies (Chazarenc et al., 2008).

Within the framework of a European research project (Research Fund for Coal and Steel (RFCS) research programme under grant agreement n° RFSP–CT–2009–00028 (SLASORB)), our study aimed to evaluate the potential use of steel slag produced in Europe as a reactive medium to treat wastewater.

The originality and importance of this paper are highlighted by the following two points:

i. The first large-scale investigation in Europe of the PRCs of steel slag: the same experimental procedures were followed to investigate a selection of samples representative of the European steel slag market. This enabled the results of different experiments to be compared to select the most suitable samples for P removal.

ii. An in-depth critical investigation of the PO_4-P removal mechanisms: only a few studies in the literature have tried to explain thoroughly the sequence of reactions leading to PO_4-P removal using steel slag (Kim et al., 2006a; Kim et al., 2006b), and many details are still unclear. Our work presents an in-depth study of the main parameters influencing PO_4-P removal. First, the kinetics of Ca^{2+} and OH^- release from slag were studied applying a pseudo-first order model. Then, the influences of pH, Ca^{2+} and initial PO_4-P concentrations on PO_4-P removal were studied in a series of batch experiments of PO_4-P removal from synthetic solutions. Finally, experiments on PO_4-P removal from real wastewater were performed to verify the behaviour of slag when it is used to treat real wastewater.

2.2 Materials and methods

2.2.1 Slag collection and preparation

The samples of EAF and BOF steel slag tested in this study were collected from 10 production sites throughout Spain, France, Luxembourg and Germany. Since chemical, mineralogical and technical properties of EAF and BOF slags produced in Europe are generally comparable and independent of their producer (Motz and Geiseler, 2001), we assumed that a sampling of 10 different sites (5 EAF, 5 BOF) was enough to establish an overview of PRCs of European steel slags. The samples were screened on an automatic grinder according to three ranges of granular size (< 5, 5-10 and > 10 mm). The granular size of 5-10 mm was selected to perform the batch experiments. This enables the results to be compared with the size of field scale filters. Before the experiments, the samples were washed first with tap water to remove fine particles and then dried at 105°C for 24 h. Energy dispersive X-ray fluorescence analyses (EDX) were performed to determine the semi-quantitative chemical composition of the slag samples (Rayny series EDX-800HS spectrometer, Shimadzu Corporation, Kyoto, Japan).

2.2.2 Kinetic experiments on Ca^{2+} and OH^- release

The kinetics of Ca^{2+} and OH^- release from slag were investigated in a series of batch experiments (adapted from ASTM 4646-87, 1993). The aim of these was to demonstrate that the increase in Ca^{2+} and pH of the solutions depended primarily on CaO-slag dissolution. For each experiment, 40 g of slag was immersed in 1 L of deionised water (conductivity < 0.1 µS/cm) contained in a glass bottle, thus leading to a slag to solution ratio of 0.04 g/mL (adapted from Nair et al., 1984). The bottle was placed on an agitation table and shaken at 125 rpm under controlled temperature conditions (20°C). Samples of solution were taken after 1, 2, 3, 4 and 7 days of agitation. The pH values and total Ca^{2+} concentrations of the samples were measured. The samples were acidified (pH 2-3, using 1 M HCl) to measure the total Ca^{2+} concentrations. The pH values of the solutions were expressed in OH^- concentrations (mg OH/L). The experimental capacities of Ca^{2+} and OH^- release from slag were calculated using equations (2.1) and (2.2), where Q_t are the capacities of Ca^{2+} and OH^- release at time t (mg/g), V is the volume of the solution (L), M is the mass of slag (g) and Ca^t and OH^t are the total Ca^{2+} and OH^- concentrations of the solutions at time t (mg /L).

$$Q_t = \frac{Ca^t V}{M} \qquad (2.1)$$

$$Q_t = \frac{OH^t V}{M} \quad (2.2)$$

Then the experimental capacities of Ca^{2+} and OH^- release were plotted according to the pseudo-first order kinetic equation of Lagergren (1898), equation (2.3), which is commonly employed to describe pseudo-first order reactions (Ho and McKay, 1998). If pseudo-first order kinetics are applicable, this suggests that one of the reactants is present in great excess over the other reactants in the reaction mixture. The parameter Q_e represents the capacities of Ca^{2+} and OH^- release at equilibrium (mg/g), t is the time (d) and k_1 is the rate constant of pseudo-first order release (1/d).

$$\ln(Q_e - Q_t) = \ln Q_e - k_1 t \quad (2.3)$$

The equilibrium capacity Q_e must be known to exploit equation (2.3) with experimental data. In this study, Q_e was considered an adjustable parameter whose value was estimated by trial and error. The experimental capacities of release observed after 7 days were used as initial Q_e-trial in order to calculate Q_e from the intercept of the plot of $\ln(Q_e\text{-trial} - Q_t)$ against t. Then the Q_e-trial was adjusted until the difference between Q_e-trial and Q_e was less than 0.1% of the value of Q_e-trial.

2.2.3 Experiments on phosphate removal from synthetic solutions

PRCs of steel slag and mechanisms of PO_4-P removal were investigated in a series of batch experiments (adapted from ASTM 4646-87, 1993). For each one, a series of 6 glass bottles each containing 1 L of a synthetic solution with different initial PO_4-P concentrations (0, 5, 10, 20, 25, 100 mg P/L) was prepared. These synthetic solutions were prepared with deionised water (conductivity < 0.1 µS/cm) and sodium diphosphate (Na_2HPO_4). Then, 40 g of slag was put into each bottle, thus leading to a slag to solution ratio of 0.04 g/mL (adapted from Nair et al. (1984). The bottles were placed on an agitation table and shaken at 125 rpm under controlled temperature conditions (20°C). The pH values and residual PO_4-P and Ca^{2+} concentrations of the solutions were measured after 7 days of agitation, when a pseudo-equilibrium in PO_4-P removal was reached. The solutions were filtered (0.45 µm filters) before residual PO_4-P and Ca^{2+} concentrations were measured.

PRCs (mg P/g slag) were calculated from equation (2.4), where V is the volume of the solution (L), M is the mass of slag (g), P_{in} is the initial PO_4-P concentration (mg P/L) and P is the residual PO_4-P concentration of the solution after 7 days of PO_4-P removal (mg P/L).

$$PRC = \frac{(P_{in} - P)V}{M} \quad (2.4)$$

Scanning electron microscopy (SEM) observations and EDX analyses were carried out to examine the slag surface before and after the PO_4-P removal experiments. The slag samples were dried overnight at 60°C and coated with conductive carbon before SEM observations (Jeol JSM 6400 F, Oxford Instruments, London, UK).

2.2.4 Experiments on phosphate removal from real wastewater

The samples of EAF-slag and BOF-slag with the highest PRCs were selected to perform additional experiments on PO_4-P removal from real wastewater. These aimed to verify the PO_4-P removal performances of slag under the chemical conditions of real wastewater. The wastewater used for these experiments was taken from the effluent of a small WWTP (septic tank and sand filter, Centre Scientifique et Technique du Bâtiment, Nantes, France). Its PO_4-P concentration ranged from 0.41 to 1.11 mg P/L, whereas its Ca^{2+} concentration ranged from 40.9 to 48.6 mg/L. Thus, the PO_4-P concentrations were adjusted by adding Na_2HPO_4 to prepare solutions with initial PO_4-P concentrations of 5, 10, 20, 25 and 100 mg P/L. Before preparing these solutions, the wastewater was sterilised (120°C for 20 minutes) to avoid the biological consumption of P. The PRCs of steel slag were determined following the same batch experimental procedure used for the experiments of PO_4-P removal from synthetic solutions.

The molar ratios of Ca removed to PO_4-P removed (mol Ca/mol P) from the solutions were considered to investigate the mechanism of PO_4-P removal. The amounts of PO_4-P removed from each solution were calculated from equation (2.5), where P_{in} is the initial PO_4-P concentration (mol P/L) and P is the residual PO_4-P concentration (mol P/L) after 7 days of reaction.

$$PO_4\text{-P removed} = P_{in} - P \quad (2.5)$$

The amounts of Ca removed from each solution were estimated from equation (2.6) where, for each experiment, Ca^0 is the Ca^{2+} concentration (mol/L) of the solution without addition of Na_2HPO_4 after 7 days of PO_4-P removal experiment, whereas Ca is the Ca^{2+} concentration (mol/L) of the solutions with addition of Na_2HPO_4 after 7 days of PO_4-P removal experiment.

$$Ca\text{ removed} = Ca^0 - Ca \quad (2.6)$$

2.2.5 Analytical methods

Phosphate and Ca analyses were performed according to the Ammonium Molybdate Spectrometric Method (EN ISO 6878, 2004) and the Atomic Absorption Spectrometric Method (EN ISO 7980, 1986), respectively. Phosphate concentrations were measured using a model U DR/4000 spectrophotometer (Hach Company, Loveland USA), whereas Ca concentrations were measured using a model A Analyst 200 spectrophotometer (Perkin Elmer Instruments). The limit of detection for the analysis was determined for each set of experiments from the analysis of blanks. All chemicals used were of analytical grade.

2.3 Results and discussion

2.3.1 Chemical composition of slag

The EDX analyses showed that the main chemical components of steel slag are Fe_2O_3, CaO and SiO_2 (Table 2.1). It was found that BOF-slag is richer in CaO than EAF-slag, whereas EAF-slag is richer in Fe_2O_3 and Al_2O_3 than BOF-slag. The high variance of MgO content may depend on the ratio of dolomite to lime in the fluxing agent used during the steelmaking process (Proctor et al., 2000; Motz and Geiseler, 2001). These results on slag composition are in agreement with the findings of other studies (Motz and Geiseler, 2001; Drizo et al., 2002; Kim et al., 2006a; Xue et al., 2009; Wang et al., 2010).

Table 2.1. EDX analyses: chemical composition of EAF-slag and BOF-slag (weight %). Results of 5 EAF-slag samples and 5 BOF-slag samples.

	EAF-slag			BOF-slag		
	Min	Max	Mean	Min	Max	Mean
Fe_2O_3	28.3	51.4	42.6	17.3	33.5	26.1
CaO	19.0	34.9	23.8	46.2	60.4	52.9
SiO_2	12.6	16.5	14.0	6.0	16.1	11.7
Al_2O_3	5.0	13.1	8.1	< 2	2.6	---
MnO	2.7	8.1	5.6	2.9	5.4	3.6
MgO	< 2	4.4	---	< 2	5.5	---

2.3.2 Kinetics of Ca^{2+} and OH^- release

The experiments showed that total Ca^{2+} concentrations and pH values of the solutions increased until a pseudo-equilibrium was reached after 7 days of agitation (Figure 2.1). These increases can be explained by CaO-slag dissolution following equation (2.7).

$$CaO + H_2O \rightarrow Ca^{2+} + 2OH^- \qquad (2.7)$$

According to equation (2.7), the high CaO content of BOF-slag (Table 2.1) may account for the higher total Ca^{2+} concentrations and pH values observed using BOF-slag.

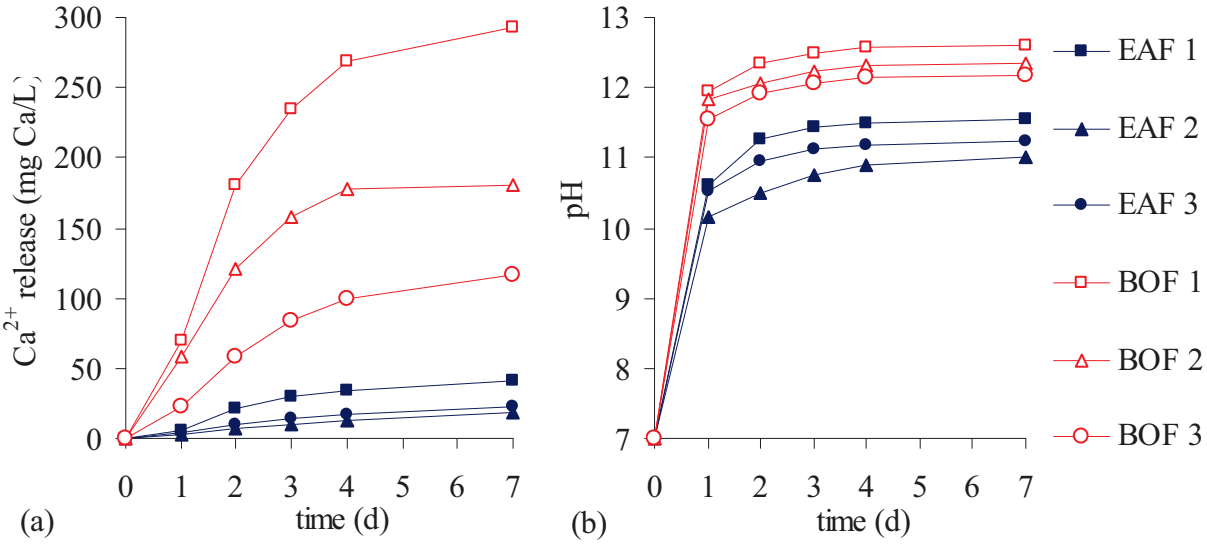

Figure 2.1. Kinetics of Ca^{2+} and OH^- release: total Ca^{2+} concentrations (a) and pH values (b) of the solutions.

Several authors have confirmed that steel slag has a particularly strong tendency to produce basic leachates as a result of a mixture of dissolution reactions of various metal oxides, including Al_2O_3, MgO and CaO (Motz and Geiseler, 2001; Jha et al., 2008; Bowden et al., 2009; Xue et al., 2009). Although Ca^{2+} concentrations and pH values are key parameters in Ca-P precipitation (Joko 1984), the kinetics of CaO-slag dissolution have, to our knowledge, never been modelled. In our study, the experimental capacities of Ca^{2+} and OH^- release were plotted according to a pseudo-first order kinetic model (equation (2.3)). The high correlation coefficients indicated that this model described the Ca^{2+} and OH^- release well (Table 2.2), suggesting that one of the reactants (CaO) was present in great excess over the other reactants in the reaction mixture. This demonstrates that the dissolution of CaO-slag is the primary reaction explaining the increase in Ca^{2+} and pH of the solutions.

As shown in Table 2.2, the equilibrium capacities Q_e and the rate constants k_1 of Ca^{2+} and OH^- release are in good agreement with each other, except for the sample BOF 2. This was probably because of the lower applicability of the first order model to describe Ca^{2+} release (R^2 0.912). The slag EAF 2 showed lower rate constants of Ca^{2+} and OH^- release than slags EAF 1 and EAF 3. This was probably due to the different weathering of the samples (EAF 1 and EAF 3 were fresh from production; EAF 2 was kept in a storage yard exposed to weathering for one year before the experiments). In fact, during the weathering of slag, CaO can react with H_2O producing $Ca(OH)_2$ (Wang et al., 2010), thus changing the rates of Ca^{2+} and OH^- release.

Table 2.2. Correlation coefficients and rate constants for the pseudo-first order kinetic model describing Ca^{2+} and OH^- release.

Slag	Ca^{2+} release			OH- release		
	Qe (mg Ca/g)	k_1 (1/d)	R^2 (-)	Qe (mg OH/g)	k_1 (1/d)	R^2 (-)
EAF 1	1.2	0.29	0.978	1.8	0.29	0.956
EAF 2	0.7	0.13	0.997	0.9	0.10	0.967
EAF 3	0.7	0.22	0.998	0.8	0.34	0.968
BOF 1	9.6	0.30	0.994	18.2	0.40	0.969
BOF 2	4.6	0.67	0.912	10.3	0.38	0.973
BOF 3	3.2	0.34	0.986	6.9	0.40	0.973

2.3.3 Phosphate removal from synthetic solutions

The results of the experiments of PO_4-P removal from synthetic solutions are shown in Table 2.3. Using EAF-slags, the PO_4–P removal efficiencies decreased (from > 80% to < 12%) according to the increase in initial PO_4–P concentrations. On the other hand, using BOF-slags high PO_4–P removal efficiencies (> 90%) have been achieved in all the range of initial PO_4–P concentrations. The decrease in PO_4-P concentrations was accompanied by a decrease in Ca^{2+} concentrations of the solutions. This indicates that the removal of PO_4-P was mainly based on the precipitation of Ca-PO_4-P complexes as already reported by Bowden et al. (2009). Several Ca-PO_4-P precipitates may be formed depending on the pH values, Ca^{2+} and PO_4-P concentrations of the solutions: amorphous calcium phosphates (ACPs), dicalcium phosphate

(DCP), dicalcium phosphate dihydrate (DCPD), octocalcium phosphate (OCP), tricalcium phosphate (TCP) and the most stable hydroxyapatite (HAP) (Valsami-Jones, 2001). Among these, HAP seems to be the most probable because the pH values, Ca^{2+} and PO_4-P concentrations of the solutions were in the range of values that support formation of HAP (Stumm and Morgan, 1996; Valsami-Jones, 2001; Kim et al., 2006b). Moreover, the decrease in PO_4-P concentrations was accompanied by a decrease in pH of the solutions (clear using EAF-slags) as already shown by Lu et al. (2008). This was probably due to the consumption of OH^- ions via HAP precipitation as shown in reaction (2.8).

$$5Ca^{2+} + 3PO_4^{3-} + OH^- \rightarrow Ca_5(PO_4)_3(OH) \downarrow \quad (2.8)$$

Table 2.3. Ranges of pH values and residual PO_4-P and Ca^{2+} concentrations after 7 days of PO_4-P removal from synthetic solutions. Results of 5 EAF-slag samples and 5 BOF-slag samples.

Initial PO_4-P (mg P/L)	EAF-slag			BOF-slag		
	pH (-)	Res. PO_4-P (mg P/L)	Ca^{2+} (mg Ca/L)	pH (-)	Res. PO_4-P (mg P/L)	Ca^{2+} (mg Ca/L)
0	11.0-11.4	---	8.8-24.8	12.1-12.5	---	148-228
5	10.6-10.9	< LQ[a]-1.05	2.8-6.7	12.1-12.4	0.40-3.53	124-216
10	10.4-10.8	0.12-5.39	0.1-3.4	12.1-12.4	0.17-7.64	137-194
20	10.3-10.5	10.96-16.58	< LQ[a]-0.9	12.0-12.4	0.28-8.67	116-191
25	10.1-10.4	15.25-20.82	< LQ[a]-0.8	12.1-12.4	0.17-3.08	100-168
100	9.9-10.3	87.45-94.29	< LQ[a]-0.8	11.6-12.3	0.23-49.15	1-53

[a] Limit of Quantification: 0.01 mg P/L, 0.07 mg Ca/L.

The PRCs of EAF-slags ranged from 0.09 to 0.28 mg P/g, whereas the PRCs of BOF-slags ranged from 0.03 to 2.49 mg P/g (Figure 2.2). The highest PRCs were observed when treating solutions with an initial PO_4-P concentration of 100 mg P/L. The PRCs of EAF-slags did not increase according to initial PO_4-P concentrations above 10 mg P/L, suggesting that a limit in PO_4-P removal was reached. On the other hand, the PRCs of BOF-slags increased according to the initial PO_4-P concentrations, suggesting that a limit in PO_4-P removal was not reached.

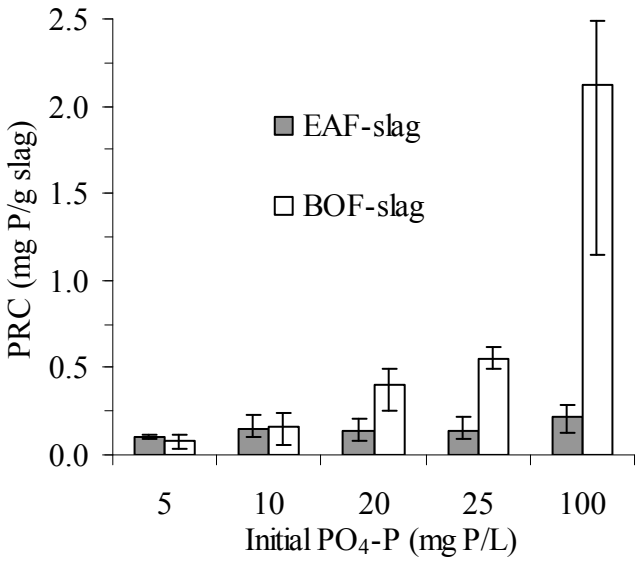

Figure 2.2. Mean PRCs after 7 days of PO_4-P removal from synthetic solutions: results of 5 EAF-slag samples and 5 BOF-slag samples. Bars indicate the range of different values of capacities.

Other authors have reported maximum PRCs of steel slag ranging from 0.8 to 89.9 mg P/g (Table 2.4). Among these literature data, BOF-slag shows higher PRCs than EAF-slag, most probably due to its higher CaO content. However, it is difficult to compare the results of different studies because of the variety of experimental procedures used.

As shown in Table 2.4, the main parameters affecting the results of batch experiments are particle size, ratio of slag to solution, initial PO_4-P concentration, agitation mode and contact time. Overall, PRCs increased when the particle size decreased and/or the ratio of slag to solution decreased, most probably because the contact surface of slag to solution was enlarged.

Table 2.4. Maximum experimental PRCs observed in batch experiments.

Authors	Slag material tested	Particle size (mm)	Ratio slag to solution (g/mL)	Initial PO_4-P (mg P/L)	Agitation mode	Contact time (h)	PO_4-P removed (%)	Maximum PRC (mg P/g)
This study	EAF	5-10	0.04	100	125 rpm	168	12	0.28
	BOF						> 99	2.49
Drizo et al., 2002	EAF	2.5-10	0.05	320	175 rpm	24	60	3.9
Xiong et al., 2008	EAF	< 2	0.04	45	200 rpm	2	71	0.8
Jha et al., 2008	BOF	< 0.02	0.002	320	N.A.	24	49	78.9
Xue et al., 2008	BOF	< 0.6	0.01	500	N.A.	3	86	43.1
Bowden et al., 2009	BOF	< 6	N.A.	500	150 rpm	24	18	89.9

Several studies have demonstrated that PO_4-P can be removed from solution by precipitation of HAP in the presence of appropriate concentrations of Ca^{2+} (Joko, 1984; Johansson and Gustafsson, 2000; Jang and Kang, 2002; Kim et al., 2006b). According to equation (2.8), Ca^{2+} concentration may limit HAP precipitation when the molar ratio of PO_4-P concentration to Ca^{2+} concentration (PO_4-P/Ca) of the solution is higher than 0.6.

The molar ratios PO_4-P/Ca of residual PO_4-P to Ca^{2+} concentrations of the solutions after 7 days of PO_4-P removal are shown in Table 2.5. These results indicate that Ca^{2+} limited HAP precipitation when EAF-slags were used to treat initial PO_4-P concentrations > 10 mg P/L (Table 2.5). This suggests that the amount of Ca^{2+} released from EAF-slags was not large enough to maintain the appropriate Ca^{2+} concentrations to enable HAP precipitation, thus limiting PO_4-P removal as shown in Figure 2.2. For BOF-slag, Ca^{2+} concentrations did not limit HAP precipitation, except for initial PO_4-P concentrations of 100 mg/L. This suggests that the amount of Ca^{2+} released from BOF-slags was large enough to maintain the appropriate Ca^{2+} concentrations to enable HAP precipitation at different initial PO_4-P concentrations, except for highly concentrated solutions (100 mg P/L).

Table 2.5. Range of molar ratios PO_4-P/Ca of residual PO_4-P to Ca^{2+} concentrations after 7 days of PO_4-P removal from synthetic solutions. Results of 5 EAF-slag samples and 5 BOF-slag samples.

Initial PO_4-P (mg P/L)	Residual PO_4-P/Ca[a] (mol P/mol Ca)	
	EAF-slag	BOF-slag
5	< 0.38	< 0.03
10	0.10-58.65	< 0.06
20	> 21.33	< 0.06
25	> 34.15	< 0.03
100	> 149.29	0.01-63.61

[a]Ca limits HAP precipitation for PO_4-P/Ca > 0.6

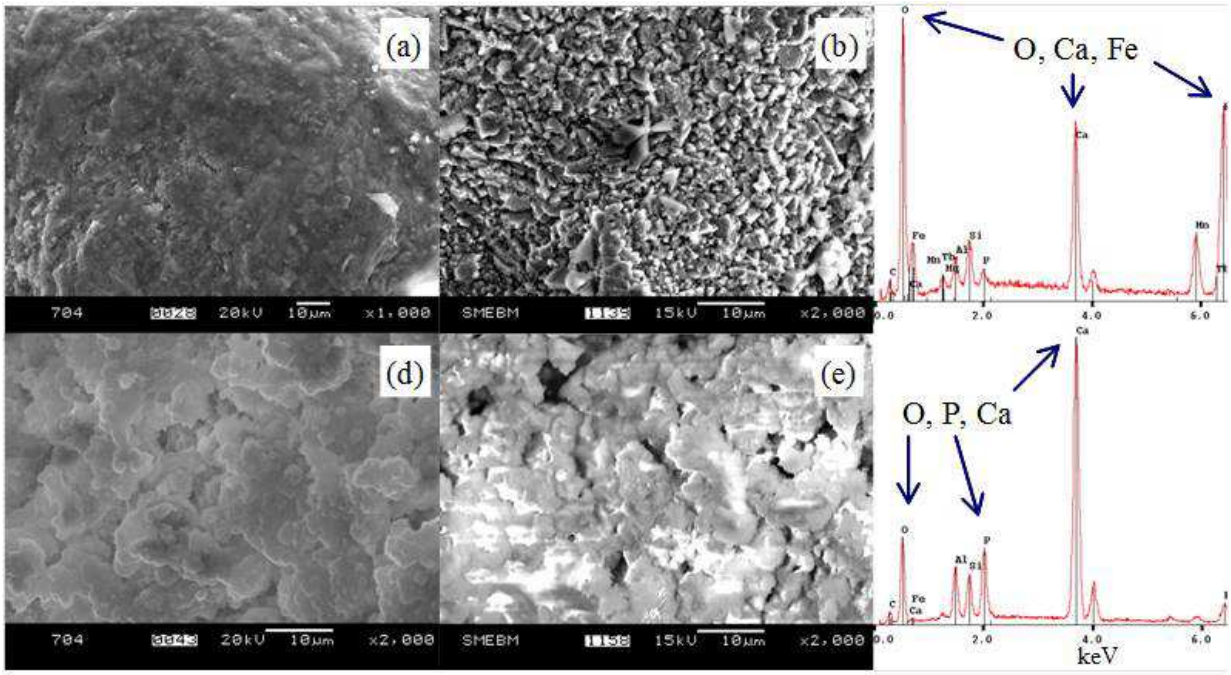

Figure 2.3. SEM observations and XRF analyses. (a) surface of BOF-slag before PO_4-P removal; (b) surface of EAF-slag before PO_4-P removal; (c) chemical analysis of the surface of EAF-slag before PO_4-P removal; (d) surface of BOF-slag after PO_4-P removal; (e) surface of EAF-slag after PO_4-P removal; (f) chemical analysis of the surface of EAF-slag after PO_4-P removal.

The slag surface before and after PO_4-P removal experiments was examined by SEM and EDX analyses (Figure 2.3). Figures 2.3a and b show the coarse surface of BOF-slag and EAF-slag, respectively, before the PO_4-P removal experiments. EDX analyses confirmed that the coarse surface of slag consisted predominantly of Fe and Ca (Figure 2.3c). Microscopic observations by SEM of slag after PO_4-P removal experiments showed that the surface was covered with a finely distributed crystalline layer (Figures 2.3d and e). The EDX analyses demonstrated that the crystalline layer consisted predominantly of Ca, P and O (Figure 2.3f), indicating crystallisation of HAP. Moreover, the HAP crystals observed on the surface of EAF- and BOF-slag (Figures 2.3d and e) had a similar shape to those observed by Kim et al. (2006a).

According to our experimental results, the main mechanism of PO_4-P removal appears to be composed of three consecutive reactive phases, as shown in Figure 2.4:

(1) CaO-slag dissolution: increase in Ca^{2+} and OH^- concentrations of the solutions;

(2) HAP precipitation: decrease in Ca^{2+}, PO_4-P and OH^- concentrations of the solutions;

(3) HAP adsorption and/or crystallisation on the slag surface.

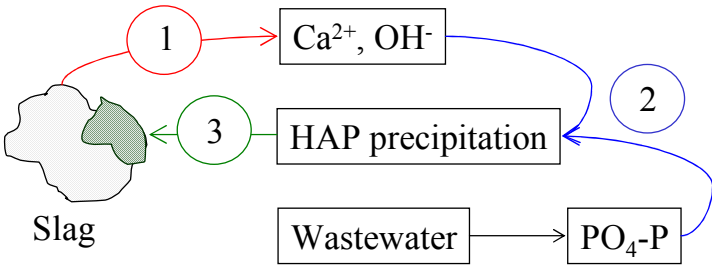

Figure 2.4. Supposed mechanism of PO_4-P removal: (1) CaO-slag dissolution; (2) HAP precipitation; (3) HAP adsorption and/or crystallisation.

2.3.4 Phosphate removal from real wastewater

The results of the experiments on PO_4-P removal from real wastewater are shown in Table 2.6. Using EAF-slag, the PO_4–P removal efficiencies decreased (from > 90% to 25%) according to the increase in initial PO_4-P concentration, whereas using BOF-slag the PO_4–P removal efficiencies were always > 90%. The decrease in PO_4-P concentrations was observed along with a decrease in pH values and Ca^{2+} concentrations of the solutions. This appears to confirm that the major PO_4-P removal mechanism was precipitation of HAP.

Table 2.6. pH values and residual PO_4-P and Ca^{2+} concentrations after 7 days of PO_4-P removal from real wastewater. Results of 1 sample of EAF-slag and 1 sample of BOF-slag.

Initial PO_4-P (mg P/L)	EAF-slag			BOF-slag		
	pH (-)	Res. PO_4-P (mg P/L)	Ca^{2+} (mg Ca/L)	pH (-)	Res. PO_4-P (mg P/L)	Ca^{2+} (mg Ca/L)
0.41-1.11	10.1	0.18	56.5	12.2	0.30	163.2
5	9.6	0.47	46.5	12.1	0.53	136.5
10	9.8	0.47	41.7	12.0	0.18	84.1
20	8.9	6.15	25.8	12.0	0.12	73.2
25	8.8	8.22	19.8	12.0	0.12	106.0
100	8.0	75.13	3.3	11.6	0.24	1.3

The PRCs of EAF-slag ranged from 0.12 to 0.63 mg P/g, whereas those of BOF-slag ranged from 0.14 to 2.50 mg P/g (Figure 2.5). The PRCs reported when treating real wastewater were higher than those reported for treating synthetic solutions. As clearly shown in Figure 2.5, PRCs of EAF-slag and BOF-slag increased according to the initial PO_4-P concentrations, suggesting that a limit of PO_4-P removal was not reached.

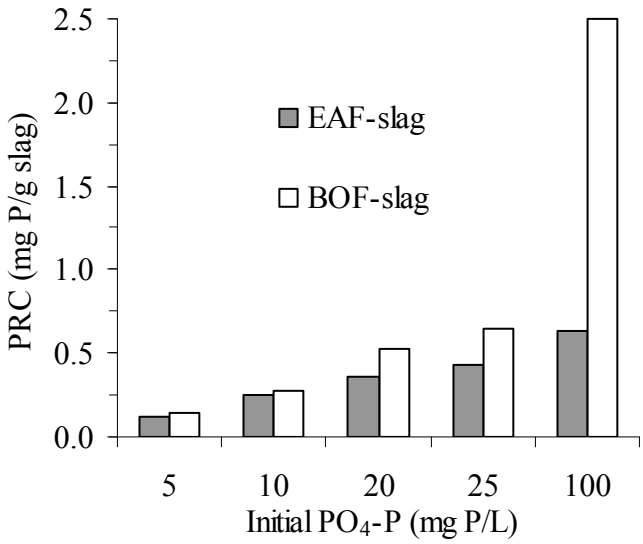

Figure 2.5. PRCs of steel slag after 7 days of PO_4-P removal from real wastewater.

The PO_4-P/Ca molar ratios of residual PO_4-P to Ca^{2+} concentrations of the solutions after 7 days of PO_4-P removal indicate that Ca^{2+} limited HAP precipitation only when EAF-slag was used to treat the most concentrated solution (100 mg P/L), whereas Ca^{2+} never limited HAP precipitation when using BOF-slag (Table 2.7). This differs from that observed when treating synthetic solutions. Most probably, the Ca^{2+} content of the wastewater used for the experiments (40.9-48.6 mg Ca/L) represented a further source of Ca^{2+} ions available for HAP precipitation, thus increasing the PO_4-removal performances. These results are in agreement with other research works (Joko, 1984; Jang and Kang, 2002; Kim et al., 2006a) in which efficient PO_4-P removal via HAP precipitation was reported under conditions of initial Ca^{2+} concentrations of 40-120 mg/L and initial PO_4-P concentrations of 3-10 mg/L.

Table 2.7. Molar ratios PO_4-P/Ca of residual PO_4-P to Ca^{2+} concentrations and molar ratios of Ca removed to PO_4-P removed after 7 days of PO_4-P removal from real wastewater.

Initial PO_4-P (mg P/L)	Residual PO_4-P/Ca[a] (mol P/mol Ca)		Ca removed/PO_4-P removed[b] (mol Ca/mol P)	
	EAF-slag	BOF-slag	EAF-slag	BOF-slag
5	0.01	< 0.01	1.70	4.61
10	0.02	< 0.01	1.20	6.22
20	0.31	< 0.01	1.71	3.50
25	0.54	< 0.01	1.69	1.78
100	29.46	0.24	1.65	1.25

[a]Ca limits HAP precipitation for PO_4-P/Ca > 0.6.

[b]Ratio Ca removed to PO_4-P removed for HAP = 1.67.

The molar ratios of Ca removed to PO_4-P removed ranged from 1.20 to 1.71 mol Ca/mol P for EAF-slag and from 1.25 to 6.22 mol Ca/mol P for BOF-slag (Table 2.7). Since the theoretical molar ratio of Ca to P (Ca/P) for HAP is 1.67, the ratios of Ca removed to PO_4-P removed < 1.67 mol Ca/mol P might be affected by specific PO_4-P adsorption onto the slag surface, whereas the ratios of Ca removed to PO_4-P removed > 1.67 mol Ca/mol P might be affected by $CaCO_3$ precipitation. In fact, PO_4-P adsorption on slag does not involve the consumption of Ca^{2+}, thus leading to molar ratios of Ca removed to PO_4-P removed lower than 1.67. On the other hand, $CaCO_3$ precipitation involves the consumption of Ca^{2+}, thus leading to molar ratios of Ca removed to PO_4-P removed higher than 1.67.

Several studies have demonstrated that $CaCO_3$ precipitation leads to a competing consumption of Ca^{2+}, thus limiting HAP precipitation (Johansson and Gustafsson, 2000; Jang and Kang, 2002). The carbonate alkalinity of the solutions and the dissolution of atmospheric CO_2 may represent the sources of carbonate that enable $CaCO_3$ precipitation.

2.4 Conclusions

This study showed that EAF and BOF steel slags produced in Europe are efficient substrates for PO_4-P removal from wastewater. The major PO_4-P removal mechanism was precipitation of Ca-PO_4-P complexes (most probably HAP), and the main parameters influencing PO_4-P removal were pH, and initial PO_4-P and Ca^{2+} concentrations. It was found that the dissolution

of CaO-slag provided Ca^{2+} ions that were available for HAP precipitation. In addition, CaO-slag dissolution led to an increase in the pH of the solution, thus favouring HAP precipitation.

However, Ca^{2+} release from slag was not always enough to maintain the appropriate Ca^{2+} concentrations to enable HAP precipitation, especially when EAF-slags were used to remove PO_4-P from highly concentrated synthetic solutions. The results of experiments on PO_4-P removal from real wastewater indicated that the Ca^{2+} content of the wastewater represented a further source of Ca^{2+} ions that were available for HAP precipitation, thus increasing the PO_4-P removal efficiencies.

The results of this study suggest that three key parameters should be considered before applying steel slag filters in real WWTPs; one parameter depends on the slag composition, the other two depend on the quality of the wastewater:

(i) CaO content of slag: dissolution of CaO provides Ca^{2+} ions and high pH values of the leachates, thus favouring HAP precipitation;

(ii) Ca^{2+} concentration of the wastewater: represents a further source of Ca^{2+} ions that are available for HAP precipitation;

(iii) Carbonate alkalinity of the wastewater: might lead to a competing consumption of Ca^{2+} due to $CaCO_3$ precipitation, thus limiting HAP precipitation.

Supporting Information

Figure AIII 1 of Annex III shows the shows synthetic solutions and samples of slag after 7 days of batch experiments: solutions showed abundant suspended white precipitates, whereas semples of slag showed white crystals covering the surface.

References of Chapter 2

ASTM D4646-87, 1993. Standard test method for 24-h batch type measurement of contaminant sorption by soils and sediments. American Society for Testing and Materials 44–47.

EN ISO 6878, 2004. Water quality - Determination of phosphorus - Ammonium molybdate spectrometric method.

EN ISO 7980, 1986. Water quality - Determination of calcium and magnesium - Atomic absorption spectrometric method.

Bowden L.I., Jarvis A.P., Younger P.L., Johnson K.L., 2009. Phosphorus removal from wastewaters using basic oxygen steel slag. Environmental Science and Technology 43(7), 2476-2481.

Chazarenc F., Kacem M., Gerente C., Andres Y., 2008. 'Active' filters: a mini-review on the use of industrial by-products for upgrading phosphorus removal from treatment wetlands. Proceedings of the 11th International Conference on Wetland Systems for Water Pollution Control. Indore, India, 1-7 Nov. 2008.

Cucarella V., Renman G., 2009. Phosphorus sorption capacity of filter materials used for on-site wastewater treatment determined in batch experiments. A comparative study. Journal of Environmental Quality 38(2), 381-392.

Drizo A., Comeau Y., Forget C., Chapuis R. P., 2002. Phosphorus saturation potential: a parameter for estimating the longevity of constructed wetland systems. Environmental Science and Technology 36(21), 4642-4648.

Drizo A., Forget C., Chapuis R.P., Comeau Y., 2006. Phosphorus removal by electric arc furnace steel slag and serpentinite. Water Research 40(8), 1547-1554.

Ho Y.S., McKay G., 1998. A comparison of chemisorption kinetic models applied to pollutant removal on various sorbents. Process Safety and Environmental Protection 76(4), 332-340.

Jang H., Kang S.H., 2002. Phosphorus removal using cow bone in hydroxyapatite crystallization. Water Research 36(5), 1324-1330.

Jha V.K., Kameshima Y., Nakajima A., Okada K., 2008. Utilization of steel-making slag for the uptake of ammonium and phosphate ions from aqueous solution. Journal of Hazardous Materials 156(1-3), 156-162.

Johansson L., Gustafsson J.P., 2000. Phosphate removal using blast furnace slags and opoka - mechanisms. Water Research 34(1), 259-265.

Johansson-Westholm L., 2006. Substrates for phosphorus removal-potential benefits for on-site wastewater treatment? Water Research 40(1), 23-36.

Joko I., 1984. Phosphorus removal from wastewater by the crystallization method. Water Science and Technology 17(2-3), 121-132.

Kim E.H., Lee D.W., Hwang H.K., Yim S., 2006a. Recovery of phosphates from wastewater using converter slag: Kinetics analysis of a completely mixed phosphorus crystallization process. Chemosphere 63(2), 192-201.

Kim E.H., Yim S., Jung H., Lee E., 2006b. Hydroxyapatite crystallization from a highly concentrated phosphate solution using powdered converter slag as a seed material. Journal of Hazardous Materials 136(3), 690-697.

Lagergren S., 1898. About the theory of so-called adsorption of soluble substances, Kungliga Svenska Vetenskapsakademiens. Handlingar 24(4), 1-39.

Lu S., Bai S., Shan H., 2008. Mechanisms of phosphate removal from aqueous solutions by blast furnace slag and steel furnace slag. Journal of Zhejiang University-Science A 9(1), 125-132.

Motz H., Geiseler J., 2001. Products of steel slags: an opportunity to save natural resources. Waste Management 21(3), 285-293.

Nair P.S., Logan T.J., Sharpley A.N., Sommers L.E., Tabatabai M.A., Yuan T.L., 1984. Interlaboratory comparation of a standardized phosphorus adsorption procedure. Journal of Environmental Quality 13(4), 591-595.

Proctor D.M., Fehling K.A., Shay E.C., Wittenborn J.L., Green J.J., Avent C., Bigham R.D., Connolly M., Lee B., Shepker T.O., Zak M.A., 2000. Physical and chemical characteristics of blast furnace, basic oxygen furnace, and electric arc furnace steel industry slags. Environmental Science and Technology 34(8), 1576-1582.

Stumm W., Morgan J.J., 1996. Aquatic chemistry – Chemical equilibria and rates in natural waters. 3rd edition, Wiley-Interscience Publication, USA (Iowa), pp. 1022.

Valsami-Jones E., 2001. Mineralogical controls on phosphorus recovery from wastewaters. Mineralogical Magazine 65(5), 611-620.

Vohla C., Kõiv M., Bavor H.J., Chazarenc F., Mander U., 2011. Filter materials for phosphorus removal from wastewater in treatment wetlands – A review. Ecological Engineering 37(1), 70-89.

Wang G., Wang Y., Gao Z., 2010. Use of steel slag as a granular material: Volume expansion prediction and usability criteria. Journal of Hazardous Materials 184(1-3), 555-560.

Xue Y., Hou H., Zhu S., 2009. Characteristics and mechanisms of phosphate adsorption onto basic oxygen furnace slag. Journal of Hazardous Materials 162(2-3), 973-980.

Xiong J., He Z., Mahmood Q., Liu D., Yang X., Islam E., 2008. Phosphate removal from solution using steel slag through magnetic separation. Journal of Hazardous Materials 152(1), 211-215.

Yamada H., Kayama M., Saito K., Hara M., 1986. A fundamental research on phosphate removal by using slag. Water Research 20(5), 547-557.

CHAPTER 3 Steel slag filters to upgrade phosphorus removal in small wastewater treatment plants: two years of column experiments

Abstract

Electric arc furnace steel slag (EAF-slag) and basic oxygen furnace steel slag (BOF-slag) were tested in continuous flow column experiments to determine their capacities to remove phosphorus (P) from a synthetic wastewater containing initially 10 mg P/L. The influences of various parameters, including ratio of width to length of the column (0.21 and 0.42), slag type (EAF and BOF), slag size (5-16 mm, 6-12 mm, 20-40 mm and 20-50 mm) and slag composition (CaO content), on P removal performances were studied. P removal mechanisms were also investigated through various chemical and mineralogical analyses, which were performed to investigate the surface of slag before and after their use in the columns. P removal occurred predominantly via CaO-slag dissolution followed by Ca phosphate precipitation. Among the findings, it was confirmed that P removal performances improved with decreasing the size of slag, most probably because the smaller the size, the greater the specific surface available for CaO-slag dissolution. Over a period of 100 weeks of column experiments, small-size slag (5-16 mm) removed more than 98% of the inlet total phosphorus, reaching retention levels of 1.71 g P/kg for EAF-slag and of 1.98 g P/kg for BOF-slag. On the contrary, big-size slag (20-50 mm) showed lower P removal efficiencies, which were negatively affected by massive releases of pre-accumulated P precipitates. However, the results of this study showed that column performances can be improved by enhancing the design of the filter. It was found that hydraulic and P removal performances improved with decreasing the aspect ratio of width to length of the column and decreasing the size of slag, most probably because filtration of P precipitates was improved.

3.1 Introduction

Phosphorus (P) is a significant component of many wastewaters (Metacalf and Eddy, 2003). It represents an essential nutrient for biomass growth in several ecosystems. However, an excessive intake of P in water bodies such as rivers, lakes or lagoons, causes an abnormal growth of algae and aquatic plants resulting in the degradation of the water quality. When algae and aquatic plants die, they sink to the bottom of the water body and decay by microbial decomposition, thus reducing the concentration of dissolved oxygen and forming P-rich sediments. Over time, these sediments release P that is available for biomass growth, thus resulting in trophic cycles and algal blooms (Recknagel et al., 1995). This phenomenon of water quality degradation due to trophic cycles is commonly referred to as "eutrophication" (Crouzet et al., 1999).

In Europe, the EU Water Framework Directive (2000/60/EC) established the environmental objective of "good water status" to be achieved in all the water bodies by 2015. Consequently, the research on potential low-cost solutions for P removal treatment systems has become a priority for scientists during the past decade. One appropriate technology for upgrading P removal in small wastewater treatment plants (WWTPs) is the filtration through materials with high affinities for P binding (Johansson-Westholm, 2006; Vohla et al., 2011).

Since the 1980s, the affinity of steel slag for P binding has been studied with the aim of using a by-product of the steel industry as filter substrate to remove P from wastewater (Yamada et al., 1986). Steel and iron industry produces mostly four types of slag: blast furnace slag (BF-slag), which originates from the iron production in a blast furnace; basic oxygen furnace slag (BOF-slag), which originates from the further refining of iron in a basic oxygen furnace; electric arc furnace slag (EAF-slag), which is derived from melting recycled scrap in an electric arc furnace; melter slag, which is produced when iron sand is converted to melter iron (Proctor et al., 2000; Pratt et al., 2007). Steel slag is primarily made of iron (Fe) and calcium oxide (CaO), as the result of the use of fluxing agents (mainly lime) during the steelmaking process (Motz and Geiseler, 2001).

Several international studies have demonstrated that steel slag is a suitable substrate for P removal from wastewater (Table 3.3). P retention capacities reported from batch experiments ranged from less than 1 to up to 80 mg P/g (Xiong et al., 2008; Bowden et al., 2009), and main mechanism of P removal was related to CaO-slag dissolution followed by Ca phosphate precipitation (Bowden et al., 2009; Barca et al., 2012). Although column experiments have

confirmed that steel slags are efficient filter substrates for P removal (Johansson, 1999; Shilton et al., 2005; Drizo et al., 2006; Bowden et al., 2009), some studies have also shown some limitations such as high pH-effluents due to excessive CaO-slag dissolution and clogging due to excessive $CaCO_3$ precipitation (Chazarenc et al., 2007; Lee et al., 2010). Therefore, further investigations are needed to investigate the influence of various parameters including slag size and composition, filter design and flow rate on treatment and hydraulic performances of steel slag filters.

The European research project SLASORB (funded by the Research Fund for Coal and Steel, RFCS) aims at developing the use EAF-slag and BOF-slag produced in Europe as substrate in filters designed to remove P from the effluents of small WWTPs. Within the framework of the project SLASORB, this study aimed to investigate the effect of different slag size and composition, and different column design on the treatment and hydraulic performances of continuous sub-horizontal flow slag filters. P removal mechanisms were also investigated through various chemical and mineralogical analyses, including X-ray fluorescence (XRF), scanning electron microscopy (SEM), energy dispersive spectrometry (EDS), X-ray diffraction (XRD) and wet chemical extractions, which were performed to investigate the surface of slag before and after their use in the columns.

3.2 Materials and methods

3.2.1 Experimental setup

Samples of slag used in this study were selected based on their P removal capacities that were determined by a comparative batch study (Barca et al., 2012). The selected samples were EAF-slag from the production site of Esch Belval (Luxemburg) and BOF-slag from the production site of Fos sur Mer (France). Two different sizes were tested: small-size slag (5-16 mm for EAF-slag, 6-12 mm for BOF-slag), and big-size slag (20-40 mm for EAF-slag, 20-50 mm for BOF-slag). These granular sizes were supposed to be large enough to prevent column clogging, as shown in previous studies (Chazarenc et al., 2007; Weber et al., 2007). The slag samples used in this study had a bulk density of about 1.8 g/cm^3 (EAF-slag) and 1.6 g/cm^3 (BOF-slag), and a bulk porosity of about 50%.

The experimental setup consisted of six columns built in two different designs (Figures 3.1): four small-size columns (about 42 L of total volume), and two big-size columns (about 84 L of total volume). The design of the columns was adapted from a previous study (Anjab,

2009), which investigated the effect of different sizes of slag on treatment and hydraulic performances in column experiments. The columns were designed according to a ratio of width to length <0.5, because low ratio of width to length may favour dissipation of initial turbulence and favour a uniform distribution of the flow along the cross section of the columns. Small size columns had a width of 0.15 m and a length of 0.7, thus leading to a ratio of width to length of about 0.21, whereas big size columns had a width of 0.3 m and a length of 0.7, thus leading to a ratio of width to length of about 0.42.

Also, the columns were designed according to a minimum ratio of width of the column to size of slag of 10, this because the ratios of width of the column to size of material higher than 10 may limit wall effect (Zeiser et al., 2001). Big size columns were filled with big-size EAF-slag and big-size BOF-slag (column codes: EAF-big and BOF-big, respectively). Two of the small-size columns were filled with small-size EAF-slag and small-size BOF-slag (column codes: EAF-small and BOF-small, respectively). The remaining two small-size columns were filled with small-size EAF-slag and small-size BOF-slag as above, but with the addition of a vertical layer of silica sand (granular size 1-2.5 mm) replacing 20% of slag volume just before the outlet, this to improve the filtration of Ca-P precipitates (column codes: EAF-small + sand and BOF-small + sand, respectively) (Figure 3.1).

During the full period of operation, the columns were fed with a synthetic P solution (about 10 mg P/L, tap water + KH_2PO_4) at a continuous sub-superficial horizontal-flow of 0.6 L/h (small-size columns) and 1.2 L/h (big-size columns), thus resulting in a void hydraulic retention time (HRTv) of about 24 h. The inlet P concentration of 10 mg P/L was selected to be representative of a municipal wastewater (4-16 mg P/L, Metcalf and Eddy, 2003). The sub-horizontal flow was adopted to limit the contact of wastewater to air and hence to reduce dissolution of atmospheric CO_2. In fact, CO_2 in water is an inhibitor of P precipitation (Valsami-Jones, 2001), and also it may favour $CaCO_3$ precipitation, thus leading to clogging in CaO-rich filter materials (Chazarenc et al., 2007). The column experiments were performed under room temperature condition (approximately 20 °C). Figure 3.2 shows the cross section view of the columns, indicating the inlet and the outlet of the columns.

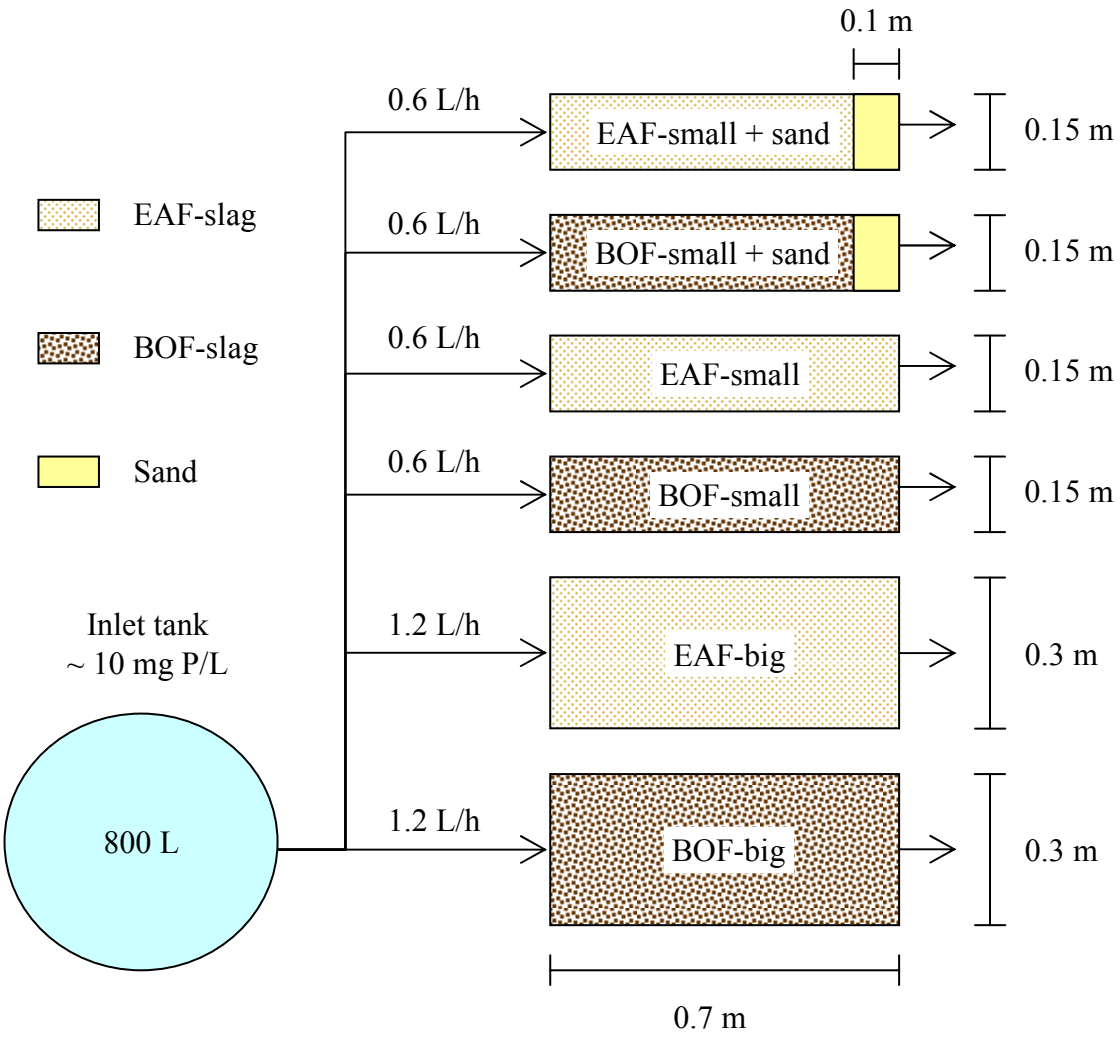

Figure 3.1. Schematic plan view of the experimental setup.

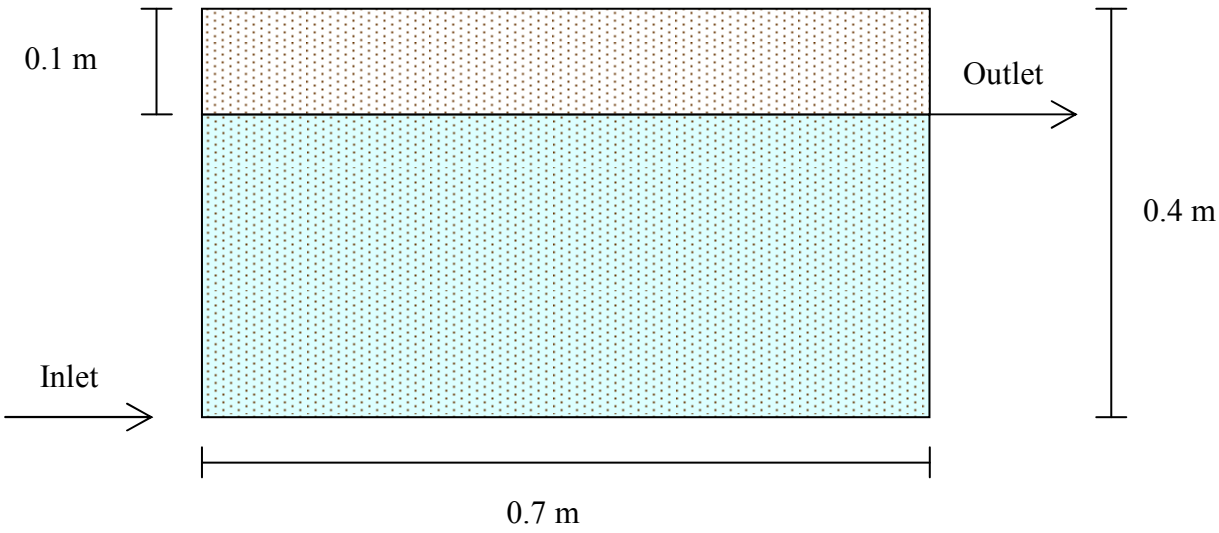

Figure 3.2. Column design: cross section view.

3.2.2 Experimental methods

3.2.2.1 Hydraulic performances

Tracer tests were performed during week 0 (before starting regular operation), during weeks 52-54, and during weeks 96-98, using fluorescein and lithium salt (LiCl) as tracer substances. These experiments aimed at evaluating hydrodynamics of the columns and their evolution over time. The effect of different column design (ratio of width to length of 0.2 and 0.4) and size of slag on hydraulic efficiency was also investigated. A well known amount of tracer was injected to each column (14 mL of a solution 1 g LiCl/L and/or 25 mL of a solution 4 g of fluorescein/L for small-size columns; 30 mL of a solution 1 g LiCl/L and/or 50 mL of a solution 4 g of fluorescein/L for big-size columns). Then, the outlet tracer concentrations were monitored over time until more than 75% of the tracer was recovered (approximately 72-96 h after the injection).

The average retention time of the fluid in the column (T_A) was calculated by the equation (3.1) (Metcalf and Eddy, 2003), where Ci is the outlet tracer concentration at the time ti (mg/L), ti is the time from the tracer injection (h), Δti is the interval between two consecutive measures (h) and n is the number of measures (-).

$$T_A = \frac{\sum ti \times Ci \times \Delta ti}{\sum Ci \times \Delta ti} \qquad \text{for } i = 1,\ldots,n; \tag{3.1}$$

Several empirical models have been used in the literature to study the internal hydrodynamics in sub-horizontal flow reactors filled with various types of filter media including sand, gravel, and clay aggregates (Chazarenc et al., 2003; Suliman et al., 2006; Alcocer et al., 2012). Most of these models were developed to reproduce the experimental retention time distribution of the flow in filter systems, and they are based on the theories of the continuous stirred tank reactor (CSTR) and of the plug flow reactor (PFR) (Werner and Kadlec, 2000). In this study, the empirical flow model of Wolf and Resnick (1963) (equation 3.2) was employed to describe the hydraulic behaviour of the slag columns. This enabled the results to be compared to those of a recent study (Alcocer et al., 2012), which employed the equation (3.2) to investigate the effect of different filter design, medium size, and inflow rate on the hydraulic performances of sub-horizontal flow filters. In equation (3.2), F(t) is the fraction of the tracer that exited the filter at the time t (-), t is the time from the tracer injection (h), T is the theoretical HRTv (h), PF is the plug flow fraction (-) and DV is the dead volume fraction (-).

$$F(t) = 1 - \exp\left[\left(\frac{t/T}{(1-PF)(1-DV)} - \frac{PF}{1-PF}\right)\right] \quad (3.2)$$

If equation (3.2) is applicable, PF indicates the fraction of fluid that presents a constant velocity along any cross-section of the filter, according to the theory of the plug flow reactor. Instead, DV indicates the fraction of fluid that stagnates in the reactor and does not participate to reactions (Alcocer et al., 2012).

3.2.2.2 Water quality monitoring

Water samples (about 100 mL) were collected from the inlet tank and from the outlet of each column approximately every two weeks during the full period of column operation. pH, total phosphorus (TP), phosphate (PO_4-P) and Ca^{2+} concentrations of the water samples were measured: pH was measured in fresh water samples; TP concentrations were determined after acidification of the samples by adding some drops of 1M HCl to dissolve suspended Ca phosphate precipitates; PO_4-P and Ca^{2+} concentrations were determined after filtration of the water samples trough 0.45 μm filters, to remove suspended Ca phosphate precipitates. Additional water samples were collected sporadically from the inlet tank to measure total alkalinity (TA).

3.2.2.3 Chemical and mineralogical investigations on slag

Column EAF-small + sand and column BOF-small + sand were deconstructed after 52 weeks of operation. Since the added value of the sand layer was not observed (by comparison with columns EAF-small and BOF-small, data not shown), it was thus decided to use their slag content (containing accumulated P) for chemical and mineralogical investigations. Only the samples taken from the zone close to the inlet of the columns were considered for chemical and mineralogical analyses, as shown in Figure 3.3: in fact, since this zone was more exposed to the inlet P-rich solution, these samples were supposed to show the higher P retention levels.

The slag samples (5-16 mm for EAF-slag, 6-12 mm for BOF-slag) were dried overnight at 55 °C before analyses, this to prevent mineralogical changes deriving from high temperature drying. Analogous chemical and mineralogical analyses were performed by using fresh slag samples (before the use in the columns). This enabled the results to be compared to evaluate the changes in chemistry and mineralogy of the surface of slag before and after the column experiments.

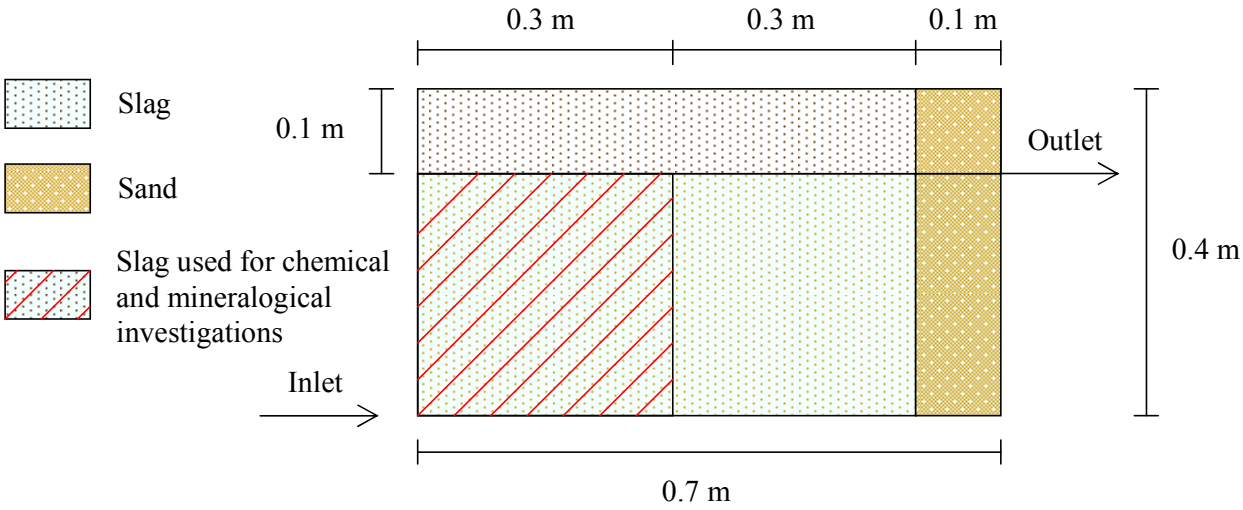

Figure 3.3. Cross section view of column EAF-small + sand and column BOF-small + sand: dotted area shows slag used for chemical and mineralogical investigation after 52 weeks of column operation.

X-ray fluorescence (XRF) and X-ray diffraction (XRD) analyses were performed to determine the semi-quantitative chemical and mineralogical composition of slag, whereas scanning electron microscopy (SEM) observations and energy dispersive spectrometry (EDS) analyses were performed to examine the surface of slag before and after 52 weeks of column experiments (column EAF-small + sand and column BOF-small + sand). The grains of slag (size <10 mm) were coated with conductive platinum before SEM observations (Jeol JSM 7600 F, Oxford Instruments, London, UK).

Additional XRD analyses were performed to investigate the mineralogical composition of the precipitates covering the surface of slag after 52 weeks of column experiments (column EAF-small + sand and column BOF-small + sand). The samples of slag were shaken manually on a grinder and the fraction < 1 mm was recovered. We assumed that this fraction represented the precipitates deposited on slag during the water filtration. Before XRD analysis, these precipitates were crushed in a mortar to produce fine and homogeneous particles.

Leaching experiments were conducted according to a procedure adapted from EN 12457-1: 2002 with original size slag (5-16 mm for EAF-slag, 6-12 mm for BOF-slag) and a ratio of extracting solution to slag of 2 L/kg, this to evaluate the production of environmental hazardous leachates from slag before and after 52 weeks of column experiments (column EAF-small + sand and column BOF-small + sand).

The sequential extraction procedure of Tiessen and Moir (1993), as adapted by Headley et al. (2003), was employed to quantify the fractions of different P compounds in slag before and after 52 weeks of column experiments (column EAF-small + sand and column BOF-small + sand). Four fractions of P were sequentially extracted from 20 g of slag in original size (5-16 mm for EAF-slag, 6-12 mm for BOF-slag):

i. Bicarbonate extractable P fraction was extracted in 200 mL of 0.5 M $NaHCO_3$. This fraction represents weakly bound P;

ii. Hydroxide extractable P fraction was extracted in 200 mL of 0.1 M NaOH. This fraction represents Fe and Al associated P;

iii. Diluted HCl extractable P fraction was extracted in 200 mL of 1 M HCl. This fraction is defined as Ca associated P;

iv. Highly concentrated HCl extractable P fraction was extracted in 50 mL of ~12 M HCl in a 20 min water bath at 80°C. This fraction represents P in very stable compounds. Drizo et al. (2002) employed the procedure of Tiessen and Moir (1993) to quantify the proportion of P bound to mineral compounds in EAF-slag, and they defined the hot concentrated HCl extract as Ca associated P in the stable residual pools.

The extractions (i), (ii) and (iii) were conducted with a slag to extracting solution ratio of 0.1 kg/L (adapted from EN 12457-2: 2002) and 16 h extraction time at 20 °C and at 125 rpm of agitation. After each extraction, the samples were washed with 25 mL of 1 M KCl to recover P re-adsorbed on slag surface, and the KCl washes were added to the supernatant solution, as already done by (Headly et al., 2003). All the extractions were performed in duplicate.

3.2.3 Analytical methods

The pH values of fresh water samples were measured using a model C 561 conductivimeter /pH-meter (Consort, Turnhout, Belgium). TP and PO_4-P analyses were performed according to the Ammonium Molybdate Spectrometric Method (EN ISO 6878, 2004), whereas Ca analyses were performed according to the Atomic Absorption Spectrometric Method (EN ISO 7980, 1986). Phosphate concentrations were measured using a model U DR/4000 spectrophotometer (Hach Company, Loveland, USA), whereas Ca concentrations were measured using a model A Analyst 200 spectrophotometer (Perkin Elmer, Waltham, USA). Total alkalinity was measured according to the titrimetric determination method (EN ISO

9963-1, 1994). The limit of detection for the analysis was determined for each set of experiments from the analysis of blanks. All chemicals used were of analytical grade.

3.3 Results and Discussion

3.3.1 Hydraulic performances

The normalized retention time distribution curves (RTD-curves) representing the ratio of outlet tracer concentration (Ci) to inlet tracer concentration (C_0) as a function of the time are shown in Figure 3.4. The time required to observe at the outlet the peak in tracer concentration ranged from about 6 to about 28 h, depending on the week of operation, size of the column, and size of slag.

Great differences were observed between the hydraulic behaviour of the columns before the regular operation (week 0) (Figure 3.4 A), and the hydraulic behaviour of columns during regular operation (weeks 52-54 and 96-98) (Figure 3.4 B and C). In fact, in week 0, RTD-curves showed several peaks of tracer at times very lower than the theoretical HRTv, thus suggesting preferential paths and short-circuiting effects (Figure 3.4 A). Then, with only the exception of column BOF-big, the hydraulic performances appeared to improve during the column operation, as suggested by the single and narrow peaks of tracer close to the theoretical HRTv, which usually indicate a plug flow with low diffusion, low short-circuiting and low wall effects (Chazarenc et al., 2003; Alcocer et al., 2012). This likely depended on the settling of the slag grains and on phenomena of $CaCO_3$ and Ca phosphate precipitation that occurred during the operation of the columns. Most probably, the precipitation of $CaCO_3$ and Ca phosphate on the surface of the slag grains during the water filtration cut off the preferential paths, thus favouring a better distribution of the flow along the cross surface of the columns. A similar effect of filter porosity reduction on hydraulic performances of sub-horizontal filters was already observed in a recent study (Suliman et al., 2006).

However, the tracer tests were performed by using different tracer substances, a chemical salt (LiCl) and an organic compound (fluorescein), and this may lead to difficulties in comparing the results of the different experiments. Nevertheless, Williams and Nelson (2011) recently showed a high repeatability of the results of tracer tests performed with two different tracer substances, a chemical salt (bromide) and an organic compound (rhodamine-WT), and this enabled the results of different tracers to be compared.

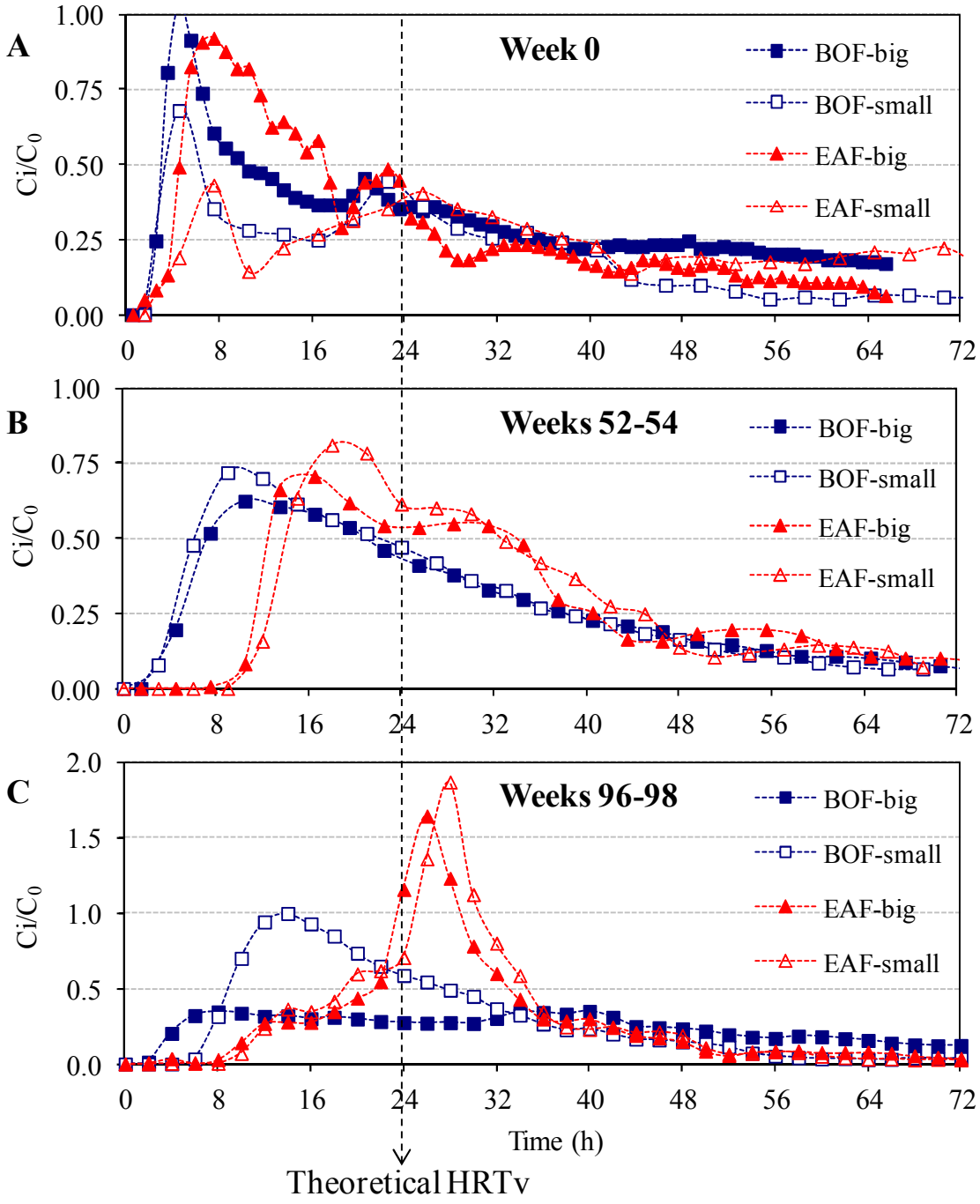

Figure 3.4. Normalized retention time distribution curves (RTD-curves) representing the ratio of outlet tracer concentrations Ci to the tracer concentration C_0 (C_0 is the ratio of the total-injected tracer mass and the void volume of the filter): (A) week 0; (B) week 52-54; (C) week 96-98.

Table 3.1 shows the average retention time T_A (calculated by equation 3.1) and the fraction of plug flow (PF) (evaluated by employing equation 3.2). The correlation coefficients for equation (3.2) were always >0.9, thus indicating that the empirical flow model described the hydrodynamics of the columns well. Dead volume fractions (DV) have been always < 0.04,

thus suggesting that only a small fraction of the fluid stagnated into the columns and most of the void volume was effectively exploited for filtration (Alcocer et al., 2012). The results shown in Table 3.1 appear to confirm that hydraulic performances of the columns improved after the start of regular operation, as suggested by the increases in PF and/or the T_A closer to the theoretical HRTv of 24 h (Table 3.1). In contrast to the other columns, BOF-big in week 96 showed a lower-slope RTD-curve (Figure 3.4 C) and an increase in T_A (Table 3.1), thus suggesting higher dispersion, higher wall effect and higher retention time. Most probably, excessive $CaCO_3$ and Ca phosphate precipitation in column BOF-big (Figure AIII.5, Annex III), rather than reduce porosity and increase the velocity of the flow, cut off the preferential paths, but, also, reduced the passage section of the fluid between the grains, thus increasing dispersion, wall effects and retention time.

Table 3.1. Tracer tests: average retention time (T_A) and fractions of plug flow (PF).

Week of operation	Tracer substance	BOF-big W/L[a] = 0.42		EAF-big W/L[a] = 0.42		BOF-small W/L[a] = 0.21		EAF-small W/L[a] = 0.21	
		T_A (h)	PF (-)	T_A (h)	PF (-)	T_A (h)	PF (-)	T_A (h)	PF (-)
0	Li	26.3	0.27	22.8	0.30	31.5	0.30	41.0	0.45
52-54	Li	30.0	0.38	33.9	0.56	25.0	0.37	31.0	0.53
96-98	Fluorescein	38.6	0.36	31.0	0.47	25.0	0.49	30.0	0.57

[a] Ratio of width to length of the columns.

It was found that, in general, small-columns filled with small size slag showed better hydraulic performances than big-columns filled with big-size slag, as indicated by the shapes of the RTD-curves and the T_A close to the theoretical HRTv of 24 h. This probably depended on the decrease in the ratio of width to length of the columns, which likely favoured the dissipation of the initial turbulence of the system, as already shown by Alcocer et al. (2012). Moreover, the use of smaller medium size probably favoured a more uniform distribution of the flow along the cross section of the column, thus reducing short-circuiting effects and showing retention times closer to the theoretical HRTv (Alcocer et al., 2012).

As regards the slag type, EAF-columns showed generally higher retention time than BOF-columns, thus suggesting a higher void volume (Suliman et al., 2006). This difference likely depended on the higher CaO content of BOF-slag. In fact hydration of CaO-slag may have led to volume increase of slag (Wang et al., 2010), thus reducing the void volume of the filters.

Since high plug flow with low dispersion, low dead volume, low short circuiting, and low wall effect is the type of behaviour that is desirable to optimize treatment in sub-surface flow filters (Kadlec and Wallace, 2009), it can be concluded that the small-columns filled with small-size slags showed the best hydraulic behaviour.

3.3.2 P removal performances

Water quality parameters over 100 weeks of column monitoring are shown in Table 3. 2. The mean outlet pH and Ca^{2+} concentrations were significantly higher than those of the inlet. This was most probably due to CaO-slag dissolution with production of Ca^{2+} and OH^- ions. The high CaO content of BOF-slag may account for the higher outlet pH and Ca^{2+} concentrations observed using BOF-slag (Table 3.4).

Table 3.2. Water quality parameters of the inlet P solution and of the outlet of the slag columns over the 100-week period of monitoring: mean values ± standard deviation (range of min-max values) n° of measures.

Parameter (unit of meas.)	Inlet P solution	Outlet of the columns			
		BOF-big	EAF-big	BOF-small	EAF-small
TP (mg P/L)	10.24 ± 0.97 (8.45-12.43) n = 46	4.51 ± 8.33 (<LQ[a]-42.79) n = 46	1.33 ± 1.53 (<LQ[a]-8.07) n = 46	0.07 ± 0.13 (<LQ[a]-0.70) n = 46	0.19 ± 0.19 (<LQ[a]-1.02) n = 46
PO_4-P (mg P/L)	10.09 ± 0.76 (8.93-11.91) n = 46	0.35 ± 1.14 (<LQ[a]-7.81) n = 46	1.04 ± 0.94 (<LQ[a]-5.40) n = 46	0.03 ± 0.07 (<LQ[a]-0.28) n = 46	0.15 ± 0.15 (<LQ[a]-0.72) n = 46
pH (-)	7.7 ± 0.2 (7.1-8.0) n = 46	10.8 ± 0.6 (9.8-12.2) n = 46	8.7 ± 0.5 (7.5-10.3) n = 46	11.5 ± 0.4 (11.1-12.6) n = 46	9.5 ± 0.8 (8.4-11.0) n = 46
Ca (mg Ca/L)	33.9 ± 7.5 (14.3-46.5) n = 45	43.7 ± 24.1 (18.7-127.8) n = 45	35.4 ± 8.3 (15.5-54.6) n = 45	83.1 ± 80.3 (45.7-466.2) n = 45	29.6 ± 7.7 (15.1-46.9) n = 45

[a] Limit of Quantification: 0.01 mg P/L.

The mean outlet TP and PO_4-P concentrations were markedly lower than those of the inlet solution, indicating very high P removal performances. Table 3.2 clearly shows that columns filled with small-size slag were more efficient in P removal than columns filled with big-size

slag. It is likely that, since the main mechanism of P removal was related to CaO-slag dissolution followed by Ca phosphate precipitation, the smaller the size of slag, the greater the specific surface available for CaO dissolution (Vohla et al., 2011). However, it was also observed that small-size slag produced a higher outlet pH than big-size, most probably as results of excessive CaO dissolution. The inlet P solution treated in this study had a mean TA of 140 mg $CaCO_3$/L (6 measures, range min-max value 80-200 mg $CaCO_3$/L) (soft water, according to French classification). TA is a measure of the concentrations of species of the carbonate system (CO_2, HCO_3^-, CO_3^{2-}), and it is usually employed as an indirect measure of the capacity of the water to resist changes in pH (Metcalf and Eddy, 2003). It is well known that carbonates are strong inhibitors for P precipitation, because they block Ca phosphate nucleation (Valsami-Jones, 2001) and also they compete with phosphate in the process of Ca carbonate precipitation (House, 1999; Johansson and Gustafsson, 2000). The relatively low TA of the inlet P solution suggested a low inhibition effect for Ca phosphate precipitation and also a low capacity to resist changes in pH, as appears to be confirmed by the strong increase in pH of the column effluents.

Figure 3.5 shows the evolution of pH values and TP, PO_4-P, and Ca^{2+} concentrations during the 100-week period of column operation. During the first 65 weeks of operation, outlet TP concentrations remained in the same low levels of outlet PO_4-P concentrations for all the columns. This suggested that, if PO_4-P precipitation occurred, P precipitated were accumulated into the columns by filtration, as already shown by Claveau-Mallet et al. (2012).

After week 65, massive releases of TP were observed in the column filled with big-size BOF-slag (BOF-big) (Figure 3.5 A), thus suggesting that a level of TP saturation was achieved. Since PO_4-P removal efficiencies of column BOF-big remained very high during the full period of operation (Figure 3.5 B), these massive releases of TP were most probably due to the release of P precipitates previously accumulated into the column. Most probably, CaO hydration and carbonation during water filtration led to a decrease in void volume available for accumulation of P precipitates. Differently from column BOF-big, column filled with small-size BOF-slag (BOF-small) showed very high TP removal performances (always >92%), thus suggesting that small-size slag was more efficient in the filtration of P precipitates than big-size slag.

As shown in Figures 3.5 C and D, the pH and Ca^{2+} concentrations of the column effluents appeared to decrease during the column operation, and this seemed to indicate that the rate of CaO-slag dissolution decreased over time.

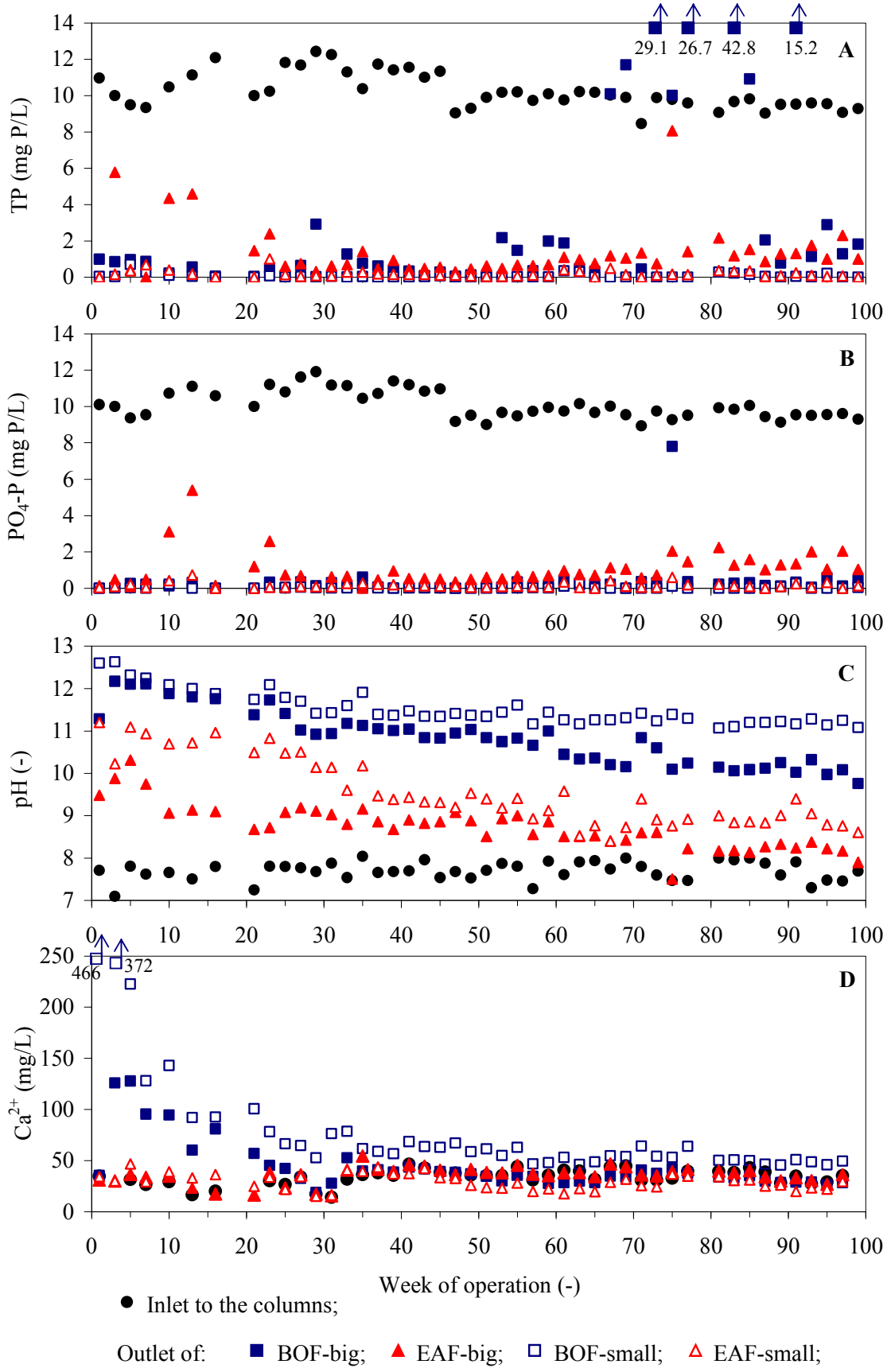

Figure 3.5. Inlet and outlet levels of TP (A), PO_4-P (B), pH (C) and Ca^{2+} (D) over 100 weeks of column monitoring.

The results of this study were compared to those of previous column experiments that tested P removal performances of Ca-rich industrial by-products (Table 3.3). Among the material tested, EAF-slag and BOF-slag showed the highest potential for TP removal, as shown by the higher TP removal efficiency (>99%, Drizo et al., 2006) and by the higher amount of TP retained (8.2 mg P/g BOF-slag, Bowden et al., 2009).

TP removal performances varied according to the chemical composition of the materials and to the experimental parameters that were established (Table 3.3). Overall, TP removal efficiencies and/or amount of TP removed appeared to increase with increasing CaO-content of the materials, increasing HRTv and with decreasing media size, most probably because the contact surface of material to solution was enlarged, thus favouring CaO dissolution and Ca phosphate precipitation. In addition, the use of smaller medium size favoured filtration of P precipitates, thus improving TP removal efficiencies.

As shown in Table 3.3, the TP retention levels ranged from less than 1 to up than 8 mg P/g of material. However, in most of the study presented in Table 3.3, TP saturation levels of the material were usually not reached, and TP retention levels appeared to increase with increasing duration of the experiments and/or with increasing TP concentrations of the inlet solutions (Drizo et al., 2002 and 2006; Bowden et al., 2009).

To date, there are not enough data in the literature to assess which type of flow (horizontal or vertical, downstream or upstream) is desirable to optimize P treatment in filters filled with Ca-rich materials (Table 3.3). However, it seemed that saturated condition is the most desirable flow condition to reduce atmospheric CO_2 dissolution in the water and hence to avoid inhibition of P precipitation (Valsami-Jones, 2001) and to prevent filter clogging due to $CaCO_3$ precipitation (Chazarenc et al., 2007).

Claveau-Mallet et al. (2012) investigated the effect of the water velocity on P removal performances of columns filled with EAF-slag. They found that P retention levels increased with decreasing the water velocity. Most probably, higher water velocity had the effect of leaching out of the columns the P precipitates, whereas lower water velocity favoured settling of the P precipitates into the columns.

Table 3.3. Main results from selected studies that tested Ca-rich industrial by-product in column experiments (adapted from Vohla et al., 2011).

Authors	Material	Size (mm)	CaO (%)	Volume (L)	Flow type[a]	Inlet TP (mg/L)	HRTv (h)	Duration (week)	TP removal (%)	TP removed (mg P/g)
This study	EAF-slag	5-16	24.9	42	HF	10.2 (mean)	24	100	98	1.71
	EAF-slag	20-40	24.9	84	HF	10.2 (mean)	24	100	86	1.51
	BOF-slag	6-12	44.1	42	HF	10.2 (mean)	24	100	99	1.98
	BOF-slag	20-50	44.1	84	HF	10.2 (mean)	24	67	94	1.26[b]
Gustafsson et al., 2008	BF-slag	0-4	21.6 (Ca)	4	UVF	4.5 (mean)	7	68	86	1.0-3.1
Drizo et al., 2002	EAF-slag	2.5-10	21.7 (Ca)	1.2	SVF	350-400	8.3	40	N.A.	1.35[b]
Drizo et al., 2006	EAF-slag	2.5-10	30.4	8	SVF	20-400	24	26	>99	2.2
Chazarenc et al., 2007	EAF-slag	2-5	27.7	6	SVF	6-12	2-4	52	80	0.3
Claveau-Mallet et al., 2012	EAF-slag	5-10	30	3	SVF	26	16.3	90	>99	~ 6
Bowden et al., 2009	BOF-slag	<20	42-44	N.A.	N.A.	100-300	8	44	24	8.4
Shilton et al., 2005	Melter slag	N.A.	N.A.	18	N.A.	10	12	30	27	N.A.
Liira et al., 2009	Oil shale ash	2-5	29.2	12.6	HF	8-15	6-12	22	>40	N.A.

[a] Horizontal Flow (HF), Saturated Vertical Flow (SVF), Unsaturated Vertical Flow (UVF).

[b] TP saturation level was achieved.

3.3.3 Chemical and mineralogical investigations on slag

Table 3.4 shows the results of XRF and XRD analyses of slag before and after 52 weeks of column experiments (column EAF-small + sand and column BOF-small + sand). XRF analyses confirmed that BOF-slag is richer in CaO than EAF-slag, whereas EAF-slag is richer in Fe_{tot} and Al_2O_3 than BOF-slag (Table 3.4). These results on slag composition are in agreement with the findings of other studies (Motz and Geiseler, 2001; Wang et al., 2010). As shown in Table 3.4, remarkable changes in chemical composition were not observed after the use of slag in column experiments.

XRD analyses showed the presence of $CaCO_3$ in the crystalline form of calcite on slag after 52 weeks of column experiments (Table 3.4). This suggested precipitation of $CaCO_3$ followed by crystallisation in the form of calcite on the slag surface during the column operation, as already shown in a previous column experiment (Bowden et al., 2009).

XRD analyses also showed that BOF-slag still had a high content of free lime (CaO_{free}) after 52 weeks after 52 weeks of column experiments (Table 3.4). This appears to contradict the knowledge about the behaviour of CaO_{free} in aqueous solution, because it is well known that CaO_{free} is highly reactive and readily dissolves in solution to produce Ca^{2+} and OH^- ions (National Lime Association, USA). Most probably, during the column experiments the surface of slag was covered over time by a secondary layer of precipitates, including Ca phosphates and $CaCO_3$. Then, these precipitates crystallized into HAP and calcite to form a finely distributed crystalline layer over the slag surface that probably hindered further CaO_{free} dissolution, as appeared to be confirmed by the decrease in pH and Ca^{2+} concentrations of the column effluent over time, during the column operation (Figures 3.5 C and D). The results of recent studies that have investigated the capacity of steel slag for sequestration of CO_2 appears to confirm that the formation of a $CaCO_3$ layer coating the slag surface after the carbonation process hinders CaO_{free} dissolution (Huijgen et al., 2005; Navarro et al., 2010).

Table 3.4. Semi quantitative chemical and mineralogical compositions of slag before and after 52 weeks of column experiments (weight %). Results from XRF and XRD analyses.

Component	EAF-slag		BOF-slag	
	Before use	After 52 weeks	Before use	After 52 weeks
Fe_{tot}	24.9	N.A.	22.4	N.A.
CaO	24.9	23.6	44.1	42.0
SiO_2	13.9	10.8	12.1	8.9
Al_2O_3	9.2	10.3	1.4	1.7
MnO	8.5	8.6	3.5	3.4
MgO	1.9	2.2	6.9	7.9
P_2O_5	0.46	0.65	1.85	1.84
Cr_2O_3	3.70	3.06	0.25	0.32
CaO_{free}	<LQ[a]	<LQ[a]	6.4	5.5
Calcite ($CaCO_3$)	<LQ[a]	2	<LQ[a]	6

[a] Limit of quantification: 0.2%.

Leaching experiments confirmed that steel slag has a strong tendency to produce high pH, conductivities and Ca leachates (Table 3.5) as the results of CaO-slag dissolution. As shown in Table 3.5, pH values, conductivity and Ca^{2+} leachates of slag after 52 weeks of column operations (column EAF-small + sand and column BOF-small + sand) were lower than those of fresh slag (before the experiments), thus indicating a decrease in the potential of CaO-slag dissolution overtime, as already suggested by Figure 3.5 C and D. However, pH values and Ca^{2+} concentrations of the leachates remained into the range of values that support Ca phosphate precipitation (Valsami-Jones, 2001; Kim et al., 2006a), thus suggesting that steel slag after 52 weeks of column experiments still had a high potential for P removal. The metal concentrations of the leachates of slag after 52 weeks of column experiments (column EAF-small + sand and column BOF-small + sand) were very similar to those of fresh samples of slag (before the use in columns) (Table 3.5), and this suggested that the rate of metal release from slag did not change after column experiments. The data shown in Table 3.5 appeared to demonstrate that steel slag does not produce environmental hazardous leachates, with the exceptions of V and Ba releases from EAF-slag, and the leachate concentrations were below the limits established by the European Council decision 2003/33/EC for waste acceptable at

landfills for inert waste. These data on slag leachates are in agreement with the findings of a previous study (Proctor et al., 2000), which confirmed the potential release of V and Ba from steel slag.

Table 3.5. Leachate concentrations of slag after 52 weeks of column operation compared to leachate concentrations of slag before column experiments (according to EN 12457-1: 2002).

Parameters	EAF-slag		BOF-slag		Limits values
	Before use	After 52 weeks	Before use	After 52 weeks	2003/33/EC[a]
pH (-)	11.4	10.7	12.3	11.9	N.A.
Cond. (mS/cm)	598	205	4410	1391	N.A.
As (mg/L)	<0.005	<0.005	<0.005	<0.005	0.2
Ba (mg/L)	0.46	0.10	0.09	0.04	14
Ca (mg/L)	53	29	472	92	N.A.
Cd (mg/L)	<0.0005	<0.0005	<0.0005	<0.0005	0.06
Cr_{tot} (mg/L)	0.006	0.001	0.005	0.007	0.4
Cu (mg/L)	0.003	<0.002	<0.002	<0.002	1.8
Fe (mg/L)	0.035	<0.01	<0.01	0.029	N.A
Mn (mg/L)	0.009	0.001	0.006	0.003	N.A.
Mo (mg/L)	0.022	0.028	0.004	0.007	0.6
Ni (mg/L)	<0.002	<0.002	<0.002	<0.002	0.4
P (mg/L)	<0.010	<0.010	<0.010	<0.010	N.A.
Pb (mg/L)	<0.002	<0.002	<0.002	<0.002	0.4
Sb (mg/L)	<0.005	<0.005	<0.005	<0.005	0.04
V (mg/L)	0.447	0.439	0.003	0.036	N.A.
Zn (mg/L)	<0.005	<0.005	<0.005	<0.005	4
Cl (mg/L)	1	2	<1	4	1100
F (mg/L)	<0.4	<0.4	0.6	<0.4	8
SO_4 (mg/L)	2	9	1	16	1120

[a] Leaching limit values for waste acceptable at landfills for inert waste, calculated at liquid to solid ratios (L/S) of 2 L/kg.

The surfaces of slag before and after 52 weeks of column experiments (column EAF-small + sand and column BOF-small + sand) were examined by SEM and EDX analyses (Figure 3.6). Before column experiments, the coarse surface of BOF-slag and EAF-slag resulted predominantly composed of Fe, Ca and O (Figures 3.6 A and B). Microscopic observations by SEM of slag after 65 weeks of filter operation showed that the surface was covered with a layer of precipitates including rhombohedral crystals and spheroidal aggregates (Figures 3.6 C and D). EDX analyses confirmed that rhombohedral crystals (>20 µm) were mostly made of Ca, C and O, thus suggesting $CaCO_3$ precipitation and crystallisation on the surface of slag. Instead, spheroidal aggregates (<20 µm) were mostly made of Ca, P and O, thus indicating Ca phosphate precipitation on the surface of slag.

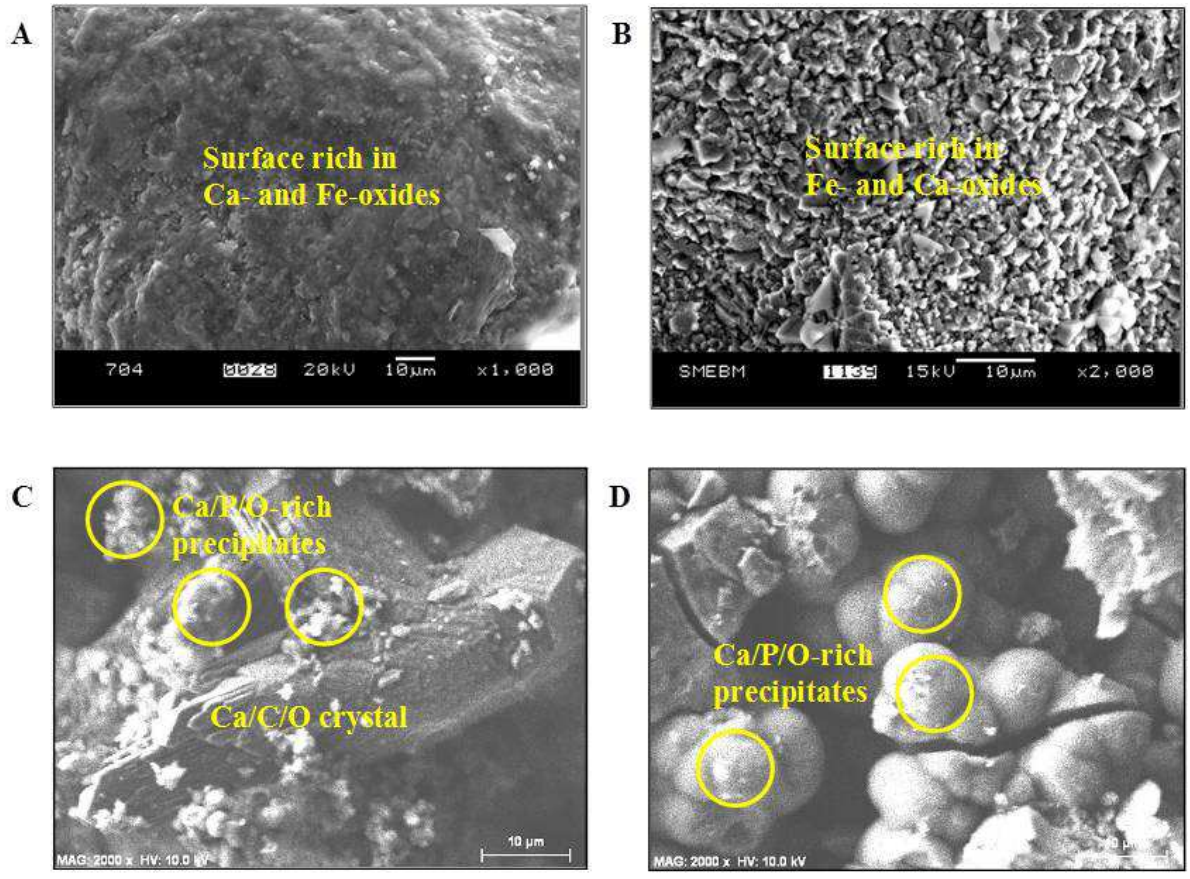

Figure 3.6. SEM observations and EDX analyses: (A) surface of BOF-slag before experiments; (B) surface of EAF-slag before experiments; (C) surface of BOF-slag after 52 weeks of column experiments; (D) surface of EAF-slag after 52 weeks of column experiments.

Figure 3.7 shows the XRD diffractograms of the precipitates covering the slag surface after 52 weeks of column experiments (column EAF-small + sand and column BOF-small + sand).

The results indicated the probable presence of crystals of hydroxyapatite (HAP) growing on the surface of slag (clear using BOF-slag). This suggested that, after precipitation, Ca phosphate began to recrystallize into the most stable HAP, as suggested by the literature (Valsami-Jones, 2001; Lundager-Madsen, 2008). Also, the XRD diffractograms (Figure 3.7) confirmed the presence of well crystallized forms of calcite covering the slag surface after 52 weeks of column operation, and this appeared to confirm $CaCO_3$ precipitation followed by crystallisation into calcite on the slag surface.

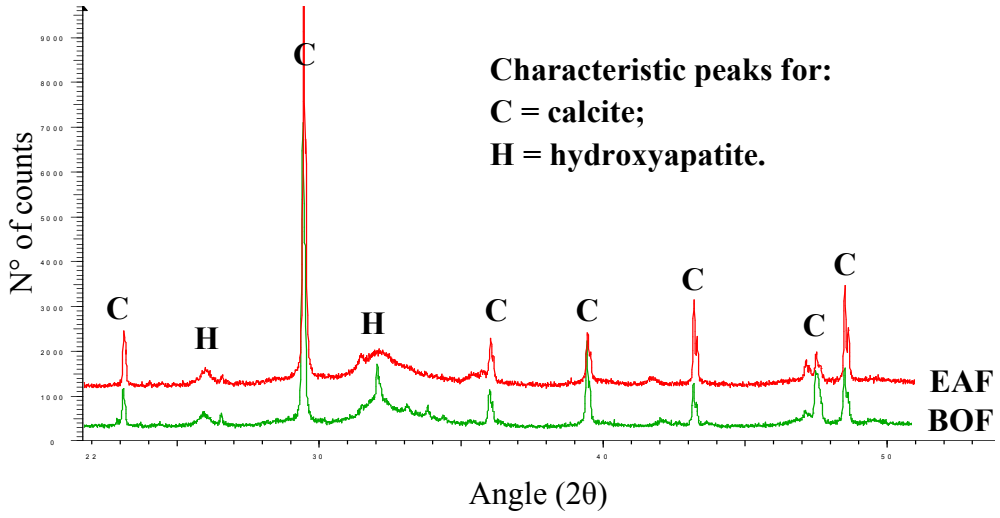

Figure 3.7. XRD diffractograms of the precipitates covering the surface of slag after 52 weeks of column experiments.

Figure 3.8 shows the results of sequential P extractions: 1.88 g P/kg was totally extracted from fresh EAF-slag (before experiments), whereas 2.64 g P/kg was totally extracted from fresh BOF-slag (before experiments). These results are in agreement with the findings of XRF analyses (Table 3.4), which showed that BOF-slag is originally richer in P than EAF-slag. Motz and Geiseler (2001) have also demonstrated by XRF analyses that BOF-slag produced in Europe is richer in P than EAF-slag. The major fractions of P in slag were Ca bound P and P in stable residual pools (>90% of the total amount of P extracted) and this suggests that the P in fresh slag is poorly mobilizable in water.

As shown in Figure 3.8, the amount of P totally extracted from slag after 52 weeks of column experiments (column EAF-small + sand and column BOF-small + sand) increased to 2.17 g P/kg for EAF-slag and to 3.66 g P/kg for BOF-slag, thus suggesting that about 0.3 g P/kg of EAF-slag and about 1.0 g P/kg of BOF-slag were accumulated on slag during 52 weeks of column operation. With EAF-slag, the main increases were observed for the fractions of

weakly bound P and Ca bound P, thus confirming the presence of Ca phosphate precipitates covering the surface of EAF-slag after column experiments. Instead, with BOF-slag the major increase was observed for the fraction of P in very stable residual pools, and this probably depended on recrystallisation of Ca phosphate precipitates into the most stable HAP. This result is consistent with the findings of a previous study (Drizo et al., 2002), who defined the hot concentrated HCl extract as Ca associated P in the stable residual pools on EAF-slag after column experiments.

Also, Figure 3.8 shows that the fractions of Al and Fe bound P were negligible compared to the other fractions of P. This suggested that P adsorption on Al and Fe hydroxides of slag was negligible compared to Ca phosphate precipitation. This most probably depended on the high pH of the column leachates (Table 4.2), because, according to the chemical equilibrium rates of phosphates in aqueous solution, pH values higher than 8 favours Ca phosphate precipitation against Al and Fe phosphate precipitation (Stumm and Morgan, 1996).

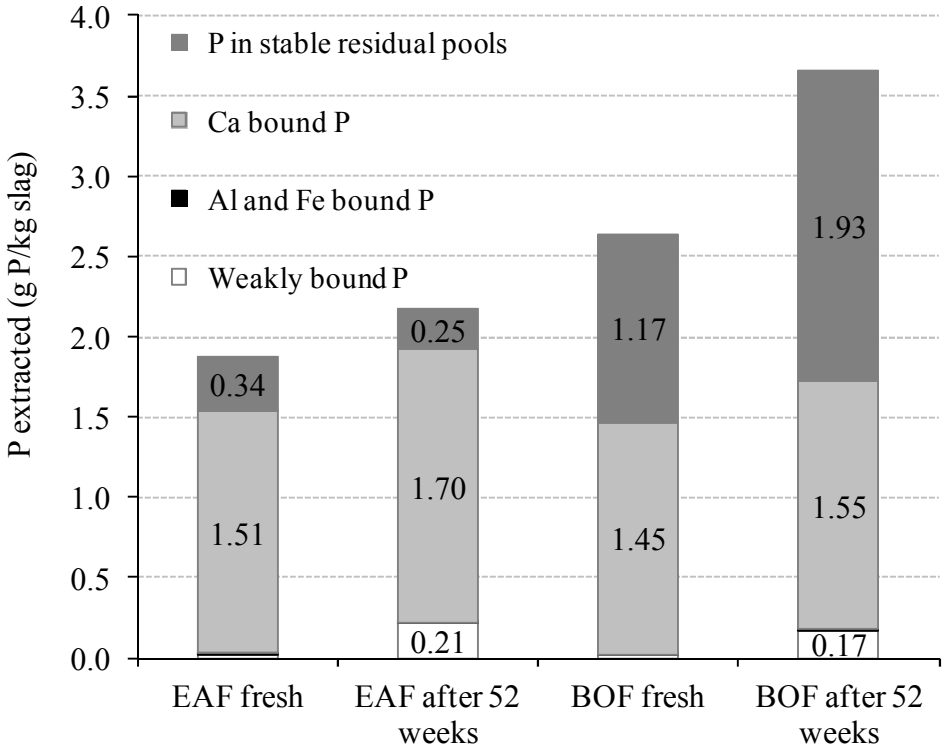

Figure 3.8. P fractionation experiments: P fractions extracted from slag before and after 52 weeks of column experiments. Average values from duplicates.

The results of chemical and mineralogical analyses of slag before and after column experiments are in agreement with the findings of previous studies (Bowden et al., 2009;

Claveau-Mallet et al., 2012), which have shown the formation of a secondary layer of Ca phosphate precipitates, HAP and $CaCO_3$ crystals (calcite) covering the surface of EAF-slag and BOF-slag after one year of column experiments.

3.3.4 Mechanism of P removal

The results of this study suggested that P removal occurred predominantly via Ca phosphate precipitation. Several Ca phosphates may be formed depending on the pH values, Ca^{2+} and PO_4-P concentrations of the solutions (Valsami-Jones, 2001): amorphous Ca phosphate (ACP), dicalcium phosphate (DCP), dicalcium phosphate dihydrate (DCPD), tricalcium phosphate (TCP), octacalcium phosphate (OCP) and hydroxyapatite (HAP).

Our experimental results clearly indicated that outlet PO_4-P concentrations decreased with increasing outlet pH (Figure 3.9), as already shown by Cleveau-Mallet et al. (2012). Most probably this happened because the solubility of various Ca phosphate decreases with increasing pH (Stumm and Morgan, 1996), thus favouring precipitation. The experimental data shown in Figure 3.5 were compared to the solubility curve of Ca phosphates depending on the pH of the solutions (Stumm and Morgan, 1996; Valsami-Jones, 2001). It was found that pH, Ca^{2+} and PO_4-P concentrations were in the range of values that support precipitation of TCP, OCP and HAP.

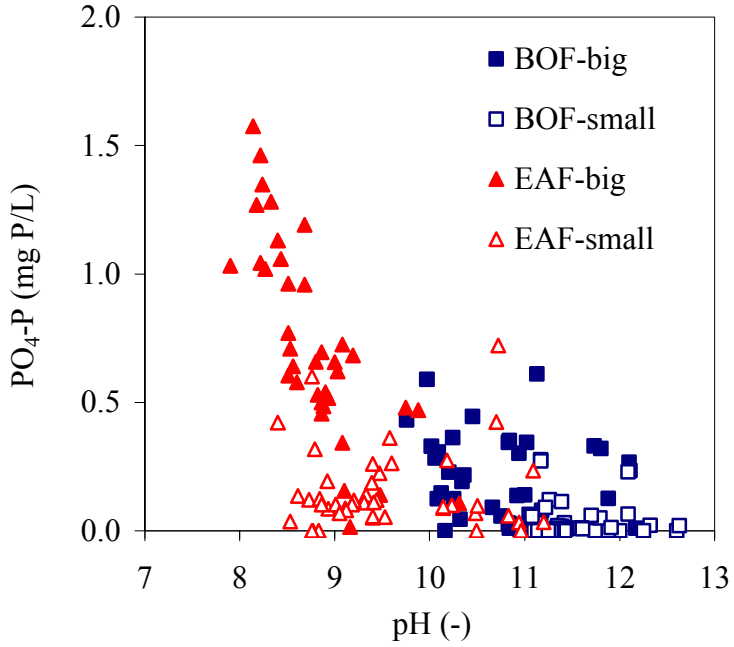

Figure 3.9. Outlet PO_4-P concentration as a function of outlet pH values.

The equations (3.3), (3.4) and (3.5) represent the precipitation of TCP, OCP and HAP, respectively (Roques, 1990; Stumm and Morgan, 1996).

$$3Ca^{2+} + 2PO_4^{3-} \rightarrow Ca_3(PO_4)_2 \downarrow \qquad (Ksp = 10^{-26}) \qquad (3.3)$$

$$4Ca^{2+} + 3PO_4^{3-} + H^- \rightarrow Ca_4H(PO_4)_3 \downarrow \qquad (Ksp = 10^{-46.9}) \qquad (3.4)$$

$$10Ca^{2+} + 6PO_4^{3-} + 2OH^- \rightarrow Ca_{10}(PO_4)_6(OH)_2 \downarrow \qquad (Ksp = 10^{-114}) \qquad (3.5)$$

According to the equations (3.3), (3.4) and (3.5), Ca^{2+} concentration may limit Ca phosphate precipitation when the molar ratio of PO_4-P concentration to Ca^{2+} concentration (PO_4-P/Ca) of the solution is higher than 0.6. During the 100-week period of monitoring, the molar ratio of outlet PO_4-P concentration to outlet Ca concentration was always <0.3 (Table 3.2), thus indicating that Ca^{2+} concentration never limited Ca phosphate precipitation. These results are in agreement with the findings of previous experiments performed at different scales of investigation (from batch to field scale), which showed efficient P removal via Ca phosphate precipitation under the conditions of initial Ca^{2+} concentrations of 40-120 mg Ca/L and initial P concentrations of 3-10 mg P/L (Jang and Kang, 2002; Kim et al., 2006b; Koiv et al., 2010; Barca et al., 2012).

Several authors in the literature have stated that precipitation of Ca phosphates usually follows the Ostwald's well-known "rule of stages": first, precipitation of less stable compounds (ACP, DCP, OCP, TCP), then, recrystallisation into the most thermodynamically stable HAP (Valsami-Jones, 2001; Lundager-Madsen, 2008). Recrystallisation of Ca phosphate precipitates into HAP appeared to be confirmed by a recent study (Bowden et al., 2009), which has recently shown that there is a succession of Ca phosphate minerals on the surface of BOF-slag during continuous flow column experiments, and that this sequence of Ca phosphate minerals progresses from the less stable (DCP, which was observed since the first month of column operation) to the most stable (HAP, which was observed since the fifth month of column operation). In our study, XRD analyses seemed to indicate the presence of growing crystals of HAP on the surface of slag after 52 weeks of column experiments (column EAF-small + sand and column BOF-small + sand) (Figure 3.7), and this appears to confirm the process of Ca phosphate recrystallisation into HAP on the surface of slag. These "recrystallised" crystals of HAP may represent seed crystals for further HAP crystallisation (Kim et al., 2006a), thus increasing P removal efficiencies of the columns on the long time.

Also, SEM observations and XRD analyses have shown the presence of crystals of calcite covering the surface of slag after 52 weeks of column experiments (column EAF-small + sand and column BOF-small + sand) (Figure 3.6 and 3.7), this suggesting $CaCO_3$ precipitation followed by crystallisation into calcite on the slag surface.

On the hand, $CaCO_3$ precipitation may have led to a competing consumption of Ca^{2+}, thus limiting Ca phosphate precipitation (Johansson and Gustafsson, 2000; Jang and Kang, 2002). On the other hand, "recrystallised" $CaCO_3$ into crystals of calcite may favour further P removal, as calcite has been recognized to provide sorption sites for P removal (Freeman and Rowell, 1981). Moreover, several studies showed that the co-precipitation of calcite with P is possible, with calcite incorporating P into the calcite crystals (House, 1999; Plant and House, 2002). These mechanisms of P sorption on calcite and P co-precipitation with calcite may be significant for the long-term P removal efficiency of the slag columns (Bowden et al., 2009). P co-precipitation with calcite appeared to be confirmed in experiments performed at different scales of investigation (batch, column, field) (Kim et al., 2006a; Liira et al., 2009; Koiv et al., 2010).

3.3.5 TP retention potential

The P saturation levels of filter materials are usually considered as a parameter to estimate the longevity of filter systems (Drizo et al., 2002). Figure 3.10 shows the TP removed as a function of the TP added to the columns over a period of 100 weeks of operation. Over the full period of monitoring, columns EAF-small and BOF-small removed more than 98% of the inlet TP reaching a TP retention level of 1.71 g P/kg of EAF-slag and 1.98 g P/kg of BOF-slag, respectively. Over the same period of operation, column EAF-big removed 86% of the inlet TP reaching a P retention level of 1.51 g P/kg of EAF-slag. As shown in Figure 3.9, the relationship between cumulative TP removed to cumulative TP added is linear for columns EAF-big, EAF-small and BOF-small, thus suggesting that a TP saturation level was not reached.

Differently from the other columns, column BOF-big showed high TP removal efficiencies until reach a TP saturation value of 1.26 g P/kg of BOF-slag after 67 weeks of operation; then, it began to release pre-accumulated P precipitates (Figure 3.10).

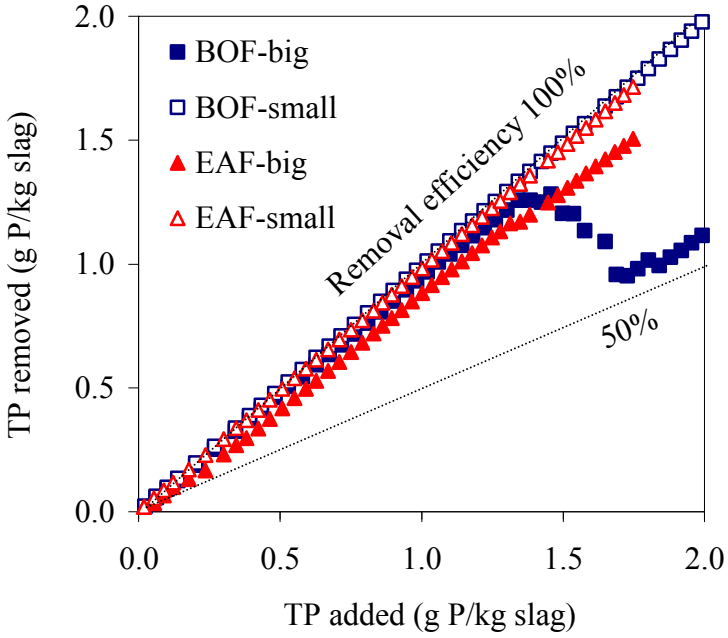

Figure 3.10. TP removed as a function of TP added to the columns over 100 weeks of operation.

The TP retention levels reported in this study were compared to those reported in previous studies (Drizo et al., 2002; Bowden et al., 2009). Drizo et al (2002) showed a saturation value of 1.35 g P/kg of EAF-slag after 40 weeks of column experiments with highly concentrated P synthetic solution (350-400 mg P/L). After 100 weeks of column operation, EAF-slag (size 5-16 mm) tested in this study showed a TP retention value 1.5 times higher than the TP saturation value reported by Drizo at al. (2002) for EAF-slag (size 2.5-10 mm). This indicated that EAF-slag tested in our study has a higher TP retention potential. Concerning slag of type BOF, Bowden et al (2009) reported a TP retention level of 8.4 g P/kg of BOF-slag after 24 weeks of highly concentrated P synthetic solution application (100-300 mg P/L) without showing signs of saturation. This suggested that BOF-slag has a very high potential for P retention, and, nowadays, there are not enough data to estimate TP saturation levels of BOF-slag in continuous flow column experiments.

3.4 Conclusions

This study showed that EAF and BOF steel slags are very efficient filter substrates for P removal from synthetic solutions. P removal predominantly occurred via CaO-slag dissolution followed by Ca phosphate precipitation. It was found that TP removal performances depended on slag type, slag size and column design.

Over a period of 100 weeks of operation, small-columns filled with small-size slag removed more than 98% of the inlet TP, reaching TP retention levels of 1.71 g P/kg for EAF-slag and of 1.98 g P/kg for BOF-slag. On the contrary, big-size column filled with big-size BOF-slag showed the lowest TP removal efficiency, which was negatively affected by massive releases of pre-accumulated P precipitates.

However, our experimental results suggested that TP removal performances can be improved by enhancing the design of the filter. In fact, it was found that hydraulic and TP removal performances of the columns improved by decreasing the aspect ratio of width to length of the column and with decreasing the size of slag, most probably because filtration of P precipitates was more efficient.

Supporting Information

Tables AII 1 and 2 in Annex II show the results of P fractionation experiments of samples of slag before and after 52 weeks of column operation. Figures AIII 2-5 in Annex III show top and panoramic view of the column system, SEM observations of slag after 52 weeks of column operation, and an image of column BOF-big (filled with BOF-slag size 20-50 mm) showing the presence of white precipitates occupying the void volume after 100 weeks of operation.

References of Chapter 3

EN 12457-1, 2002. Characterisation of waste. Leaching. Compliance test for leaching of granular waste materials and sludges. One stage batch test at a liquid to solid ratio of 2 l/kg for materials with high solid content and with particle size below 4 mm (without or with size reduction).

EN 12457-2, 2002. Characterisation of waste. Leaching. Compliance test for leaching of granular waste materials and sludges. One stage batch test at a liquid to solid ratio of 10 l/kg for materials with high solid content and with particle size below 4 mm (without or with size reduction).

EN ISO 6878, 2004. Water quality - Determination of phosphorus - Ammonium molybdate spectrometric method.

EN ISO 7980, 1986. Water quality - Determination of calcium and magnesium - Atomic absorption spectrometric method.

EN ISO 9963-1, 1994. Water quality - Determination of alkalinity - Part 1: Determination of total and composite alkalinity.

Alcocer D.J.R., Giacoman V.G., Champagne P., 2012. Assessment of the plug flow and dead volume ratios in a sub-surface horizontal-flow packed-bed reactor as a representative model of a sub-surface horizontal constructed wetland. Ecological Engineering 40, 18-26.

Anjab Z.A., 2009. Développement d'un lit de scorie d'aciérie pour la dephosphatation des eaux usées. Master Thesis (in French), Ecole Polytechnique de Montréal, Canada.

Barca C., Gérente C., Meyer D., Chazarenc F., Andrès Y., 2012. Phosphate removal from synthetic and real wastewater using steel slags produced in Europe. Water Research 46(7), 2376-2384.

Bowden L.I., Jarvis A.P., Younger P.L., Johnson K.L., 2009. Phosphorus removal from wastewaters using basic oxygen steel slag. Environmental Science and Technology 43(7), 2476-2481.

Chazarenc F., Merlin G., Gonthier Y., 2003. Hydrodynamics of horizontal subsurface flow constructed wetlands. Ecological Engineering 21 (2-3), 165-173.

Chazarenc F., Brisson J., Comeau Y., 2007. Slag columns for upgrading phosphorus removal from constructed wetland effluents. Water Science and Technology 56(3), 109-115.

Claveau-Mallet D., Wallace S., Comeau Y., 2012. Model of phosphorus precipitation and crystal formation in electric arc furnace steel slag filters. Environmental Science and Technology 46(3), 1465-1470.

Crouzet P., Leonard J., Nixon S., Rees Y., Parr W., Laffon L., Bogestrand J., Kristensen P., Lallana C., Izzo G., Bokn T., Bak J., 1999. Nutrients in European Ecosystems. European Environment Agency, www.eea.eu.int, Environmental Assessment Report n° 4.

Drizo A., Comeau Y., Forget C., Chapuis R. P., 2002. Phosphorus saturation potential: a parameter for estimating the longevity of constructed wetland systems. Environmental Science and Technology 36(21), 4642-4648.

Drizo A., Forget C., Chapuis R.P., Comeau Y., 2006. Phosphorus removal by electric arc furnace steel slag and serpentinite. Water Research 40(8), 1547-1554.

Freeman J.S, Rowel D.L., 1981. The adsorption and precipitation of phosphate onto calcite. International Journal of Soil Science 32(1), 75-84.

Gustafsson J.P., Renman A., Renman G., Poll K., 2008. Phosphate removal by mineral-based sorbents used in filters for small-scale wastewater treatment. Water Research 42 (1-2), 189-197.

Headley T.R., Huett D.O., Davison L., 2003. Seasonal variation in phosphorus removal processes within reed beds – mass balance investigations. Water Science and Technology 48(5), 59-66.

House W.A., 1999. The physico-chemical conditions for the precipitation of phosphate with calcium. Environmental Technology 20(7), 727-733.

Huijgen W.J.J, Witkamp G.J., Comans R.N.J., 2005. Mineral CO_2 sequestration by steel slag carbonation. Environmental Science and Technology 39(24), 9676-9682.

Jang H., Kang S.H., 2002. Phosphorus removal using cow bone in hydroxyapatite crystallization. Water Research 36(5), 1324-1330.

Johansson L., 1999. Blast furnace slag as phosphorus sorbents – column studies. Science of Total Environment 229, 89-97.

Johansson L., Gustafsson J.P., 2000. Phosphate removal using blast furnace slags and opoka - mechanisms. Water Research 34(1), 259-265.

Johansson-Westholm L., 2006. Substrates for phosphorus removal-potential benefits for on-site wastewater treatment? Water Research 40(1), 23-36.

Kadlec R.H., Wallace S.D., 2009. Treatment Wetlands. Second Edition. Taylor and Francis Group, Boca Raton, FL, USA.

Kim E.H., Yim S., Jung H., Lee E., 2006a. Hydroxyapatite crystallization from a highly concentrated phosphate solution using powdered converter slag as a seed material. Journal of Hazardous Materials 136(3), 690-697.

Kim E.H., Lee D.W., Hwang H.K., Yim S., 2006b. Recovery of phosphates from wastewater using converter slag: Kinetics analysis of a completely mixed phosphorus crystallization process. Chemosphere 63(2), 192-201.

Koiv M., Liira M., Mander U., Motlep R., Vohla C., Kirsimae K., 2010. Phosphorus removal using Ca-rich hydrated oil shale ash as filter material – The effect of different phosphorus loadings and wastewater compositions. Water Research 44(18), 5232-5239.

Lee M.S., Drizo A., Rizzo D.M., Druschel G., Hayden N., Twohig E., 2010. Evaluating the efficiency and temporal variation of pilot-scale constructed wetlands and steel slag phosphorus removing filters for treating dairy wastewater. Water Research 44(14), 4077-4086.

Liira M., Kõiv M., Mander Ü., Mõtlep R., Vohla C., Kirsimäe K., 2009. Active filtration of phosphorus on Ca-rich hydrated oil-shale ash: does longer retention time improve the process? Environmental Science and Technology 43(10), 3809-3814.

Lundager-Madsen H.E., 2008. Influence of foreign metal ions on crystal growth and morphology of brushite ($CaHPO_4,2H_2O$) and its transformation to octacalcium phosphate and apatite. Journal of Crystal Growth 310(10), 2602-2612.

Metcalf and Eddy, Inc. 2003. Wastewater Engineering - Treatment and reuse. 4th edition, McGraw-Hill, USA (New York).

Motz H., Geiseler J., 2001. Products of steel slags: an opportunity to save natural resources. Waste Management 21(3), 285-293.

Navarro C., Diaz M., Villa-Garcia M.A., 2010. Physico-chemical characterization of steel slag. Study of its behavior under simulated environmental conditions. Environmental Science and Technology 44(14), 5383-5388.

Plant L.J., House W.A., 2002. Precipitation of calcite in the presence of inorganic phosphate. Colloid and Surfaces A – Physicochemical and Engineering Aspects 203(1-3), 143-153.

Pratt C., Shilton A., Pratt S., Haverkamp R.G., Bolan N.S., 2007. Phosphorus removal mechanisms in active slag filters treating waste stabilization pond effluent. Environmental Science and Technology 41(9), 3296-3301.

Proctor D.M., Fehling K.A., Shay E.C., Wittenborn J.L., Green J.J., Avent C., Bigham R.D., Connolly M., Lee B., Shepker T.O., Zak M.A., 2000. Physical and chemical characteristics of blast furnace, basic oxygen furnace, and electric arc furnace steel industry slags. Environmental Science and Technology 34(8), 1576-1582.

Recknagel F., Hosomi M., Fukushima T., Kong D.S., 1995. Short and long term control of external and internal phosphorus loads in lakes. A scenario analysis. Water Research 29(7), 1767-1779.

Roques H., 1990. Fondements théoriques du traitement chimique des eaux. Volume II, Technique et Documentation – Lavoisier, Paris (France), pp. 382.

Shilton A. N., Pratt S., Drizo A., Mahmood B., Banker S., Billings L., Glenny S., Luo D., 2005. Active filters for upgrading phosphorus removal from pond systems. Water Science and Technology 51(12), 111-116.

Stumm W., Morgan J.J., 1996. Aquatic chemistry – Chemical equilibria and rates in natural waters. 3rd edition, Wiley-Interscience Publication, USA (Iowa), pp. 1022.

Suliman F., French H.K., Haugen L.E., Sovik A.K., 2006. Change in flow transport patterns in horizontal subsurface flow constructed wetlands as a result of biological growth. Ecological Engineering 27(2), 124-133.

Tiessen H., Moir J.O., 1993. Characterization of available P by sequential extraction. In: Soil sampling and methods of analysis. M.R. Carter Editor, Canadian Society of Soil Science. Lewis Publisher, London, Ch. 10, 75-86.

Valsami-Jones E., 2001. Mineralogical controls on phosphorus recovery from wastewaters. Mineralogical Magazine 65(5), 611-620.

Vohla C., Kõiv M., Bavor H.J., Chazarenc F., Mander U., 2011. Filter materials for phosphorus removal from wastewater in treatment wetlands – A review. Ecological Engineering 37(1), 70-89.

Wang G., Wang Y., Gao Z., 2010. Use of steel slag as a granular material: Volume expansion prediction and usability criteria. Journal of Hazardous Materials 184(1-3), 555-560.

Weber D., Drizo A., Twohig E., Bird S., Ross D., 2007. Upgrading constructed wetlands phosphorus reduction from a dairy effluent using electric arc furnace steel slag filters. Water Science and Technology 56(3), 135-143.

Werner T.M., Kadlec R.H., 2000. Wetland residence time distribution modelling. Ecological Engineering 15(1-2), 77-90.

Williams C.F., Nelson S.D., 2011. Comparison of Rhodamine-WT and bromide as a tracer for elucidating internal wetland flow dynamics. Ecological Engineering 37(10), 1492-1498.

Wolf, D., Resnick, W. 1963. Residence time distribution in real system. Journal of Industrial and Engineering Chemical Fundamentals, 2(4):28-293.

Xiong J., He Z., Mahmood Q., Liu D., Yang X., Islam E., 2008. Phosphate removal from solution using steel slag through magnetic separation. Journal of Hazardous Materials 152(1), 211-215.

Yamada H., Kayama M., Saito K. and Hara M. (1986). A fundamental research on phosphate removal by using slag. Water Research 20(5), 547-557.

Zeiser T., Lammers P., Klemm E., Li Y.W., Bernsdorf J., Brenner G., 2001. CFD-calculation of flow, dispersion and reaction in a catalyst filled tube by the lattice Boltzmann method. Chemical Engineering Science 56(4), 1697-1704.

CHAPTER 4 Steel slag filters to upgrade phosphorus removal in constructed wetlands: two years of field experiments

Abstract

Electric arc furnace steel slag (EAF-slag) and basic oxygen furnace steel slag (BOF-slag) were used as filter substrates in sub-horizontal flow filters (6 m^3 each) designed to remove phosphorus (P) from the effluent of a constructed wetland. The influences of parameters, including slag composition, void hydraulic retention time (HRTv), temperature, and wastewater quality, on filter performances were studied. Over a period of 85 weeks of filter operation, EAF-slag removed 36% of the inlet total P, whereas BOF-slag removed 59% of the inlet total P. P removal occurred predominantly via CaO-slag dissolution followed by Ca phosphate precipitation. P removal efficiencies improved with increasing temperature and HRTv, most probably because the increase in temperature and HRTv affected the rate of CaO-slag dissolution and Ca phosphate precipitation. It was observed that at long HRTv (>3 days) slag filters may produce high pH in the effluents (>9) as the results of excessive CaO-slag dissolution. However, at shorter HRTv (1-2 days) pH values were elevated only during the first 5 weeks of operation, and then stabilized below a pH of 9. The kinetics of P removal were investigated employing a first order equation, and a model for filter design was proposed.

4.1 Introduction

Phosphorus (P) is an essential nutrient for biomass growth. However, excessive intake of P into water bodies such as rivers, lakes or lagoons causes eutrophication and degradation of the water quality. Therefore, legislation on P rejects into the surrounding environment is becoming stricter worldwide, including for small wastewater treatment plants (WWTPs) such as constructed wetland systems (CWSs). One appropriate technology for upgrading P removal from CWS is filtration through materials with high affinities for P binding (Johansson-Westholm, 2006; Vohla et al., 2011).

Since the 1980s, the affinity of steel slag for P binding has been studied with the aim of using a by-product of the steel industry as filter substrate to treat wastewater (Yamada et al., 1986). Steel and iron industry produces mostly four types of slag: (i) blast furnace slag (BF-slag), which originates from the iron production in a blast furnace; (ii) basic oxygen furnace slag (BOF-slag), which originates from the further refining of iron in a basic oxygen furnace; (iii) electric arc furnace slag (EAF-slag), which is derived from melting recycled scrap in an electric arc furnace; (iv) melter slag, which is produced when iron sand is converted to melter iron (Proctor et al., 2000; Pratt et al., 2007). Steel slag is primarily made of iron (Fe) and calcium oxide (CaO), as a result of the use of fluxing agents (mainly lime) during the steelmaking process (Motz and Geiseler, 2001).

Many international studies have demonstrated that steel slag is an efficient substrate for P removal from wastewater: P retention capacities reported from batch experiments range from less than 1 to up to 80 mg P/g (Xiong et al., 2008; Bowden et al., 2009), and the main mechanism of P removal was related to CaO-slag dissolution followed by Ca phosphate precipitation (Bowden et al., 2009; Barca et al., 2012). Pilot scale experiments have confirmed that steel slag is an efficient filter substrates for P removal (Johansson, 1999; Shilton et al., 2005; Drizo et al., 2006), but they showed also some limitations such as high pH-effluents and clogging due to $CaCO_3$ precipitation (Chazarenc et al., 2007; Lee et al., 2010). However, most of these experiments were performed with synthetic P solutions, which do not contain all components occurring in real CWS effluents that may affect P removal (e.g., humic acids, organic colloids, competing anions) (Valsami-Jones, 2001; Pratt et al., 2007). Indeed, large differences in filter performance were observed when treating real CWS effluents (Shilton et al., 2005; Chazarenc et al., 2007).

Nowadays, only a few experiments have been conducted to determine P removal performances of steel slag under field conditions (Shilton et al., 2006; Korkusuz et al., 2007; Weber et al., 2007; Cassini et al., 2010). Moreover, long-term data on performances of slag filters are scarce (Shilton et al., 2006), and further long-term experiments are needed to define the behaviour of steel slag under real operating conditions.

Within the framework of the European research project "SLASORB" (funded by Research Fund for Coal and Steel, RFCS), our study aimed to investigate the hydraulic and treatment performances of steel slag produced in Europe in demonstration-scale filters designed to remove P from the effluent of a CWS, and to propose design equations based on the experimental results.

The originality and importance of this study are highlighted by the following two points:

(i) The first field-scale investigation in Europe of the P removal performances of steel slag: two sub-horizontal flow filters of 6 m^3 of volume (one filled with EAF-slag, one filled with BOF-slag) were fed with the effluent of a CWS. The influences of several parameters, including slag composition, void hydraulic retention time (HRTv), temperature, and wastewater quality, on P removal performances were studied. Tracer tests were also performed to investigate the hydrodynamic of the filters and its evolution during the filter operation.

(ii) An in-depth critical investigation of the P removal mechanisms: to our knowledge, only a study in the literature has tried to explain thoroughly the P removal mechanisms of steel slag (type melter slag) in long-term field experiments (Pratt et al., 2007). Our work presents an in-depth study of the P removal mechanisms of BOF-slag and EAF-slag that had been used to remove P from the effluent of a CWS. Elemental analysis, scanning microscopy observations and chemical extractions were performed to elucidate the process of P removal. The understanding of the removal mechanisms aided design and enabled to evaluate the lifespan of the slag filters.

4.2 Materials and methods

4.2.1 Experimental setup

4.2.1.1 The CWS of La Motte d'Aigues

The municipal WWTP of "*La Motte d'Aigues*" (Provence-Alpes-Cote d'Azur, France) (1359 inhabitants according to INSEE, 2009) is a classical example of CWS in France (Liénard, 1987). It consists of two stages of vertical flow constructed wetlands (VFCWs): the first reed-planted bed (1440 m^2 of surface) is followed by the second reed-planted bed (960 m^2 of surface) (Figure 4.1). The WWTP of "*La Motte d'Aigues*" has a treatment capacity of about 240 m^3/d and actual load of about 160 m^3/d, which correspond to about 1050 people equivalent (p.e.) (150 L/(p.e.)*d). The raw wastewater is sent to the first bed without any pre-treatment, with the exception of a preliminary screening to remove solids larger than 4 cm in diameter. Two stage VFCW in France provides high removal performances for chemical oxygen demand (COD), total suspended solid (TSS) and total Kjeldahl nitrogen (TKN) (Molle et al., 2005). However, P removal performances of VFCWs in France are poor (<20%, according to Molle, 2008). The CWS of "*La Motte d'Aigues*" was chosen to perform the field experiments because its treatment capacity is high enough to ensure a sufficient amount of wastewater in input to the filters at any time during the day.

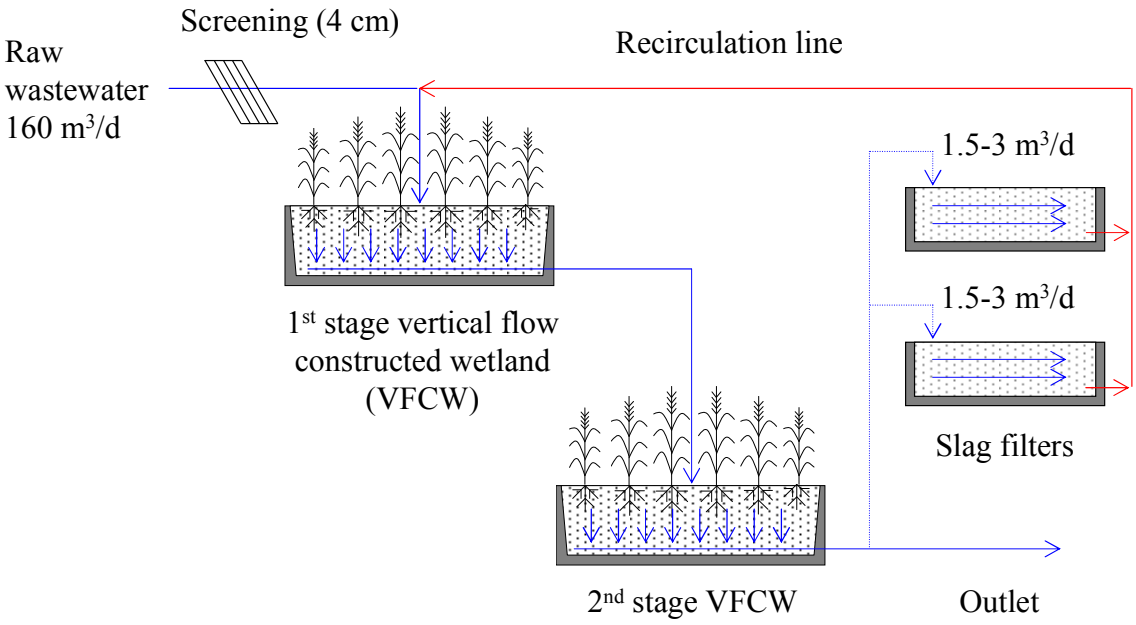

Figure 4.1. Schematic view of the La Motte d'Aigues WWTP with the addition of the demonstration-scale steel slag filters.

4.2.1.2 The demonstration scale steel slag filters

Two demonstration field-scale filters were designed to upgrade P removal performances of the CWS of "*La Motte d'Aigues*". The filters were filled one with EAF-slag from the production sites of Sestao, Spain (EAF-filter), one with BOF-slag from the production sites of Fos Sur Mer, France (BOF-filter). These slag samples were selected by comparative batch experiments that were performed to determine the phosphate removal capacities of several samples of slag produced in Europe (Barca et al., 2012). The bulk density of slag was about 1.8 g/cm^3 for EAF-slag and 1.6 g/cm^3 for BOF-slag. X-ray fluorescence analyses showed that main chemical components of EAF-slag used in this study were Fe_2O_3 (43.7%), CaO (26.0%) and SiO_2 (14.4%), whereas main components of BOF-slag were CaO (54.6%), Fe_2O_3 (27.0%), and SiO_2 (13.3%) (Barca et al., 2012). Figure 4.2 shows the granular size distribution curves of the slag samples used to fill the filters. The main fraction of slag was comprised in the granular size range of 20-40 mm (96.8% for EAF-slag, 77.9% for BOF-slag). This granular size was considered to be large enough to prevent filter clogging, as reported by other authors (Shilton et al., 2006; Chazarenc et al., 2007; Weber et al., 2007; Vohla et al., 2011).

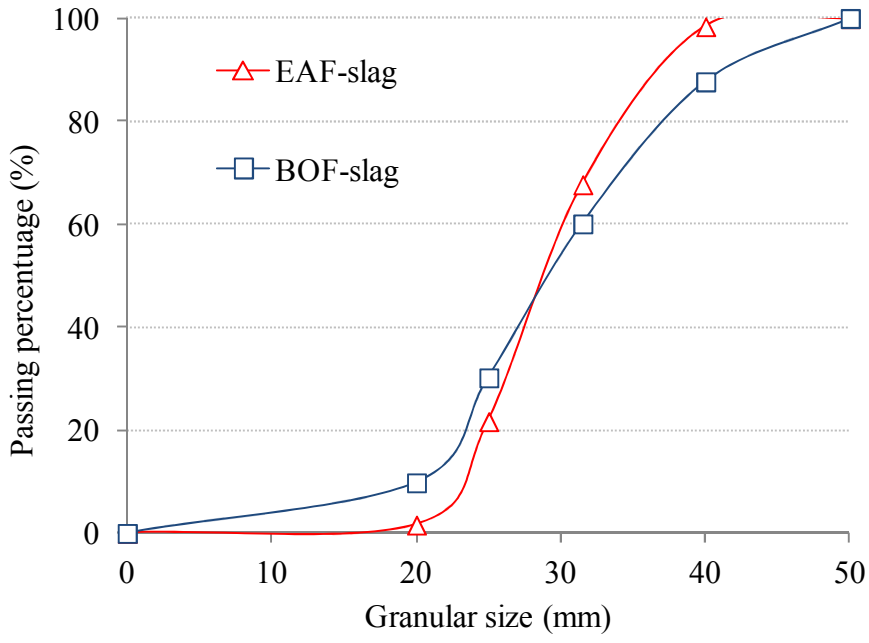

Figure 4.2. Granular size distribution of the slag samples tested in field experiments.

Figure 4.3 shows the design of the slag filters. Each filter had a total volume of about 6 m^3 and a void volume of about 3 m^3, thus corresponding to a filter porosity of about 50%. Then,

the steel slag filters were fed with a fraction (2-4%) of the effluent from the CWS of "*La Motte d'Aigues*" and operated with sub-surface horizontal flow and batch loads (24 batches/day), this to simulate the typical CWS-feeding conditions. The sub-horizontal flow was adopted to limit the dissolution of atmospheric CO_2 in water, because CO_2 in water is an inhibitor of P precipitation (Valsami-Jones, 2001). The HRTv of the filters was initially calibrated to 1 day by the use of a flow meter. Then, HRTv was increased to 2 days after week 9 of operation, this to evaluate the effect of the HRTv on P removal performances. The filters were also equipped with thermometers, to monitor air and water temperature, and piezometers, to study the kinetics of P removal.

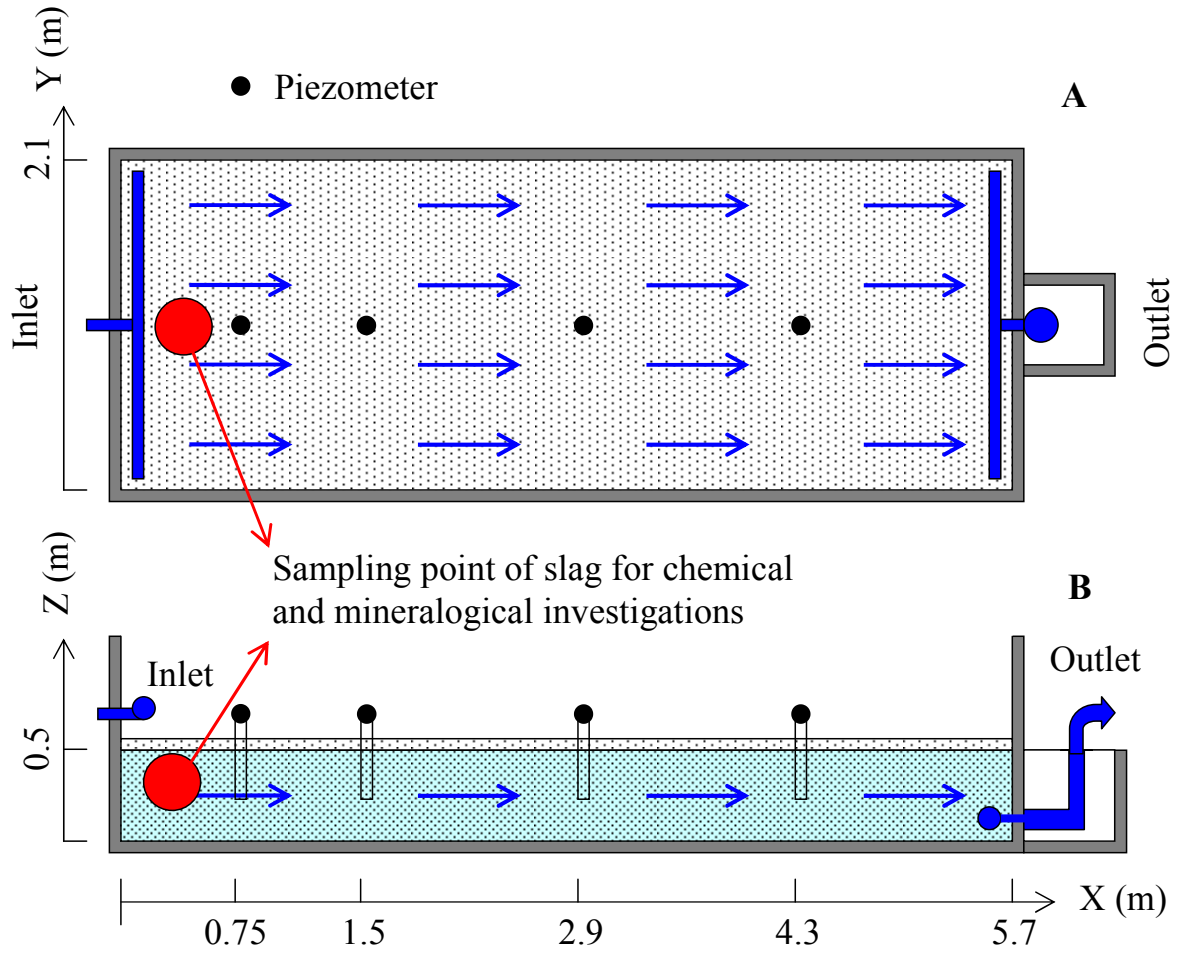

Figure 4.3. Field-scale slag filters: plan (A) and cross section (B) views. Red circles show the sampling point of slag for chemical and mineralogical investigations.

4.2.2 Experimental methods

4.2.2.1 Hydraulic performances

Tracer tests were performed in week 1, 9, 22, 29 and 44 by using fluorescein as tracer substance. These experiments aimed at evaluating the hydrodynamics of the filters and its evolution over time. 5 L of a solution 1 g fluorescein/L (5 g fluorescein/filter) were instantaneously injected to the inlet of each filter. Then, outlet tracer concentrations were monitored until more than 90% of the mass of the tracer was recovered (72 h after the tracer injection), and the curves of the outlet tracer concentrations as a function of the time were drawn (retention time distribution curves, RTD-curves).

The average retention time of the fluid into the filter (T_A) was calculated by the equation (4.1) (Metcalf and Eddy, 2003), where Ci is the outlet tracer concentration at the time ti (mg/L), ti is the time from the tracer injection (h), Δti is the interval between two consecutive measures (h) and n is the number of measures (-).

$$T_A = \frac{\sum ti \times Ci \times \Delta ti}{\sum Ci \times \Delta ti} \qquad \text{for } i = 1,\ldots,n; \tag{4.1}$$

In the literature, several empirical flow models have been used to study the internal hydrodynamics of sub-horizontal flow filters (Chazarenc et al., 2003; Suliman et al., 2006; Alcocer et al., 2012). Most of these models were developed to reproduce the experimental retention time distribution of the flow in filter systems, this by using the theories of the continuous stirred tank reactor (CSTR) and of the plug flow reactors (PFR) (Werner and Kadlec, 2000). In this study, the empirical flow model of Wolf and Resnick (1963) (equation (4.2)) was employed to describe the hydraulic behaviour of the slag filters. This enabled the results to be compared to those of a recent study (Alcocer et al., 2012), which employed the equation (4.2) to investigate the effect of different filter design, medium size, and inflow rate on the hydraulic performances of sub-horizontal flow filters of different sizes. In equation (4.2), F(t) is the fraction of the tracer that exited the filter at the time t (-), t is the time from the tracer injection (h), T is the theoretical HRTv (h), PF is the plug flow fraction (-) and DV is the dead volume fraction (-).

$$F(t) = 1 - \exp\left[\left(\frac{t/T}{(1-PF)(1-DV)} - \frac{PF}{1-PF}\right)\right] \tag{4.2}$$

If equation (4.2) is applicable, PF indicates the fraction of fluid that presents a constant velocity along any cross-section of the filter, according to the theory of the PFR. Instead, DV indicates the fraction of fluid that stagnates in the reactor and does not participate to reactions (Alcocer et al., 2012). All the tracer tests were performed at theoretical HRTv of 1 day, this to enable the results of the different tests to be compared.

4.2.2.2 Water quality monitoring

During the first 44 weeks of filter operation, water samples (0.8 L) were collected weekly from the inlet and from the outlet of the filters. After week 44, the sampling frequency was reduced to about 1 sample per month. Each water sample was composed of 4 sub-samples (0.2 L each) taken at different times (at 4:00, 10:00, 16:00 and 22:00), this to recreate a water sample as representative as possible of the whole day of sampling. pH, total phosphorus (TP), phosphate (PO_4-P) and Ca^{2+} concentrations of the water samples were measured. TP concentrations were determined after acid digestion, whereas PO_4-P and Ca^{2+} concentrations were determined after filtration (0.45 μm filter) of the water samples. Additional water samples were collected approximately every two months from the inlet and outlet of the filters to determine TSS, COD, total alkalinity (TA) and total nitrogen (TN).

4.2.2.3 P removal kinetics

During the first year of filter operation, water samples were collected about fortnightly from the piezometers, and their TP concentrations were measured. These investigations aimed at determining the P removal kinetics of the slag filters and their evolution over time. The experimental data were modelled with the k-C* model of Kadlec and Knight (1996) (equation 3), which derived from the first-order equation proposed by USEPA (1988) to model pollutant removal in CWS. The parameter C is the TP concentration at the distance x from the inlet (mg P/L), C_0 is the inlet TP concentration (mg P/L), C* is the background outlet TP concentration (mg P/L), k_V is the volumetric constant rate of TP removal (1/d), HRTv is the theoretical retention time (d), x is the distance from the inlet (m) and L is the filter length (m). The k-C* model (equation 4.3) is based on the assumptions of plug flow and that k_V and C* are constants, except for possible seasonal effects (Kadlec, 2000).

$$\frac{C - C^*}{C_0 - C^*} = \exp\left(-k_V \times HRTv \times \frac{x}{L}\right) \qquad (4.3)$$

4.2.2.4 Chemical and mineralogical investigations on slag

A series of analyses was carried out to investigate chemical and mineralogical properties of slag before and after its use in field experiments. In week 52, 65 and 85 of operation, samples of slag were taken at half-depth of the inlet-zone of the filters, as shown in Figure 4.3. Since this zone was the most exposed to inlet P-rich wastewater, these samples were likely to have had a high amount of P bound to their surfaces. The samples of slag (20-40 mm) were dried overnight at 55 °C before the analyses, this to reduce the risk of mineralogical changes due to high temperature drying.

Leaching experiments were conducted according to a procedure adapted from EN 12457-1 (2002) with original size slag (20-40 mm) and a ratio of extracting solution to slag of 2 L/kg, this to evaluate the production of environmental hazardous leachates from slag before and after 52 weeks of field experiments.

Scanning electron microscopy (SEM) observations and energy dispersive X-ray fluorescence (EDX) analyses were performed to examine the surface of grains of slag before and after 65 weeks of field experiments. The samples were coated with conductive platinum before SEM observations (Jeol JSM 7600 F, Oxford Instruments, London, UK).

Finally, the sequential extraction procedure of Tiessen and Moir (1993), as adapted by Headley et al. (2003), was employed to quantify the fractions of different P compounds in slag before and after 85 weeks of field experiments. Four fractions of P were extracted from 350 g of slag (size 20-40 mm):

i. Bicarbonate extractable P fraction was extracted in 700 mL of 0.5 M $NaHCO_3$. This fraction represents weakly bound P;

ii. Hydroxide extractable P fraction was extracted in 700 mL of 0.1 M NaOH. This fraction represents Fe and Al associated P;

iii. Diluted HCl extractable P fraction was extracted in 700 mL of 1 M HCl. This fraction is defined as Ca associated P;

iv. Highly concentrated HCl extractable P fraction was extracted in 200 mL of ~12 M HCl in a 20 min water bath at 80°C. This fraction represents P in very stable residual pools.

The extractions (i), (ii) and (iii) were conducted with a slag to extracting solution ratio of 0.5 kg/L (adapted from EN 12457-1, 2002) and 16 h extraction time at 20 °C and at 125 rpm of agitation. After each extraction, the samples were washed with 25 mL of 1 M KCl to recover P re-adsorbed on slag surface, and the KCl washes were added to the supernatant solution, as already done by (Headly et al., 2003). All the extractions were performed in duplicate.

4.2.2.5 Analytical methods

The pH values of fresh water samples were measured using a model C 561 conductivimeter /pH-meter (Consort, Turnhout, Belgium). TP and PO_4-P analyses were performed according to the Ammonium Molybdate Spectrometric Method (EN ISO 6878, 2004), whereas Ca analyses were performed according to the Atomic Absorption Spectrometric Method (EN ISO 7980, 1986). Phosphate concentrations were measured using a model Helios Epsilon spectrophotometer (Thermo Fischer Scientific, Waltham, USA), whereas Ca concentrations were measured using a model A Analyst 200 spectrophotometer (Perkin Elmer, Waltham, USA). Total alkalinity was measured according to the titrimetric determination method (EN ISO 9963-1, 1994), whereas COD and TN concentrations were analysed by cuvette tests (HACH LANGE, Düsseldorf, Germany). The limit of detection for the analysis was determined for each set of experiments from the analysis of blanks. All chemicals used were of analytical grade.

4.3 Results and discussion

4.3.1 Hydraulic performances

With few exceptions (EAF-filter week 29 and 44), the retention time distribution curves (RTD-curves) showed a single and narrow peak of tracer after 12-24 hours from the tracer injection (Figure 4.4). This usually indicates low diffusion and/or dispersion of the tracer inside the filter and suggests a plug flow with low short-circuiting and low wall effects (Chazarenc et al., 2003; Alcocer et al., 2012).

The average retention times of the fluid into the filters (T_A) (calculated with equation 4.1) ranged from 17.4 to 25.7 h (Table 4.1), and were close to the theoretical HRTv of 24 h. The experimental data of tracer tests were plotted according to equation (4.2) to evaluate the PF and DV fractions (Table 4.1). The correlation coefficients were always $R^2 > 0.95$, thus indicating that equation (4.2) described the hydraulic performances well. With very few exceptions (EAF-filter week 1, BOF-filter week 29), PFs were >0.5, thus suggesting a plug

flow regime. DVs were always <0.3, thus suggesting that most of the void volume of the filters was available for filtration and participated to the reactions (Chazarenc et al., 2003). Since high PF with low dispersion and low DV is the type of behaviour that is desirable to optimize treatment in sub-surface flow filters (Kadlec and Wallace, 2009), it can be concluded that, overall, slag filters did not show major hydraulic fails.

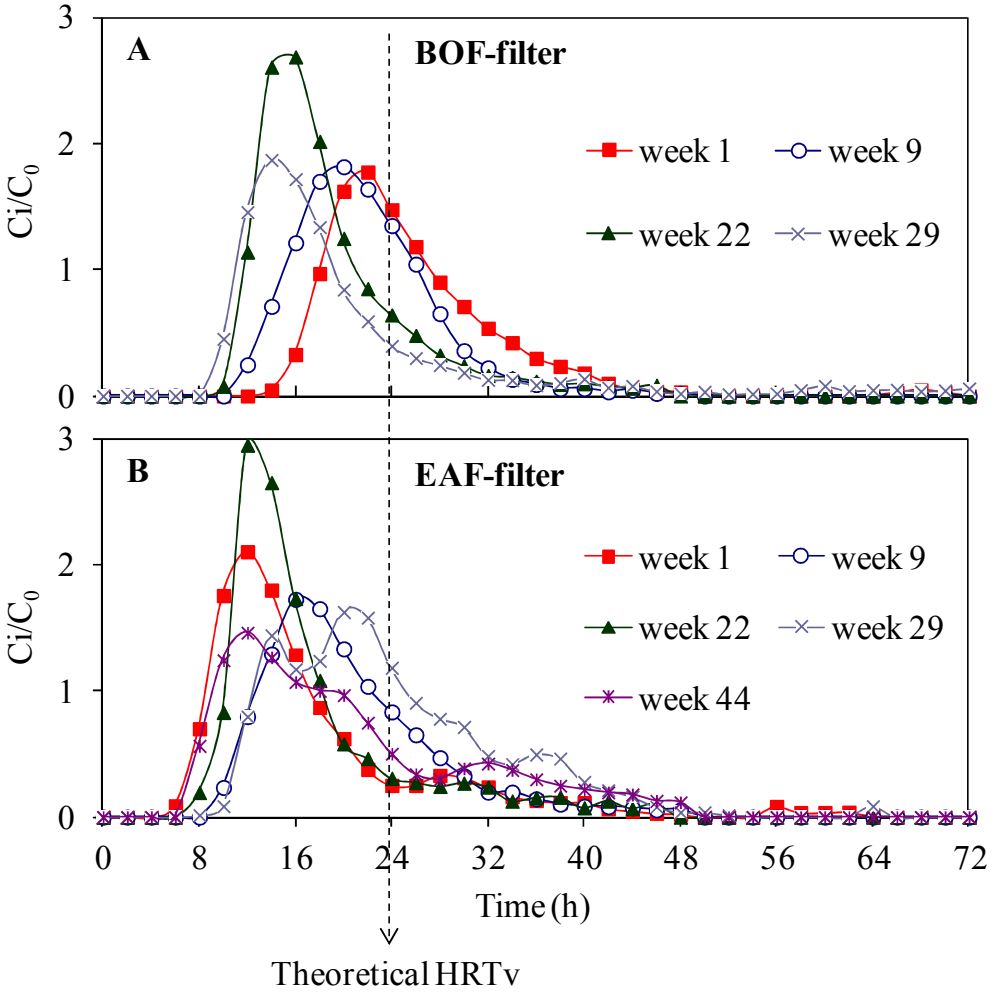

Figure 4.4. Normalized retention time distribution curves (RTD-curves) representing the ratio of outlet tracer concentration Ci to the tracer concentration C_0 (C_0 is the ratio of the total-injected tracer mass and the void volume of the filter): (A) BOF-filter; (B) EAF-filter.

Hydrodynamics of EAF-filter seemed to not change significantly over time, whereas BOF-filter showed an increase in DV and a decrease in PF fractions after week 22 of operation. This likely depended on reactions of slag hydration, slag carbonation and Ca carbonate precipitation during water filtration (Huijgen et al., 2005; Liira et al., 2009; Wang et al., 2010), which probably resulted in the decrease in pore size. Then, the smaller pore size

yielded a lower PF due to the higher dispersion resulting from the fluid flowing through the smaller spaces (Alcocer et al., 2012). However, this change in internal hydrodynamics of the BOF-filter did not seem to affect the T_A, as shown in Table 4.1. Most probably, rather than obtaining reduced porosity and hence decreased retention time, the smaller pore size had also the effect to reduce preferential paths, thus preserving the T_A close to the value of the theoretical HRTv.

Table 4.1. Hydraulic behaviour of the slag filters: average retention time (T_A) and fractions of plug flow (PF) and dead volume (DV).

Week of operation	EAF-filter			BOF-filter		
	T_A (h)	PF (-)	DV (-)	T_A (h)	PF (-)	DV (-)
Week 1	17.5	0.40	0.30	25.7	0.72	0.01
Week 9	20.6	0.64	0.18	21.8	0.74	0.15
Week 22	17.4	0.50	0.30	19.0	0.61	0.25
Week 29	23.8	0.63	0.08	20.6	0.18	0.27
Week 44	20.5	0.52	0.16	N.A.	N.A.	N.A.

4.3.2 Water quality monitoring

Water quality parameters at inlet (CWS effluent) and outlet of the slag filters during the 96-week period of monitoring are presented in Table 4.2. The outlet pH and Ca^{2+} concentrations were significantly higher compared to those of the inlet of the filters. Dissolution of CaO-slag during the water filtration may explain these increases in Ca^{2+} and pH of the filter effluents.

The PO_4-P was the primary form of P in the inlet wastewater. This indicated a high potential for chemical precipitation and adsorption, because PO_4-P is a form of P that is readily available for P precipitation and adsorption onto metal hydroxides (Stumm and Morgan, 1996). The mean outlet concentrations of TP and PO_4-P were markedly lower compared to those of the inlet of the filters, and this indicated P removal. As shown in Table 4.2, PO_4-P was the primary form of P of the filter effluents. Since Ca phosphate precipitation was supposed to be the main mechanism of P removal using Ca-rich materials (Vohla et al., 2011), it is likely that Ca phosphate precipitates were removed from the solution by filtration and then accumulated into the filters, as already observed by Claveau-Mallet et al. (2012) in column experiments.

Table 4.2. Water quality parameters over the 96 weeks of filter monitoring: mean values ± standard deviation (range of min-max values) and number of measures (n).

Parameters	Inlet slag-filters (CWS effluent)	Outlet EAF-filter	Outlet BOF-filter
TP (mg P/L)	8.5 ± 1.3 (5.9-12.0) n = 54	4.7 ± 1.7 (0.9-8.4) n = 54	3.5 ± 1.7 (0.1-7.6) n = 54
PO_4-P (mg P/L)	7.8 ± 1.3 (4.4-11.0) n = 46	4.4 ± 1.6 (0.8-8.2) n = 46	3.3 ± 1.5 (0.1-7.4) n = 46
Ca^{2+} (mg Ca/L)	127 ± 22 (47-152) n = 37	142 ± 20 (75-175) n = 37	134 ± 20 (72-173) n = 37
TN (mg N/L)	39.6 ± 8.8 (26.7-45.1) n = 4	37.9 ± 6.6 (29.0-44.5) n = 4	38.4 ± 6.6 (28.6-43.0) n = 4
TA (mg $CaCO_3$/L)	282 ± 39 (205-340) n = 8	336 ± 48 (247-380) n = 8	296 ± 53 (215-355) n = 8
COD (mg O_2/L)	32.0 ± 7.3 (15.0-42.0) n = 19	25.1 ± 6.2 (16.1-33.8) n = 19	24.9 ± 8.1 (8.5-39.0) n = 19
TSS (mg/L)	<10 n = 12	<10 n = 12	<10 n = 12
pH (-)	7.2 ± 0.2 (6.7-7.7) n = 54	8.3 ± 0.2 (7.7-9.0) n = 54	8.6 ± 0.7 (8.0-12.0) n = 54

As shown in Table 4.2, the CWS effluent treated in this study had a mean TA of 282 mg $CaCO_3$/L (very hard water, according to French classification), thus suggesting a high carbonate alkalinity. The high carbonate alkalinity probably limited P removal as it is well known that carbonate is a strong inhibitor of P precipitation (House, 1999; Johansson and Gustafsson, 2000). Jang and Kang (2002) have demonstrated in batch experiments that the efficiency of P removal via HAP precipitation decreases with increasing bicarbonate alkalinity of the solutions. The TSS, TN and COD concentrations of the CWS effluent treated in this study were similar to the average outlet concentrations of two stage VFCWs in France (Molle et al., 2005). As shown in Table 4.2, the use of slag filters did not lead to significant further reductions of those pollutants.

4.3.3 P removal efficiencies

TP and pH levels at the inlet and outlet of the slag filters during the 96-week period of monitoring are shown in Figures 4.5 A and B, respectively, whereas Figure 4.4 C shows the air and water temperature evolution. The field experiments were started with a HRTv of 1 day. During the first 9 weeks of operation, TP removal efficiencies appeared to decrease according to the decrease in temperature. After week 9, the HRTv was increased from 1 to 2 days, and this led to a temporary increase in TP removal efficiencies. However, the efficiencies decreased drastically during the winter season (after week 16). Then, the TP removal efficiencies began to gradually increase with increasing temperature in spring (week 25-40) (Figure 4.6). This suggested that TP removal efficiency of steel slag increases with increasing temperature, as already observed in column experiments by Shilton et al. (2005).

Inlet and outlet TP levels observed in this study (Figure 4.5 A) were very similar to those reported in a recent study (Shilton et al., 2006), which used melter-slag to upgrade P removal in a CWS in New Zeeland (HRT approximately 3 days). Also, Shilton et al. (2006) showed a clear seasonal fluctuation of TP removal efficiencies during the 10 years of filter operation: the lowest outlet TP concentrations (<2 mg P/L) were observed during the warm seasons (September-March), whereas higher outlet TP concentrations (>4 mg P/L) were observed during the cold seasons (March-September). Therefore, steel slag filters are supposed to be more efficient in warmer climates (Shilton et al., 2005).

During week 22, 29 and 44 the HRTv was temporarily set to 1 day to perform the tracer tests. This decrease in HRTv led to a temporary decrease in TP removal efficiencies. In week 14, 15 and 36, the HRTv increased (from 2 to approximately 4 days) because of clogging of the feeding pipes. The increase in HRTv resulted in a temporary increase in TP removal performances. This seemed to indicate that TP removal efficiencies of slag filters increase with increasing HRTv, as already demonstrated in previous column experiments (Shilton et al., 2005; Drizo et al., 2006). However, excessively long HRTv (>3 days) may produce high pH effluents as the result of excessive CaO-slag dissolution. This problem of high pH effluents was clear for BOF-filter, most probably because BOF-slag is richer in CaO than EAF-slag. In addition, long HRTv may promote reactions of CaO hydration and $CaCO_3$ precipitation, thus causing volume expansion and favouring filter clogging (Liira et al., 2009; Wang et al., 2010). Our experimental results showed that, at HRTv of 1-2 days, the effluent pH was elevated only during the first 5 weeks of operation, and then it stabilized around a pH

of 8.5 (maximum value of pH for discharges from urban waste water treatment plants in France, Arrête du 2 Février 1998). These results on effluent pH were in agreement with the findings of previous pilot-scale experiments (Weber et al., 2007; Lee et al., 2010).

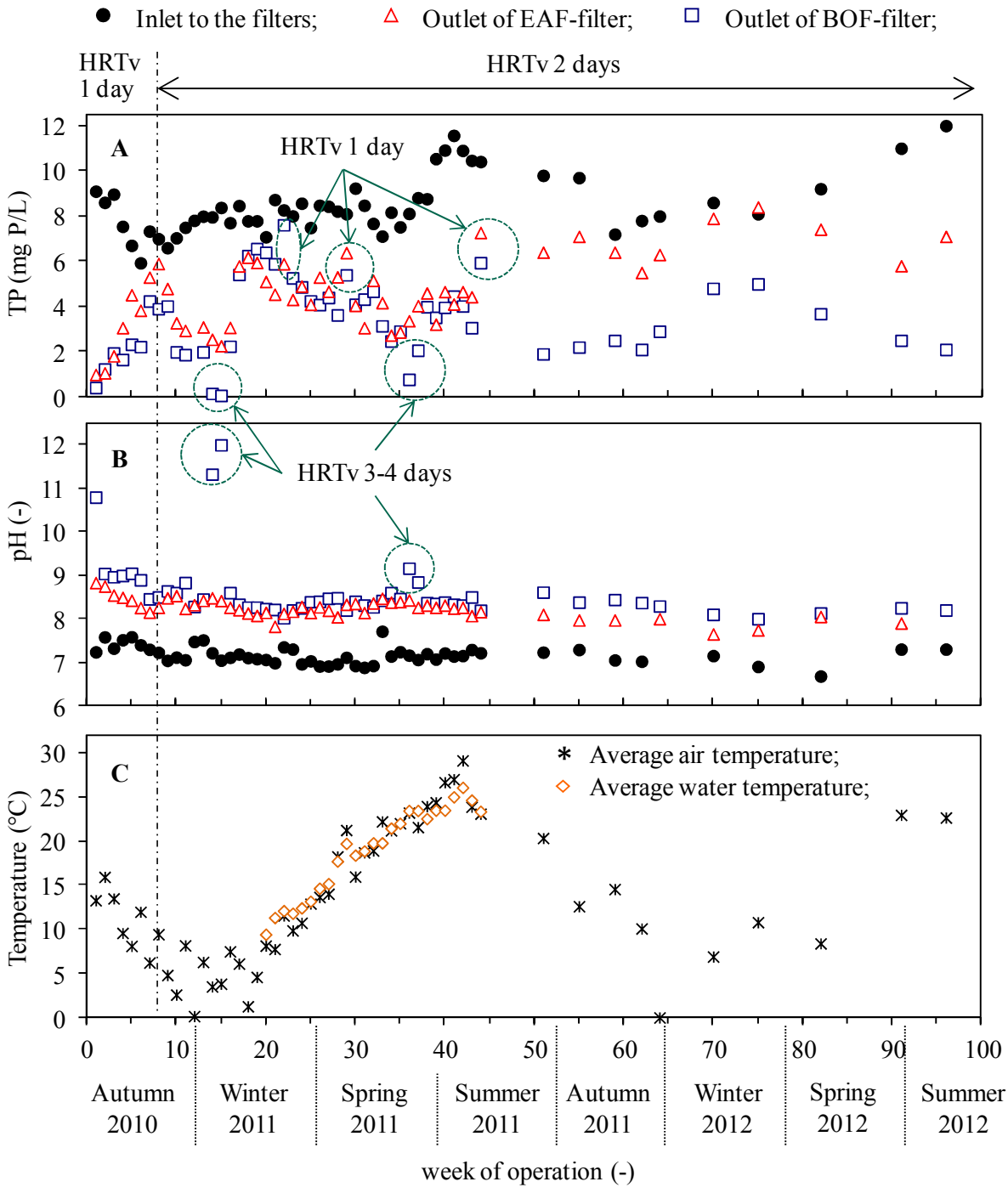

Figure 4.5. Inlet and outlet levels of TP (A) and pH (B), and air and water temperature (C) over a period of 96 weeks of operation of steel slag filters.

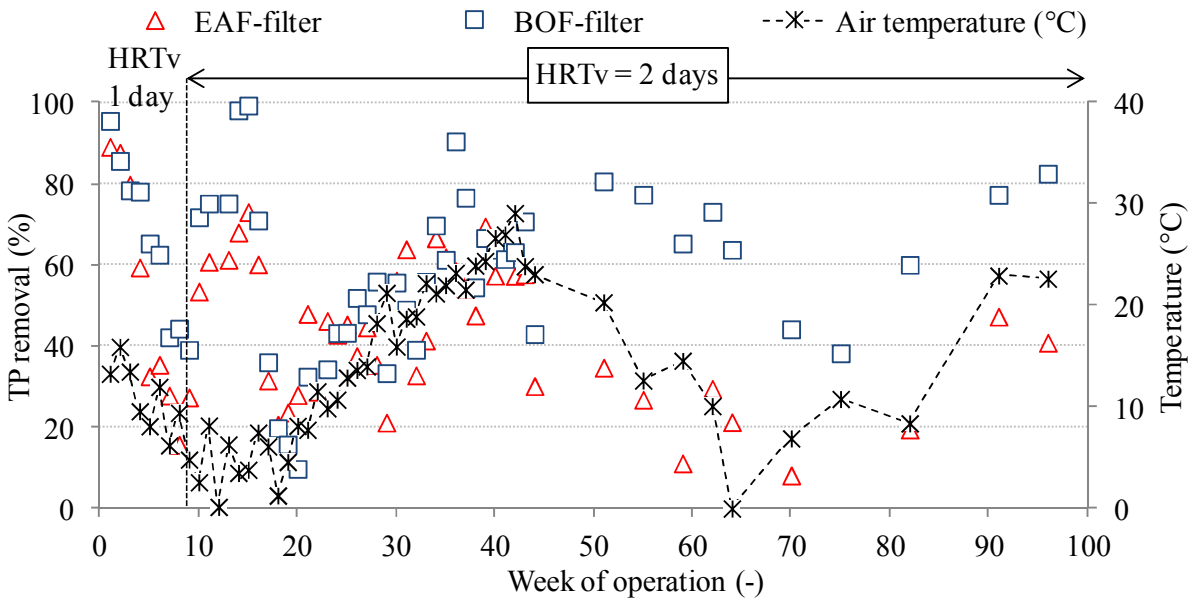

Figure 4.6. Correlation between TP removal efficiencies of EAF and BOF-filter and average air temperature over the 96-week period of operation.

Results of this study were compared to those of previous experiments that used CaO-rich materials in filters designed to upgrade P removal in CWSs (Table 4.3). BOF-slag and sediments of oil shale ash showed the highest P removal performances (>99%) (Koiv et al., 2010; Cassini et al., 2010). However, the duration of these studies is too limited (<12 months, except for Shilton et al., 2006). In addition, in most of the studies TP saturation levels of the materials were not reached, thus leading to difficulties when evaluating the lifespan of the filters. The main mechanism of P removal using EAF-slag, BOF-slag and oil shale ash was related to CaO dissolution followed by Ca phosphate precipitation, whereas melter slag mainly removed P by adsorption onto metal hydroxides (Pratt et al., 2007). Overall, TP removal performances seemed to improve with increasing CaO content and/or by decreasing the size of the materials. It is likely that the greater the CaO content of the material, the greater the potential for Ca phosphate precipitation. Also, the smaller is the size of the material, the greater is the specific surface available for CaO dissolution (Vohla et al., 2011). However, the smaller is the size, the greater is the risk of clogging due to CaO hydration and $CaCO_3$ precipitation (Chazarenc et al., 2007). For these reasons, the use of medium size larger than 5 mm is recommended when using Ca-rich materials as filter substrate (Vohla et al., 2011).

Table 4.3. Selected field studies that used CaO-rich industrial by-products to upgrade P removal in CWSs (adapted from Vohla et al., 2011).

Authors	Filter material	Experimental design, Flow type[a] (filter vol.)	Size (mm)	CaO (% w.)	Inlet TP[b] (mg/L)	HRTv (day)	Duration (month)	TP removal (%)	TP removed (mg P/g)
This study	EAF-slag	1 HF (6 m^3)	20-40	26.0	8.5	1-2	22	37%	0.32
	BOF-slag	1 HF (6 m^3)	20-40	54.6	8.5	1-2	22	62%	0.61
Koiv et al., 2010	Sediments of oil shale ash	1 UVF (0.86 m^3) 1 HF (1.24 m^3) in series	5-20	29.2	4.9	5-15	6	>99	0.69 (VF) 0.61 (HF)
Korkusuz et al., 2007	Gravel (25%) BF-slag (50%) Sand (25%)	1 UVF (18 m^3)	<3	33.5	6.6	3	12	52	0.08[c]
Cassini et al., 2010	BOF-slag	1 HF (7.2 m^3)	d_{10}[d] < 32	40	7.8	1.7	5	>99	N.A.
Shilton et al., 2006	Melter slag	10 HF (1440 m^3 each) in parallel	10-20	15.9	8.4	3	10 years	72 (first 5 years) 37 (last 5 years)	1.23 (5 years) 1.5 (10 years)
Weber et al., 2007	EAF-slag	4 SVF (0.02 m^3 each)[e] in parallel	5-14	N.A.	N.A.	0.5-1	9	79-81	1.67-1.7

[a] Horizontal Flow (HF), Saturated Vertical Flow (SVF), Unsaturated Vertical Flow (UVF).

[b] Average value of inlet TP.

[c] Determined by P extraction experiment.

[d] Diameter of the sieve which passes 10% (weight) of the particles.

[e] Pore volume only, total volume of the filters not available.

4.3.4 P removal kinetics

TP concentrations of the samples taken from the piezometers were plotted according to the k-C* kinetic model of Kadlec and Knight (1996) (equation 4.3). The minimum outlet TP concentration observed during this study (0.1 mg P/L, Table 4.2) was used as C*-value when employing equation (4.3). With very few exceptions (EAF-filter week 3; BOF-filter week 5), correlation coefficients (R^2) were higher than 0.7, and this suggested that the k-C* kinetic model described the TP removal kinetics well. Figure 4.7 shows the evolution of the k_V-values during the filter operation. In week 1 of operation, the k_V-values were 3.30 d^{-1} using EAF-slag and 4.09 d^{-1} using BOF-slag. Then, k_V-values gradually decreased to stabilize around a value of 0.5 d^{-1} after week 16. This decrease in k_V-values appeared to be well correlated with the decrease in temperature in winter. After week 32, the k_V-values seemed to slightly improve with increasing temperature in spring. These results suggested that temperature affected the kinetic of P removal, most probably because the solubility of various Ca phosphates decreases with increasing temperature, thus favouring precipitation (McDowell et al., 1977; Ferreira et al., 2003), thus increasing the rate of Ca phosphate precipitation.

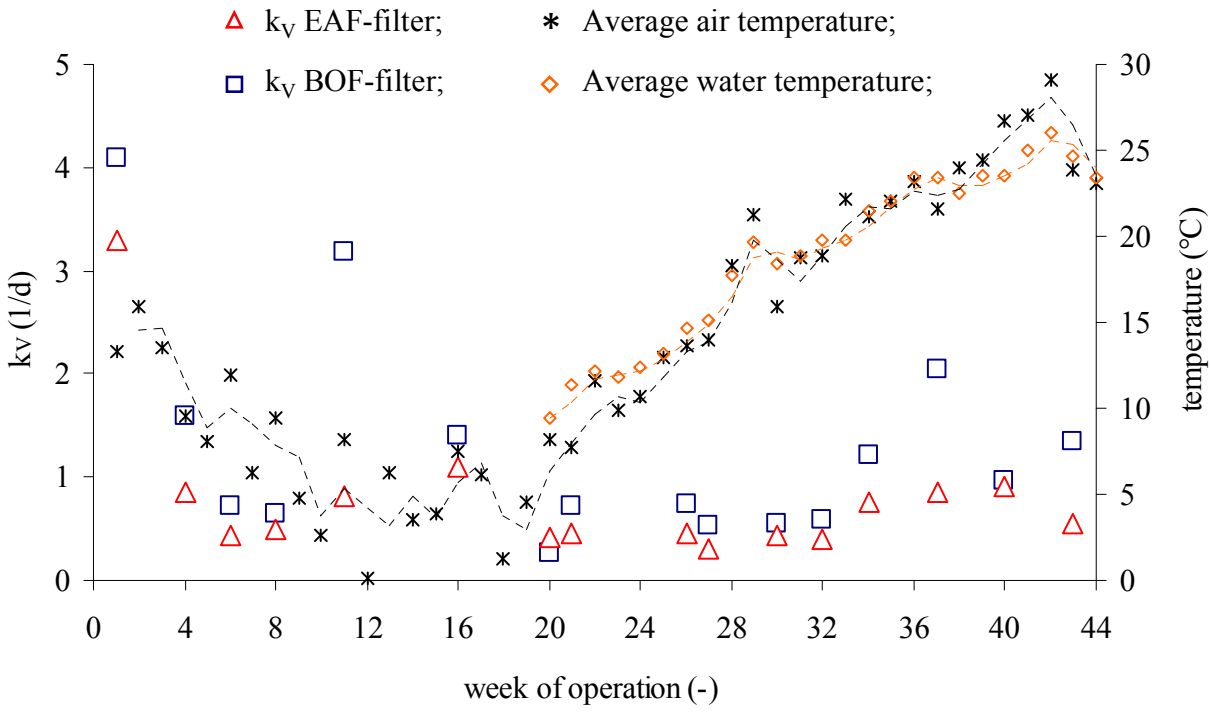

Figure 4.7. Volumetric constant rates (k_V) for the k-C* kinetic model (Kadlec and Knight, 1996) describing TP removal over a 44-week period of the filter operation.

The results of simulation studies showed that in general k_V-values are not affected by the inlet pollutant concentration, whereas the C* values are strongly affected by the inlet concentration (Kadlec, 2000). However, in this study, the variation of the inlet TP during the kinetic investigations seemed to be too low to affect significantly the C* values (Figure 4.5 A).

4.3.5 Chemical and mineralogical investigations on slag

Leaching experiments showed that steel slag after 52 weeks of demonstration-scale filter operation still produced high pH, conductivities and Ca leachates (Table 4.4), thus indicating that steel slag still had a high potential for CaO dissolution. The increase in SO_4 leachates after field experiment may indicate precipitation of Ca sulphate (probably gypsum) on the slag surface during wastewater filtration. Most probably, the precipitation of Ca sulphate led to a competing consumption of Ca ions, thus limiting Ca phosphate precipitation. The metal concentrations of the leachates of slag did not seem to vary remarkably during the filter operation. The data shown in Table 4.4 appeared to demonstrate that steel slag does not produce environmental hazardous leachates, with the exceptions of V and Ba releases from EAF-slag, and the leachate concentrations were below the limits established by the European Council decision 2003/33/EC for waste acceptable at landfills for inert waste. These data on slag leachates are in agreement with the findings of a previous study (Proctor et al., 2000), which confirmed the potential release of V and Ba from steel slag.

The surfaces of steel slag before and after 65 weeks of filter operation were examined by SEM and EDX analyses (Figure 4.8). The coarse surface of fresh BOF-slag and EAF-slag resulted predominantly composed of Fe, Ca and O. Microscopic observations by SEM of slag after 65 weeks of filter operation showed that the surface was covered with a layer of precipitates including rhombohedral crystals and spheroidal aggregates (Figures 4.8 C and D), as already observed in column experiments (Chapter 3). EDX analyses confirmed that rhombohedral crystals (>10 μm) were mostly made of Ca, C and O, thus suggesting $CaCO_3$ precipitation and crystallisation on the surface of slag. Instead, spheroidal aggregates (<10 μm) were mostly made of Ca and P, thus indicating Ca phosphate precipitation on the surface of slag, and then suggesting co-precipitation of Ca carbonate and Ca phosphate.

These results are in agreement with the finding of previous laboratory and field-scale experiments (Bowden et al., 2009; Liira et al., 2009; Koiv et al., 2010), which have shown the formation of a secondary layer of Ca phosphate precipitates mixed to $CaCO_3$ crystals (calcite) covering the surface of Ca-rich materials after their use in filters.

Table 4.4. Leachate concentrations of slag after 52 weeks of demonstration-scale filter operation compared to leachate concentrations of slag before the use in field experiments (according to EN 12457-1, 2002).

Parameter	EAF-slag		BOF-slag		Limit values 2003/33/EC[a]
	Before use	After 52 weeks	Before use	After 52 weeks	
pH (-)	11.9	11.5	12.6	12.4	N.A.
Cond. (mS/cm)	1.05	0.99	5.29	3.92	N.A.
As (mg/L)	<0.005	0.003	<0.005	<0.002	0.2
Ba (mg/L)	0.21	0.15	0.11	0.12	14
Ca (mg/L)	87	88	496	335	N.A.
Cd (mg/L)	<0.0005	<0.0005	<0.0005	<0.0005	0.06
Cr_{tot} (mg/L)	0.014	<0.001	0.002	0.001	0.4
Cu (mg/L)	<0.002	0.008	<0.002	<0.002	1.8
Fe (mg/L)	0.72	0.021	<0.01	0.012	N.A
Mn (mg/L)	0.09	0.001	0.003	0.002	N.A.
Mo (mg/L)	0.017	0.06	0.006	0.025	0.6
Ni (mg/L)	<0.002	<0.002	<0.002	<0.002	0.4
P (mg/L)	<0.010	<0.010	<0.010	0.014	N.A.
Pb (mg/L)	<0.002	0.043	<0.002	<0.002	0.4
Sb (mg/L)	<0.005	0.018	<0.005	<0.005	0.04
V (mg/L)	0.111	0.131	<0.002	0.002	N.A.
Zn (mg/L)	0.007	0.072	<0.005	<0.005	4
Cl (mg/L)	5	17	<1	7	1100
F (mg/L)	0.9	1.3	<0.4	<0.4	8
SO_4 (mg/L)	3	32	<1	5	1120

[a] Leaching limit values for waste acceptable at landfills for inert waste, calculated at liquid to solid ratios (L/S) of 2 L/kg.

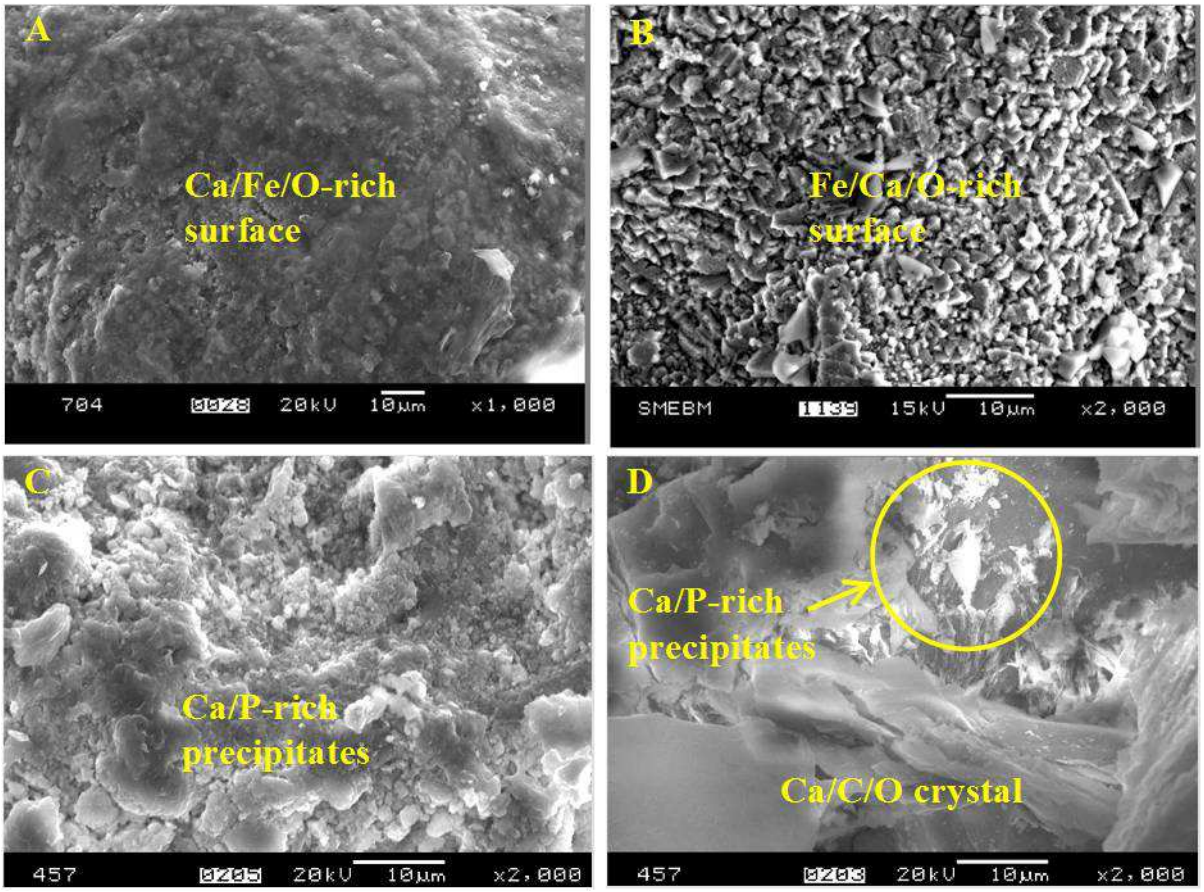

Figure 4.8. SEM observations and EDX analyses: (A) surface of BOF-slag before experiments; (B) surface of EAF-slag before experiments; (C) surface of BOF-slag after 65 weeks of demonstration-scale filter operation; (D) surface of EAF-slag after 65 weeks of demonstration-scale filter operation.

Figure 4.9 shows the results of P fractionation experiments: 0.30 g P/kg was totally extracted from fresh EAF-slag (before field experiments), whereas 1.03 g P/kg was totally extracted from fresh BOF-slag (before filed experiments). The major fractions of P in slag were Ca bound P and P in stable residual pools (>90% of the total amount of P extracted) and this suggests that the P in fresh slag is poorly mobilizable in water.

As shown in Figure 4.9, the total amount of P extracted from slag after 85 weeks of filter operation increased to 0.54 g P/kg for EAF-slag and 1.30 g P/kg for BOF-slag, and this confirmed P accumulation on slag. The main increases were observed for the fractions of weakly bound P, Ca bound P, and P in stable residual pools. Drizo et al. (2002) employed the procedure of Tiessen and Moir (1993) to quantify the proportion of P bound to mineral compounds in EAF-slag, and they defined the hot concentrated HCl extract as Ca associated P in the stable residual pools. This suggests that the surface of slag after 85 weeks of field

experiments was covered of a mix of less stable (amorphous) and very stable (crystalline) Ca phosphates, as it is known that crystalline Ca phosphates are more stable than amorphous Ca phosphates (Valsami-Jones, 2001). These results on P fractionation are consistent with the findings of a previous field experiment that used BF-slag as filter substrate in a CWS (Korkusuz et al., 2007). Also, the results of P fractionation experiments suggested the presence of Al and Fe bound P in EAF-slag after 85 weeks of filed experiments, as already observed by Drizo et al. (2002) using EAF-slag in column experiments. Instead, Al and Fe bound P in BOF-slag appeared to be negligible (Figure 4.9). The higher Fe and Al content of EAF-slag likely may account for the higher fraction of Al and Fe bound P in EAF-slag.

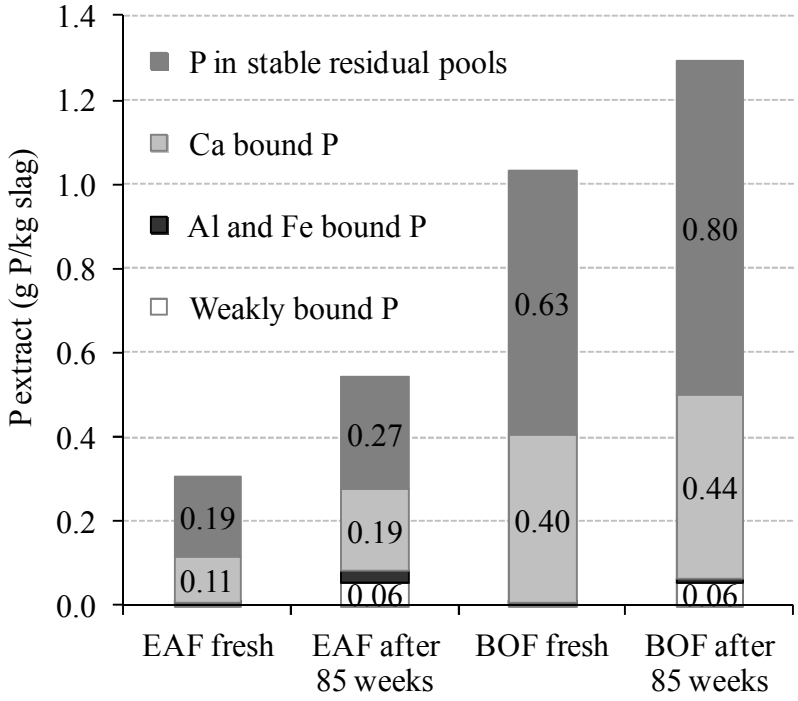

Figure 4.9. P fractionation experiments: P fractions extracted from slag before (fresh) and after 85 weeks of demonstration-scale filter operation. Average values of duplicates.

4.3.6 Mechanism of P removal

The results of this study suggested that P removal occurred predominantly via Ca phosphate precipitation. Several Ca phosphates may be formed depending on the pH values, Ca^{2+} and PO_4-P concentrations of the solutions (Valsami-Jones, 2001): amorphous Ca phosphate (ACP), dicalcium phosphate (DCP), dicalcium phosphate dihydrate (DCPD), octacalcium phosphate (OCP), tricalcium phosphate (TCP), hydroxyapatite (HAP) and fluorapatite (FAP). In our experiments, it was found that outlet TP concentrations decreased with increasing outlet pH (Figure 4.10), most probably because the solubility of various Ca phosphates

decreases with increasing pH (Stumm and Morgan, 1996), thus favouring precipitation. The experimental data shown in Figure 4.5 and Table 4.2 were compared to the solubility curve of Ca phosphates as a function of the pH of the solutions (Stumm and Morgan, 1996; Valsami-Jones, 2001). It was found that pH, Ca^{2+} and PO_4-P concentrations were in the range of values that support precipitation of TCP, OCP and HAP.

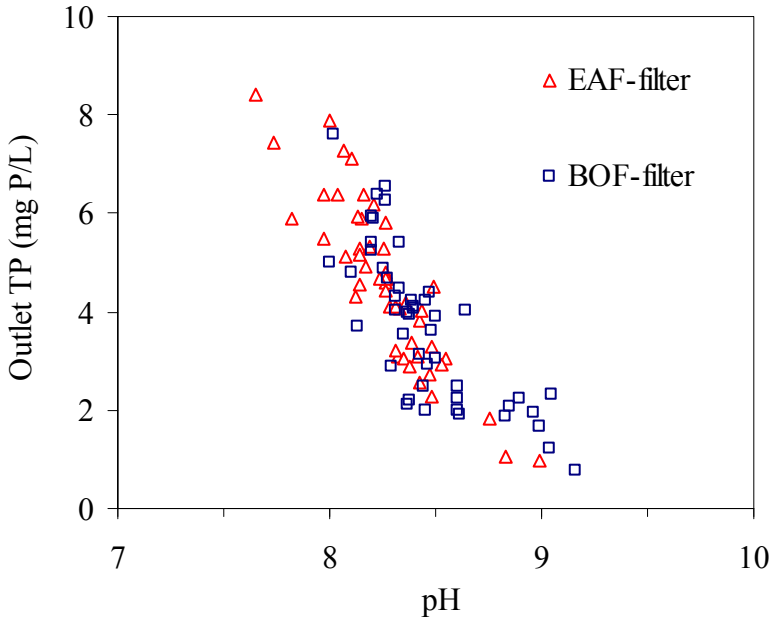

Figure 4.10. Outlet TP concentrations as a function of outlet pH values.

The equations (4.4), (4.5) and (4.6) describe the precipitation of TCP, OCP and HAP at 25 °C, respectively (Stumm and Morgan, 1996):

$$3Ca^{2+} + 2PO_4^{3-} \rightarrow Ca_3(PO_4)_2 \downarrow \qquad (Ksp = 10^{-26}) \qquad (4.4)$$

$$4Ca^{2+} + 3PO_4^{3-} + H^- \rightarrow Ca_4H(PO_4)_3 \downarrow \qquad (Ksp = 10^{-46.9}) \qquad (4.5)$$

$$10Ca^{2+} + 6PO_4^{3-} + 2OH^- \rightarrow Ca_{10}(PO_4)_6(OH)_2 \downarrow \qquad (Ksp = 10^{-114}) \qquad (4.6)$$

According to the equations (4.4), (4.5) and (4.6), Ca^{2+} concentration may limit Ca phosphate precipitation when the molar ratio of PO_4-P concentration to Ca^{2+} concentration (PO_4-P/Ca) of the solution is higher than 0.6. During the 96-week period of monitoring, the molar ratio PO_4-P/Ca of the wastewater was always <0.3 (Table 4.2), thus indicating that Ca^{2+} concentration never limited Ca phosphate precipitation. These results are in agreement with the findings of previous experiments at different scales of investigation (from batch to field scale), which showed efficient P removal via Ca phosphate precipitation under the conditions

of initial Ca^{2+} concentrations of 40-120 mg Ca/L and initial P concentrations of 3-10 mg P/L (Jang and Kang, 2002; Kim et al., 2006a; Koiv et al., 2010; Barca et al., 2012).

Several authors in the literature have stated that precipitation of Ca phosphates usually follows the Ostwald's well-known "rule of stages": first, precipitation of less stable compounds (ACP, DCP, OCP), and then, recrystallisation into the most thermodynamically stable HAP (Valsami-Jones, 2001; Lundager-Madsen, 2008). Recrystallisation of Ca phosphate precipitates into HAP appeared to be confirmed by Bowden et al. (2009), who have shown that there is a succession of Ca phosphate minerals on the surface of BOF-slag during continuous flow column experiments, and that this sequence of Ca phosphate minerals progresses from the less stable (DCP, which was observed since the first month of column operation) to the most stable (HAP, which was observed since the fifth month of column operation). "Recrystallised" crystals of HAP may represent seed crystals for further HAP crystallisation (Kim et al., 2006b), thus improving P removal efficiencies. However, under field conditions, crystallisation of HAP may be affected by several inhibitors including Mg^{2+}, CO_2, carbonates, humic, fulvic and tannic acids (House, 1999; Valsami-Jones, 2001), which usually occur in real wastewater. For these reasons, Ca phosphate recrystallisation into HAP is expected to intervene over a longer period of filter operation. In our experiments, the recrystallisation of pre-deposited Ca phosphate into HAP might explain the improvement in TP removal efficiencies of BOF-filter during the second year of operation (Figure 4.5). The presence of HAP crystals covering slag after 85 weeks of filter operation appeared to be confirmed by the increase in the fraction of P in the stable residual pools on slag (Figure 4.9).

4.3.7 Slag filter lifespan

P saturation levels of filter materials are usually considered as a parameter to estimate the longevity of filter systems (Drizo et al., 2002). Figure 4.11 shows the TP removed as a function of the TP added by the CWS effluent to the filters over 96 weeks of operation. Over the full period of monitoring, BOF-filter removed 62% of the inlet TP reaching a P retention level of about 0.61 g P/kg BOF-slag. The ratio of TP removed to TP added to BOF-filter remained higher than 0.5 over the full period of monitoring, thus suggesting that P saturation was not reached. Over the same period of operation, EAF-filter removed 37% of the inlet TP reaching a P retention level of about 0.32 g P/kg EAF-slag. The ratio of TP removed to TP added to EAF-filter fell below a value of 0.5 since week 22 of operation, thus suggesting a decrease in TP removal efficiencies over time.

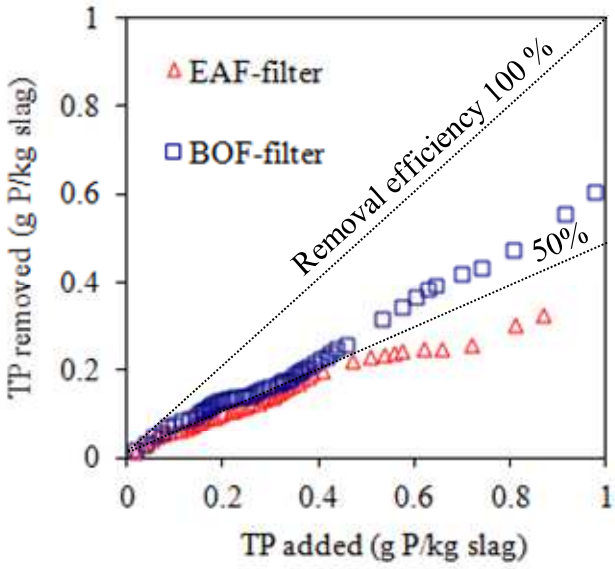

Figure 4.11. TP removed as a function of TP added by the CWS effluent to the filters over 96 weeks of operation.

P retention levels reported in this study were compared to those found by Shilton et al. (2006) using meter-slag in filters designed to remove P from the effluent of a CWS (mean inlet TP of 8 mg P/L; HRTv of 3 days). Shilton at al. (2006) showed good P removal performances until reach a P saturation level of 1.23 g P/kg melter-slag after 5 years of filter operation. The P saturation level reported by Shilton et al. (2006) is higher than those of this study, thus suggesting that, at the current rate of P retention, slag filters may operate for several years before reaching P saturation. However, estimating the lifespan of EAF and BOF filters by using data of meter slag is very approximate. Therefore, further long term studies are needed to determine the P saturation levels of EAF and BOF-slag under field conditions.

Several international studies have demonstrated that P retention capacities of P saturated slag might be regenerated by physical and chemical techniques, including drying, agitation, crushing and acid washes (Drizo et al., 2008; Pratt et al., 2009; Pratt and Shilton, 2010). These techniques may favour HAP crystallisation (drying), unclog adsorption sites to create fresh surface for CaO dissolution and P adsorption (agitation and crushing), and remove (eventually recover) P bound on slag (acid washes). After regeneration, steel slag may be reused as filter substrate for a new cycle of water treatment.

4.3.8 Design recommendation

Equation (4.7), which derived from the k-C* model of Kadlec and Knight (1996), was employed to determine the volume per capita of the filters (V) as a function of the expected outlet TP concentration (C_E). In equation (4.7), V is the volume per capita of the filter (m^3/p.c.), Q is the water flow per capita (m^3/(p.c.*d)), ρ is the filter porosity (-), k_V is the volumetric constant rate of P removal (1/d), C_0 is the inlet TP concentration (mg P/L), C_E is the expected outlet TP concentration (mg P/L) and C* is the background outlet TP concentration (mg P/L).

$$V = \frac{Q}{\rho \times k_V} \ln\left(\frac{C_0 - C^*}{C_E - C^*}\right) \qquad (4.7)$$

The less favourable conditions for P removal, which were observed during the winter (weeks 14-26), were considered when employing equation (4.7). The following experimental values for the input parameters were used: k_V of 0.61 d^{-1} for EAF-filter and of 0.78 d^{-1} for BOF-filter (average k_V-values during weeks 14-26), Q of 0.15 m^3/(p.c.*d), C_0 of 8 mg P/L, ρ of 0.5 and C* of 0.1 mg P/L. Figure 4.12 shows the filter volume per capita as a function of the expected TP concentration.

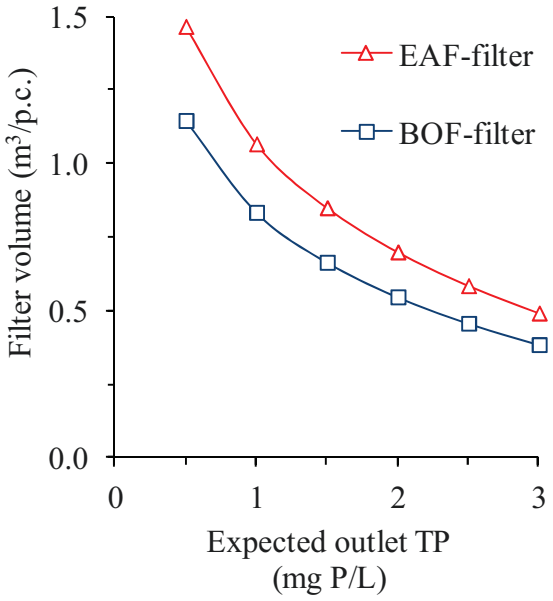

Figure 4.12. Filter volume per capita (m^3/p.c.) as a function of the expected outlet TP concentration.

The results indicated that the filter volume (V) increases with decreasing the expected outlet TP concentration (C_E) (Figure 4.12). However, greater filter volumes may require longer HRTv, thus increasing the risk of high pH of the effluents.

4.4 Conclusions

This study showed that EAF and BOF-slag produced in Europe are efficient filter substrates to remove P from the effluent of a constructed wetland. Over a period of almost 2 years of operation, the filter filled with EAF-slag removed 37% of the inlet total P, whereas the filter filled with BOF-slag removed 62% of the inlet total P. P removal occurred predominantly via CaO-slag dissolution followed by Ca phosphate precipitation. P removal efficiencies improved with increasing temperature and HRTv, most probably because this affected the rates of CaO-slag dissolution and Ca phosphate precipitation.

Overall, the results of this study showed that BOF-slag is more efficient than EAF-slag for P removal from real effluents, and a smaller volume of BOF-slag is required to reach good treatment standards.

Supporting Information

Tables AII 3 and 4 in Annex II show the results of P fractionation experiments of samples of slag before and after 85 weeks of field experiments. Figures AIII 6-8 in Annex III show plan view, panoramic view, and details on the design of the demonstration-scale slag filters.

References of Chapter 4

EN 12457-1: 2002. Characterisation of waste. Leaching. Compliance test for leaching of granular waste materials and sludges. One stage batch test at a liquid to solid ratio of 2 l/kg for materials with high solid content and with particle size below 4 mm (without or with size reduction).

EN ISO 6878: 2004. Water quality - Determination of phosphorus - Ammonium molybdate spectrometric method.

EN ISO 7980: 1986. Water quality - Determination of calcium and magnesium - Atomic absorption spectrometric method.

EN ISO 9963-1: 1994. Water quality - Determination of alkalinity - Part 1: Determination of total and composite alkalinity.

INSEE, 2009. *Institut National de la Statistique et des Etudes Economiques* (France), http://www.insee.fr.

Alcocer D.J.R., Giacoman V.G., Champagne P., 2012. Assessment of the plug flow and dead volume ratios in a sub-surface horizontal-flow packed-bed reactor as a representative model of a sub-surface horizontal constructed wetland. Ecological Engineering 40, 18-26.

Barca C., Gérente C., Meyer D., Chazarenc F., Andrès Y., 2012. Phosphate removal from synthetic and real wastewater using steel slags produced in Europe. Water Research 46(7), 2376-2384.

Bowden L.I., Jarvis A.P., Younger P.L., Johnson K.L., 2009. Phosphorus removal from wastewaters using basic oxygen steel slag. Environmental Science and Technology 43(7), 2476-2481.

Cassini S.T., Avelar J.C., Gonçalves R.F., Pinotti L.M., Keller R., 2010. Evaluation of steel slag as filter bed of constructed wetland in post treatment of anaerobic baffled reactor treating wastewater. Proceedings of the 12th International Conference on Wetland Systems for Water Pollution Control. Venice, Italy, 4-7 Oct. 2010.

Chazarenc F., Merlin G., Gonthier Y., 2003. Hydrodynamics of horizontal subsurface flow constructed wetlands. Ecological Engineering 21 (2-3), 165-173.

Chazarenc F., Brisson J., Comeau Y., 2007. Slag columns for upgrading phosphorus removal from constructed wetland effluents. Water Science and Technology 56(3), 109-115.

Claveau-Mallet D., Wallace S., Comeau Y., 2012. Model of phosphorus precipitation and crystal formation in electric arc furnace steel slag filters. Environmental Science and Technology 46(3), 1465-1470.

Drizo A., Comeau Y., Forget C., Chapuis R. P., 2002. Phosphorus saturation potential: a parameter for estimating the longevity of constructed wetland systems. Environmental Science and Technology 36(21), 4642-4648.

Drizo A., Forget C., Chapuis R.P., Comeau Y., 2006. Phosphorus removal by electric arc furnace steel slag and serpentinite. Water Research 40(8), 1547-1554.

Drizo A., Cummings J., Weber D., Twohig E., Druschel G., Bourke B., 2008. New evidence for rejuvenation of phosphorus retention capacity in EAF steel slag. Environmental Science and Technology 42(16), 6191-6197.

Ferreira A., Oliveira C., Rocha F., 2003. The different phases in the precipitation of dicalcium phosphate dihydrate. Journal of Crystal Growth, 252 (4), 599-611.

Headley T.R., Huett D.O., Davison L., 2003. Seasonal variation in phosphorus removal processes within reed beds – mass balance investigations. Water Science and Technology 48(5), 59-66.

Huijgen W.J.J, Witkamp G.J., Comans R.N.J., 2005. Mineral CO_2 sequestration by steel slag carbonation. Environmental Science and Technology, 39 (24), 9676-9682.

House W.A., 1999. The physico-chemical conditions for the precipitation of phosphate with calcium. Environmental Technology 20(7), 727-733.

Jang H., Kang S.H., 2002. Phosphorus removal using cow bone in hydroxyapatite crystallization. Water Research 36(5), 1324-1330.

Johansson L., 1999. Blast furnace slag as phosphorus sorbent – column studies. The Science of the Total Environment 229(1-2), 89-97.

Johansson L., Gustafsson J.P., 2000. Phosphate removal using blast furnace slags and opoka - mechanisms. Water Research 34(1), 259-265.

Johansson-Westholm L., 2006. Substrates for phosphorus removal-potential benefits for on-site wastewater treatment? Water Research 40(1), 23-36.

Kadlec R. H., Knight R. L., 1996. Treatment Wetlands. Lewis Publishers, USA (Florida), pp. 893.

Kadlec R.H., 2000. The inadequacy of first-order treatment wetland models. Ecological Engineering 15 (1-2), 105-119.

Kadlec R.H., Wallace S.D., 2009. Treatment Wetlands. Second Edition. Taylor and Francis Group, Boca Raton, FL, USA.

Kim E.H., Lee D.W., Hwang H.K., Yim S., 2006a. Recovery of phosphates from wastewater using converter slag: Kinetics analysis of a completely mixed phosphorus crystallization process. Chemosphere 63(2), 192-201.

Kim E.H., Yim S., Jung H., Lee E., 2006b. Hydroxyapatite crystallization from a highly concentrated phosphate solution using powdered converter slag as a seed material. Journal of Hazardous Materials 136(3), 690-697.

Korkusuz E.A., Beklioglu M., Demirer G.,N., 2007. Use of blast furnace granulated slag as a substrate in vertical flow reed beds: field application. Bioresource Technology 98(11), 2089-2101.

Koiv M., Liira M., Mander U., Motlep R., Vohla C., Kirsimae K., 2010. Phosphorus removal using Ca-rich hydrated oil shale ash as filter material – The effect of different phosphorus loadings and wastewater compositions. Water Research 44(18), 5232-5239.

Lee M.S., Drizo A., Rizzo D.M., Druschel G., Hayden N., Twohig E., 2010. Evaluating the efficiency and temporal variation of pilot-scale constructed wetlands and steel slag phosphorus removing filters for treating dairy wastewater. Water Research 44(14), 4077-4086.

Liénard A., 1987. Domestic wastewater treatment in tanks with Emergent Hydrophytes: latest results of a recent plant in France. Water Science and Technology 19(12), 373-375.

Liira M., Kõiv M., Mander Ü., Mõtlep R., Vohla C., Kirsimäe K., 2009. Active filtration of phosphorus on Ca-rich hydrated oil-shale ash: does longer retention time improve the process? Environmental Science and Technology 43(10), 3809-3814.

Lundager-Madsen H.E., 2008. Influence of foreign metal ions on crystal growth and morphology of brushite ($CaHPO_4$,$2H_2O$) and its transformation to octacalcium phosphate and apatite. Journal of Crystal Growth 310(10), 2602-2612.

Metcalf and Eddy, Inc., 2003. Wastewater Engineering - Treatment and reuse. 4th edition, McGraw-Hill, USA (New York).

Mc Dowell H., Gregory T.M., Brown W.E., 1977. Solubility of $Ca_5(PO_4)_3(OH)$ in the system $Ca(OH)_2$-H_3PO_4-H_2O at 5, 15, 25 and 37°C, Journal of Research, National Bureau of Standards, 81A(2-3), 273-281.

Molle P., Liénard A., Boutin C., Merlin G., Iwema A., 2005. How to treat raw sewage with constructed wetlands: an overview of the French system. Water Science and Technology 51(9), 11-21.

Molle P., 2008. Élimination du phosphore par filtres plantés de roseaux. Technique de l'Ingénieur RE101, pp. 8.

Motz H., Geiseler J., 2001. Products of steel slags: an opportunity to save natural resources. Waste Management 21(3), 285-293.

Pratt C., Shilton A., Pratt S., Haverkamp R.G., Bolan N.S., 2007. Phosphorus removal mechanisms in active slag filters treating waste stabilization pond effluent. Environmental Science and Technology 41(9), 3296-3301.

Pratt C., Shilton A., Haverkamp R.G., Pratt S., 2009. Assessment of physical techniques to regenerate active slag filters removing phosphorus from wastewater. Water Research 43(2), 277-282.

Pratt C., Shilton A., 2010. Active slag filters – simple and sustainable phosphorus removal from wastewater using steel industry by-product. Water Science and Technology 62(8), 1713-1718.

Proctor D.M., Fehling K.A., Shay E.C., Wittenborn J.L., Green J.J., Avent C., Bigham R.D., Connolly M., Lee B., Shepker T.O., Zak M.A., 2000. Physical and chemical characteristics of blast furnace, basic oxygen furnace, and electric arc furnace steel industry slags. Environmental Science and Technology 34(8), 1576-1582.

Shilton A. N., Pratt S., Drizo A., Mahmood B., Banker S., Billings L., Glenny S., Luo D., 2005. Active filters for upgrading phosphorus removal from pond systems. Water Science and Technology 51(12), 111-116.

Shilton A. N., Elmetri I., Drizo A., Pratt S., Haverkamp R. G., Bilby S. C., 2006. Phosphorus removal by an "active" slag filter - a decade of full scale experience. Water Research 40(1), 113-118.

Stumm W., Morgan J.J., 1996. Aquatic chemistry – Chemical equilibria and rates in natural waters. 3rd edition, Wiley-Interscience Publication, USA (Iowa), pp. 1022.

Suliman F., French H.K., Haugen L.E., Sovik A.K., 2006. Change in flow transport patterns in horizontal subsurface flow constructed wetlands as a result of biological growth. Ecological Engineering 27(2), 124-133.

Tiessen H., Moir J.O., 1993. Characterization of available P by sequential extraction. In: Soil sampling and methods of analysis. M.R. Carter Editor, Canadian Society of Soil Science. Lewis Publisher, London, Ch. 10, 75-86.

USEPA, 1988. Constructed wetland and aquatic plant systems for municipal wastewater treatment – Design manual. United States Environmental Protection Agency, pp. 92.

Valsami-Jones E., 2001. Mineralogical controls on phosphorus recovery from wastewaters. Mineralogical Magazine 65(5), 611-620.

Vohla C., Kõiv M., Bavor H.J., Chazarenc F., Mander U., 2011. Filter materials for phosphorus removal from wastewater in treatment wetlands – A review. Ecological Engineering 37(1), 70-89.

Wang G., Wang Y., Gao Z., 2010. Use of steel slag as a granular material: Volume expansion prediction and usability criteria. Journal of Hazardous Materials 184(1-3), 555-560.

Weber D., Drizo A., Twohig E., Bird S., Ross D., 2007. Upgrading constructed wetlands phosphorus reduction from a dairy effluent using electric arc furnace steel slag filters. Water Science and Technology 56(3), 135-143.

Werner T.M., Kadlec R.H., 2000. Wetland residence time distribution modelling. Ecological Engineering 15(1-2), 77-90.

Wolf, D., Resnick, W. 1963. Residence time distribution in real system. Journal of Industrial and Engineering Chemical Fundamentals, 2(4):28-293.

Xiong J., He Z., Mahmood Q., Liu D., Yang X., Islam E., 2008. Phosphate removal from solution using steel slag through magnetic separation. Journal of Hazardous Materials 152(1), 211-215.

Yamada H., Kayama M., Saito K. and Hara M. (1986). A fundamental research on phosphate removal by using slag. Water Research 20(5), 547-557.

SYNTHESIS AND GENERAL CONCLUSION

This PhD thesis aimed at developing the use of steel slag (EAF-slag and BOF-slag) produced in Europe as filter substrate to remove P from the effluents of small wastewater treatment plants. An integrated approach was followed, with investigations at different scales.

i. Batch experiments were performed to establish an overview of the PO_4-P removal capacities of steel slag produced in Europe, and then to select the most suitable samples for P removal;

ii. Continuous flow column experiments were performed to investigate the effect of various parameters including slag size and composition, and column design (aspect ratio of width to length) on treatment and hydraulic performances of slag filters;

iii. Finally, field experiments were performed to investigate hydraulic and treatment performances of demonstration-scale slag filters designed to remove P from the effluent of a constructed wetland, and to propose design equations based on the experimental results.

Figure C 1 summarizes the main mechanisms of P removal and the main reactions limiting P precipitation that were observed in this study.

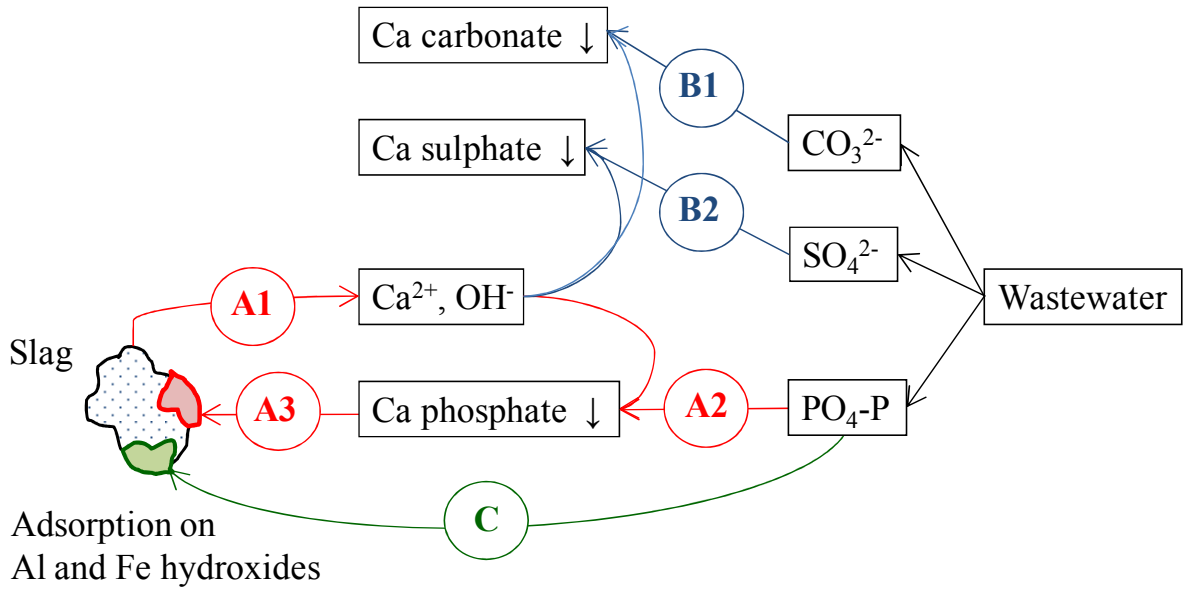

Figure C 1. Main mechanisms of P removal and reactions limiting P precipitation. P precipitation: (A1) CaO-slag dissolution; (A2) Ca phosphate precipitation; (A3) Ca phosphate recrystallisation on slag surface. Reaction limiting P precipitation: (B1) Ca carbonate precipitation; (B2) Ca sulphate precipitation. PO_4-P adsorption on Al and Fe hydroxides (C).

The results of experiments performed at different scales of investigation (batch, column, and field) demonstrated that EAF-slag and BOF-slag produced in Europe are efficient substrate for P removal from wastewater. The major mechanism of P removal was related to CaO-slag dissolution followed by Ca phosphate precipitation and its recrystallisation into hydroxyapatite (HAP) (Figure C 1). The experimental results of field experiments suggested that reactions of Ca sulphate and Ca carbonate may lead to a competing consumption of Ca ions, thus limiting Ca phosphate precipitation. Also, P fractionation experiments indicated that PO_4-P adsorption onto Al and Fe hydroxides was a further mechanism of P removal when using EAF-slag, which is richer in Al and Fe than BOF-slag. Overall, BOF-slag showed a higher affinity for P removal than EAF-slag. According to the proposed mechanism of P removal (Figure C 1), the higher CaO content of BOF-slag may account for the higher P removal capacities and for the higher P removal efficiencies observed when using BOF-slag.

Batch experiments have shown that the maximum capacities of PO_4-P removal from synthetic solutions ranged from 0.13 to 0.28 mg P/g using EAF-slag and from 1.14 to 2.49 mg P/g using BOF-slag. Also, results of batch experiments showed that an adequate concentration of Ca^{2+} is required to remove PO_4-P from wastewater via Ca phosphate precipitation mechanisms. In fact, it was found that P removal efficiencies drastically decreased when the molar ratio of PO_4-P to Ca^{2+} concentrations of the solution increased up to 0.6, thus indicating that there was not enough Ca^{2+} to enable Ca phosphate precipitation. The samples of EAF-slag and BOF-slag presenting the highest affinities for P binding were selected to perform continuous flow column experiments and demonstration field-scale experiments.

Continuous flow column experiments showed that EAF-slag and BOF-slag are efficient substrates for P removal from synthetic P solutions. Over a period of 100 weeks of operation, columns filled with small-size slag (5-16 mm EAF-slag; 6-12 mm BOF-slag) removed more than 98% of inlet TP, reaching TP retention levels of 1.71 g P/kg of EAF-slag and 1.98 g P/kg of BOF-slag. However, column filled with big-size slag (20-40 mm EAF-slag; 20-50 mm BOF-slag) showed some massive releases of TP, which were attributed to the release of P precipitates previously accumulated into the column. The experimental results suggested that hydraulic and TP removal performances may be improved by enhancing the design of the filters: hydraulic and treatment performances of the columns improved with decreasing the aspect ratio of width to length of the column (from 0.42 to 0.21) and with decreasing the size of slag (from 20-40 mm EAF-slag and 20-50 mm BOF-slag, to 5-16 mm EAF-slag and 6-12 mm BOF-slag), most probably because filtration of P precipitates was more efficient.

Field experiments confirmed that EAF-slag and BOF-slag are efficient substrate for P removal from the effluent of a constructed wetland. Over a period of 85 weeks of filter operation, EAF-slag removed 36% of the inlet TP reaching a TP retention level of about 0.26 g P/kg EAF-slag, whereas BOF-slag removed 59% of the inlet TP reaching a TP retention level of about 0.47 g P/kg BOF-slag. TP removal efficiencies increased with increasing HRTv, most probably because CaO dissolution and Ca phosphate precipitation were favoured. However, it was found that long HRTv (>3 days) may produce high pH of the effluents (>9), as the result of excessive CaO-slag dissolution. The results of this study demonstrated that at shorter HRTv (1-2 days), slag filters produced effluent pH that were elevated only during the first 5 weeks of operation, and then stabilized below a pH of 9.

However, significant differences in P removal performances between column experiments and field experiments were observed (Figure C 2).

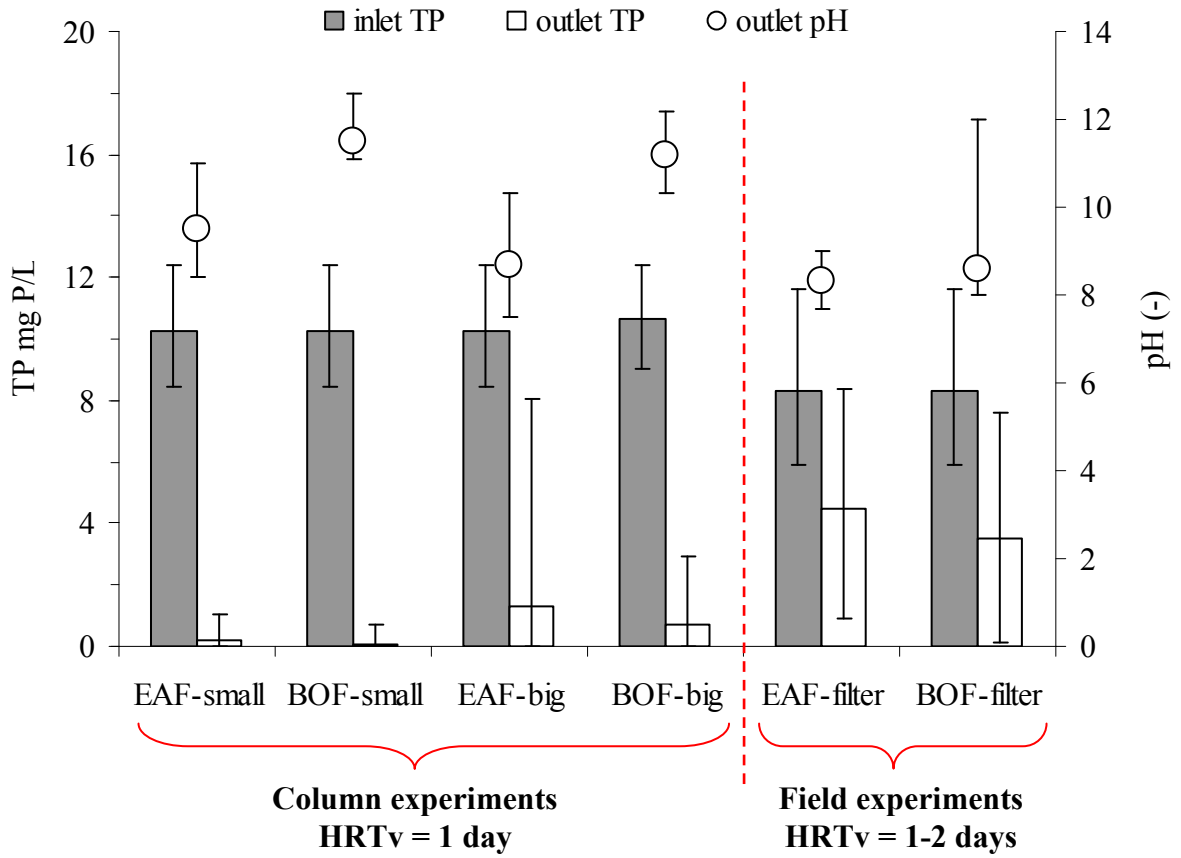

Figure C 2. Mean inlet TP concentration, mean outlet TP concentration and mean outlet pH values over 100 weeks of column experiments (with the exception of column BOF-big of which are presented the results of the first 65 weeks, until TP saturation was reached) and over 96 weeks of field experiments. Bars indicate the range minimum-maximum values.

Overall, column experiments showed higher outlet pH than field experiments, thus suggesting a higher rate of CaO-slag dissolution. Also, column experiments showed higher TP removal performances than field experiments, most probably because the higher value of pH favoured Ca phosphate precipitation, as appears to be confirmed by the clear trend of decrease in outlet PO_4-P concentrations with increasing outlet pH (Figure C 3). Therefore, the rate of CaO-slag dissolution appears to be the main parameter that controls the pH, and hence the P removal efficiency of steel slag.

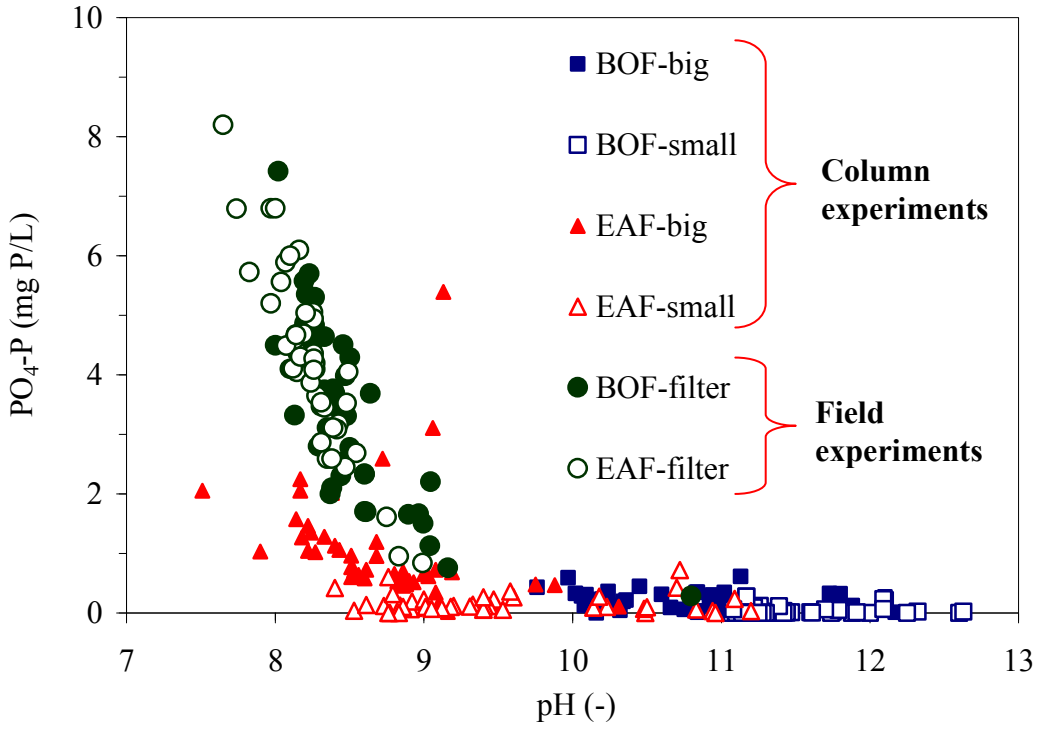

Figure C 3. Outlet PO_4-P concentration as a function of outlet pH values: results over 100 weeks of column experiments and 96 weeks of field experiments.

The differences in operating parameter such as loading mode, temperature and inlet wastewater composition may have affected the rate of CaO-slag and hence may explain the differences in outlet pH between column experiments and field experiments.

Effect of loading mode

Continuous flow column experiments were performed according to a continuous sub-superficial horizontal flow of about 0.6 L/h (small-size columns) and 1.2 L/h (big-size columns), thus resulting in a HRTv of about 1 day. Instead, field experiments were conducted with a discontinuous sub-horizontal flow with batch loads of 1500-3000 L/h (24 batches per

day), thus resulting in a HRTv of 1-2 days. The different loading rates may have led to different rates of CaO-slag dissolution due to the different internal hydrodynamics of the filters. However, tracer tests showed similar internal hydrodynamics between columns and field filters, thus suggesting that the difference in loading rates between columns and field filters probably did not affect the rate of CaO-slag dissolution.

Effect of temperature

Continuous flow column experiments were performed under stationary temperature conditions (around 20 °C), therefore fluctuation in treatment performances depending on temperature were not observed. Instead, field experiments were conducted under field conditions, with air temperature ranging from less than 0 °C to up than 30 °C, and a seasonal fluctuation in treatment performances was observed. Most probably, the increase in temperature favoured CaO-slag dissolution, and hence Ca phosphate precipitation. Batch experiments have demonstrated that the rate of CaO-slag dissolution increased with increasing temperature up to 10 °C (Annex I).

Effect of wastewater composition

Continuous flow column experiments were performed with a synthetic P solution made of tap water and salt of phosphorus (KH_2PO_4), whereas field experiments were performed with the effluent of a constructed wetland. Table C 1 shows the mean compositions of the synthetic P solution and of the constructed wetland effluent treated in column and field experiments, respectively. Only the parameters that mainly affect Ca phosphate precipitation are shown in Table C 1.

Table C 1. Mean composition of the inlet of the columns and of the inlet of the field-scale filters over a period of 100 weeks of column experiments and of 96 weeks of field experiments: mean value ± standard deviation (min-max value) number of measures (n).

Parameter	Inlet of the columns and inlet of the field-scale filters	
	Column experiments synthetic P solution	Field experiments constructed wetland effluent
TP (mg P/L)	10.2 ± 1.0 (8.4-12.4) n = 46	8.5 ± 1.3 (5.9-12.0) n = 54
PO_4-P (mg P/L)	10.1 ± 0.8 (8.9-11.9) n = 46	7.8 ± 1.3 (4.4-11.0) n = 46
pH (-)	7.7 ± 0.2 (7.1-8.0) n = 46	7.2 ± 0.2 (6.7-7.7) n = 54
Ca^{2+} (mg Ca/L)	33.9 ± 7.5 (14.3-46.5) n = 45	127 ± 22 (47-152) n = 37
TA (mg $CaCO_3$/L)	140 ± 46 (80-200) n = 6	282 ± 39 (205-340) n = 8
COD (mg O_2/L)	N.A.	32.0 ± 7.3 (15.0-42.0) n = 19

As shown in Table C 1, the major differences in composition between the constructed wetland effluent (inlet of field-scale filters) and the synthetic P solution (inlet of columns) were observed for total alkalinity (TA), Ca^{2+} and COD concentrations.

The constructed wetland effluent had a mean TA of 282 mg $CaCO_3$/L (very hard water, according to French classification), whereas the synthetic P solution (inlet of columns) had a mean TA of 140 mg $CaCO_3$/L (soft water, according to French classification). Since TA is a measure of the capacity of the water to resist changes in pH, the high TA of the constructed wetland effluent may have buffered the increase in pH due to CaO dissolution, and this may have limited Ca phosphate precipitation. In addition, the high TA of the constructed wetland effluent suggested a high potential for Ca carbonate precipitation, which may have further limited Ca phosphate precipitation. Also, the higher Ca^{2+} concentration of the constructed wetland effluent may have limited the dissolution rate of CaO, thus limiting Ca phosphate precipitation. Finally, the COD concentrations of the constructed wetland effluent may indicate the presence of organic colloids, and / or humic, fulvic and tannic acids that affected Ca phosphate nucleation and recrystallisation into hydroxyapatite.

PERSPECTIVES

The results of this PhD thesis indicated that the use of filters filled with EAF-slag and BOF-slag is an efficient technique to upgrade P removal in small wastewater treatment plants. The large number of steel making plants in Europe may represent a diffuse and low cost source of steel slag for wastewater treatment.

However, the results of this study clearly indicated that P removal performances of slag filters may vary depending on the temperature and wastewater composition, most probably because they affect the rate of CaO-slag dissolution and hence Ca phosphate precipitation. Therefore, further experiments at different scales of investigation are needed to elucidate the effect of various parameters, including temperature, total alkalinity and loading rate on P removal:

i. Batch experiments: additional batch experiments should be performed to determine the rates of Ca^{2+} and OH^- release from slag as a function of the alkalinity of the water. Steel slag may be put into solutions at different total alkalinity, and samples of solutions may be taken until equilibrium in Ca^{2+} and pH of the solution will be reached. Then, the experimental data on Ca^{2+} and OH^- concentrations may be modelled by using the pseudo first order kinetic equation of Lagergren (as already done in Chapter 2) to determine the rate of Ca^{2+} and OH^- release as a function of the alkalinity. The results of these experiments may give important information to evaluate the effect of alkalinity on the increase in pH and hence the efficiency of Ca phosphate precipitation when treating real wastewater;

ii. Column experiments: further experiments should be performed to establish the kinetics of CaO-slag dissolution under continuous flow condition. Column filled with steel slag may be equipped of piezometers placed at different distances from the inlet, and then fed with tap water (without P). Samples of solution may be taken from the piezometers to determine pH and Ca^{2+} concentrations. Then, the experimental data on Ca^{2+} and OH^- concentrations may be modelled by using a first order kinetic model (as already done in Chapter 4) to determine the volumetric rate of CaO-slag dissolution. The knowledge of the kinetics of CaO-slag dissolution under process condition may give important information to improve the design of the slag filters for P removal; also, slag filters may be designed for different purposes, such as, for examples, the adjustment of pH of acid effluents coming from processes of nitrification;

iii. Field experiments: to date, the number of field scale experiments that used steel slag to upgrade P removal in existing wastewater treatment plants is too limited, and further field-scale application are needed to evaluate the treatment performances of slag filters under different climates and wastewater composition. Also, the effect of different loading on P removal performances should be studied by decreasing and/or increasing the volume and the frequency of the batch loads, and altering feeding period to resting periods. These experiments may give important information to improve the design and the loading strategy of the slag filters in order to enhance the phenomena of Ca phosphate precipitation and crystallisation.

ANNEX I The effect of temperature on the kinetic of CaO-slag dissolution

Introduction

Several international studies have demonstrated that steel slag is an efficient substrate for phosphate (PO_4-P) removal from wastewater mostly via Ca phosphate precipitation mechanisms (Drizo et al., 2006; Kim et al., 2006; Bowden et al., 2009; Claveau-Mallet et al., 2012). The main parameters influencing Ca phosphate precipitations are initial Ca^{2+} and PO_4-P concentrations and pH values of the solutions (Stumm and Morgan, 1996; Valsami-Jones, 2001). It is well known from the chemical equilibrium rate in aqueous solutions that the solubility of the most stable Ca phosphate, including hydroxyapatite (HAP) and octacalcium phosphate (OCP) decrease with increasing pH of the solution (Stumm and Morgan, 1996; Valsami-Jones, 2001). Consequently, pH appears to be a parameter of great importance to estimate Ca phosphate precipitation, and pH >8.5 are usually needed to reach good performances of P removal via Ca phosphate precipitation mechanisms (Roques, 1990). Several authors found that steel slag produced a high pH as a result of a mixture of dissolution reactions of various metal oxides, including Al_2O_3, MgO and CaO (Bowden et al., 2009; Xue et al., 2009). Equation (AI.1) describes a general reaction of metal oxide (Me_xO_y) dissolution (Xue et al., 2009).

$$Me_xO_y + yH_2O \rightarrow xMe^{(2y/x)+} + 2yOH^- \qquad \text{(AI.1)}$$

The high pH-leachates of steel slag may favour Ca phosphate precipitation, because it is well known that the solubility of several Ca phosphates, including octacalcium phosphate (OCP), tricalcium phosphate (TCP) and hydroxyapatite (HAP) decreases with increasing pH (Stumm and Morgan, 1996; Valsami-Jones, 2001).

Barca et al. (2012) have demonstrated that kinetics of Ca^{2+} and OH^- release from slag followed a pseudo-first order kinetic model, thus suggesting that one of the reactants (CaO) was present in greater excess over the other reactants in the reaction mixture. This confirmed that the dissolution of CaO-slag was the primary reaction explaining the high pH-leachates of steel slag. It is well known that temperature affects kinetic of reactions by the variation of the rate constant of the reaction (Stumm and Morgan, 1996). Therefore, studying the kinetics of Ca^{2+} and OH^- releases at different temperature it is required to determine the effect of temperature on the rate constant of CaO-slag dissolution.

Within the framework of an internship performed at the Ecole Polytechnique de Montréal (Canada), this study aimed to evaluate the effect of temperature on the rate constant of CaO-slag dissolution. The kinetics of Ca^{2+} release from slag were investigated in a series of batch experiments performed at different temperatures. Then, the influence of temperature on the rate constant of CaO-slag dissolution was determined. The results of this study represent a valid support to estimate the pH-leachates of steel slag and hence the Ca phosphate precipitation when steel slag is used to treat wastewater at different temperature conditions.

Materials and Methods

Slag collection and preparation

The samples of steel slag tested in this study were collected from the outlet of an electric arc furnace (EAF) in Canada (Contrecoeur, Quebec, Canada). The granular size 5-10 mm was selected to perform the experiments, this because 5-10 mm is a medium size that is commonly employed in filters. The main chemical components of the EAF-slag tested in this study are reported in Table AI 1 (Claveau-Mallet et al., 2012). Its chemical composition appears to be comparable to those of EAF-slags produced in Europe (Motz and Geiseler, 2001). Before the experiments, the samples were washed with tap water to remove fine particles and then dried at 105°C for 24h.

Table AI 1. Main chemical components of EAF-slag used to determine the effect of temperature on CaO-slag dissolution (Claveau-Mallet et al., 2012).

Components	weight %
Fe_2O_3	33
CaO	30
SiO_2	16
MgO	12

Kinetic experiments on CaO slag dissolution

The effect of temperature on the kinetics of CaO-slag dissolution was studied in a series of batch experiments (adapted from ASTM 4646-87, 1993), which were performed at different

temperature (5, 10, 20 and 30°C). Figure AI 1 shows the schematic representation of the batch experiments.

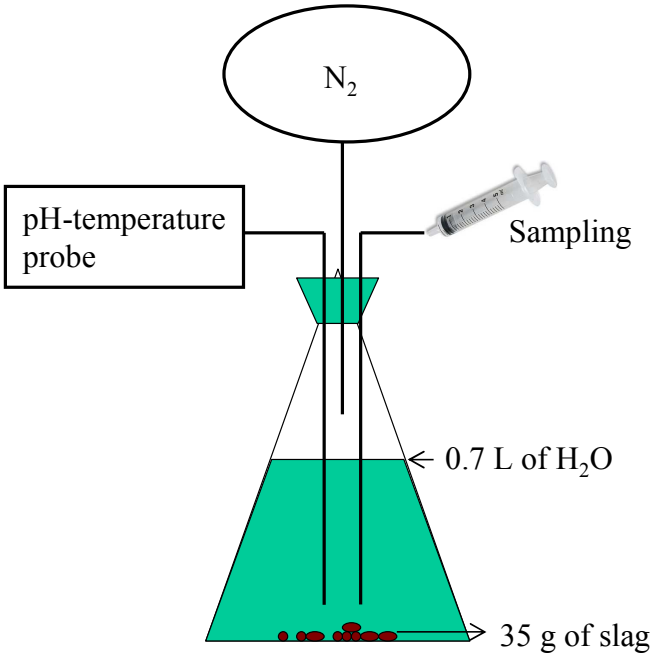

Figure AI 1. Schematic representation of the batch experiments to determine the effect of temperature on CaO-slag dissolution (adapted from Dacquin, 2011).

For each experiment, 35g of slag were immersed into a 1L glass bottle containing 0.7 L of deionised water (resistivity >18 MΩ*cm), with a ratio slag to solution of 0.05 g/mL. Then, the bottle was capped and connected to a balloon filled with N_2 to avoid $CaCO_3$ precipitation due to dissolution of atmospheric CO_2 in the solution. The bottle was placed on an agitation table and shaken at 125 rpm. The pH and temperature values of the solutions were monitored by a pH-temperature probe inserted into the bottle (Figure AI 1).

Samples of solution about (5 mL) were taken after 0.125, 0.25, 1, 2, 3, 4 and 7 days of agitation, when pseudo equilibrium in pH values of the solutions was reached. Ca^{2+}, Fe^{3+}, Al^{3+} and Mg^{2+} concentrations of the samples were measured to evaluate the dissolution of the main metal oxides composing steel slag (Motz and Geiseler, 2001). The samples were filtered (0.45 µm filters) before Ca^{2+}, Fe^{3+}, Al^{3+} and Mg^{2+} measurements. The experimental pH values were compensated by using equation (AI 2) to be referred to the reference temperature of 25°C. This enabled the results of the different experiments to be compared. In equation (AI 2), pH_{25} is the pH at 25°C (-), pH_T is the pH at the temperature T (-), pK_{25} is the dissociation constant of water at 25°C (-) and pK_T is the dissociation constant of water at the temperature T (-).

Stumm and Morgan (1996) reported the following values of pK_T depending on temperature: 14.73 at 5°C, 14.53 at 10°C, 14.17 at 20°C, 14 at 25°C and 13.83 at 30°C.

$$pH_{25} = pH_T + (pK_{25} - pK_T) \quad \text{(AI 2)}$$

The experimental capacities of Ca^{2+} release from slag were calculated using equations (AI 3), where Qt is the capacity of Ca^{2+} release at time t (mg/g), V is the volume of the solution (L), M is the mass of slag (g) and Cat is the Ca^{2+} concentration of the solution at time t (mg /L).

$$Q_t = \frac{Ca^t V}{M} \quad \text{(AI 3)}$$

Then the experimental capacities of Ca^{2+} release were plotted according to the pseudo-first order kinetic equation of Lagergren (1898), equation (AI 4). The equation (AI 4) is commonly employed to describe pseudo-first order reactions (Ho and McKay, 1998). If pseudo-first order kinetic is applicable, this suggests that one of the reactants is present in great excess over the other reactants in the reaction mixture. The parameter Qe represents the capacity of Ca^{2+} release at equilibrium (mg/g), t is the time (d) and k_1 is the rate constant of pseudo-first order release (1/d).

$$\ln(Q_e - Q_t) = \ln Q_e - k_1 t \quad \text{(AI 4)}$$

The equilibrium capacity Qe must be known to exploit equation (AI 4) with experimental data. In this study, Qe was considered an adjustable parameter whose value was estimated by trial and error. The experimental capacities of release observed after 7 days were used as initial Qe-trial in order to calculate Qe from the intercept of the plot of ln(Qe-trial – Qt) against t. Then the Qe-trial was adjusted until the difference between Qe-trial and Qe was less than 0.1% of the value of Qe-trial, and the rate constant k_1 was calculated from the slope of the plot of ln(Qe – Qt) against t. Finally, the curve of k_1 as a function of temperature was plotted to determine the effect of temperature on the kinetic of CaO-slag dissolution.

Analytical methods

The pH measurements were performed using a model Excel XL15 pH/mV/temperature meter (Thermo Fischer Scientific, Waltham, USA). Ca^{2+}, Fe^{3+}, Al^{3+} and Mg^{2+} concentrations were measured using a model A Analyst 200 spectrophotometer (Perkin Elmer Instruments,

Waltham, USA). The limit of detection for the analysis of Ca^{2+}, Fe^{3+} and Mg^{2+} was 0.01 mg/L, whereas the limit of detection for the analysis of Al^{3+} was 0.1 mg/L. All chemicals used were of analytical grade, and all the experiments were performed in duplicate.

Results and discussion

The kinetic experiments showed that pH values and Ca^{2+}, Al^{3+} and Mg^{2+} concentrations of the solutions increased until a pseudo-equilibrium was reached after 7 days of agitation (Figure AI 2). The Fe^{3+} concentrations of the solutions have been always lower than the limit of detection. This indicates dissolution of several metal slag-oxides including CaO, Al_2O_3 and MgO. As shown in Figure AI 2, Ca^{2+} concentrations were greater than Al^{3+} concentrations of one order of magnitude, and greater than Mg^{2+} concentrations of two orders of magnitude. This suggests that the increases in pH derived predominantly from CaO-slag dissolution following equation (AI 5).

$$CaO + H_2O \rightarrow Ca^{2+} + 2OH^- \qquad \text{(AI 5)}$$

It was found that pH values and total amount of Ca^{2+} released from slag after 7 days of agitations increased with increasing temperature (Figure AI 2, A and B), and this indicates that temperature affected CaO-slag dissolution.

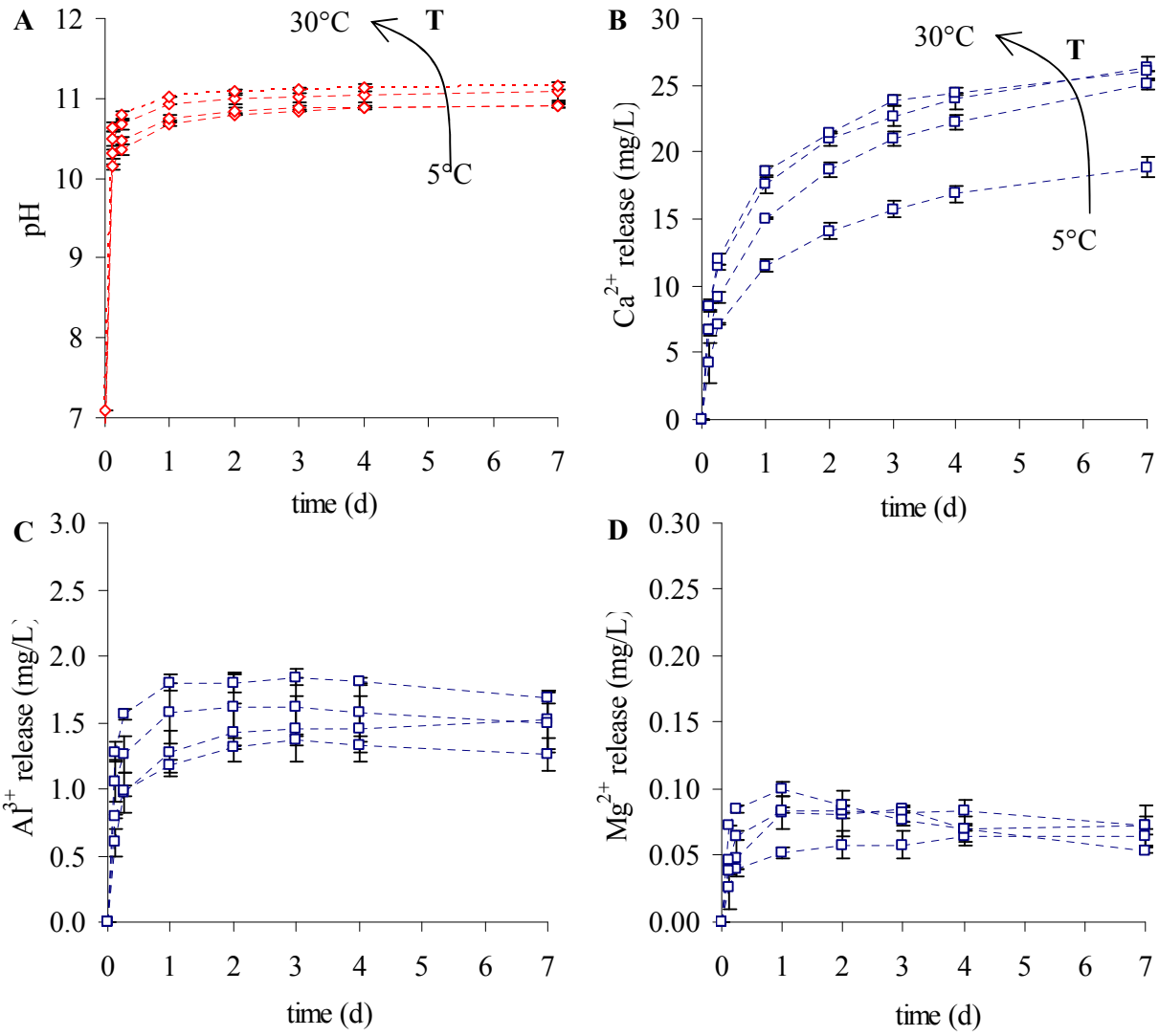

Figure AI 2. Kinetics of Ca^{2+}, Al^{3+} and Mg^{2+} release from EAF-slag at different temperatures (T) (5, 10, 20 and 30°C): pH values compensated at 25°C (A), Ca^{2+} concentrations (B), Al^{3+} concentrations (C) and Mg^{2+} concentrations (D) of the solutions. Mean values of duplicates, bars indicate the range min-max values.

The experimental capacities of Ca^{2+} (calculated by equations (AI 3)) were plotted according to a pseudo-first order kinetic model (equation (AI 4)). The high correlation coefficients indicated that this model described the Ca^{2+} release well (Table AI 2), confirming that one of the reactants (CaO) was present in great excess over the other reactants in the reaction mixture. This demonstrates that the dissolution of CaO-slag is the primary reaction explaining the increase in Ca^{2+} and pH of the solutions.

Table AI 2. Correlation coefficients and rate constants for the pseudo-first order kinetic model describing Ca^{2+} release at different temperature.

Temperature (°C)	Duplicate A			Duplicate B		
	Qe (mg Ca/g)	k_1 (1/d)	R^2 (-)	Qe (mg Ca/g)	k_1 (1/d)	R^2 (-)
5	0.35	0.76	0.958	0.38	0.78	0.937
10	0.48	0.77	0.948	0.47	0.75	0.938
20	0.48	0.90	0.928	0.51	0.88	0.936
30	0.50	1.06	0.932	0.50	0.99	0.944

The rate constants of Ca^{2+} release were stable around a value of 0.76 d^{-1} for temperature of 5 and 10°C. Then, the rate constants of Ca^{2+} release increased linearly (of a value of about 0.013 d^{-1} for each degree of temperature) with increasing temperature from 10 to 30°C (Figure AI 3). This indicates that temperature also affected the kinetic of CaO-slag dissolution.

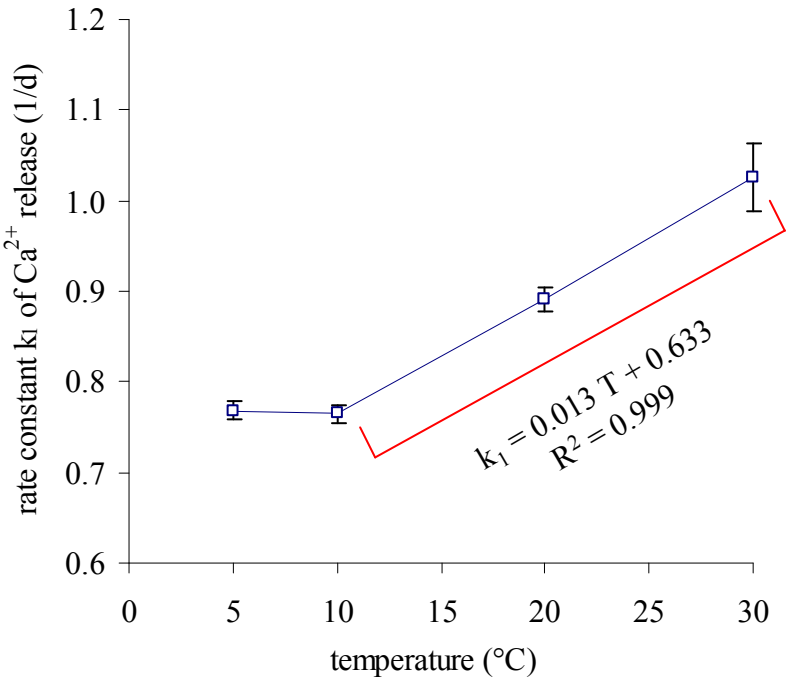

Figure AI 3. Rate constant k_1 for the pseudo first order kinetic model describing Ca^{2+} release. Mean values of duplicates, bars indicate the range min-max value of rate constants.

Finally, the experimental pH values were expressed in OH^- concentrations (mol/L) by equation (AI 6), where pK_T is the dissociation constant of water at temperature T (-) and pH_T is the pH of the solution at temperature T (-).

$$OH = 10^{-(pK_T - pH_T)} \quad \text{(AI 6)}$$

Then, the molar ratio of Ca^{2+} released to OH^- released (Ca/OH) from steel slag was investigated to identify the most probable reaction generating Ca^{2+} and OH^- releases (Figure AI 4).

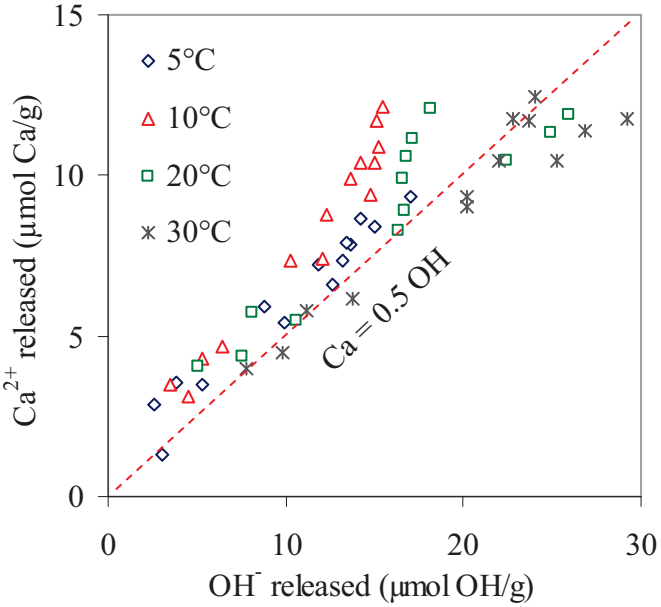

Figure AI 4. Direct correlation between the release of Ca^{2+} and the release of OH^- in the kinetic experiments performed at different temperature. Dropped line represents the theoretical molar ratio of Ca^{2+} released to OH^- released for CaO dissolution.

According to equation (AI 5), the theoretical molar ratio of Ca^{2+} released to OH^- released in the reaction of CaO dissolution is 0.5. As shown in Figure AI 4, the experimental molar ratios of Ca^{2+} released to OH^- released are close to the theoretical ratio of 0.5. This seems to confirm that CaO-slag dissolution was the primary reaction explaining the increases in Ca^{2+} and pH of the solutions. The experimental ratios Ca/OH <0.5 might be affected by the dissolution of other slag-oxides (Al_2O_3, MgO), which produced further release of OH^-, thus decreasing the ratio Ca/OH below 0.5. On the other hand, the experimental ratios Ca/OH >0.5 might be affected by Ca^{2+} release from Ca-silicate following equation (AI 7) (Huijgen et al., 2005).

$$CaSiO_3 + 2H^+ \rightarrow Ca^{2+} + SiO_2 + H_2O \qquad \text{(AI 7)}$$

As shown in equation (2.15), Ca^{2+} release from Ca-silicate is not accompanied by release of OH^-, thus increasing the ratio Ca/OH up the theoretical value of 0.5.

Conclusion

This study confirmed that dissolution of CaO-slag was the primary reaction explaining the release of Ca^{2+} and OH^- from steel slag. The kinetic experiments showed that temperature affected the kinetic of CaO-slag dissolution. It was found that the rate constants of Ca^{2+} release increased linearly (from a mean value of 0.76 to a mean value of 1.02 d^{-1}) with increasing temperature from 10 to 30°C. This indicated that the rate of CaO-slag dissolution increased with increasing temperature. Since the main mechanism of PO_4-P removal using steel slag was supposed to be related to CaO-slag dissolution followed by Ca phosphate precipitation, the results of this study suggest that the PO_4-P removal efficiency of steel slag may improve with increasing temperature.

References of Annex 1

ASTM D4646-87, 1993. Standard test method for 24-h batch type measurement of contaminant sorption by soils and sediments. American Society for Testing and Materials, 44–47.

Barca C., Gérente C., Meyer D., Chazarenc F., Andrès Y., 2012. Phosphate removal from synthetic and real wastewater using steel slags produced in Europe. Water Research 46(7), 2376-2384.

Bowden L.I., Jarvis A.P., Younger P.L., Johnson K.L., 2009. Phosphorus removal from wastewaters using basic oxygen steel slag. Environmental Science and Technology 43(7), 2476-2481.

Claveau-Mallet D., Wallace S., Comeau Y., 2012. Model of phosphorus precipitation and crystal formation in electric arc furnace steel slag filters. Environmental Science and Technology 46(3), 1465-1470.

Dacquin C., 2011. Cinétique de dissolution des scories pour la dephosphatation d'effluent. Internship report, Ecole Polytechnique de Montreal, Montreal (Canada).

Drizo A., Forget C., Chapuis R.P., Comeau Y., 2006. Phosphorus removal by electric arc furnace steel slag and serpentinite. Water Research 40(8), 1547-1554.

Ho Y.S., McKay G., 1998. A comparison of chemisorption kinetic models applied to pollutant removal on various sorbents. Process Safety and Environmental Protection 76(4), 332-340.

Huijgen W.J.J., Witkamp G.J., Comans R.N.J., 2005. Mineral CO_2 sequestration by steel slag carbonation. Environmental Science and Technology 39(24), 9676-9682.

Lagergren S., 1898. About the theory of so-called adsorption of soluble substances, Kungliga Svenska Vetenskapsakademiens. Handlingar 24(4), 1-39.

Kim E.H., Lee D.W., Hwang H.K., Yim S., 2006. Recovery of phosphates from wastewater using converter slag: Kinetics analysis of a completely mixed phosphorus crystallization process. Chemosphere 63(2), 192-201.

Motz H., Geiseler J., 2001. Products of steel slags: an opportunity to save natural resources. Waste Management 21(3), 285-293.

Roques H., 1990. Fondements théoriques du traitement chimique des eaux. Volume II, Technique et Documentation – Lavoisier, Paris (France), pp. 382.

Stumm W., Morgan J.J., 1996. Aquatic chemistry – Chemical equilibria and rates in natural waters. 3rd edition, Wiley-Interscience Publication, USA (Iowa), pp. 1022.

Valsami-Jones E., 2001. Mineralogical controls on phosphorus recovery from wastewaters. Mineralogical Magazine 65(5), 611-620.

Xue Y., Hou H., Zhu S., 2009. Characteristics and mechanisms of phosphate adsorption onto basic oxygen furnace slag. Journal of Hazardous Materials 162(2-3), 973-980.

ANNEX II Results of P fractionation experiments

Table AII 1. Results of P fractionation of samples of EAF-slag before and after 52 weeks of column experiments.

P fractions (mg P/g slag)	EAF-slag before experiments		EAF-slag after 52 weeks of column experiments	
	Test A	Test B	Test A	Test B
Weakly bound P	0.02	0.02	0.20	0.23
Al and Fe bound P	<0.01	<0.01	<0.01	<0.01
Ca bound P	1.41	1.60	1.64	1.77
Ca bound P in stable pools	0.44	0.25	0.28	0.22
Total P extracted	1.88	1.88	2.12	2.23

Table AII 2. Results of P fractionation of samples of BOF-slag before and after 52 weeks of column experiments.

P fractions (mg P/g slag)	BOF-slag before experiments		BOF-slag after 52 weeks of column experiments	
	Test A	Test B	Test A	Test B
Weakly bound P	0.02	0.02	0.16	0.18
Al and Fe bound P	<0.01	<0.01	<0.01	<0.01
Ca bound P	1.40	1.49	1.50	1.60
Ca bound P in stable pools	1.15	1.19	1.91	1.95
Total P extracted	2.58	2.70	3.58	3.74

Table AII 3. Results of P fractionation of samples of EAF-slag before and after 85 weeks of field experiments.

P fractions (mg P/g slag)	EAF-slag before experiments		EAF-slag after 85 weeks of field experiments	
	Test A	Test B	Test A	Test B
Weakly bound P	0.01	0.01	0.05	0.07
Al and Fe bound P	<0.01	<0.01	0.02	0.04
Ca bound P	0.03	0.19	0.14	0.24
Ca bound P in stable pools	0.19	0.19	0.24	0.29
Total P extracted	0.22	0.39	0.45	0.63

Table AII 4. Results of P fractionation of samples of BOF-slag before and after 85 weeks of field experiments.

P fractions (mg P/g slag)	BOF-slag before experiments		BOF-slag after 85 weeks of field experiments	
	Test A	Test B	Test A	Test B
Weakly bound P	0.01	0.01	0.05	0.06
Al and Fe bound P	<0.01	<0.01	0.01	0.01
Ca bound P	0.41	0.39	0.35	0.52
Ca bound P in stable pools	0.71	0.55	0.84	0.75
Total P extracted	1.12	0.94	1.25	1.34

ANNEX III Photos and images of batch, column and field experiments

Batch experiments

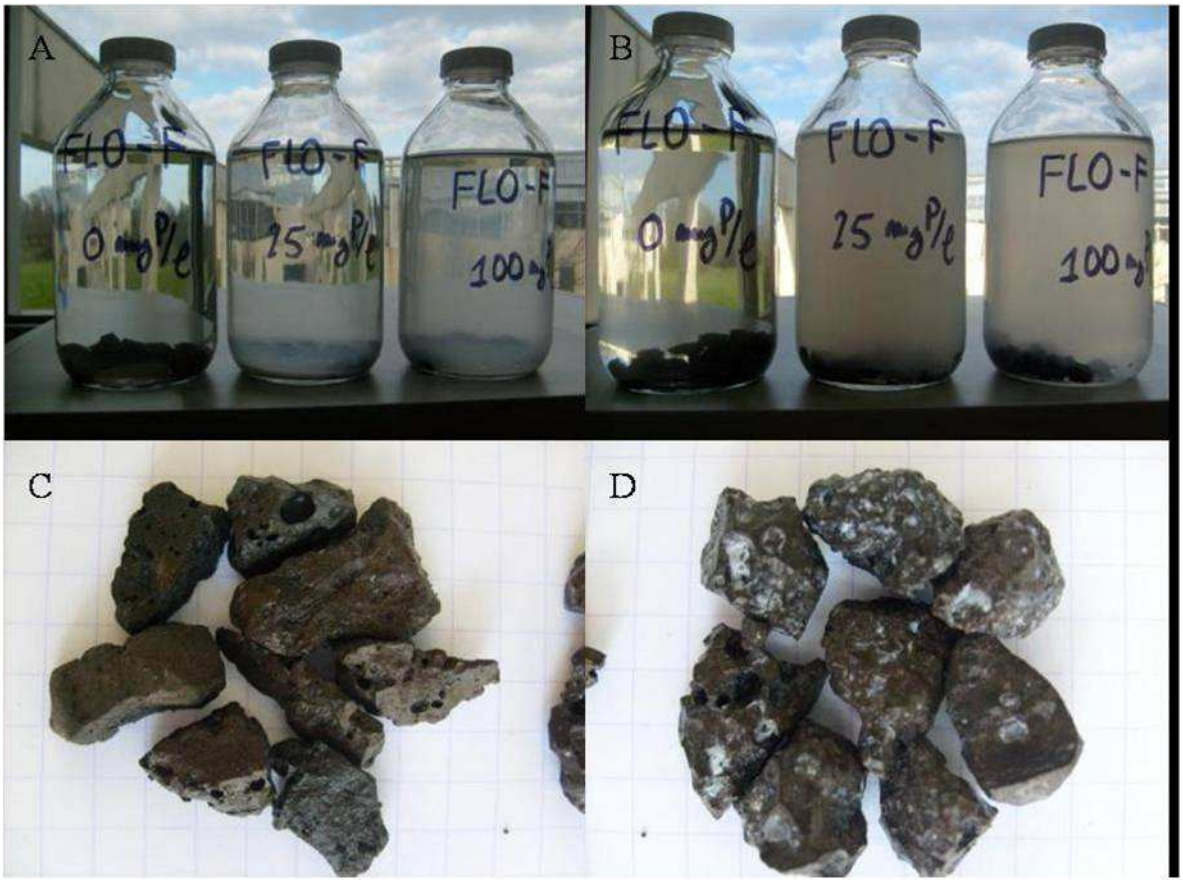

Figure AIII 1. BOF-slag, Batch test after 7 days of P sorption from solutions with initial P concentrations of 0, 25 and 100 mg P/L: (A) bottles before agitation show white precipitates settled in the bottom; (B) bottles after agitation show white precipitates suspended in the solution, with the exception for initial P solution of 0 mg P/L; (C) BOF-slag from bottles containing initial P solution 0 mg P/L doas not show the presence of white precipitates asdorbed on the surface; (D) BOF-slag from bottles containing initial P solution 100 mg P/L shows the presence of white precipitates asdorbed on the surface.

Column experiments

Figure AIII 2. Top view of the column system (photo of Daniel Meyer, 2011).

Figure AIII 3. Panoramic view of the column system (photo of Daniel Meyer, 2011).

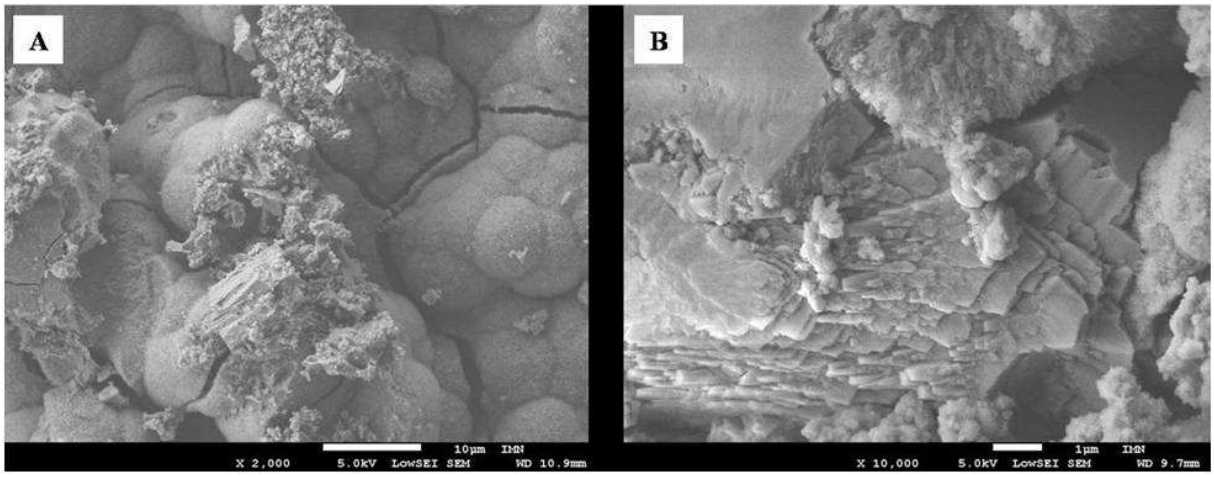

Figure AIII 4. SEM observation of surface of slag after 52 weeks of column experiments: (A) Secondary layer of Ca phosphate precipitates covering the surface of EAF-slag. The figure shows clearly the crack due to the drying of the secondary layer; (B) Multilayer calcite crystals ($CaCO_3$) covering the surface of BOF-slag after column experiments.

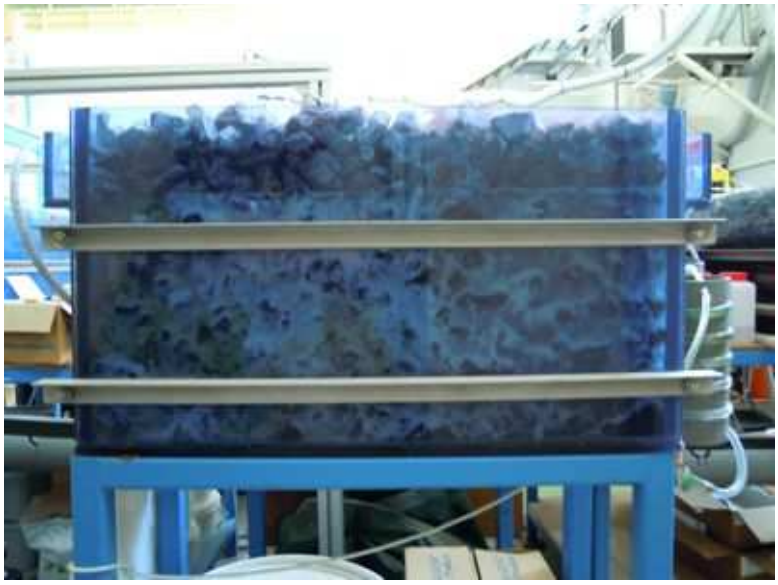

Figure AIII 5. Column filled with big-size BOF-slag (20-50 mm) shows the presence of white precipitates occupying the void volume after 100 weeks of operation.

Field experiments

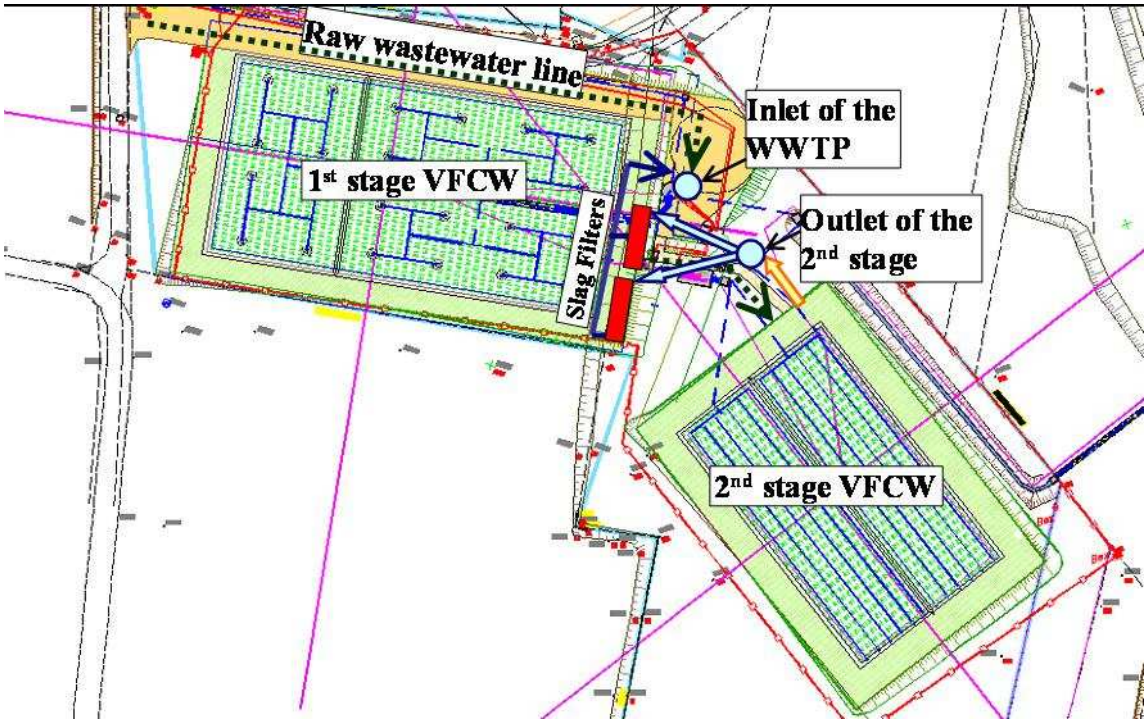

Figure AIII 6. Plan view of the two stages vertical flow constructed wetland (VFCW) of La Motte d'Aigues with the addition of the demonstration-scale slag filters treating a fraction of the outlet from the second stage VFCW.

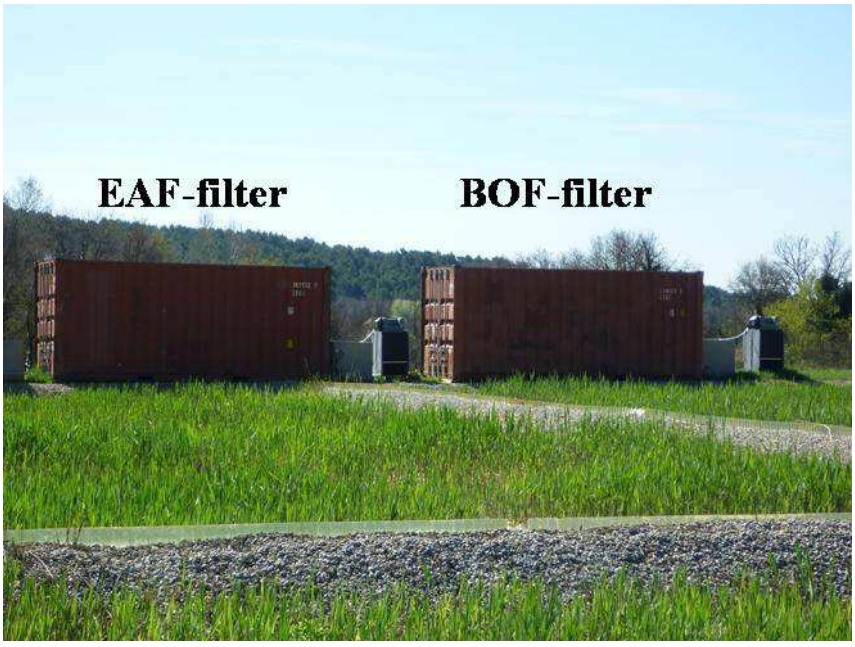

Figure AIII 7. Panoramic view of the demonstration-scale slag filters: two old containers were reused to construct the slag filters (photo Arthur Robinet).

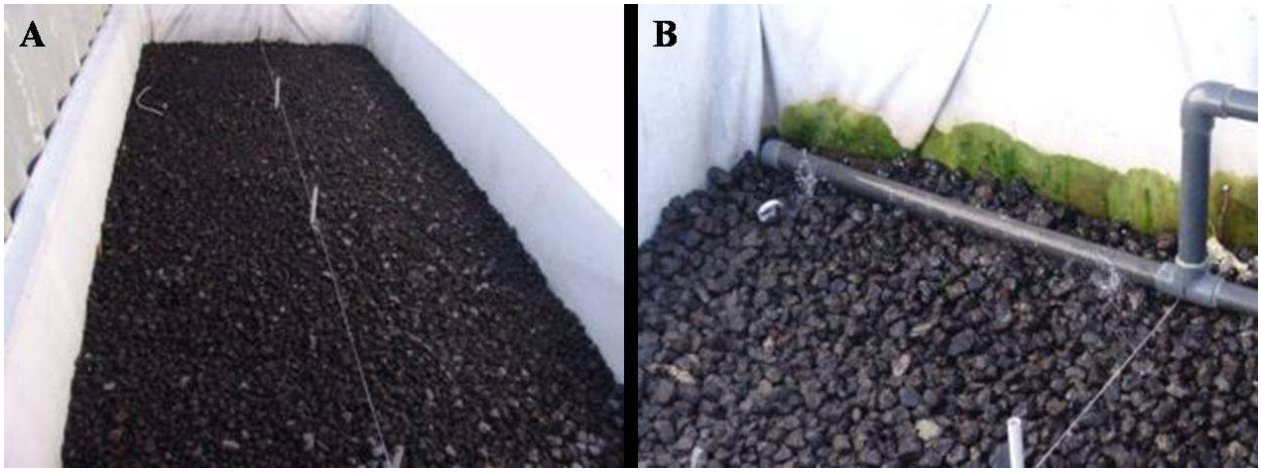

Figure AIII 8. Details on design of demonstration-scale slag filters: (A) piezometers; (B) feeding pipe.

RESUME EN FRANCAIS

Index

Introduction

Cette thèse est issue de la collaboration entre l'Ecole des Mines de Nantes et l'entreprise Epur Nature (Caumont sur Durance, France) dans le cadre du projet européen SLASORB (steel slag as sorbent for phosphorus removal from wastewater). L'objectif principal de ce travail était de développer l'utilisation de filtres garnis d'un coproduit de l'industrie (laitiers d'aciérie) pour améliorer le traitement du phosphore (P) au sein des petites stations d'épuration des eaux usées.

Une approche intégrée a été suivie, avec des investigations à différents échelles: (i) Des expériences en flacons ont été réalisées pour établir les capacités de rétention du P des laitiers produits en Europe, et ainsi sélectionner les échantillons les plus adaptés pour l'élimination du P; (ii) Des expériences en colonnes ont été menées pour étudier l'effet de différents paramètres, notamment la taille et la composition du laitier, sur les performances épuratoires de filtres de taille réduite; (iii) Enfin, des expériences de terrain à pleine échelle ont été conduites afin d'évaluer les performances hydrauliques et épuratoires de deux unités de démonstration conçues pour le traitement du P au sein d'une station de traitement des eaux résiduaire par un marais artificiel.

Les essais en flacons et en colonnes ont été réalisés au sein du Département Systèmes Energétiques et Environnement (DSEE) de Nantes Ecole des Mines, alors que les expériences sur le terrain ont été effectuées au sein de la station de traitement des eaux usées de La Motte D'Aigues (Vaucluse, France), sous la supervision technique de l'entreprise Epur Nature.

Les résultats de cette étude ont démontré que les laitiers d'aciérie produits en Europe sont des substrats efficaces pour l'élimination du P des eaux usées.

CHAPITRE 1 Revue de littérature

1.1 Le phosphore et la pollution des eaux

Le phosphore (P) est un élément nutritif essentiel à la croissance de la biomasse. Cependant, un apport excessif de P dans des bassins hydriques à faible renouvellement d'eau, comme les rivières, lacs ou lagunes, peut conduire à une croissance anormale des algues et de plantes aquatiques ce qui amène à une dégradation de la qualité de l'eau. Ce phénomène de dégradation de la qualité de l'eau due à un excès de P est communément appelé «eutrophisation» (Crouzet et al., 1999).

Aujourd'hui, il est bien connu que la réduction des apports en P est nécessaire pour réduire le risque d'eutrophisation. Par conséquent, les législations sur les rejets du P dans l'environnement sont de plus en plus strictes dans le monde entier, en particulier pour les zones qui présentent un risque élevé d'eutrophisation. La directive de l'Union Européenne sur le traitement des eaux urbaines résiduaires (91/271/CEE) a établit les limites suivantes pour les rejets du P au sein de stations d'épuration dans les zones sensibles à l'eutrophisation:

iii. Stations de taille moyenne (10000 -100000 EH[2]): moyenne annuelle de concentration de phosphore total (TP) de 2 mg P/L et une réduction du 80% du TP;

iv. Stations de grande taille (> 100000 EH): moyenne annuelle de concentration de phosphore total (TP) de 1 mg P/L et une réduction du 80% du TP.

1.2 Les formes de phosphore dans les eaux

Le P dans les eaux usées existe sous trois formes principales: phosphates, polyphosphates et phosphore organique (Roques, 1990). Les phosphates sont désignés comme les sels de l'acide phosphorique (H_3PO_4), qui se dissocie en solutions sous les formes de $H_2PO_4^-$, HPO_4^{2-} et

[2] L'équivalent habitant (EH) est une unité de mesure de la pollution organique biodégradable représentant la charge moyenne de cette pollution produite par habitant et par jour. Il est précisé dans la directive qu'un EH produit 60 g de DBO_5 (demande biochimique en oxygène en cinq jours) par jour.

PO_4^{3-} (PO_4-P). Le phosphate est une forme de P qui est facilement disponible pour la précipitation chimique, l'adsorption et l'assimilation biologique.

Les polyphosphates sont des chaînes de phosphates liés entre eux par un atome d'oxygène (Roques, 1990). Les polyphosphates dans les eaux usées proviennent principalement des détergents ménagers. Au cours des 20 dernières années, la teneur en P des détergents a été considérablement réduite dans de nombreux pays en Europe (Crouzet et al., 1999). Par conséquent, le contenu de polyphosphates dans les eaux usées a été fortement réduit.

Le phosphore organique des eaux usées municipales provient essentiellement des déjections humaines. En France, la production moyenne de phosphore organique est d'environ 1,5 g P/(EH) d (Roque, 1990). Cela signifie que, compte tenu d'une consommation d'eau d'environ 150 L/(EH) d, la concentration de phosphore organique dans les eaux usées non traitées est proche d'une valeur de 10 mg P/L.

Le P change de forme au fil du temps: les polyphosphates et le phosphore organique sont réduits en phosphates au travers de phénomènes d'hydrolyse et de transformations microbiennes. Pour avoir une mesure stable du P contenu dans les eaux, il est d'usage de réaliser la détermination de la teneur en phosphore total (TP). Cette dernière est mesurée par spectrophotométrie après la conversion de toutes les formes de phosphore en phosphate via un prétraitement par digestion acide et suivit de la formation d'un composé coloré (EN ISO 6878, 2004).

Les concentrations typiques de TP des eaux usées domestiques sont comprises entre 4 et 16 mg P/L (Metcalf et Eddy, 2003), ce qui implique l'utilisation de techniques visant spécifiquement le traitement du P afin de répondre aux normes de rejets.

1.3 Techniques conventionnelles pour le traitement du phosphore

Les techniques les plus courantes utilisées pour l'élimination du phosphore dans les stations d'épuration utilisent des procédés de précipitation chimique ou à de l'élimination biologique.

1.3.1 Précipitation chimique

Les traitements conventionnels pour l'élimination du P font souvent appel à des mécanismes de précipitation chimique. Plusieurs sels, notamment le sulfate d'aluminium ($Al_2(SO_4)_3$), le chlorure ferrique ($FeCl_3$) et la chaux (CaO) sont généralement ajoutés aux eaux pour favoriser la précipitation du P sous la forme de phosphates d'Al, Fe et Ca.

1.3.2 Dephosphatation biologique

Les technologies de dephosphatation biologique sont basées sur la capacité de certains microorganismes à accumuler le P au-dessus du besoin métabolique, lorsque des phases aérobies et anaérobies sont alternées. Cette technique de traitement du P exige un contrôle continu des paramètres de procédé: en fait, un changement inattendu de phase aérobie-anaérobie peut conduire à une libération soudaine du P accumulé dans les microorganismes.

1.4 Rétention du P par filtration au travers de matériaux réactifs

Les techniques classiques basées sur les procédés de précipitation chimique ou de dephosphatation biologique sont en général d'application difficile au sein des petites installations de traitement des eaux résiduaires domestiques de nature extensive et rustique, tels que les marais artificiels.

En fait, les techniques de précipitation chimique impliquent le contrôle continu des paramètres chimiques qui gèrent les équilibres dissolution-précipitation des sels de phosphore (pH, alcalinité, etc.). De plus, l'élimination et le traitement des boues de précipités représentent un coût supplémentaire. La technique de la dephosphatation biologique quand à elle est assez complexe et inadaptée aux besoins des petites installations. En fait, elle exige le contrôle continu des phases aérobies/anaérobies, ce qui demande l'emploi de personnel qualifié et entraîne des coûts d'exploitation élevés.

Durant les dernières décennies, plusieurs études internationales ont démontré que la technique de la filtration à travers des matériaux réactifs ayant une grande affinité pour l'enlèvement du P est une technique adaptée aux besoins des petites installations.

1.4.1 Substrats potentiels pour l'enlèvement du P

Au cours des deux dernières décennies, un grand nombre de matériaux a été testés pour l'enlèvement du P. Ces matériaux peuvent être classés en trois catégories principales en fonction de leur source d'origine (Johansson-Westholm, 2006): matériaux naturels, matériaux artificiels produits spécifiquement pour le traitement du P et coproduits de l'industrie, y compris les laitiers d'aciérie.

Les laitiers d'aciérie

Deux principaux types de laitiers d'aciérie sont produits par l'industrie sidérurgique en Europe: i) les laitiers de four de conversion (laitier BOF), qui sont issus de la production de

l'acier; ii) les laitiers de four à arc électrique (laitier EAF), qui sont issus d'un four à arc électrique principalement utilisé pour le recyclage de l'acier (Proctor et al., 2000). Selon les statistiques EUROSLAG, plus de 20 millions de tonnes de laitiers d'aciérie ont été produits en Europe en 2006. Environ 80% des ces résidus ont été utilisé dans plusieurs domaines d'application tels que la production de ciment ou la construction routière et 10% ont été recyclé au sein des sites de production. Toutefois, les 10% restant n'ont pas été réutilisé et sont envoyé en sites de stockage. Ceci suggère un fort marché potentiel de réutilisation des laitiers pour le traitement des eaux usées. Les laitiers d'aciérie sont composés principalement de fer (Fe), silice (SiO_2) et chaux (CaO) (Motz et Geiseler, 2001).

CHAPITRE 2 Sélection des laitiers: expériences en flacon

2.1 Introduction

Les expériences en flacon sont couramment effectuées pour évaluer la capacité de rétention des phosphates (PRC) d'un matériau. En fait, le PRC est un paramètre important pour le choix d'un substrat pour un système de filtration (Drizo et al., 2002). Plusieurs études internationales ont démontré que les laitiers d'aciérie représentaient un substrat approprié pour l'élimination du PO_4-P des eaux usées (Drizo et al., 2006; Kim et al., 2006; Bowden et al., 2009). Les valeurs de PRC observées dans des expériences en flacon ont été comprises entre moins de 1 et plus de 80 mg P/g (Drizo et al., 2002; Jha et al., 2008; Xiong et al., 2008; Xue et al., 2009; Bowden et al., 2009). Cependant, il est difficile de comparer les résultats des différentes études à cause de la différence entre les paramètres expérimentaux qui ont été appliqués, comme temps de contact, taille de laitiers, concentration en P des solutions (Chazarenc et al., 2008; Cucarella and Reenman, 2009).

Cette étude a visé à évaluer l'affinité des laitiers d'aciérie produits en Europe pour le traitement du P. Des tests en flacon ont été menées pour évaluer les PRCs d'échantillons de laitiers représentatifs du marché Européen. Les mêmes paramètres expérimentaux ont été suivis pour les tests en flacon. Cela a permis de comparer les résultats des différents tests afin de sélectionner les échantillons les plus adaptés au traitement du P. Enfin, ces échantillons ont été choisis pour effectuer des expériences en colonne et sur le terrain.

2.2 Matériels et méthodes

2.2.1 Collection et préparation des laitiers

Les échantillons de laitiers EAF et BOF testés dans cette étude ont été recueillies auprès de 10 sites de production à travers l'Europe. La granulométrie de 5-10 mm a été choisie pour réaliser les essais en flacon, car cette taille est comparable à la taille de matériau filtrant utilisé dans des conditions opératoires réelles. Des analyses de fluorescence aux rayons X (XRF) ont été effectuées pour déterminer la composition chimique semi-quantitative des échantillons.

2.2.2 Expériences de rétention du phosphate

Les PRCs des échantillons de laitiers d'aciérie ont été déterminés par une série d'expériences en flacon (adapté de la norme ASTM 4646-87, 1993). Pour chaque expérience, une série de 6 bouteilles en verre contenants chacune 1 L d'une solution synthétique de PO_4-P (0, 5, 10, 20, 25, 100 mg P/L) a été préparée. Ces solutions synthétiques ont été préparées avec de l'eau déminéralisée et du phosphate de sodium (Na_2HPO_4). Ensuite, 40 g de laitier ont été mis dans chaque bouteille (rapport laitier/solution de 0.04 g/mL), et les bouteilles ont été placées sur une table d'agitation et agitées à 125 tours par minute à la température de 20 °C. Les valeurs de pH et les concentrations résiduelles de PO_4-P et de Ca^{2+} ont été mesurées après 7 jours d'agitation. Les analyses du PO_4-P et du Ca ont été réalisées selon les méthodes prévues par les normes Européennes (EN ISO 6878, 2004, et EN ISO 7980, 1986, respectivement).

Les PRCs (mg P/g de laitier) ont été calculées à partir de l'équation (2.1), où V est le volume de la solution (L), M est la masse de laitier (g), P_{in} est la concentration initiale de PO_4-P (mg P/L) et P est la concentration résiduelle de PO_4-P après 7 jours de réaction (mg P/L).

$$PRC = \frac{(P_{in} - P)V}{M} \qquad (2.1)$$

2.3 Résultats et discussion

2.3.1 Composition chimique des laitiers

Les analyses XRF ont confirmé que les principaux composants chimiques des laitiers étaient le Fe_2O_3, le CaO et le SiO_2 (tableau 2.1). Il a été constaté que les laitiers BOF sont plus riches en CaO que les laitiers EAF, tandis que les laitiers EAF sont plus riches en Fe_2O_3 et Al_2O_3.

2.3.2 Capacités de rétention des phosphates

Les résultats des expériences en flacon sont présentés dans le tableau 2.2. Une augmentation des concentrations en Ca^{2+} et des valeurs de pH a été observée lorsque les laitiers ont été mis en contact avec les solutions. Ceci a été très probablement du à la dissolution du CaO des laitiers, avec la libération d'ions Ca^{2+} et OH^-. Après 7 jours d'expériences en flacon, une forte diminution des concentrations de PO_4-P a été observée (tableau 2.2). Cette diminution a été accompagnée par une diminution des concentrations de Ca^{2+} des solutions, et cela suggère la précipitation de complexes Ca-PO_4-P, comme rapporté dans un' étude précédente (Bowden et al., 2009).

Tableau 2.1. Analyses XRF: composition chimique des laitiers EAF et BOF (% poids). Résultats de 5 échantillons EAF et 5 échantillons BOF.

	Laitier EAF			Laitier BOF		
	Min	Max	Moyenne	Min	Max	Moyenne
Fe_2O_3	28.3	51.4	42.6	17.3	33.5	26.1
CaO	19.0	34.9	23.8	46.2	60.4	52.9
SiO_2	12.6	16.5	14.0	6.0	16.1	11.7
Al_2O_3	5.0	13.1	8.1	< 2	2.6	---
MnO	2.7	8.1	5.6	2.9	5.4	3.6
MgO	< 2	4.4	---	< 2	5.5	---

Tableau 2.2. Plages de valeurs de pH et concentrations résiduelles de PO_4-P et de Ca^{2+} après 7 jours d'expériences en flacon. Résultats de 5 échantillons de laitiers EAF et 5 échantillons de laitiers BOF.

Initial PO_4-P (mg P/L)	Laitiers EAF			Laitiers BOF		
	pH (-)	Res. PO_4-P (mg P/L)	Ca^{2+} (mg Ca/L)	pH (-)	Res. PO_4-P (mg P/L)	Ca^{2+} (mg Ca/L)
0	11.0-11.4	---	8.8-24.8	12.1-12.5	---	148-228
5	10.6-10.9	< LQ[a]-1.05	2.8-6.7	12.1-12.4	0.40-3.53	124-216
10	10.4-10.8	0.12-5.39	0.1-3.4	12.1-12.4	0.17-7.64	137-194
20	10.3-10.5	10.96-16.58	< LQ[a]-0.9	12.0-12.4	0.28-8.67	116-191
25	10.1-10.4	15.25-20.82	< LQ[a]-0.8	12.1-12.4	0.17-3.08	100-168
100	9.9-10.3	87.45-94.29	< LQ[a]-0.8	11.6-12.3	0.23-49.15	1-53

[a] Limite de Quantification: 0.01 mg P/L, 0.07 mg Ca/L.

Plusieurs précipités de Ca-PO_4-P peuvent être formés, en fonction des valeurs de pH, Ca^{2+} et PO_4-P des solutions: phosphates de calcium amorphes (ACPs), phosphate dicalcique (DCP), phosphate dicalcique dihydraté (DCPD), phosphates octocalcique (OCP), phosphate tricalcique (TCP) et l'hydroxyapatite (HAP), qui parmi les complexes Ca-PO_4-P est le plus stable (Valsami-Jones, 2001). Au cours des expériences en flacon, la précipitation de HAP

semble être la plus probable parce que les valeurs de pH, Ca^{2+} et PO_4-P des solutions ont été comprises dans la plage de valeurs qui permet la formation de HAP (Stumm et Morgan, 1996; Valsami-Jones, 2001). En outre, la diminution de la concentration de PO_4-P a été accompagnée par une diminution du pH des solutions (clairement observé en utilisant les laitiers EAF), ce qui confirme les résultats de Lu et al. (2008). Ce résultat suggère la consommation d'ions OH^- par précipitations de HAP, comme montré par la réaction (2.2).

$$5Ca^{2+} + 3PO_4^{3-} + OH^- \rightarrow Ca_5(PO_4)_3(OH) \downarrow \qquad (2.2)$$

Les PRCs des laitiers EAF ont varié entre 0.09 et 0.28 mg P/g, tandis que les PRCs des laitiers BOF ont varié entre 0.03 et 2.49 mg P/g (figure 2.1). Les plus fortes valeurs de PRCs ont été observées pour les solutions à forte concentration initiale de PO_4-P (100 mg P/L). Les PRCs des laitiers EAF n'ont pas augmenté avec l'augmentation des concentrations initiales de PO_4-P au dessus de 10 mg P/L, ce qui suggère qu'une limite de rétention en PO_4-P a été atteinte. Au contraire, les PRCs des laitiers BOF ont augmenté avec l'augmentation des concentrations initiales de PO_4-P, ce qui suggère que la limite de rétention de PO_4-P n'a pas été atteinte.

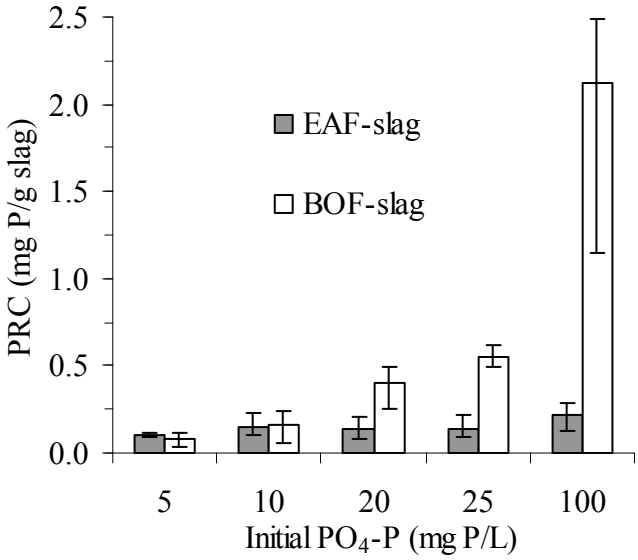

Figure 2.6. Valeurs moyennes de PRC après 7 jours de tests en flacon: résultats de 5 échantillons de laitiers EAF et 5 échantillons de laitiers BOF. Les barres indiquent la plage de valeurs des capacités.

Selon l'équation (2.2), la concentration de Ca^{2+} peut limiter la précipitation de HAP lorsque le rapport molaire des concentrations de PO_4-P et Ca^{2+} de la solution (PO_4-P/Ca) est supérieur à 0.6. Les rapports molaires PO_4-P/Ca des solutions après 7 jours d'essais en flacon sont

présentés dans le tableau 2.3. Les résultats indiquent que le Ca^{2+} a limité la précipitation de HAP lorsque les laitiers EAF ont été utilisés pour traiter des concentrations >10 mg P/L (tableau 2.3). Ceci suggère que la quantité de Ca^{2+} libérée des laitiers EAF par dissolution de la CaO n'a pas été suffisante pour permettre la précipitation du P en solutions pour des concentrations initiales de PO_4-P >10 mg P/L. Ceci peut également expliquer le limite en rétention de PO_4-P montré en figure 2.1. Au contraire, la quantité de Ca^{2+} libérée des scories BOF apparait être suffisante pour produire une bonne précipitation du P en solutions à différents concentrations initiales.

Tableau 2.3. Valeurs des rapports molaires de PO_4-P/Ca des solutions après 7 jours d'essais en flacon. Résultats de 5 échantillons de laitiers EAF et 5 échantillons de laitiers BOF.

PO_4-P Initial (mg P/L)	PO_4-P/Ca[a] Résiduel (mol P/mol Ca)	
	Laitiers EAF	Laitiers BOF
5	< 0.38	< 0.03
10	0.10-58.65	< 0.06
20	> 21.33	< 0.06
25	> 34.15	< 0.03
100	> 149.29	0.01-63.61

[a]Le Ca limite la précipitation de HAP pour PO_4-P/Ca > 0.6

2.4 Conclusions

Cette étude a montré que les laitiers d'aciérie produits en Europe sont des substrats efficaces pour le traitement du PO_4-P des eaux usées. Le principal mécanisme de rétention apparait être lié à la dissolution du CaO des laitiers suivie de la précipitation de complexes Ca-P (très probablement HAP). Il a été démontré que la dissolution du CaO a fourni les ions Ca^{2+} et OH^- qui sont nécessaires pour la précipitation de l'HAP. Toutefois, le relargage de Ca^{2+} à partir de laitiers EAF n'a pas été toujours suffisant pour la précipitation de HAP en solutions fortement concentrées en PO_4-P. Cependant, la teneur en Ca^{2+} des eaux usées peut représenter une source supplémentaire d'ions Ca^{2+} disponibles pour la précipitation de HAP, et cela peut conduire à une augmentation des efficacités d'élimination du PO_4-P.

Les résultats de cette étude ont montré qui le PRCs des laitiers EAF et BOF produits en Europe sont généralement comparables et indépendantes du site de production. Par conséquent, la distance du lieu de production a été considérée comme étant le principal paramètre pour le choix des laitiers.

CHAPITRE 3 Filtres garnis de laitiers d'aciérie pour la rétention du phosphore au sein de petites installations d'épuration: deux année d'expériences en colonne

3.1 Introduction

Plusieurs études internationales ont confirmé au travers d'expériences en colonne que les laitiers d'aciérie sont des substrats efficaces pour la rétention du P (Johansson, 1999; Shilton et al., 2005; Drizo et al., 2006; Bowden et al., 2009). Cependant, des études ont également montré certaines limitations, comme le pH élevé des effluents et le risque de colmatage suite à la dissolution du CaO des laitiers et de la précipitation de $CaCO_3$ (Chazarenc et al., 2007; Lee et al., 2010). Par conséquent, d'autres investigations en colonne sont nécessaires afin d'améliorer le design des filtres à laitier et ainsi réduire le risque de colmatage et de relargage basique.

Cette étude a visé principalement à étudier l'effet de la taille et de la composition de laitiers sur les performances de filtres garnies de laitiers EAF et BOF. Les mécanismes d'élimination du P ont également été étudiés avec l'utilisation de plusieurs techniques d'analyses chimiques et minéralogiques, tels que la microscopie électronique à balayage (MEB), la spectrométrie à dispersion d'énergie (EDS) et la diffraction des rayons X (XRD). Ces analyses ont permis d'étudier la surface des laitiers avant et après leur utilisation dans les colonnes.

3.2 Matériels and méthodes

3.2.1 Dispositif expérimental

Les échantillons de laitiers utilisés dans cette étude ont été choisis en fonction de leurs PRCs qui ont été déterminées par une étude comparative en flacon (Barca et al., 2012 et chapitre précédent). Deux tailles des laitiers ont été testées: petite taille (5-16 mm pour le laitier EAF, 6-12 mm pour le laitier BOF), et grande taille (20-40 mm pour le laitier EAF, 20-50 mm pour le laitier BOF). Ces tailles granulométriques ont été choisies pour éviter le colmatage des colonnes (Chazarenc et al., 2007).

Le dispositif expérimental était composé de quatre colonnes réalisées selon deux designs différents (figure 3.1): deux colonnes de petite taille (environ 42 L de volume total), et deux colonnes de grande taille (environ 84 L de volume total). La conception des colonnes a été adaptée à partir d'une étude récente (Anjab, 2009). Les colonnes de grande taille ont été remplies avec les laitiers EAF et BOF de grande taille (colonnes EAF-big et BOF-big, respectivement), tandis que les colonnes de petite taille ont été remplies avec les laitiers EAF et BOF de petite taille (colonnes EAF-small et BOF-small, respectivement).

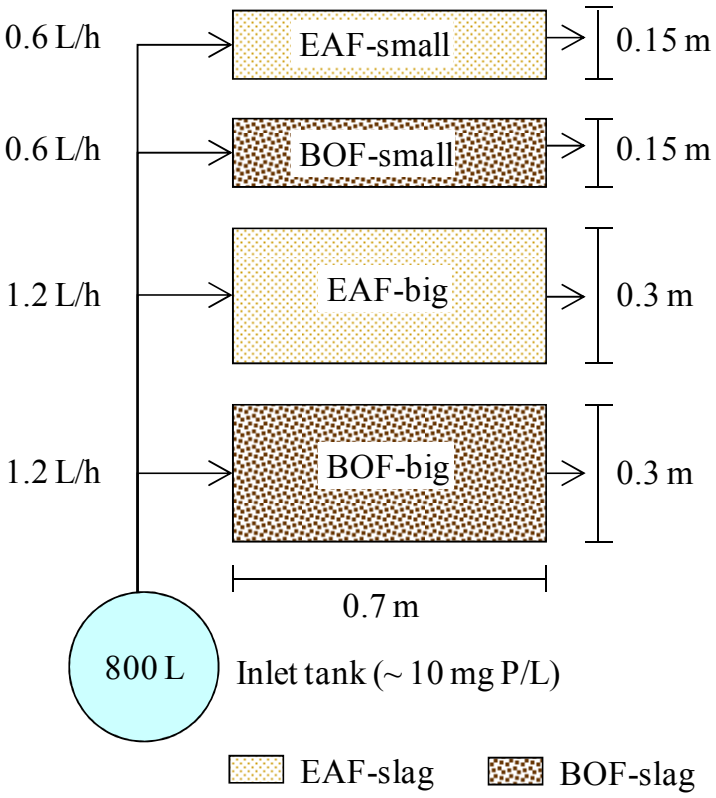

Figure 3.11. Vue schématique en plan du dispositif expérimental.

Pendant toute la durée des opérations, les colonnes ont été alimentées avec une solution synthétique de P (environ 10 mg P/L, eau du robinet + KH_2PO_4), par un flux continu horizontal sous surfacique de 0.6 L/h (colonnes de petite taille) et 1.2 L/h (colonnes de grande taille). Cela correspond à un temps de séjour hydraulique évalué sur le volume des vides (HRTv) d'environ 24 h. La concentration en phosphore d'entrée de 10 mg P/L a été choisie en accord avec la concentration typique d'une eau usée domestique (4-16 mg P/L, Metcalf et Eddy, 2003). Le flux sous surfacique a été adopté pour limiter le contact entre la solution et l'air, et ainsi réduire la dissolution du CO_2 atmosphérique. En fait, le CO_2 est un inhibiteur de la précipitation du P (Valsami-Jones, 2001). Les expériences en colonne ont été effectuées

dans des conditions de température de laboratoire (environ 20 °C). La figure 3.2 montre la vue en coupe transversale des colonnes.

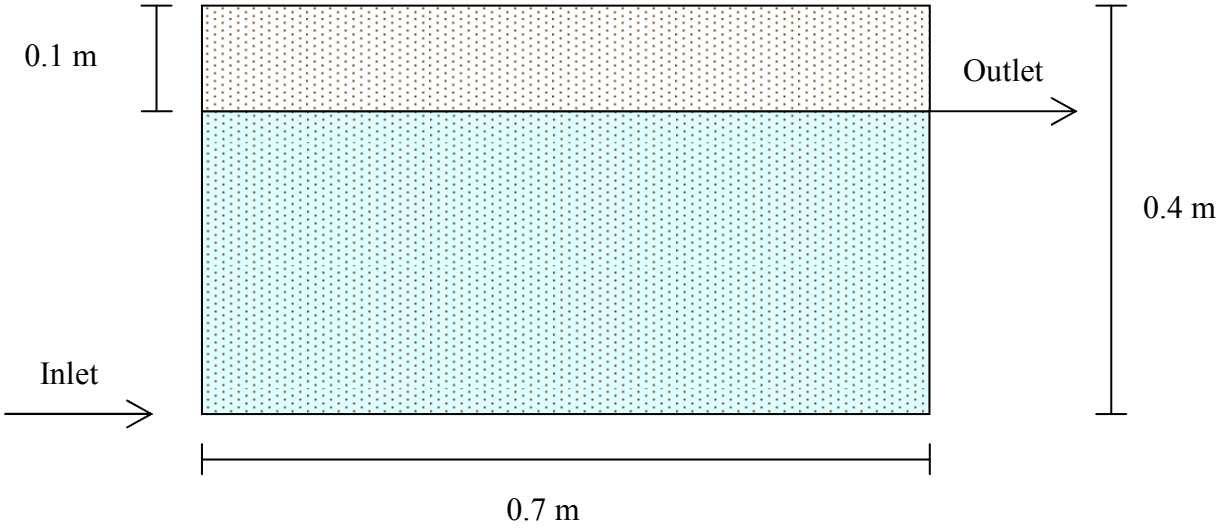

Figure 3.12. Conception des colonnes: vue en coupe transversale.

3.2.2 Méthodes expérimentales

Suivi des performances épuratoires

Des échantillons d'environ 100 mL ont été prélevés à l'entrée et à la sortie de chaque colonne environ toutes les deux semaines pendant 100 semaines. Les valeurs de pH, phosphore total (TP), phosphate (PO_4-P) et Ca^{2+} des échantillons ont été mesurés. Les analyses de TP et PO_4-P ont été réalisées selon la méthode spectrométrique au molybdate d'ammonium (EN ISO 6878, 2004), alors que les analyses de Ca ont été réalisées selon la méthode par spectrométrique d'absorption atomique (EN ISO 7980, 1986).

Analyses chimiques et minéralogiques des laitiers

Des observations MEB et des analyses EDS ont été effectuées pour examiner la surface des laitiers avant et après 52 semaines d'opération des colonnes. Ces analyses ont permis d'évaluer les changements chimiques de la surface des laitiers après l'utilisation dans le traitement du P.

Des analyses de XRD ont été effectuées pour étudier la composition minéralogique des précipités qui recouvrent la surface des laitiers prélevés des colonnes après 52 semaines d'opération. Les échantillons de laitiers ont été tamisés et la fraction <1 mm a été récupéré. Il a été fait l'hypothèse que cette fraction représente les précipités déposés sur les laitiers lors de la filtration de l'eau. Avant d'effectuer les analyses XRD, les précipités ont été écrasés dans un mortier afin de produire des particules fines et homogènes.

3.3 Résultats et Discussion

3.3.1 Performances épuratoires

La figure 3.5 montre l'évolution des valeurs de pH, TP, PO_4-P et Ca^{2+} au cours de 100 semaines de fonctionnement des colonnes. Les valeurs de pH et Ca^{2+} à la sortie étaient significativement plus élevés que les valeurs à l'entrée. Ce résultat est très probablement lié à la dissolution de CaO des laitiers pendant la filtration de l'eau, avec production de ions Ca^{2+} et OH^-. La plus forte teneur en CaO des laitiers BOF peut expliquer les pH et les concentrations en Ca^{2+} plus élevés qui ont été observés avec les laitiers BOF. En outre, il a été observé que les laitiers de petite taille ont produit des pH plus élevés que les laitiers de grande taille, très probablement parce que plus la taille de laitier est petite, et plus la surface spécifique disponible pour la dissolution de CaO est grande (Vohla et al., 2011). Les figures 3.5 C et D montrent que les valeurs de pH et en Ca^{2+} des effluents diminuent au cours de l'opération des colonnes, ce qui semble indiquer une diminution du taux de dissolution de CaO au fil du temps.

Au cours des 65 premières semaines d'opération, les valeurs de TP et PO_4-P à la sortie étaient, en moyenne, 10 fois plus basses des celles à l'entrée, ce qui indique des très bonnes performances de rétention du P. Ces résultats suggèrent un mécanisme de rétention du P composé de trois phases réactives consécutives: i) dissolution de la CaO des laitiers; ii) précipitation de complexes Ca-P; iii) filtration et accumulation des précipités dans les colonnes, comme montré par Claveau-Mallet et al. (2012).

Après la semaine 65, des rejets massifs de TP ont été observés pour la colonne remplie de laitiers BOF de grande taille (BOF-big) (figure 3.5 A). Ces rejets massifs de TP étaient très probablement dus au relargage de précipités de P précédemment accumulés dans la colonne. Au contraire, la colonne remplie de laitiers BOF de petite taille (BOF-small) a toujours montré de très bonnes performances épuratoires en TP (> 92%), ce qui suggère que le laitier de petite taille était plus efficace dans la filtration des précipités de P.

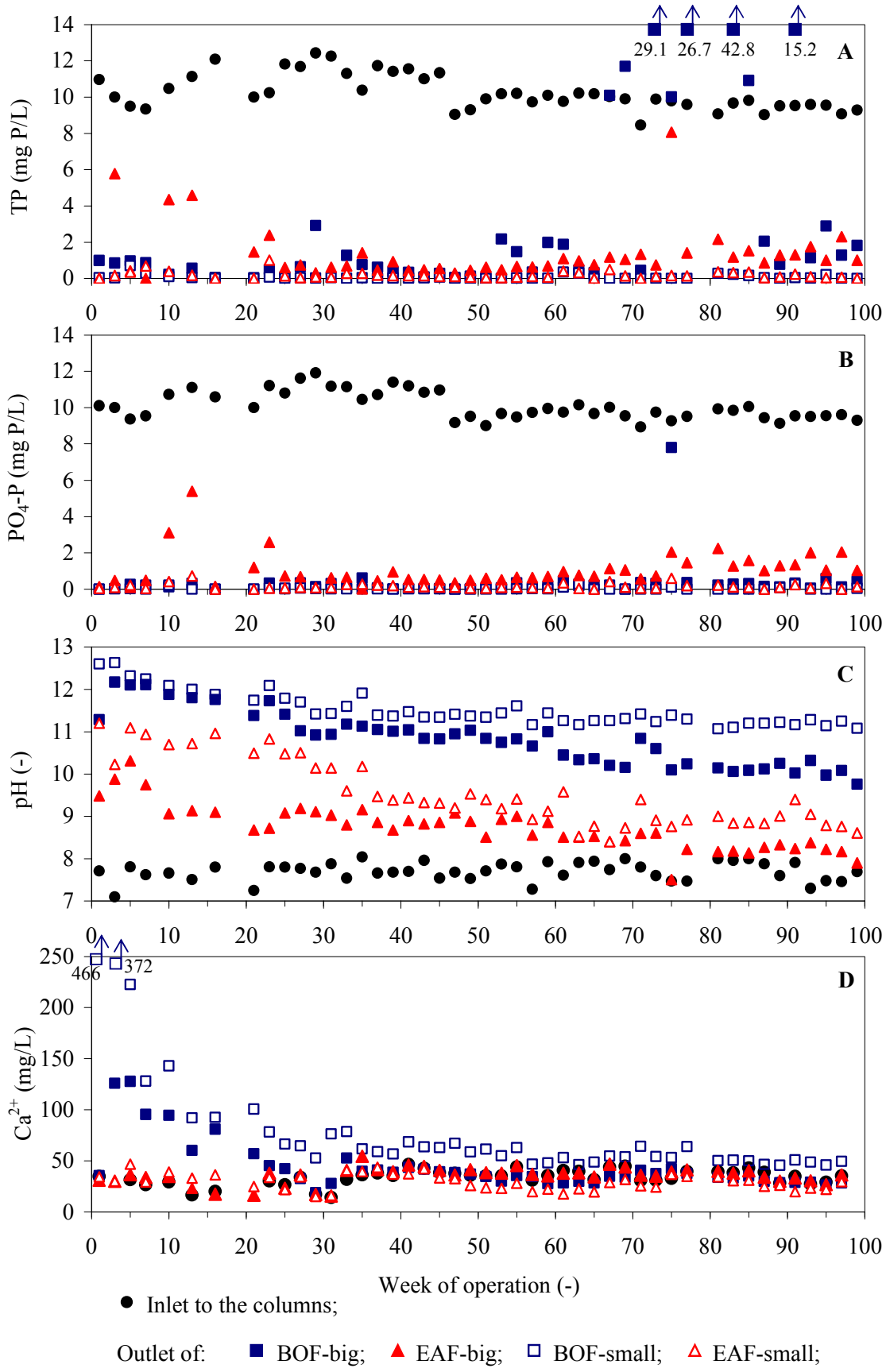

Figure 3.13. Valeurs de TP (A), PO_4-P (B), pH (C) et Ca^{2+} (D) à l'entrée et à la sortie des colonnes au cours de 100 semaines d'opération.

3.3.2 Chimie et minéralogie des laitiers

Les surfaces des laitiers avant et après 52 semaines d'expérience en colonne ont été examinées par analyses MEB et EDX (figure 3.6). Avant les expériences en colonne, les surfaces brutes des laitiers étaient principalement composés de Fe, Ca et O (figures 3.6 A et B). Les observations MEB des laitiers après 52 semaines d'opération des colonnes ont montré que la surface était recouverte d'une couche de précipités constitué de cristaux rhomboédriques et d'agrégats sphériques (figures 3.6 C et D). Les analyses EDX ont confirmé que les cristaux rhomboédriques (>20 µm) étaient essentiellement composés de Ca, C et O, ce qui suggère la précipitation et la cristallisation de $CaCO_3$ sur la surface des laitiers. Au contraire, les agrégats sphéroïdaux (<20 µm) étaient essentiellement composés de Ca, P et O, indiquant ainsi la précipitation de phosphates de Ca à la surface des laitiers.

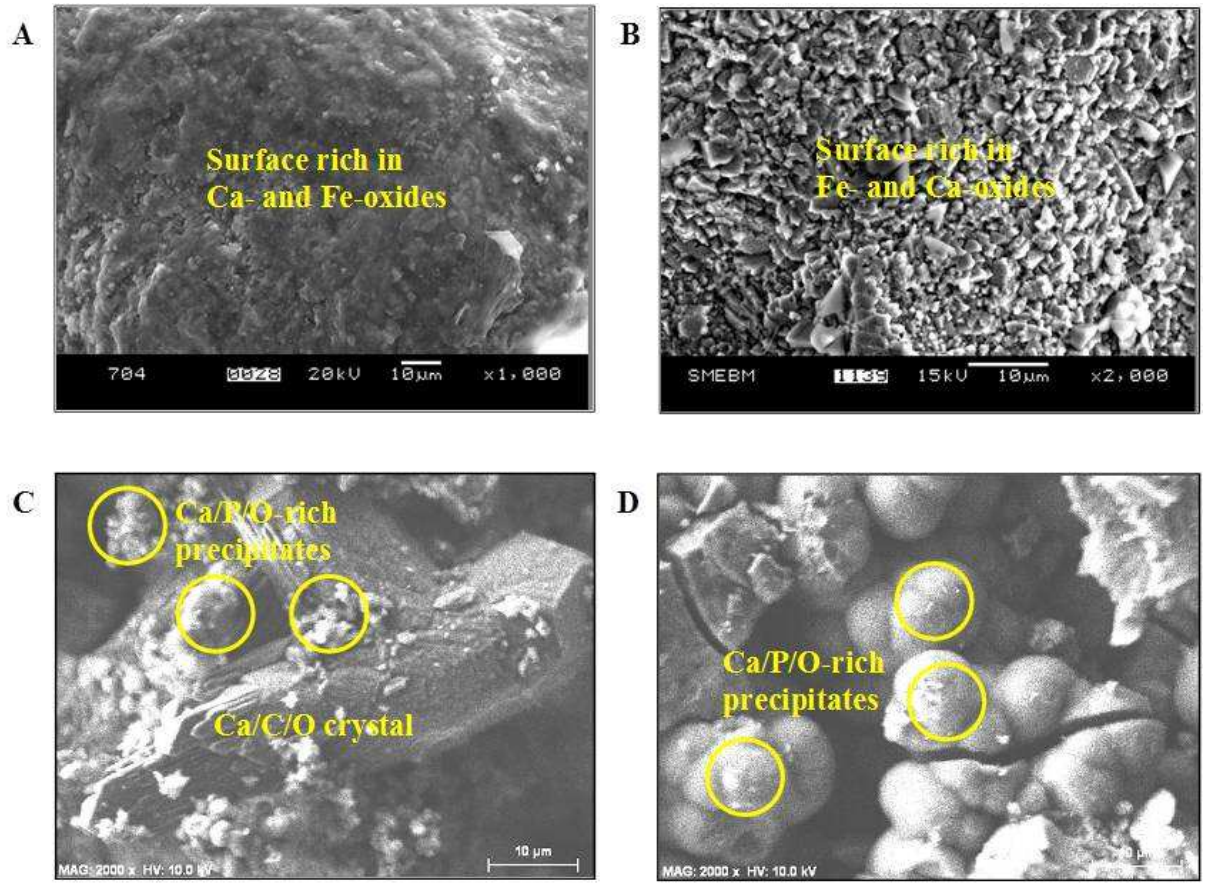

Figure 3.14. Observations MEB et analyses EDX: (A) surface de laitier BOF avant les expériences; (B) surface de laitier EAF avant les expériences; (C) surface de laitier BOF après 52 semaines d'expériences en colonne; (D) surface de laitier EAF après 52 semaines d'expériences en colonne.

La figure 3.7 montre les diffractogrammes XRD des précipités qui recouvrent la surface du laitier après 52 semaines d'expérience en colonne. Les résultats indiquent la présence probable de cristaux d'hydroxyapatite (HAP) en train de se former sur la surface du laitier. Cela suggère que, après la précipitation, les phosphates de Ca commencent à recristalliser sous la forme plus stable d'HAP (Valsami-Jones, 2001). En outre, les diffractogrammes (Figure 3.7) ont confirmé la présence de formes bien cristallisées de calcite recouvrant la surface du laitier après 52 semaines d'opération des colonnes, ce qui semble confirmer la précipitation de $CaCO_3$ et sa cristallisation en forme de calcite sur la surface du laitier.

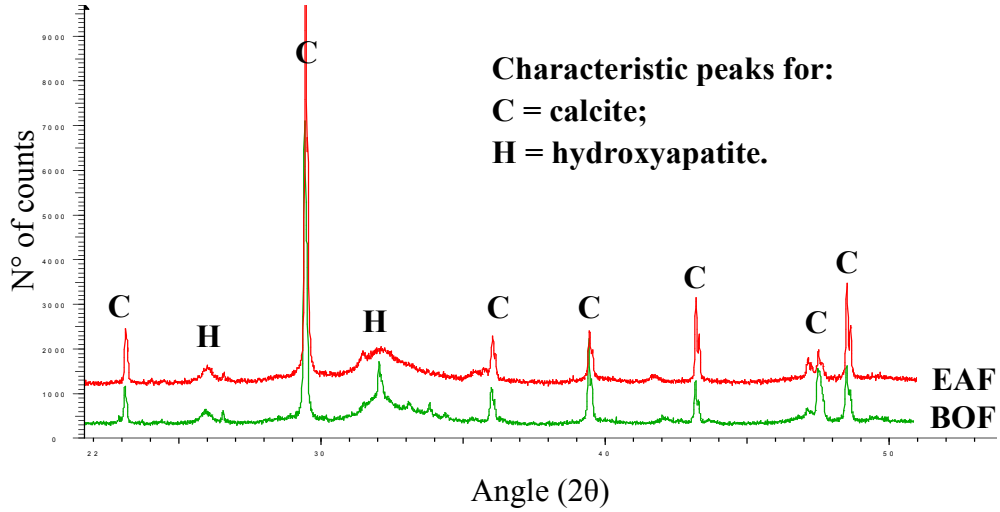

Figure 3.15. Diffractogrammes XRD des précipités qui recouvrent la surface des scories après 52 semaines d'expérimentation des colonnes.

3.4 Conclusions

Cette étude a montré que les laitiers EAF et BOF sont des matériaux très efficaces pour l'élimination du P des eaux en condition de procédé contrôlé. En général, il a été observé que les efficacités de rétention du P augmentent avec l'augmentation du contenu en CaO et avec la diminution de la taille des laitiers, très probablement parce que plus la taille est petite, et plus la surface spécifique pour la dissolution de CaO est grande.

Sur une période de 100 semaines de fonctionnement, les colonnes remplies de laitiers de petite taille ont retenu plus du 98% de TP à l'entrée, et elles ont atteint des niveaux de rétention de TP de 1,71 g P/kg EAF et de 1,98 g de P/kg BOF. Au contraire, les colonnes remplies de laitiers de grande taille ont montré des efficacités de rétention plus faibles.

CHAPITRE 4 Filtres garnis de laitiers d'aciérie pour la rétention du phosphore au sein de petites installations d'épuration d'eaux usée: deux années d'expériences sur le terrain

4.1 Introduction

De nombreuses études internationales ont démontré l'efficacité de filtres garnis de laitiers d'aciérie pour la rétention du P des eaux (Johansson, 1999; Shilton et al., 2005; Drizo et al., 2006). Cependant, la plupart de ces expériences ont été réalisées avec des solutions synthétiques de P, qui ne contiennent pas tous les éléments qui sont présents dans les eaux usées réelles et qui peuvent affecter les mécanismes d'élimination du P (par exemple, les acides humiques, les colloïdes organiques, les anions en compétition) (Valsami-Jones, 2001; Pratt et al., 2007). En effet, des grandes différences en performances épuratoires du P ont été observées lors du traitement des eaux usées réelles (Shilton et al., 2005; Chazarenc et al., 2007). Au jour d'aujourd'hui, peu d'expériences ont été menées pour déterminer les performances épuratoires en P de filtres à laitiers dans des conditions réelles (Shilton et al., 2006; Korkusuz et al., 2007; Weber et al., 2007; Cassini et al., 2010). En outre, les expériences de longue durée sont très rares (Shilton et al., 2006), et d'autres études sont nécessaires pour définir le comportement des filtres à laitiers en conditions opératoires réelles et sur le long terme. Cette étude vise à étudier les performances hydrauliques et de traitement de filtres garnis de laitiers produits en Europe. Deux filtres à laitiers ont été conçus pour traiter le P de l'effluent d'un marais artificiel planté de roseaux. Les effets des principaux paramètres de procédés (HRTv, température) sur les efficacités épuratoires ont été étudiés.

4.2 Matériels et méthodes

4.2.1 Dispositif expérimental

Deux filtres à l'échelle de démonstration ont été conçus pour traiter une fraction (2-4%) de l'effluent de la station de traitement des eaux usées domestiques de "La Motte d'Aigues"

(1359 habitants, Provence-Alpes-Côte d'Azur, France, INSEE, 2009) (Figure 4.1). L'implantation de "La Motte d'Aigues" est un exemple de système à deux étages de marais artificiels à flux vertical (VFCWs) (Liénard, 1987). Le VFCWs en France sont capables d'assurer de bonnes efficacités de traitement de la demande chimique d'oxygène (DCO), de la matière en suspension et de l'azote Kjeldahl, mais ils présentent en général des efficacités de traitement du P assez faibles (<20%, Molle et al., 2008).

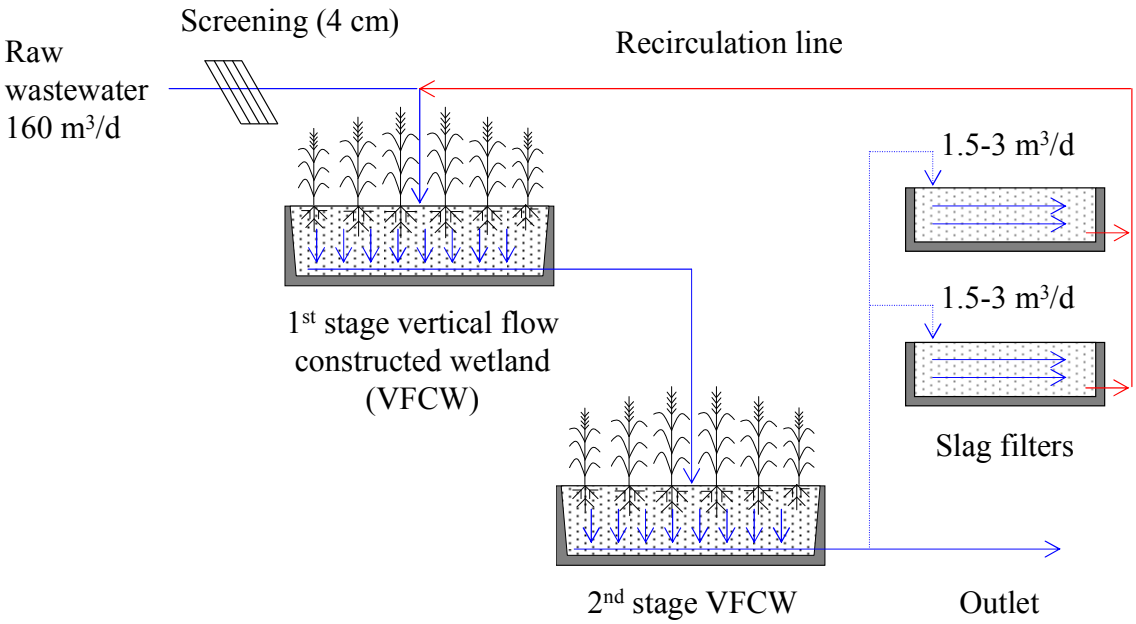

Figure 4.13. Vue schématique de la station d'épuration de La Motte d'Aigues avec l'ajout des filtres à laitiers.

Les filtres ont été remplis l'un avec du laitiers EAF, taille 20-40 mm (EAF-filter), l'autre avec du laitiers BOF, taille 20-40 mm (BOF-filter). Les échantillons de laitiers utilisés dans cette étude ont été choisis en fonction de leurs PRCs, qui ont été déterminées préalablement (chapitre 2). La densité apparente du laitier était d'environ 1.8 g/cm^3 pour le laitier EAF et 1.6 g/cm^3 pour le laitier BOF.

La figure 4.2 montre la conception des filtres. Chaque filtre a un volume total d'environ 6 m^3 et un volume de vide d'environ 3 m^3, ce qui correspond à une porosité d'environ le 50%. Les filtres ont été opérés avec un flux sous-superficiel horizontal et une alimentation en batch (24 batches/jour), afin de simuler les caractéristiques typiques d'alimentation des marais artificiels. Le temps de séjour calculé sur le volume de vide des filtres (HRTv) a été initialement étalonné à 1 jour, à l'aide d'un débitmètre. Puis, le HRTv a été porté à 2 jours après la semaine 9 d'opération, afin d'évaluer l'effet du HRTv sur les performances de

rétention du P. Les filtres ont été équipés de thermomètres pour le suivi de la température de l'eau et de l'air.

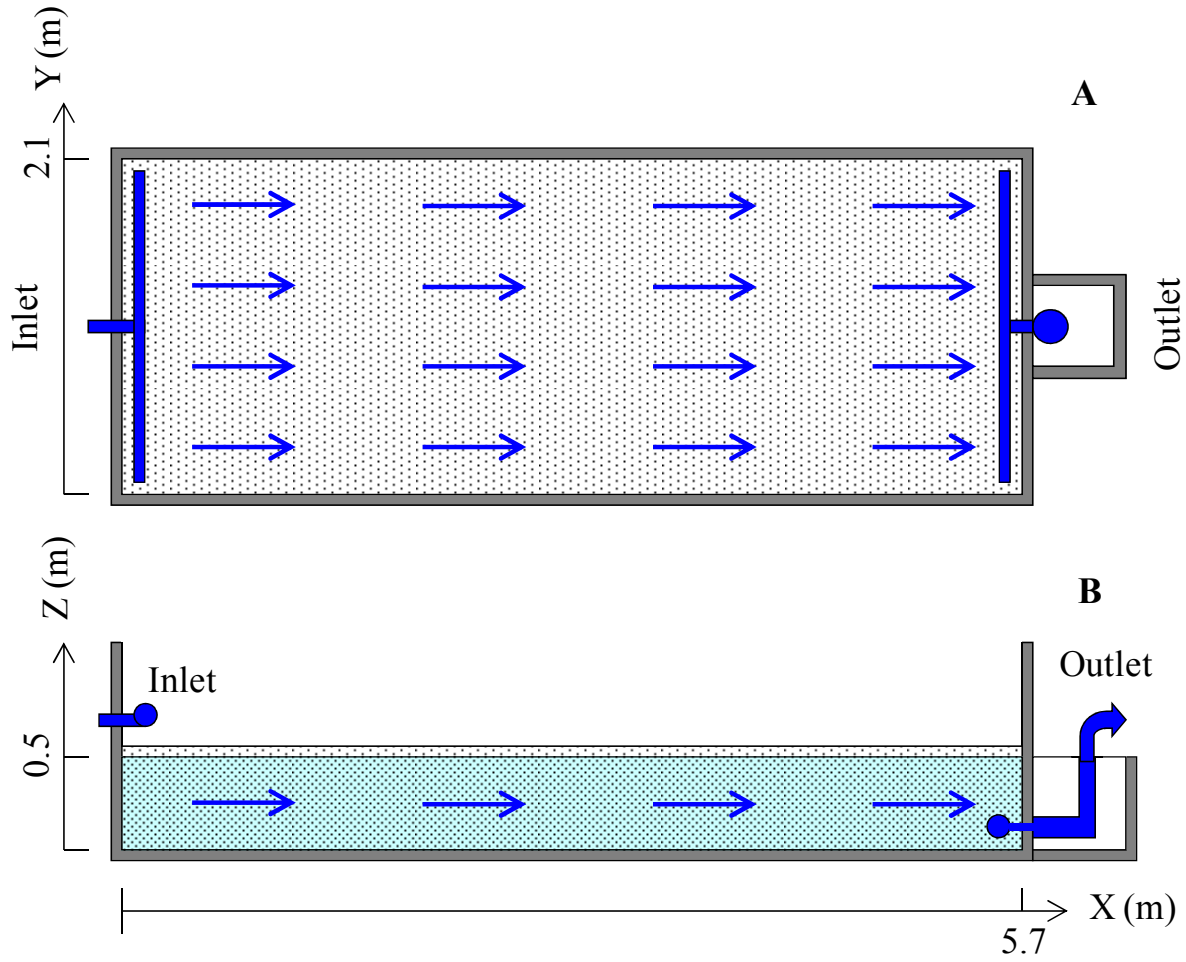

Figure 4.14. Filtrés à laitiers pleine échelle: vue en plan (A) et en section (B).

4.2.2 Méthodes expérimentales

4.2.2.1 *Etude hydraulique*

Des tests de traçage ont été réalisés en semaine 1, 9, 22, 29 et 44 d'opération à l'aide de fluorescéine. Ces expériences visaient à évaluer l'hydrodynamique des filtres et son évolution au fil du temps. 5 litres d'une solution à 1 g de fluorescéine/L (5 g de fluorescéine/filtre) ont été injectés instantanément à l'entrée de chaque filtre. Puis, les concentrations de traceur en sortie des filtres ont été suivies jusqu'à ce que plus de 90% de la masse du traceur a été récupérée à la sortie des filtres. Les courbes des concentrations de traceurs en fonction du temps ont été tracées (courbes de distribution des temps de rétention, RTD-courbes).

Le temps de séjour moyen du traceur dans le filtre (T_A) a été calculé par l'équation (4.1) (Metcalf et Eddy, 2003), où Ci est la concentration du traceur à la sortie à l'instant ti (mg/L), ti est le temps passé à partir de l'injection de traceur (h), Δti est l'intervalle entre deux mesures consécutives (h) et n est le nombre de mesures (-).

$$T_A = \frac{\sum ti \times Ci \times \Delta ti}{\sum Ci \times \Delta ti} \qquad \text{for } i = 1,\ldots,n; \tag{4.1}$$

Le modèle empirique d'écoulement de Wolf et Resnick (1963) (équation 4.2) a été utilisé pour décrire le comportement hydraulique interne des filtres. L'équation (4.2) est issue de l'application de la théorie du réacteur agité en continu (CSTR) et du réacteur à écoulement piston (PFR) (Alcocer et al., 2012). Dans l'équation (4.2), F (t) représente la fraction du traceur qui a quitté le filtre à l'instant t (-), t est le temps passé du moment de l'injection du traceur (h), T est le temps de séjour théorique (h), PF est la fraction à écoulement piston (-) et DV est la fraction du volume mort (-).

$$F(t) = 1 - \exp\left[\left(\frac{t/T}{(1-PF)(1-DV)} - \frac{PF}{1-PF}\right)\right] \tag{4.2}$$

4.2.2.2 *Suivi des performances épuratoires*

Au cours des 44 premières semaines d'opération, des échantillons d'eau (0.8 L) ont été prélevés chaque semaine à l'entrée et à la sortie des filtres. Après la semaine 44, la fréquence d'échantillonnage a été réduite à environ 1 échantillon par mois. Les valeurs de pH, phosphore total (TP), phosphate (PO_4-P) et Ca^{2+} des échantillons d'eau ont été mesurées. Les analyses de TP et PO_4-P ont été réalisées selon la méthode spectrométrique au molybdate d'ammonium (EN ISO 6878, 2004), alors que les analyses de Ca ont été réalisées selon la méthode par spectrométrique d'absorption atomique (EN ISO 7980, 1986).

4.3 Résultats et discussion

4.3.1 Performances hydrauliques

Les courbes de distribution des temps de rétention (RTD-courbes, Figure 4.3) ont montré en général un pic unique et étroit de traceur à la sortie des filtres après 12-24 heures de l'injection du traceur (sauf le filtre EAF, semaine 29). Cela suggère une faible diffusion et/ou dispersion

du traceur à l'intérieur des filtres, et semble indiquer un écoulement piston avec de faibles effets de paroi et de court-circuit (Chazarenc et al., 2003; Alcocer et al., 2012).

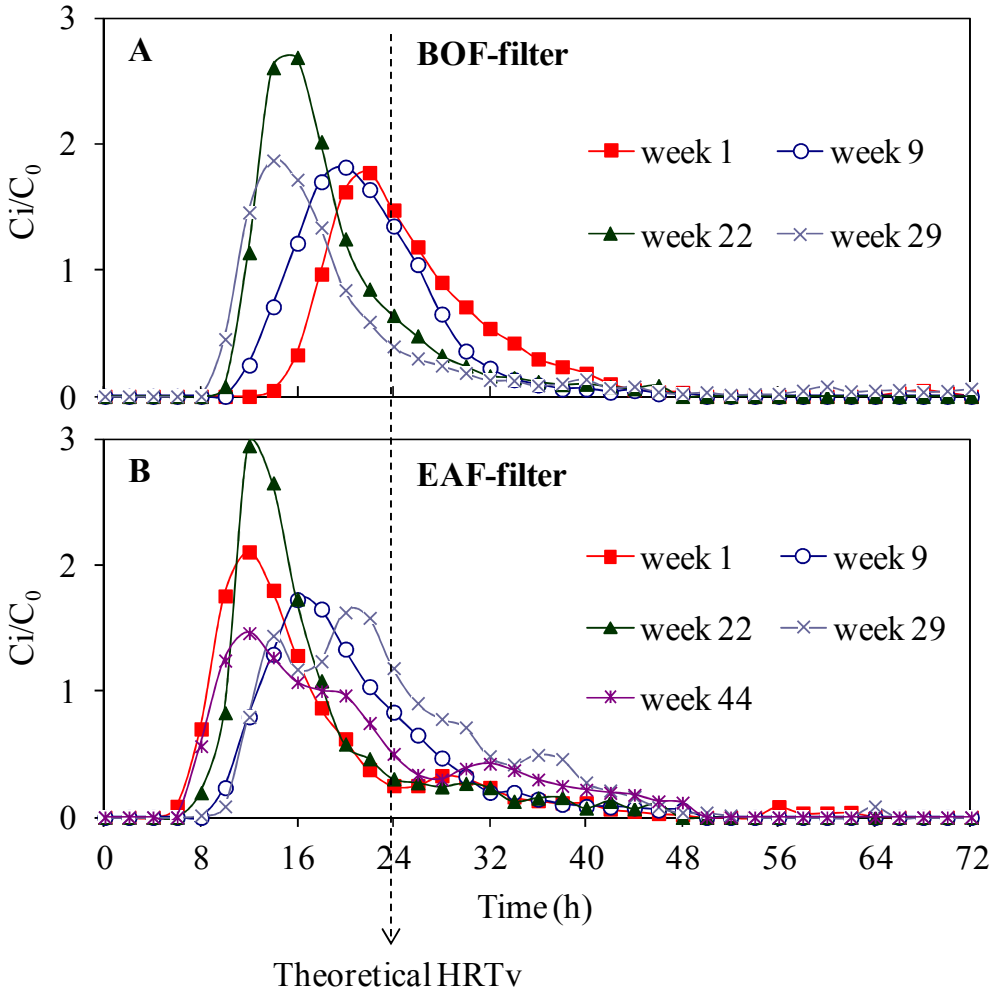

Figure 4.15. Courbes normalisées de distribution des temps de rétention (RTD-courbes) représentant le rapport entre la concentration du traceur en sortie (Ci) et la concentration équivalente de traceur à l'entrée (C_0 = masse de tracer/volume total des vides) en fonction du temps (HRT_V théorique = 24 h): (A) EAF-filter; (B) BOF-filter.

Les temps de rétention moyen du traceur dans les filtres (T_A) (calculé avec l'équation 4.1) ont été compris entre 17,4 et 25,7 h (tableau 4.1), qui sont des valeurs assez proches du HRTv théorique (24 h). Les données expérimentales des tests de traçage ont été modélisées selon l'équation (4.2) pour évaluer les fractions de PF et DV (tableau 4.1). Les coefficients de corrélation étaient toujours $R^2 > 0.95$, ce qui indique que l'équation (4.2) a bien décrit les comportements hydrauliques. Avec seulement quelques rares exceptions (EAF-filtre semaine 1, BOF-filtre semaine 29), les valeurs de PF étaient >0.5, ce qui suggère un régime

d'écoulement piston. Les valeurs de DV étaient toujours <0.3, ce qui suggère que la plus grande partie du volume de vide des filtres était disponible pour la filtration (Chazarenc et al., 2003). Le comportement hydrodynamique du filtre EAF ne semble pas changer de façon notable au fil du temps. Au contraire, le filtre BOF a montré une augmentation du DV et une diminution du PF après la semaine 22 d'opération. Cela a été, très probablement, du à la diminution de la taille des pores en raison de phénomènes de précipitation de $CaCO_3$ et de carbonatation à la surface du laitier. En fait, la diminution de la taille des pores peut avoir favorisé la diffusion et/ou la dispersion du tracer, ce qui entraîne une baisse du PF (Alcocer et al., 2012).

Tableau 4.1. Comportement hydraulique des filtres à laitier: temps de rétention moyen (T_A) et fractions d'écoulement piston (PF) et le volume mort (DV).

Semaine	Filtre EAF			Filtre BOF		
	T_A (h)	PF (-)	DV (-)	T_A (h)	PF (-)	DV (-)
1	17.5	0.40	0.30	25.7	0.72	0.01
9	20.6	0.64	0.18	21.8	0.74	0.15
22	17.4	0.50	0.30	19.0	0.61	0.25
29	23.8	0.63	0.08	20.6	0.18	0.27
44	20.5	0.52	0.16	N.A.	N.A.	N.A.

4.3.2 Performances épuratoires

Les paramètres de qualité de l'eau à l'entrée et à la sortie des filtres de laitiers au cours de 85 semaines de suivi sont présentés dans le tableau 4.2. Les concentrations moyennes de TP et PO_4-P en sortie des filtres étaient nettement plus faibles par rapport à celles de l'entrée, ce qui confirme la rétention du P au cours de la filtration de l'eau. Comme présenté dans le tableau 4.2, le pH et le Ca^{2+} à la sortie des filtres étaient plus élevés par rapport à ceux de l'entrée. La dissolution de la CaO du laitier lors de la filtration de l'eau peut expliquer les augmentations en Ca^{2+} et le pH des effluents.

Tableau 4.2. Paramètres de qualité de l'eau au cours des 85 semaines de suivi des filtres: valeurs moyennes ± écart-type (plage de valeurs min-max) et nombre de mesures (n).

Paramètres	Entrée des filtres	Sortie du filtre EAF	Sortie du filtre BOF
TP (mg P/L)	8.3 ± 1.2 (5.9-11.6) n = 52	4.5 ± 1.7 (0.9-8.4) n = 52	3.5 ± 1.7 (0.1-7.6) n = 52
PO_4-P (mg P/L)	7.7 ± 1.1 (4.4-10.3) n = 44	4.2 ± 1.6 (0.8-8.2) n = 44	3.4 ± 1.5 (0.1-7.4) n = 44
Ca^{2+} (mg Ca/L)	127 ± 22 (47-152) n = 37	142 ± 20 (75-175) n = 37	134 ± 20 (72-173) n = 37
pH (-)	7.2 ± 0.2 (6.9-7.7) n = 52	8.3 ± 0.2 (7.7-9.0) n = 52	8.6 ± 0.7 (8.0-12.0) n = 52

Les niveaux de TP et de pH à l'entrée et à la sortie des filtres de laitiers au cours des 85 semaines de suivi sont présentés dans les figures 4.4 A et B, respectivement, tandis que la figure 4.4 C montre l'évolution de la température moyenne de l'air et de l'eau.

Les expériences sur le terrain ont débuté avec un HRTv de 1 jour. Pendant les 9 premières semaines de fonctionnement, les efficacités de rétention du TP ont semblé diminuer en fonction de la diminution de la température. Après la semaine 9, le HRTv a été augmenté de 1 à 2 jours, et cela a conduit à une augmentation temporaire des efficacités d'élimination du TP. Cependant, les rendements ont diminué considérablement au cours de l'hiver (après la semaine 16). Ensuite, les rendements d'élimination du TP ont commencé à augmenter progressivement avec l'augmentation de la température au printemps (semaine 25-40). Cela suggère que l'efficacité de l'enlèvement du TP augmente lorsque la température augmente, comme cela a été déjà observé au cours d'expériences en colonne (Shilton et al., 2005). Les valeurs de TP en entrée et sortie des filtres de laitiers observées dans cette étude (figure 4.4 A) étaient très similaires à celles rapportées dans une étude récente (Shilton et al., 2006), qui a utilisé des laitiers d'aciérie pour traiter l'effluent d'un marais artificiel en Nouvelle Zélande (HRTv environ 3 jours). Shilton et al. (2006) ont confirmé la fluctuation saisonnière des efficacités d'élimination du TP au cours des 10 années de fonctionnement des filtres à laitiers: les concentrations plus faibles de TP en sortie (<2 mg P/L) ont été observées pendant les

saisons chaudes (Septembre-Mars), tandis que les concentrations plus élevées de TP en sortie (>4 mg P/L) ont été observées pendant les saisons froides (Mars-Septembre). Par conséquent, les filtres à laitiers sont censés être plus efficaces dans des climats chauds (Shilton et al., 2005).

Au cours des semaines 22, 29 et 44, le HRTv a été temporairement fixé à 1 jour pour effectuer les essais de traçage. Cette diminution de HRTv a conduit à une diminution temporaire de l'efficacité d'élimination du TP. En semaine 14, 15 et 36, le HRTv est augmenté (de 2 à environ 4 jours) en raison du colmatage des tuyaux d'alimentation. L'augmentation du HRTv a donné lieu à une augmentation temporaire des performances de rétention du TP. Cela semble indiquer que l'efficacité de rétention du TP augmente avec l'augmentation du HRTv, comme déjà démontré dans des études en colonne (Shilton et al., 2005; Drizo et al., 2006). Cependant, des HTRv trop longs peuvent produire des effluents avec des pH élevés à cause de la dissolution excessive de CaO des laitiers. Ce problème d'élévation de pH était clair surtout pour le filtre BOF, probablement parce que les laitiers BOF sont plus riches en CaO que les laitiers EAF. En outre, des long HRTv peuvent favoriser les réactions d'hydratation du CaO et de précipitation de $CaCO_3$, réactions qui provoquent l'expansion du volume des grains et favorisent le colmatage des filtres (Liira et al., 2009; Wang et al., 2010). Les résultats expérimentaux de cette étude ont montré que pour des valeurs de HRTv de 1-2 jours, les pH des effluents ont été élevés uniquement pendant les 5 premières semaines de fonctionnement, puis les pH se sont stabilisés au dessous d'une valeur de 9. Ces résultats sur le pH des effluents sont en accord avec les résultats d'expériences menées à l'échelle pilote (Weber et al., 2007; Lee et al., 2010).

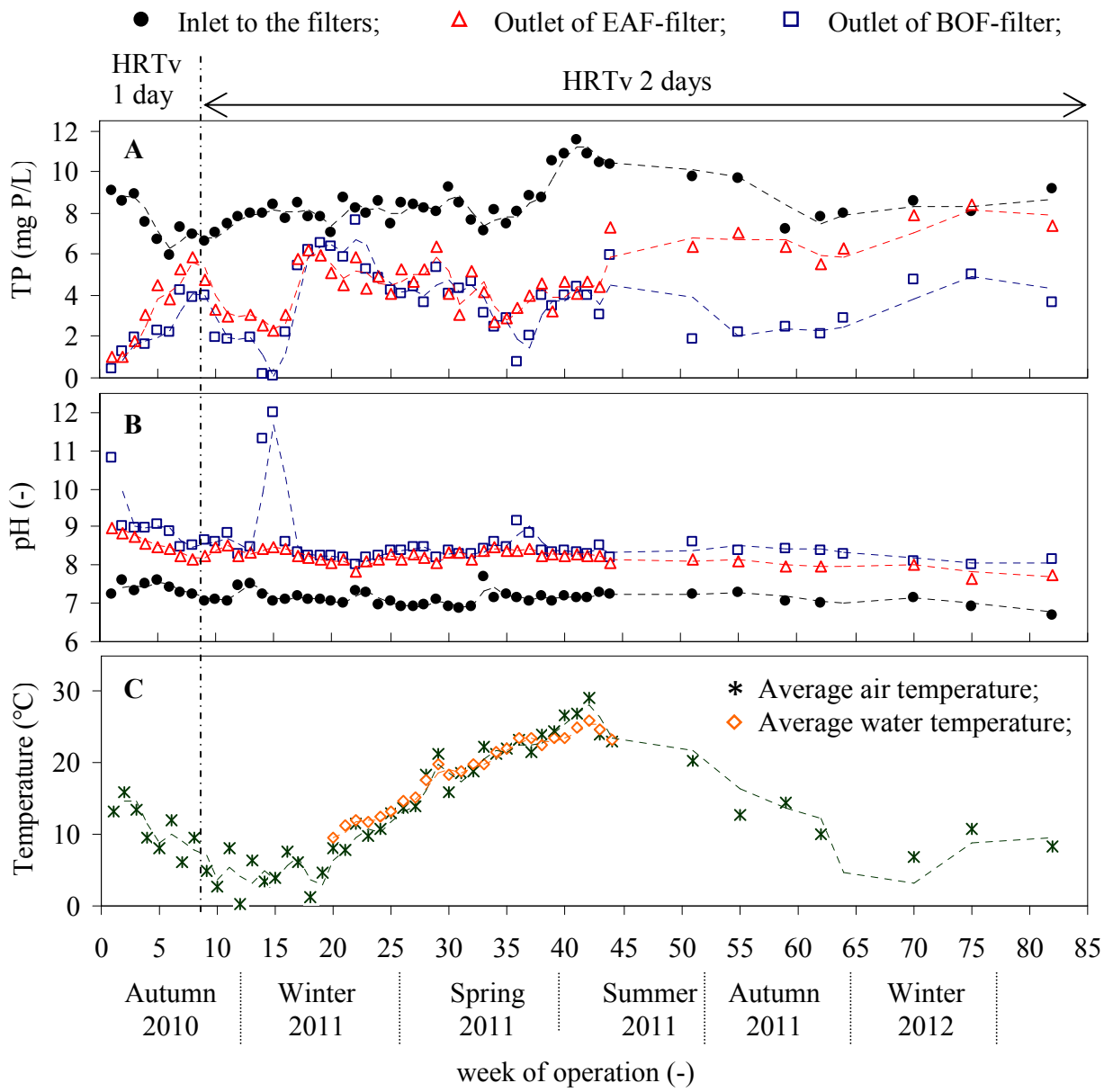

Figure 4.16. Niveaux de TP (A) et de pH (B) à l'entrée et à la sortie des filtres à laitiers, et valeurs moyennes des températures de l'air et de l'eau (C) sur une période de 85 semaines d'opération.

4.3.3 Mécanisme de rétention du P

Les résultats de cette étude suggèrent que la précipitation de phosphates de Ca a été le principal mécanisme d'enlèvement du P. Plusieurs formes de phosphate de Ca peuvent précipiter en fonction des valeurs de pH, des concentrations de Ca^{2+} et PO_4-P des solutions (Valsami-Jones, 2001): phosphate de Ca amorphe (ACP), phosphate dicalcique (DCP), phosphate octacalcique (OCP), phosphate tricalcique (TCP), hydroxyapatite (HAP) et fluorapatite (FAP). Les données expérimentales présentées dans le tableau 4.2 ont été

comparées aux courbes de solubilité des phosphates de Ca en fonction du pH (Stumm et Morgan, 1996; Valsami-Jones, 2001). Il a été constaté que les valeurs de pH, Ca^{2+} et PO_4-P étaient dans la plage de valeurs qui supportent la précipitation de TCP, OCP et HAP.

Les équations (4.3), (4.4) et (4.5) décrivent respectivement la précipitation de TCP, OCP et HAP à 25 °C (Stumm et Morgan, 1996):

$$3Ca^{2+} + 2PO_4^{3-} \rightarrow Ca_3(PO_4)_2 \downarrow \qquad (Ksp = 10^{-26}) \qquad (4.3)$$

$$4Ca^{2+} + 3PO_4^{3-} + H^- \rightarrow Ca_4H(PO_4)_3 \downarrow \qquad (Ksp = 10^{-46.9}) \qquad (4.4)$$

$$10Ca^{2+} + 6PO_4^{3-} + 2OH^- \rightarrow Ca_{10}(PO_4)_6(OH)_2 \downarrow \qquad (Ksp = 10^{-114}) \qquad (4.5)$$

D'après les équations (4.3), (4.4) et (4.5), la concentration de Ca^{2+} peut limiter la précipitation de phosphate de Ca lorsque le rapport molaire entre les concentrations de PO_4-P sur Ca^{2+} (PO_4-P/Ca) est supérieur à 0.6. Au cours des expériences sur terrain, le rapport molaire PO_4-P/Ca des eaux usées était toujours <0.3 (tableau 4.2), ce qui indique que la concentration de Ca^{2+} n'a pas limité la précipitation de phosphate de Ca.

Plusieurs auteurs ont confirmé que la précipitation des phosphates de Ca suit habituellement la "règle des phases" d'Ostwald: d'abord, la précipitation des composés moins stables (ACP, DCP, OCP), puis recristallisation dans la forme thermodynamiquement plus stable de l'HAP (Valsami-Jones, 2001; Lundager-Madsen, 2008). La recristallisation de phosphate de Ca en HAP semble être confirmée par Bowden et al. (2009), qui ont montré qu'il existe une succession de minéraux de phosphate de Ca à la surface des laitiers BOF au cours d'expériences en colonne, et que cette séquence de minéraux de phosphate de Ca progresse de la forme la moins stable (DCP, qui a été observé à partir du premier mois de fonctionnement de la colonne) à la plus stable (HAP, qui a été observée après le cinquième mois de fonctionnement de la colonne). Il a été observé dans la littérature que les cristaux de HAP représentent des germes pour la cristallisation d'autres cristaux d'HAP (Kim et al., 2006). Donc, la recristallisation en forme d'HAP des phosphates de Ca peut amener à une amélioration des efficacités d'élimination du P au fil du temps. Cependant, la cristallisation de l'HAP peut être gênée par plusieurs inhibiteurs qui sont présent dans les eaux usées, comme les ions Mg^{2+}, le CO_2, les carbonates, et les acides humiques, fulviques et tanniques (House, 1999; Valsami-Jones, 2001). Dans notre étude, la recristallisation des phosphate de Ca en

HAP pourrait expliquer l'amélioration des performance épuratoires en P qui ont été observées pour le filtre BOF au cours de la deuxième année de fonctionnement (Figure 4.4).

4.3.4 Durée de vie des filtres à laitiers

Les niveaux de rétention du P à saturation d'un substrat représente un important paramètre pour estimer la longévité d'un filtre (Drizo et al., 2002). La figure 4.5 montre les quantités cumulées de TP retenues dans les filtres en fonction des quantités cumulées de TP ajoutées (par l'effluent du marais artificiel) à l'entré des filtres. Au cours des 85 semaines de fonctionnement, le filtre BOF a enlevé 59% du TP à l'entrée, et il a atteint un niveau de rétention du P d'environ 0.47 g P/kg laitier BOF. Au cours de la même période d'opération, le filtre EAF a enlevé 36% du TP à l'entrée et il a atteint un niveau de rétention du P d'environ 0.26 g de P/kg laitier EAF.

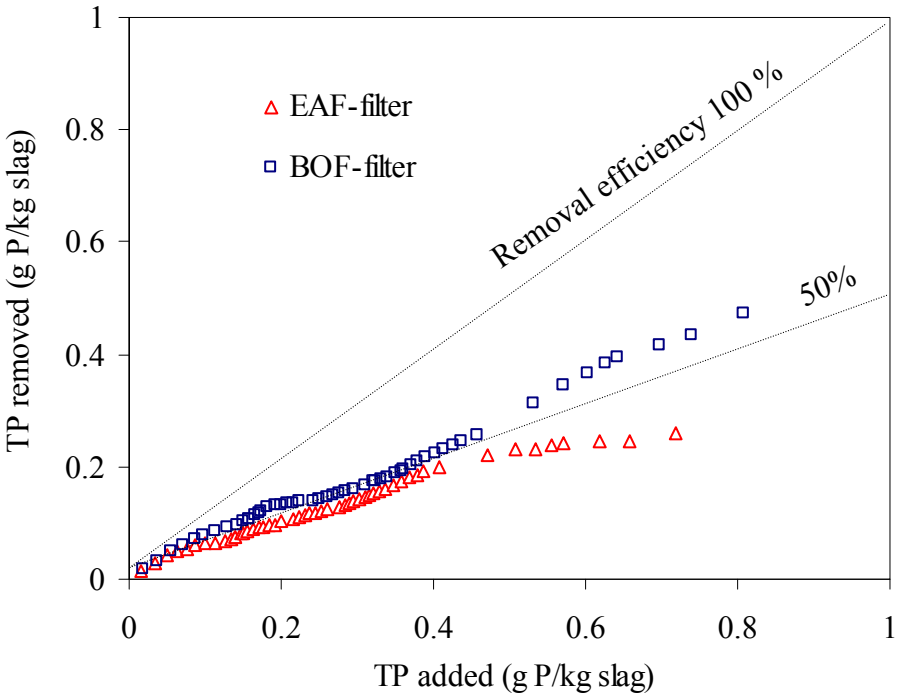

Figure 4.17. TP éliminé en fonction du TP ajouté à l'entrée des filtres (par l'effluent du marais artificiel) au cours de 85 semaines d'opération.

Les niveaux de rétention du P observés dans cette étude ont été comparés à ceux obtenu par Shilton et al. (2006), qui ont utilisé des filtres garnis de laitier de type "melter" (laitier issu de la fusion de sable riche en fer) pour le traitement du P de l'effluent d'un marais artificiel (TP moyenne à l'entrée des filtres: 8 mg P/L; HRTv de 3 jours). Shilton et al. (2006) ont montré de

bonnes performances de d'enlèvement du P jusqu'à atteindre un niveau de saturation en P de 1.23 g P/kg de laitier type "melter" après 5 années d'opération. Le niveau de saturation en P rapporté par Shilton et al. (2006) est plus élevé que ceux observés dans cette étude, ce qui suggère que, au taux actuel de rétention du P, les filtres à laitier peuvent fonctionner pour plusieurs années avant d'atteindre la saturation en P. Cependant, l'estimation de la durée de vie de filtres garnis de laitiers EAF et BOF en utilisant les données de laitiers type "melter" est très approximative. Par conséquent, il est nécessaire d'effectuer d'autres études de longue durée pour déterminer la durée de vie de filtres à laitiers EAF et BOF dans des conditions d'opération réelles.

4.4 Conclusions

Les résultats de cette étude ont confirmé que les laitiers EAF et BOF sont des substrats efficaces pour la rétention du P de l'effluent d'un marais artificiel planté de roseaux. Il a été observé que les performances épuratoires en TP augmentent avec l'augmentation de la température et du HRTv, très probablement parce que la température et le HRTv ont un effet sur les cinétiques de dissolution de CaO et sur la précipitation des phosphates de Ca.

Synthèses et conclusions générales

Les résultats des expériences réalisées à différentes échelles d'investigation (batch, colonne, et sur le terrain) ont démontré que les laitiers EAF et BOF produits en Europe sont des substrats efficaces pour l'élimination du P des eaux usées. Le principal mécanisme d'élimination du phosphore apparait être composé de trois phases consécutives: 1) dissolution de la CaO des laitiers; 2) précipitation de phosphate de Ca; 3) recristallisation des phosphates de Ca en forme d'hydroxyapatite (HAP) (Figure C 1).

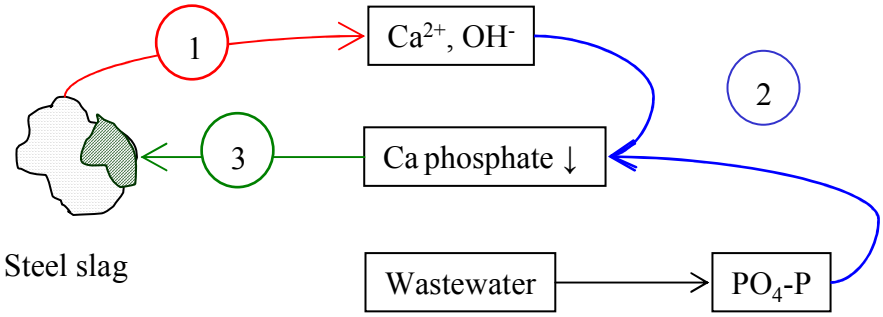

(1) CaO-slag dissolution;

(2) Ca phosphate precipitation;

(3) Ca phosphate crystallization into hydroxyapatite (HAP).

Figure C 4. Principal mécanisme de rétention du P avec les laitiers d'aciérie.

Pour l'ensemble des résultats, les laitiers BOF ont montré une plus grande affinité pour la rétention du P. Selon le mécanisme proposé (Figure C 1), la plus forte teneur en CaO du laitier BOF peut justifier les plus fortes capacités de rétention du P observées lors de l'utilisation des laitiers BOF.

Toutefois, des fortes différences ont été observées entre les efficacités de rétention du P des expériences en colonnes et celles des expériences utilisant un effluent réel (Figure C 2). Dans l'ensemble, les expériences en colonne ont montré des efficacités de rétention du P et aussi des valeurs de pH à la sortie plus élevées, ce qui suggère un taux de dissolution de CaO plus élevé.

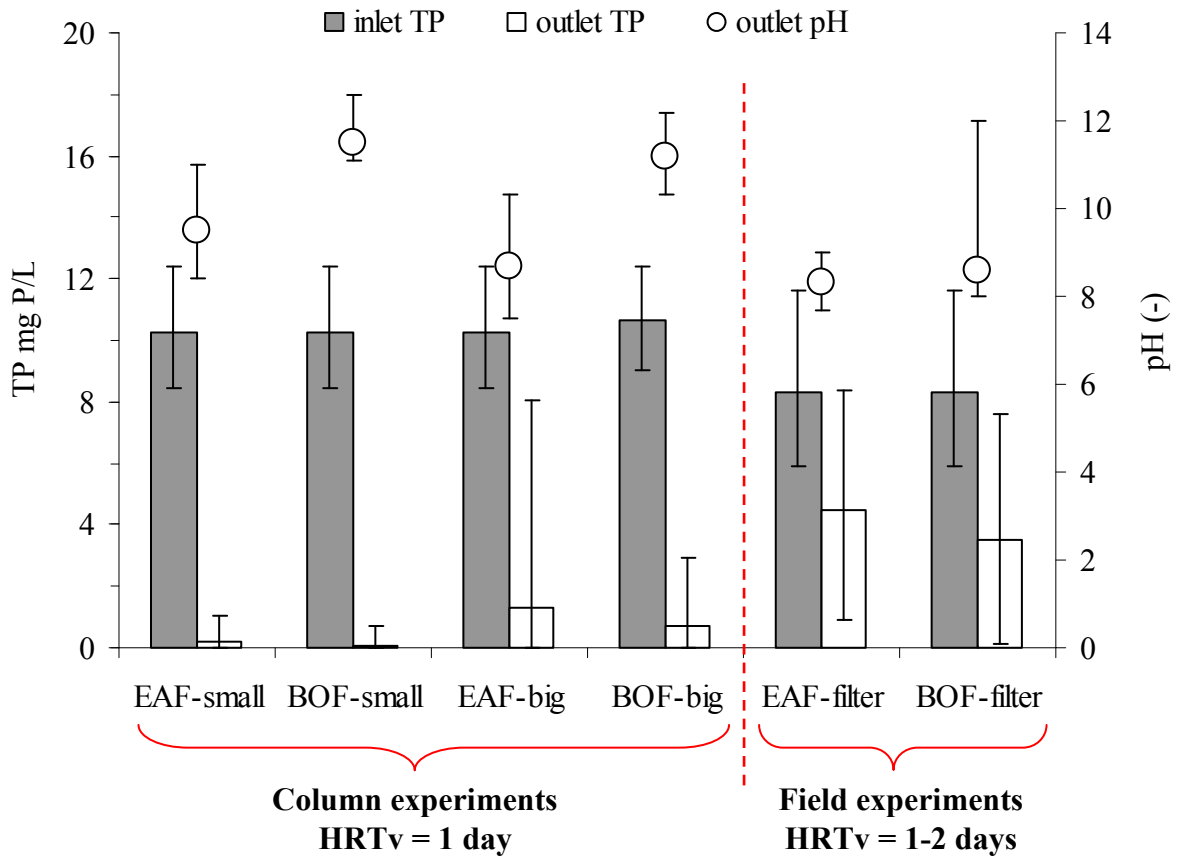

Figure C 5. Concentrations moyennes de TP à l'entré et à la sortie, et valeurs moyennes de pH en sortie au cours de 100 semaines d'expérience en colonnes (à l'exception de la colonne BOF-big dont sont présentés les résultats des 65 premières semaines) et au cours de 85 semaines d'expériences de terrain. Les barres indiquent la plage minimum-maximum des valeurs.

Les différences entre les paramètres de procédé, telles que la température et la composition des eaux usées, peuvent avoir affecté le taux de dissolution de CaO des laitiers, et donc, pourraient expliquer les différences des valeurs de pH en sortie et en efficacités de rétention du P entre les expériences en colonne et celles menées sur le terrain.

Effet de la température

Les expériences en colonne ont été réalisées dans des conditions de température de laboratoire (environ 20 °C), et par conséquent, des fluctuations en performances épuratoires liées à la température n'ont pas été observées. Au contraire, les expériences sur le terrain ont été menées en condition de température de l'air variable entre moins de 0 °C jusqu'à plus de 30 °C, et cela a conduit à une fluctuation saisonnière des performances épuratoires en P. Très probablement,

l'augmentation de la température a favorisé la dissolution du CaO des laitiers, et par conséquent la précipitation de phosphates de Ca.

Effet de la composition de l'eau

Les expériences en colonne ont été réalisées avec une solution synthétique de P faite avec de l'eau du robinet et du sel de phosphore (KH_2PO_4), tandis que les expériences sur le terrain ont été effectuées avec un effluent réel d'un marais artificiel. Le tableau C 1 montre les compositions moyennes de la solution synthétique de P et de l'effluent du marais artificiel. Comme montré par le tableau C 1, les principales différences de composition entre l'effluent du marais artificiel (entrée des filtres pleine échelle) et la solution synthétique de P (entrée des colonnes) ont été observées pour l'alcalinité totale (TA), les concentrations en Ca^{2+} et la DCO.

Tableau C 2. Composition moyenne de l'eau à l'entrée des colonnes et des filtres pleine échelle sur une période de 100 semaines d'expériences en colonnes et 85 semaines d'expériences sur terrain: valeur moyenne ± écart-type (valeur minimum-maximum) nombre de mesures (n).

Paramètres	Colonnes Solution synthétique	Filtres pleine échelle Effluent du marais artificiel
TP (mg P/L)	10.2 ± 1.0 (8.4-12.4) n = 46	8.3 ± 1.2 (5.9-11.6) n = 52
PO_4-P (mg P/L)	10.1 ± 0.8 (8.9-11.9) n = 46	7.7 ± 1.1 (4.4-10.3) n = 44
pH (-)	7.7 ± 0.2 (7.1-8.0) n = 46	7.2 ± 0.2 (6.9-7.7) n = 52
Ca^{2+} (mg Ca/L)	33.9 ± 7.5 (14.3-46.5) n = 45	127 ± 22 (47-152) n = 37
TA (mg $CaCO_3$/L)	140 ± 46 (80-200) n = 6	282 ± 39 (205-340) n = 8
DCO (mg O_2/L)	N.A.	32.0 ± 7.3 (15.0-42.0) n = 19

L'effluent du marais artificiel présentait une valeur de TA moyenne de 282 mg $CaCO_3$/L (eau très dure, selon la classification française), alors que la solution synthétique de P (entrée des colonnes) avait une valeur de TA moyenne de 140 mg $CaCO_3$/L (eau douce, selon la classification française). La mesure du TA représente la capacité de l'eau à résister aux changements de pH: les valeurs de TA élevées de l'effluent du marais artificiel peuvent avoir tamponné l'augmentation du pH (due à la dissolution de la CaO), et cela peut avoir limité la

précipitation de phosphates de Ca. En outre, la concentration élevée de Ca^{2+} de l'effluent du marais artificiel peut avoir limité le taux de dissolution de CaO, et cela par conséquent peut avoir limité la précipitation de phosphate de Ca. Enfin, les concentrations de DCO de l'effluent réel peuvent indiquer la présence de colloïdes organiques et/ou acides humiques, fulviques et tanniques qui sont des inhibiteurs de la nucléation des phosphate de Ca et de la cristallisation de l'hydroxyapatite.

Références

ASTM D4646-87, 1993. Standard test method for 24-h batch type measurement of contaminant sorption by soils and sediments. American Society for Testing and Materials 44–47.

EN ISO 6878: 2004. Water quality - Determination of phosphorus - Ammonium molybdate spectrometric method.

EN ISO 7980: 1986. Water quality - Determination of calcium and magnesium - Atomic absorption spectrometric method.

INSEE, 2009. *Institut National de la Statistique et des Etudes Economiques* (France), http://www.insee.fr.

Alcocer D.J.R., Giacoman V.G., Champagne P., 2012. Assessment of the plug flow and dead volume ratios in a sub-surface horizontal-flow packed-bed reactor as a representative model of a sub-surface horizontal constructed wetland. Ecological Engineering 40, 18-26.

Anjab Z.A., 2009. Développement d'un lit de scorie d'aciérie pour la dephosphatation des eaux usées. Master Thesis (in French), Ecole Polytechnique de Montréal, Canada.

Barca C., Gérente C., Meyer D., Chazarenc F., Andrès Y., 2012. Phosphate removal from synthetic and real wastewater using steel slags produced in Europe. Water Research 46(7), 2376-2384.

Bowden L.I., Jarvis A.P., Younger P.L., Johnson K.L., 2009. Phosphorus removal from wastewaters using basic oxygen steel slag. Environmental Science and Technology 43(7), 2476-2481.

Cassini S.T., Avelar J.C., Gonçalves R.F., Pinotti L.M., Keller R., 2010. Evaluation of steel slag as filter bed of constructed wetland in post treatment of anaerobic baffled reactor treating wastewater. Proceedings of the 12th International Conference on Wetland Systems for Water Pollution Control. Venice, Italy, 4-7 Oct. 2010.

Chazarenc F., Merlin G., Gonthier Y., 2003. Hydrodynamics of horizontal subsurface flow constructed wetlands. Ecological Engineering 21 (2-3), 165-173.

Chazarenc F., Brisson J., Comeau Y., 2007. Slag columns for upgrading phosphorus removal from constructed wetland effluents. Water Science and Technology 56(3), 109-115.

Chazarenc F., Kacem M., Gerente C., Andres Y., 2008. 'Active' filters: a mini-review on the use of industrial by-products for upgrading phosphorus removal from treatment wetlands. Proceedings of the 11th International Conference on Wetland Systems for Water Pollution Control. Indore, India, 1-7 Nov. 2008.

Claveau-Mallet D., Wallace S., Comeau Y., 2012. Model of phosphorus precipitation and crystal formation in electric arc furnace steel slag filters. Environmental Science and Technology 46(3), 1465-1470.

Crouzet P., Leonard J., Nixon S., Rees Y., Parr W., Laffon L., Bogestrand J., Kristensen P., Lallana C., Izzo G., Bokn T., Bak J., 1999. Nutrients in European Ecosystems. European Environment Agency, www.eea.eu.int, Environmental Assessment Report n° 4.

Cucarella V., Renman G., 2009. Phosphorus sorption capacity of filter materials used for on-site wastewater treatment determined in batch experiments. A comparative study. Journal of Environmental Quality 38(2), 381-392.

Drizo A., Comeau Y., Forget C., Chapuis R. P., 2002. Phosphorus saturation potential: a parameter for estimating the longevity of constructed wetland systems. Environmental Science and Technology 36(21), 4642-4648.

Drizo A., Forget C., Chapuis R.P., Comeau Y., 2006. Phosphorus removal by electric arc furnace steel slag and serpentinite. Water Research 40(8), 1547-1554.

House W.A., 1999. The physico-chemical conditions for the precipitation of phosphate with calcium. Environmental Technology 20(7), 727-733.

Jha V.K., Kameshima Y., Nakajima A., Okada K., 2008. Utilization of steel-making slag for the uptake of ammonium and phosphate ions from aqueous solution. Journal of Hazardous Materials 156(1-3), 156-162.

Johansson L., 1999. Blast furnace slag as phosphorus sorbent – column studies. The Science of the Total Environment 229(1-2), 89-97.

Johansson-Westholm L., 2006. Substrates for phosphorus removal-potential benefits for on-site wastewater treatment? Water Research 40(1), 23-36.

Kim E.H., Yim S., Jung H., Lee E., 2006. Hydroxyapatite crystallization from a highly concentrated phosphate solution using powdered converter slag as a seed material. Journal of Hazardous Materials 136(3), 690-697.

Korkusuz E.A., Beklioglu M., Demirer G.,N., 2007. Use of blast furnace granulated slag as a substrate in vertical flow reed beds: field application. Bioresource Technology 98(11), 2089-2101.

Lee M.S., Drizo A., Rizzo D.M., Druschel G., Hayden N., Twohig E., 2010. Evaluating the efficiency and temporal variation of pilot-scale constructed wetlands and steel slag phosphorus removing filters for treating dairy wastewater. Water Research 44(14), 4077-4086.

Liénard A., 1987. Domestic wastewater treatment in tanks with Emergent Hydrophytes: latest results of a recent plant in France. Water Science and Technology 19(12), 373-375.

Liira M., Kõiv M., Mander Ü., Mõtlep R., Vohla C., Kirsimäe K., 2009. Active filtration of phosphorus on Ca-rich hydrated oil-shale ash: does longer retention time improve the process? Environmental Science and Technology 43(10), 3809-3814.

Lu S., Bai S., Shan H., 2008. Mechanisms of phosphate removal from aqueous solutions by blast furnace slag and steel furnace slag. Journal of Zhejiang University-Science A 9(1), 125-132.

Lundager-Madsen H.E., 2008. Influence of foreign metal ions on crystal growth and morphology of brushite ($CaHPO_4,2H_2O$) and its transformation to octacalcium phosphate and apatite. Journal of Crystal Growth 310(10), 2602-2612.

Metcalf and Eddy, Inc., 2003. Wastewater Engineering - Treatment and reuse. 4th edition, McGraw-Hill, USA (New York).

Molle P., 2008. Élimination du phosphore par filtres plantés de roseaux. Technique de l'Ingénieur RE101, pp. 8.

Motz H., Geiseler J., 2001. Products of steel slags: an opportunity to save natural resources. Waste Management 21(3), 285-293.

Pratt C., Shilton A., Pratt S., Haverkamp R.G., Bolan N.S., 2007. Phosphorus removal mechanisms in active slag filters treating waste stabilization pond effluent. Environmental Science and Technology 41(9), 3296-3301.

Proctor D.M., Fehling K.A., Shay E.C., Wittenborn J.L., Green J.J., Avent C., Bigham R.D., Connolly M., Lee B., Shepker T.O., Zak M.A., 2000. Physical and chemical characteristics of blast furnace, basic oxygen furnace, and electric arc furnace steel industry slags. Environmental Science and Technology 34(8), 1576-1582.

Roques H., 1990. Fondements théoriques du traitement chimique des eaux. Volume II, Technique et Documentation – Lavoisier, Paris (France), pp. 382.

Shilton A. N., Pratt S., Drizo A., Mahmood B., Banker S., Billings L., Glenny S., Luo D., 2005. Active filters for upgrading phosphorus removal from pond systems. Water Science and Technology 51(12), 111-116.

Shilton A. N., Elmetri I., Drizo A., Pratt S., Haverkamp R. G., Bilby S. C., 2006. Phosphorus removal by an "active" slag filter - a decade of full scale experience. Water Research 40(1), 113-118.

Stumm W., Morgan J.J., 1996. Aquatic chemistry – Chemical equilibria and rates in natural waters. 3rd edition, Wiley-Interscience Publication, USA (Iowa), pp. 1022.

Valsami-Jones E., 2001. Mineralogical controls on phosphorus recovery from wastewaters. Mineralogical Magazine 65(5), 611-620.

Vohla C., Kõiv M., Bavor H.J., Chazarenc F., Mander U., 2011. Filter materials for phosphorus removal from wastewater in treatment wetlands – A review. Ecological Engineering 37(1), 70-89.

Wang G., Wang Y., Gao Z., 2010. Use of steel slag as a granular material: Volume expansion prediction and usability criteria. Journal of Hazardous Materials 184(1-3), 555-560.

Weber D., Drizo A., Twohig E., Bird S., Ross D., 2007. Upgrading constructed wetlands phosphorus reduction from a dairy effluent using electric arc furnace steel slag filters. Water Science and Technology 56(3), 135-143.

Wolf, D., Resnick, W. 1963. Residence time distribution in real system. Journal of Industrial and Engineering Chemical Fundamentals, 2(4):28-293.

Xiong J., He Z., Mahmood Q., Liu D., Yang X., Islam E., 2008. Phosphate removal from solution using steel slag through magnetic separation. Journal of Hazardous Materials 152(1), 211-215.

Xue Y., Hou H., Zhu S., 2009. Characteristics and mechanisms of phosphate adsorption onto basic oxygen furnace slag. Journal of Hazardous Materials 162(2-3), 973-980.

Cristian Barca

Steel slag filters to upgrade phosphorus removal in small wastewater treatment plants

Mise au point de filtres garnis de matériaux réactifs destinés au traitement des eaux usées au sein de petites installations

Abstract

This thesis aimed at developing the use of electric arc furnace steel slag (EAF-slag) and basic oxygen furnace steel slag (BOF-slag) in filters designed to upgrade phosphorus (P) removal in small wastewater treatment plants. An integrated approach was followed, with investigation at different scales: (i) Batch experiments were performed to establish an overview of the P removal capacities of steel slag produced in Europe, and then to select the most suitable samples for P removal; (ii) Continuous flow column experiments were performed to investigate the effect of various parameters including slag size and composition, and column design on treatment and hydraulic performances of lab-scale slag filters; (iii) Finally, field experiments were performed to investigate hydraulic and treatment performances of demonstration-scale slag filters designed to remove P from the effluent of a constructed wetland. The experimental results indicated that the major mechanism of P removal was related to CaO-slag dissolution followed by precipitation of Ca phosphate and recrystallisation into hydroxyapatite (HAP). Over 100 weeks of continuous feeding of a synthetic P solution (mean inlet total P 10.2 mg P/L), columns filled with small-size slag (6-12 mm BOF-slag; 5-16 mm EAF-slag) removed >98% of inlet total P, whereas columns filled with big-size slag (20-50 mm BOF-slag and 20-40 mm EAF-slag) removed 56 and 86% of inlet total P, respectively. Most probably, the smaller was the size of slag, the greater was the specific surface for CaO-slag dissolution and adsorption of Ca phosphate precipitates. Field experiments confirmed that EAF-slag and BOF-slag are efficient substrate for P removal from the effluent of a constructed wetland (mean inlet total P 8.3 mg P/L). Over a period of 85 weeks of operation, EAF-slag removed 36% of inlet total P, whereas BOF-slag removed 59% of inlet total P. P removal efficiencies increased with increasing temperature and void hydraulic retention time (HRTv), most probably because the increase in temperature and HRTv affected the rate of CaO dissolution and Ca phosphate precipitation. However, it was found that long HRTv (>3 days) may produce high pH of the effluents (>9), as the result of excessive CaO-slag dissolution. However, the results of field experiments demonstrated that at shorter HRTv (1-2 days), slag filters produced pH that were elevated only during the first 5 weeks of operation, and then stabilized below a pH of 9. Finally, a dimensioning equation based on the experimental results was proposed.

Keywords
Phosphorus removal; steel slag filter; constructed wetlands; Ca phosphate precipitation; hydroxyapatite.

Résumé

L'objectif de ce travail est la mise au point de filtres garnis de laitiers d'aciéries destinés au traitement du phosphore (P) des eaux usées au sein de petites installations. Deux types de laitiers on été testés: laitiers de four à arc électrique (EAF), et laitiers d'aciérie de conversion (BOF). Une approche intégrée a été suivie, avec investigations à différentes échelles: (i) Des expériences en flacons ont été réalisées pour établir les capacités de rétention du P de laitiers produits en Europe, et ainsi sélectionner les échantillons les plus adaptés pour l'élimination du P; (ii) Des expériences en colonnes ont été menées pour étudier l'effet de divers paramètres, notamment la taille et la composition du laitier, sur les performances hydrauliques et épuratoires des filtres; (iii) Enfin, des expériences sur terrain ont été conduites afin d'évaluer les performances hydrauliques et épuratoires de deux unités démonstration conçues pour le traitement du P au sein d'un marais artificiel. Les résultats expérimentaux ont indiqué que le principal mécanisme d'élimination du P est lié à la dissolution du CaO des laitiers, suivie de la précipitation de phosphate de Ca et recristallisation en hydroxyapatite (HAP). Après 100 semaines d'alimentation avec une solution de P (concentration moyenne de P totale 10,2 mg P/L), les colonnes remplies de laitiers de petite taille (BOF 6-12 mm et EAF 5-16 mm) ont retenu >98% du P total en entrée, tandis que les colonnes remplies de laitiers de grande taille (BOF 20-50 mm et EAF 20-40) ont retenu 56 et 86% du P total en entrée, respectivement. Il apparaît que, plus la taille des laitiers est petite, plus la surface spécifique disponible pour la dissolution du CaO et pour l'adsorption des phosphates de Ca est grande. Les expériences sur terrain ont confirmé que les laitiers sont efficaces pour le traitement du P de l'effluent d'un marais artificiel (concentration moyenne du P totale 8,3 mg P/L). Sur une période de 85 semaines d'opération, de laitiers EAF ont retenu le 36% du P total en entrée, tandis que les laitiers BOF ont retenu le 59% du P total en entrée. L'efficacité de rétention du P apparaît augmenter avec la température et le temps de rétention hydraulique (HRT), très probablement parce que l'augmentation de la température et du HRT a favorisé la dissolution de la CaO et la précipitation de phosphate de Ca. Toutefois, il a été constaté que HRT >3 jours peuvent produire des pH élevés (>9), à la suite d'une excessive dissolution de CaO. Cependant, les résultats des unités démonstration ont montré que, à HRT de 1-2 jours, les filtres produisent des pH élevés seulement pendant les 5 premières semaines de fonctionnement, puis les pH se stabilisent en dessous de 9. Enfin, une équation de dimensionnement sur la base des résultats expérimentaux a été proposée.

Mots-clés
Rétention du phosphore; scories d'aciérie; marais artificiel; précipitation des phosphates; hydroxyapatite.

l'université nantes angers le mans
PÔLE DE RECHERCHE ET D'ENSEIGNEMENT SUPÉRIEUR

ECOLE DES MINES DE NANTES